# Bulletin
# of
# The Geological Society of America

VOLUME 70 October 1959 NUMBER 10

## CONTENTS

Pages

Temperature variations due to the formation of a geosyncline. By B. F. Grossling ..... 1253–1282

Inspissation of post-Oligocene sediments in southern Louisiana. By Robert W. Crouch ..... 1283–1292

Emplacement of three granitic plutons in southeastern Ontario, Canada. By Ajit Kumar Saha ..... 1293–1326

Stratigraphic-sedimentary significance of contemporary climate and relief in four regions of the Andes Mountains. By H. F. Garner ..... 1327–1368

Geology of Continental Shelf off Louisiana: its influence on offshore foundation design. By Harold N. Fisk and Bramlette McClelland ..... 1369–1394

Short Note

Layered intrusions of Willow Lake type. By Arie Poldervaart and William H. Taubeneck ..... 1395–1398

Subscription $15.00 per year.

Printing Office: Mt. Royal & Guilford Aves., Baltimore 2, Md.

Communications for publications should be addressed to The Geological Society of America, Dr. H. R. Aldrich, Secretary, 419 West 117 Street, New York 27, N. Y.

Please give notice of change of address 4 weeks in advance. Claims for nonreceipt of the Bulletin of a given month must be sent to the Secretary of the Society before the end of the second succeeding month.

Second-class postage paid at Baltimore, Md.
Accepted for mailing at special rate of postage provided for in Section 1103 Act of October 3, 1917, authorized on July 8, 1918.

## PAPERS IN PRESS FOR FORTHCOMING ISSUES

Tertiary Geology of a Portion of the Central Cascade Mountains, Washington. By Robert F. Foster

Petrology and Metamorphism of the Wilmington Complex, Delaware. By Richard F. Ward

Geology and Structure of the Northwest Trinidad Mountains, Las Villas Province, Cuba. By Patrick Arthur Hill

Thickness and Consolidation of Deep-Sea Sediments. By Edwin L. Hamilton

Thrust Faulting and Chaos Structure, Silurian Hills, San Bernardino County, California. By Donald H. Kupfer

Structure and Petrology of the Northeast Part of the Soda Mountains, San Bernardino County, California. By L. Trowbridge Grose

BULLETIN OF THE GEOLOGICAL SOCIETY OF AMERICA
VOL. 70, PP. 1253-1282, 17 FIGS. OCTOBER 1959

# TEMPERATURE VARIATIONS DUE TO THE FORMATION OF A GEOSYNCLINE

By B. F. Grossling

## Abstract

The perturbation of the thermal equilibrium, produced by subsidence and sedimentation in the earth's outer layers is investigated by means of two models. In one the heat reaching the surface is assumed to come from the deep interior, in the other, to be generated in the crust.

The models consist of three horizontal layers, the top one representing the sedimentary layers, the middle one representing the crystalline part of the continental crust, and the lowest one representing the plastic substratum. It is assumed that at a particular instant the thickness of the top layer is increased. A theory is developed to determine the subsequent temperature variations. Also, asymptotic values are found for large times.

A finite subsidence velocity introduces an uncertainty in the time of origin of the rapid-subsidence model. For events which occur long after the subsidence, the instantaneous assumption is adequate. Moreover, it is adequate without this restriction in the lower part of the crust and in the substratum.

For large times, the deviation from the final steady state is a linear function of the depth. When the heat comes from the interior, the temperature deviation from the final steady state varies as $t^{-3/2}$, whereas when the heat is generated in the crust, it varies as $t^{-1/2}$.

The temperature variations are evaluated for subsidences of 6 and 13 km. The sedimentary layer is assumed to be 2 km thick initially, and the crystalline crust is assumed to be 30 km thick. The time variation of the different components of the temperature variations gives an insight into the propagation of thermal disturbances in the earth. Thermal adjustment requires millions of years.

After subsidence, the temperature increases rapidly during the first 20 million years or so. Thereafter, the rate of increase is much smaller. The increase is much more rapid in the sediments than in the lower part of the crust. At the base of the crust, the increase is about 22°–23° C per km of subsidence, if the thermal conductivity is 0.006 cgs. However, if the conductivity decrease with temperature in the range of crustal temperatures was taken into consideration, much larger increases would be obtained.

The times required for thermal adjustment are large enough to be significant in certain geological processes. The temperature increase after subsidence should affect the rate of lithification of sediments and the strength of the crust.

Both the stresses and the temperature of a certain portion of sediment increase with subsidence. At depths greater than a few hundred feet, the confining stress on the grain matrix corresponds, practically without any time lag, to the current depth of burial. On the other hand, the adjustment of the temperature lags appreciably. Thus, lithification may be incomplete at certain depths because the temperature is still far below its final value. Lithification is likely to be completed within the first 20 million years after the subsidence.

During the folding stage of a geosyncline, the shearing rate of the crustal rocks increases appreciably. The crustal "solid viscosity" may decrease markedly when the temperature reaches the value it has at the base of an undisturbed crust. Thus, the crustal strength decreases relatively quickly up to about 20 million years after the subsidence and thereafter much more slowly. Because of this decrease, the folding stage of a geosyncline would occur 15–20 million years after the subsidence.

If heat comes from the deep interior, there is, for a certain time, a zone of cooling in the substratum. The corresponding increase in the solid viscosity of the substratum may effectively lock, for a certain time, the subsequent uplift of the crust.

## CONTENTS

### TEXT


| | Page |
|---|---|
| Introduction | 1254 |
| Notation | 1255 |
| Statement of problem | 1256 |
| Theory of rapid subsidence | 1257 |
| General considerations | 1257 |
| Model in which the heat comes from the deep interior | 1259 |
| Initial conditions | 1259 |
| Determination of $\Delta T^{\mathrm{I}}$ | 1259 |
| Determination of $\Delta T^{\mathrm{II}}$ | 1259 |
| Approximation for large $t$ | 1260 |
| Determination of $\Delta T^{\mathrm{III}}$ | 1260 |
| Model in which the heat is generated in the crust | 1261 |
| Transient temperature distribution $\Delta T_b^{\mathrm{I}}$ | 1261 |
| Radioactive slabs | 1262 |
| Radiogenic heat conducted to the earth's interior | 1263 |
| Application of rapid-subsidence theory to a geosyncline | 1264 |
| General considerations | 1264 |
| Components of temperature deviation when the heat comes from the deep interior | 1264 |
| Components of temperature deviation when the heat is generated in the crust | 1267 |
| Discussion of rapid-subsidence assumption | 1269 |
| Temperature variations after subsidence of a geosyncline | 1272 |
| Significance of temperature variations | 1273 |
| Significance for lithification | 1273 |
| Significance for evolution of geosynclines | 1278 |
| Conclusions | 1280 |
| References cited | 1280 |


### ILLUSTRATIONS


| Figure | Page |
|---|---|
| 1. Types of steady temperature distribution, (a) due to heat from the deep interior, (b) due to heat generated in the crust | 1256 |
| 2. Effect of a rapid subsidence on temperature distribution | 1258 |
| 3. Distortion of the temperature profile in the substratum after a rapid subsidence | 1261 |
| 4. Transient distribution $\Delta T_b^{\mathrm{I}}$ at $t = 0$ | 1262 |
| 5. Radioactive slabs | 1262 |
| 6. Convention about distances $D$ and $d$ | 1263 |
| 7. Decay of surface disturbance ($\Delta T^{\mathrm{I}} + \Delta T^{\mathrm{II}}$) | 1265 |
| 8. Decay of the temperature perturbation $\Delta T^{\mathrm{III}}$ produced by deformation of the substratum by a rapid subsidence | 1266 |
| 9. Decay of temperature distribution $\Delta T_b^{\mathrm{I}}$ | 1268 |
| 10. Temperature build-up by radioactive material of upper slab | 1270 |
| 11. Temperature build-up by radioactive material of lower slab | 1271 |
| 12. Temperature increase after rapid subsidence and sedimentation when the heat comes from the earth's deep interior | 1274 |
| 13. Temperature increase after rapid subsidence and sedimentation when the heat is produced by the radioactivity of the crust and sedimentary layer | 1275 |
| 14. Evolution of the temperature profile after rapid subsidence and sedimentation | 1276 |
| 15. Increase of temperature after a rapid subsidence | 1277 |
| 16. Stress distribution in the crust produced by a compressional force $Q$ | 1278 |
| 17. Variation of the crustal strength because of the increase of temperature which follows a rapid subsidence | 1279 |


### TABLES


| Table | Page |
|---|---|
| 1. Values of principal parameters | 1264 |
| 2. Dimensions of radioactive slabs | 1269 |
| 3. Ultimate temperature increase $T_2$ at base of crust | 1277 |


## INTRODUCTION

Geosynclines have formed commonly during the evolution of the earth's crust. These are generally a few hundred kilometers wide and several hundred kilometers long. The earth's surface gradually bends downward into a troughlike depression. In most cases sedimentation keeps pace with subsidence, so that the trough is constantly filled. Flow of the plastic substratum permits the subsidence of the crust.

The subsidence of the crust and the piling up of sediments in the trough upset the thermal equilibrium. During the subsidence, the isotherms are displaced downward; when subsidence ceases, they move upward, thus gradually approaching their new steady-state positions. Hence, the formation of a geosyncline causes temperature variations in the outer layers of the earth. This paper studies these temperature variations.

Because most rock properties depend somewhat on the temperature, the temperature variations obtained here should interest investigators in other fields of geology. Mechanical properties such as strength and plasticity depend on the temperature. The evolution of

geosynclines depends on these properties. Some sediments are buried to great depths by subsidence, and their temperature and confining pressure increase. Since temperature and pressure are important for lithification, a knowledge of the temperature variations should be of interest in dating and studying transformation of sediments into indurated rocks.

The temperature variations depend on the initial or normal temperature distribution in the outer layers. There is, however, some uncertainty about this. All the heat reaching the surface could be accounted for by radioactive material in the upper 30 km of the crust. Many geologists assume, however, that some heat comes from the deep interior and represents a gradual cooling of a once-hot earth. This paper considers both these assumptions about the source of the heat.

Several studies have been made of perturbations of the temperature distribution in the earth's crust. Jeffreys (1931) investigated the thermal effect of adding to the crust a thick cover of sediments, but he determined only the temperature at the base of the sediments and the surface gradient. The sedimentary cover was regarded as added instantaneously. He assumed radioactive sources of heat were present in the crust and absent in the sediments. Furthermore, he assumed an initial distribution of temperature having a constant gradient.

If the radioactivity were uniformly distributed, the equilibrium-temperature distribution would be parabolic in the zone of the radioactive sources. Since Jeffreys was interested only in the temperature at the base of the sediments and in the gradients at the surface, the resulting discrepancy is not great. However, determination of the temperature variations throughout the crust and substratum depends on the initial temperature distribution. Therefore, the temperature variations are discussed under the two hypotheses about the nature of the heat. This paper also considers the effect of the distortion of the plastic substratum, which is important for the determination of the temperature variation in the lower part of the crust.

Jeffreys (1938) and Bullard (1938) studied the effect of topographic inequalities on the geothermal gradients at the surface. Except in very mountainous country, this effect is only a few per cent of the normal values. Coster (1947) examined the effect of anticlinal structure using an electrical model. Benfield (1949) and Birch (1950) studied the simultaneous effect of uplift and erosion.

## Notation

The following notation is used in this paper:

| | |
|---|---|
| $T$ | Temperature, °C |
| $T_{(i)}$ | Term of $i$-th degree in a power expansion of $T$ |
| $t$ | Time, sec or $10^6$ yr |
| $\rho$ | Density, g cm$^{-3}$ |
| $c$ | Specific heat, cal g$^{-1}$ (°C)$^{-1}$ |
| $k$ | Thermal conductivity, cal cm$^{-1}$ sec$^{-1}$ (°C)$^{-1}$ |
| $\alpha$ | Thermal diffusivity, cm$^2$ sec$^{-1}$ |
| $Q$ | Rate of heat flow per unit area, cal cm$^{-2}$ sec$^{-1}$ |
| $m$ | Fraction of the total heat generated in the crust which is conducted to the earth's interior |
| $q$ | Rate of radiogenic-heat generation, cal cm$^{-3}$ sec$^{-1}$ |
| $q_1$ | Rate of radiogenic-heat generation for first layer, cal cm$^{-3}$ sec$^{-1}$ |
| $q_2$ | Rate of radiogenic-heat generation for second layer, cal cm$^{-3}$ sec$^{-1}$ |
| $z$ | Depth, measured from earth's surface, positive downward, cm or km |
| $z'_0$ | Initial depth of a given horizon of the substratum, measured from the base of the crust, positive downward, cm or km |
| $z'$ | Final depth of a given horizon of the substratum, measured from the base of the crust, positive downward, cm or km |
| $a$ | Depth-attenuation coefficient of the subsidence, cm$^{-1}$ |
| $h_0$ | Initial depth of the base of the first layer, cm or km |
| $h$ | Final depth of the base of the first layer, cm or km |
| $H_0$ | Initial depth of the base of the second layer, cm or km |
| $H$ | Final depth of the base of the second layer, cm or km |
| $s$ | Subsidence, cm or km |
| $d$ | Smallest of the distances from a point to the two faces of a plane parallel slab, cm or km |
| $D$ | Largest of the distances from a point to the two faces of a plane parallel slab, cm or km |
| $z_1$ | Reduced value of $z$; $z_1 = z/2(\alpha t)^{\frac{1}{2}}$, dimensionless. The addition of the subindex 1 to a length symbol will denote division by $2(\alpha t)^{\frac{1}{2}}$ |
| $u$ | Reduced variable, $u = \zeta/2(\alpha t)^{\frac{1}{2}}$ |
| $E$ | Steady-state temperature gradient when the heat comes from the deep interior, °C cm$^{-1}$ or °C km$^{-1}$ |
| $T_1$ | Ultimate temperature increase because of subsidence for $0 \leqslant z \leqslant s$, when the heat comes from the deep interior, $T_1 = Es$ |
| $\Delta T^1$ | *or* $\Delta T^1(z, t)$. Temperature function, which at $t = 0$ is equal to $-T_1$ in the interval |

$0 \leqslant z \leqslant \infty$; and which is $\Delta T^{\mathrm{I}} = 0$ for $z = 0$ and $t > 0$

$\Delta T^{\mathrm{II}}$ *or* $\Delta T^{\mathrm{II}}(z, t)$. Temperature function, which at $t = 0$ is a linear function of $z$ between the point $z = 0$, $\Delta T^{\mathrm{II}} = T_1$ and the point $z = s$, $\Delta T^{\mathrm{II}} = 0$; and which is $\Delta T^{\mathrm{II}} = 0$ for $z = 0$ and $t > 0$

$\Delta T^{\mathrm{III}}$ *or* $\Delta T^{\mathrm{III}}(z, t)$. Temperature function, which at $t = 0$ is equal to the deviation from $T = Ez$ produced by the distortion of the substratum

$\Delta T_a$ *or* $\Delta T_a(z, t)$. Temperature deviation from the final steady state, when the heat comes from the deep interior

$\Delta T_A$ *or* $\Delta T_A(z, t)$. Temperature variation from the initial steady state, when the heat comes from the deep interior

$T_2$ Ultimate temperature increase in the substratum, when the heat is generated in the crust

$\Delta T_b^{\mathrm{I}}$ *or* $\Delta T_b^{\mathrm{I}}(z, t)$. Temperature function equal at $t = 0$ to the initial deviation from the initial steady state, when the heat is generated in the crust

$\Delta T_b^{\mathrm{II}}$ *or* $\Delta T_b^{\mathrm{II}}(z, t)$. Temperature build-up produced by the radiogenic heat sources added by the subsidence

$\Delta T^{\mathrm{IV}}$ *or* $\Delta T^{\mathrm{IV}}(z, t)$. Temperature function, which at $t = 0$ is a linear function of $z$ between the point $z = 0$, $\Delta T^{\mathrm{IV}} = T_2$ and the point $z = s$, $\Delta T^{\mathrm{IV}} = 0$; and which is $\Delta T^{\mathrm{IV}} = 0$ for $z = 0$ and $t > 0$

$\Delta T^{\mathrm{V}}$ *or* $\Delta T^{\mathrm{V}}(z, t)$. Temperature function, which for $t = 0$ is a linear function of $z$ between the point $z = 0$, $\Delta T^{\mathrm{V}} = T_2$ and the point $z = H_0 + s/2$, $\Delta T^{\mathrm{V}} = 0$; and which is $\Delta T^{\mathrm{V}} = 0$ for $z = 0$ and $t > 0$

$\Delta T_b$ *or* $\Delta T_b(z, t)$. Temperature deviation from the final steady state, when the heat is generated in the crust

$\Delta T_B$ *or* $\Delta T_B(z, t)$. Temperature variation from the initial steady state, when the heat is generated in the crust

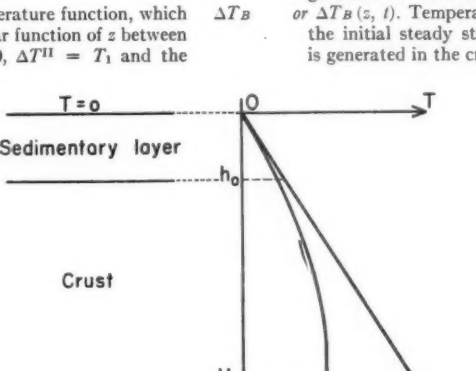


FIGURE 1.—TYPES OF STEADY TEMPERATURE DISTRIBUTION, (a) DUE TO HEAT FROM THE DEEP INTERIOR, (b) DUE TO HEAT GENERATED IN THE CRUST

## STATEMENT OF PROBLEM

If the conditions in the vertical plane through the middle of a geosyncline are considered, determination of the temperature variations owing to sedimentation and subsidence can be regarded as a one-dimensional problem. This is because the width of a geosyncline is several times the crustal thickness, and its length is again large in comparison to its width.

This paper, therefore, considers three horizontal layers—the top one representing the sedimentary layers, the middle one representing the crystalline part of the continental crust, and the lowest one a plastic substratum which can be assumed to extend downward to infinity. The thermal conductivity and diffusivity are taken to be the same for the three layers. It is assumed that the top surface of the uppermost layer is kept at a constant temperature (which may be taken as zero) and that before the subsidence, the temperature distribution has reached the steady state. The three layers are shown in Figure 1, as well as two alternatives, (a) and (b), for the initial temperature distribution. The upward flow of heat from the deep interior, shown at (a), may represent either a gradual cooling of an orginally hot earth or may be due to other deep heat sources. It will be referred to as heat from the deep interior. For alternative (b) the radioactiv

sources of heat are assumed to be distributed with different but uniform densities in the two uppermost layers.

At a particular instant the thickness of the top layer may increase, owing to deposition of sediments, assumed to be laid at zero temperature. If the topmost surface is taken as a level of reference, then the two topmost layers are displaced downward. If the subsidence occurs sufficiently quickly, the initial temperature distribution will be bodily displaced with the material but otherwise will be practically unchanged. This will be termed rapid subsidence. If the subsidence occurs slowly, the temperature distribution will readjust continuously.

The equations satisfied by the temperature must be considered. For one-dimensional heat flow in an isotropic rigid body with internal heat sources, the temperature satisfies the equation given by Carslaw and Jaeger (1948, p. 59, equation 1)

$$\frac{\partial T}{\partial t} = \alpha \frac{\partial^2 T}{\partial z^2} + \frac{q}{\rho c}, \tag{1}$$

where $\alpha$ equals $k/\rho c$ equals thermal diffusivity, $k$ equals thermal conductivity, $\rho$ equals density, $c$ equals specific heat, and $q$ equals rate of heat generation per unit volume.

When the body changes shape simultaneously with heat flow, equation 1 must be modified. If, around a volume $V$, a closed surface $S$ is displaced by the distortion of the body, the balance of heat across $S$ gives the following equation:

$$\int_{(S)} k \operatorname{grad} T \cdot \mathbf{dS} = \frac{d}{dt} \left\{ \int_{(V)} \rho c T \, dV \right\}. \tag{2}$$

In this equation $d/dt$ represents differentiation following the elements of the volume. When the volume $V$ is very small, the equation reduces to

$$k \operatorname{div} \operatorname{grad} T = \rho c \left( \frac{\partial T}{\partial t} + \frac{\partial T}{\partial s} \frac{ds}{dt} \right), \tag{3}$$

where $ds$ is the displacement in the direction of the motion. The density $\rho$ is taken to be independent of time. From equation 3,

$$\frac{\partial T}{\partial t} = \alpha \left( \frac{\partial^2 T}{\partial x^2} + \frac{\partial^2 T}{\partial y^2} + \frac{\partial^2 T}{\partial z^2} \right) - v \frac{\partial T}{\partial s}, \tag{4}$$

where $v$ is the velocity. When the problem is two-dimensional, both with respect to heat flow and distortion, one of the second derivatives of $T$ can be made zero by choosing one axis, say $y$, along the length. Furthermore, in the particular case of a subsiding geosyncline, another axis, say $z$, can be chosen in the vertical plane along its axis. On the axial zone, the isotherms will be very nearly horizontal planes, hence, $\dfrac{\partial^2 T}{\partial x^2} \simeq 0$. Also, the velocity will have only $z$ components. Therefore, according to Carslaw and Jaeger (1948, p. 127),

$$\frac{\partial T}{\partial t} = \alpha \frac{\partial^2 T}{\partial z^2} - v \frac{\partial T}{\partial z}. \tag{5}$$

## Theory of Rapid Subsidence

### *General Considerations*

The model in which the heat comes from the deep interior will be considered first.

For cooling of a once-hot earth, it can be verified that after 2000 million years the gradient is practically constant down to a depth of more than 200 km. Only that part of the temperature profile above about 150-km depth is really important for the determination of the temperature variations. Hence, there is no serious error in assuming a uniform gradient, denoted here by $E$, to represent the heat flow coming from the deep interior.

The subsidence of the crust is accompanied by a downward displacement of the initially linear temperature distribution. Since the deformation and flow of the substratum must tend to zero with increasing depth, the temperature at great depth is not affected initially by the subsidence. Therefore, the initial temperature distribution $T = Ez$ is replaced by a distorted distribution, which corresponds to the line $OAB$ and the curve $BC$ in Figure 2A, (1). The curve $BC$ at sufficiently great depth approaches the original distribution.

The distorted distribution can be replaced by (1) distribution $T = Ez$, plus (2) deviation $\Delta T_a$. The first distribution represents a steady state which is maintained by the new heat that comes from the hot interior and does not need further study. The second is a transient effect that gradually decays to zero. The transient effect will be discussed hereafter.

In the other model, the heat is produced by radioactivity of the crust. For the analysis of the problem a distinction should be made between old and new radiogenic heat. The old heat is in the ground prior to the subsidence;

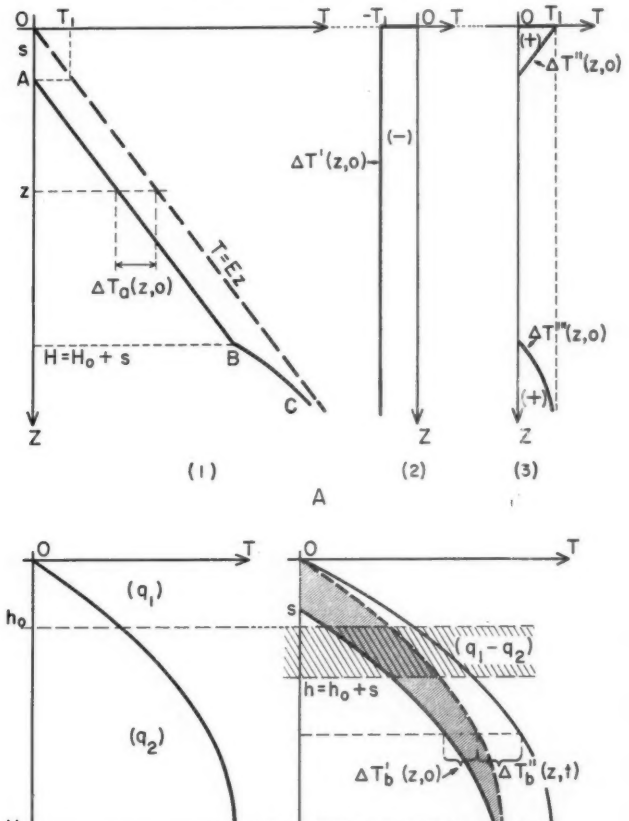


FIGURE 2.—EFFECT OF A RAPID SUBSIDENCE ON TEMPERATURE DISTRIBUTION

In A, heat comes from the deep interior; the deviation from the initial condition is resolved in partial terms shown at (2) and (3). In B, heat comes from a radiogenic source; (1) shows initial condition, (2) shows displaced-temperature distribution.

the new heat is generated after the subsidence. The old radiogenic heat is represented by the initial temperature distribution. The sedimentary layer is assumed to have a homogeneous distribution of radiogenic heat sources $q_1$, and the crust a similar kind of distribution, $q_2$ (Fig. 1). The error introduced by assuming that $q_1$ and $q_2$ are constants is very small because the half lives of the radioactive elements involved are much larger than the times of interest here.

The steady-temperature distribution produced by the radioactive sources is obtained by solving the differential equation

$$k\frac{d^2T}{dz^2} + q = 0. \qquad (6$$

There are five boundary conditions to satisfy, namely $T = 0$ at $z = 0$, $[T] = 0$ at $z = h_0$ and at $z = H_0$, and $\left[k\frac{dT}{dz}\right] = 0$ at $z = h_0$ and at $z = H_0$. The symbol [ ] denotes the change across a boundary of the quantity enclosed by the symbol. The integration of equation 6 introduces six arbitrary constants. Since the boundary conditions are only five, one arbitrary constant remains undetermined. This constant corresponds to flow of heat coming from below the radioactive layers. The part of the solution which corresponds to the radiogenic heat only is

$$T = -\frac{q_1 z^2}{2k} + \frac{(h_0 q_1 + H_0 q_2 - h_0 q_2)z}{k}, \quad (7a)$$

$$T = -\frac{q_2 z^2}{2k} + \frac{q_2 H_0 z}{k} + \frac{h_0^2(q_1 - q_2)}{2k} \quad (7b)$$

and

$$T = \frac{(h_0^2 q_1 + H_0^2 q_2 - h_0^2 q_2)}{2k} \quad (7c)$$

for the first, second, and third layers, respectively. These equations describe the initial equilibrium-temperature distribution which is rigidly displaced by the subsidence. Since no radioactive sources are assumed to exist in the substratum, the equilibrium temperature there is constant. Hence, there is no distortion of the temperature profile due to the deformation of the substratum.

The displaced temperature distribution can be considered as the superposition of the initial plus a transient distribution $-\Delta T_b^{\mathrm{I}}$ (Fig. 2B). Furthermore, the subsidence alters the distribution of radioactive matter because of the displacement of the crust and of the thickening of the sedimentary layer. This alteration is equivalent to the addition of two radioactive slabs, one extending from $z = h_0$ to $z = h_0 + s$ and with sources $(q_1 - q_2)$, and the other extending from $z = H_0$ to $z = H_0 + s$ and with sources $q_2$, as shown in Figure 2B.

Therefore, the total deviation $\Delta T_b$ from the new equilibrium condition is the sum of (1) transient term $-\Delta T_b^{\mathrm{I}}$, and (2) what is left of the ultimate temperature build-up, namely $-[\Delta T_b^{\mathrm{II}}]_t^{\infty}$, produced by the new heat sources. The symbol $\Delta T_b^{\mathrm{II}}$ denotes the temperature build-up produced by these sources.

### *Model in which the Heat Comes from the Deep Interior*

*Initial conditions.*—In the model in which the heat comes from the deep interior, the temperature variation, *OABC* at (1) in Figure 2A, immediately after a subsidence $s$, is the superposition of the steady-temperature distribution $T = Ez$ plus the temperature distributions $\Delta T^{\mathrm{I}}(z, 0)$, $\Delta T^{\mathrm{II}}(z, 0)$, and $\Delta T^{\mathrm{III}}(z, 0)$, as shown at (2) and (3) in Figure 2A. The symbol $\Delta T^{\mathrm{I}}(z, t)$ denotes the temperature function which is the decay of an initial distribution $\Delta T^{\mathrm{I}}(z, 0)$. The sum $(\Delta T^{\mathrm{I}} + \Delta T^{\mathrm{II}})$ represents the perturbation produced by the surface, and $\Delta T^{\mathrm{III}}$ represents the perturbation produced by the base of the crust and by the deformation of the substratum.

The definitions of $\Delta T^{\mathrm{I}}$, $\Delta T^{\mathrm{II}}$, and $\Delta T^{\mathrm{III}}$ for $t = 0$ are as follows: (1) $\Delta T^{\mathrm{I}}(z, 0)$ is a function which has a constant value $-T_1$ from $z = 0$ to $z = \infty$; (2) $\Delta T^{\mathrm{II}}(z, 0)$ is a linear function of $z$ which extends from $z = 0$, where it has the value $T_1$, to $z = s$, where it is zero, and which is zero elsewhere; that is,

$$\Delta T^{\mathrm{II}}(z, 0) = T_1(1 - z/s), \qquad (0 \leqslant z \leqslant s);$$

and (3) $\Delta T^{\mathrm{III}}(z, 0)$ is a function which results from the deformation of the substratum; it extends over the range $z \geqslant H$.

*Determination of* $\Delta T^{\mathrm{I}}$.—The term $\Delta T^{\mathrm{I}}$ is easy to consider. The temperature distribution in a semi-infinite solid whose surface is kept at zero temperature and whose initial temperature is $-T_1$ (constant) is given by Carslaw and Jaeger (1948, p. 41, equation 4) as

$$\Delta T^{\mathrm{I}} = -T_1 \operatorname{erf} z_1, \quad (8)$$

where $z_1 = z/2(\alpha t)^{\frac{1}{2}}$. Throughout this paper, a subindex 1 is added to a length symbol to denote division by $2(\alpha t)^{\frac{1}{2}}$. The term $T_1$ is $T_1 = Es$.

*Determination of* $\Delta T^{\mathrm{II}}$.—The value of $\Delta T^{\mathrm{II}}$ is determined by considering an infinite solid with an initial temperature distribution $f(z)$ equal to $T_1(1 - z/x)$ in the interval $0 \leqslant z \leqslant s$ and equal to $-T_1(1 + z/x)$ in the interval $0 \geqslant z \geqslant -s$. With these two distributions, the temperature at $z = 0$ is constantly zero, as required by one of the boundary conditions. The temperature in an infinite solid, when the initial temperature distribution is $f(z)$, is given by Carslaw and Jaeger (1948, p. 34, equation 1) as

$$T = \frac{1}{2\sqrt{\pi\alpha t}} \int_{-\infty}^{+\infty} f(z') \cdot \exp\{-(z - z')^2/4\alpha t\}\, dt. \quad (9)$$

If $f(z)$ is replaced by the function indicated and the equation is integrated,

$$\Delta T^{II} = T_1\{i^1 \operatorname{erfc}(z-s)_1 - i^1 \operatorname{erfc}(z+s)_1\}/2s_1 - T_1 \operatorname{erfc} z_1, \quad (10)$$

where $z_1 = z/2(\alpha t)^{\frac{1}{2}}$, etc., and $i^1$ erfc is the first integral of the error function (Hartree, 1935, p. 85).

*Approximation for large t.*—An initial temperature distribution $f(z)$ and the corresponding antisymmetrical one in order to have $T = 0$ at $z = 0$ are now considered. If the distribution is antisymmetrical and it extends only throughout finite values of $z$, then the asymptotic value of the temperature obtained from equation 9 is

$$T = \frac{zM}{2\sqrt{\pi}(\alpha t)^{3/2}}. \quad (11)$$

Here $M$ is the first moment with respect to the $z = 0$ plane of that part of the temperature distribution $f(z)$ lying on the positive side of $z = 0$. Hence, for large $t$, the distribution becomes linear in $z$ and decays as $t^{-3/2}$. For the particular case of $\Delta T^{II}$,

$$\Delta T^{II} = 2T_1 x_1^2 z_1/3\sqrt{\pi}. \quad (12)$$

*Determination of* $\Delta T^{III}$.—Determination of the actual deformation of the substratum produced by the subsidence of the crust requires consideration of the shape assumed by the crust and also the variation, in the substratum, of the viscosity and the strength with depth. Furthermore, the melting point may be reached at a depth of about 80 km (Gutenberg, 1951).

These complexities can be avoided if it is assumed that the displacement at a certain depth, corresponding to a small subsidence of the crust, decreases exponentially with the depth below the crust and further that if the crust is progressively displaced downward, the small incremental displacements are described by the same law. This kind of deformation requires thinning in the $z$ direction and spreading in the horizontal directions.

If the vertical displacements are referred to a vertical axis $z'$ directed downward, with its origin at the base of the crust, and $\Delta s$ is an elemental subsidence of the crust, then

$$\Delta z' = -\Delta s\{1 - \exp(-az')\}. \quad (13)$$

The parameter $a$ introduced in this equation is a depth-attenuation coefficient. The integration of $\Delta s$, as given by equation 13, from $s = 0$ to $s = s$, after the result is transformed, gives

$$z_0 = z + \frac{1}{a}\log[1 + \{\exp(-as) - 1\} \cdot \exp\{-a(z-H)\}], \quad (14)$$

where now $z_0$ and $z$ are the initial and final depths, respectively, below the earth's surface of a layer $P$ (Fig. 3).

For a rapid subsidence, a temperature $T$ at depth $z_0$ is carried to depth $z$. That is, if $T = Ez_0$ is the initial temperature distribution, then after the subsidence

$$T = Ez + \frac{E}{a}\log[1 + \{\exp(-as) - 1\} \cdot \exp\{-a(z-H)\}]. \quad (15)$$

The second term on the right side is the distortion with respect to the initial steady state. The deviation $\Delta T^{III}$ with respect to the final steady state is $Es$ minus this distortion, *i.e.*,

$$\Delta T^{III} = \frac{E}{a}\log[\exp as - (\exp as - 1) \cdot \exp\{-a(z-H)\}]. \quad (16)$$

This term is positive, as shown at (3) in Figure 2A.

At $t = 0$, the distribution $\Delta T^{III}$ for $z > H$ is considered, and, so that the boundary condition $\Delta T^{III} = 0$ at $z = 0$ may be satisfied, its antisymmetrical for $z < -H$ is added. With these two distributions, the temperature at any time $t$ can be deduced from equation 9. The argument of the logarithm in equation 16 is denoted by $(1 + x)$. It is easy to verify, for the range of values of the different quantities which enter into it, that $x$ is at most a fraction of 1. Thus, the approximation $\log(1 + x) \simeq x$ can be used. With this approximation the integration of equation 9 gives

$$\Delta T^{III} = T_1\{\theta(H + z, t) - \theta(H - z, t)\}, \quad (17)$$

where

$$\theta(z, t) = \tfrac{1}{2}[\exp(az + a^2\alpha t) \cdot \{1 - \operatorname{erf}(a\sqrt{\alpha t} + z/2\sqrt{\alpha t})\} + \operatorname{erf} z/2\sqrt{\alpha t}]. \quad (18)$$

A useful asymptotic value of $\Delta T^{III}$, obtained by expanding $\theta(z, t)$ in powers of $(\alpha t)^{-\frac{1}{2}}$ and letting $t$ increase, is

$$\Delta T^{III} = T_1 \cdot \left[\frac{z}{\sqrt{\pi \alpha t}} - \frac{az^3 + 3H(2 + aH)z}{12a\sqrt{\pi}(\alpha t)^{3/2}}\right]. \quad (19)$$

Furthermore, the asymptotic value of the surface gradient is

$$\left(\frac{d}{dz}\Delta T^{III}\right)_{z=0} = T_1 \cdot \left[\frac{1}{\sqrt{\pi\alpha t}} - \frac{H(2+aH)}{4a\sqrt{\pi}(\alpha t)^{3/2}}\right]. \quad (20)$$

Therefore, for large $t$, $\Delta T^{III}$ varies as $t^{-\frac{1}{2}}$, *i.e.*, less rapidly than $\Delta T^{II}$, which varies as $t^{-3/2}$.

The distribution described by equation 21 gives $\Delta T_b{}^{I} = 0$ at $z = H_0 + s/2$. In the interval $H_0 < z < H$, $\Delta T_b{}^{I}$ is an arc of parabola, arc $BC$, which is tangent to the $z$ axis at $C$. The arc $BC$ differs very little from the broken line $BDC$.

Thus, $\Delta T_b{}^{I}$ at $t = 0$ can be considered as the difference of the triangular distributions $\Delta T^{V}(z, 0) = \overline{ODF}$ and $\Delta T^{IV}(z, 0) = \overline{OAF}$. Since the initial form of $\Delta T^{II}$ is also triangular, the time decay of the two distributions can be

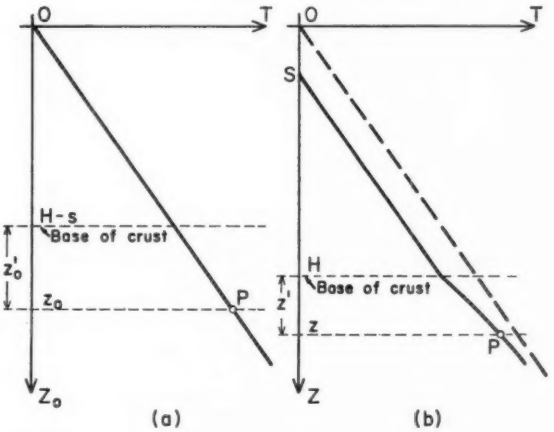


FIGURE 3.—DISTORTION OF THE TEMPERATURE PROFILE IN THE SUBSTRATUM AFTER A RAPID SUBSIDENCE

### *Model in which the Heat is Generated in the Crust*

*Transient temperature distribution* $\Delta T_b{}^{I}$.—In the analysis of the effect of rapid subsidence on the model in which heat is generated in the crust, it was found that a part of the disturbance is a transient temperature distribution $\Delta T_b{}^{I}$ (Fig. 2B).

Prior to the subsidence, the temperature distribution is assumed to have reached the steady state; this is described by equations 7a–7c. The temperature distribution in the crust, when the initial distribution is rigidly displaced through a distance $s$, is obtained by replacing $z$ by $(z - s)$ in equation 7b. Therefore, in the range $s < z < H_0$, the difference $\Delta T_b{}^{I}$ of the two distributions is a linear function of $z$, namely

$$\Delta T_b{}^{I} = -\frac{q_2 s}{k} z + \frac{q_2 s}{2k}(s + 2H_0), \quad (21)$$

and is represented by the line $AB$ in Figure 4. It is also practically linear in the range $0 < z < s$.

obtained from equation 10 by replacing $T$ with $T_2$ and by keeping $s$ for $\Delta T^{IV}$ and replacing $s$ by $(H_0 + s/2)$ for $\Delta T^{V}$.

The term $T_2$, which is equal to $\overline{OF}$ in Figure 4, is obtained by making $z = 0$ in equation 21, which gives

$$T_2 = \frac{q_2 s(s + 2H_0)}{2k}. \quad (22)$$

The term $T_2$ is equal to the ultimate temperature increase in the substratum if $q_1 = q_2$. Also, it has another interpretation. It is easily shown that the steady-state temperature below a slab with heat-source intensity $q_2$ extending from $z = H_0$ to $z = H_0 + s$ is equal to $T_2$.

In the other model the temperature variations were expressed in terms of $T_1 = Es$ instead of $T_2$. If the two models are required to give the same thermal gradient at the surface, the following relationship exists:

$$T_1 = \frac{H_0 - (1 - q_1/q_2)h_0}{H_0 + s/2} T_2. \quad (23)$$

Since $s/2 \ll H_0$ and $q_1/q_2 \simeq 1$, $T_2$ is not too different from $T_1$. For this reason, the temperature variations for the two models can be compared directly when expressed in terms of $T_1$ and $T_2$.

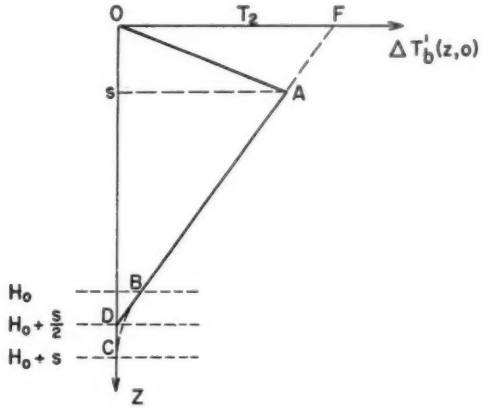


FIGURE 4.—TRANSIENT DISTRIBUTION $\Delta T_b^{\mathrm{I}}$ AT $t = 0$

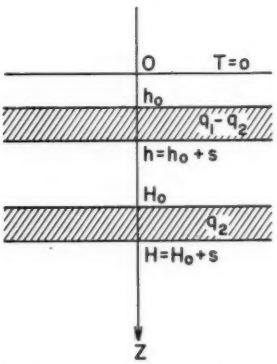


FIGURE 5.—RADIOACTIVE SLABS

*Radioactive slabs.*—In the preliminary analysis of the radiogenic model the effect of the alteration of the initial distribution of radioactive matter was mentioned. This alteration consists in the addition of two slab distributions of radioactivity, as shown in Figure 5.

The temperature distribution generated by these slabs can be determined by considering a horizontal slab of uniform thickness which extends from $z = h$ to $z = H$, which contains heat sources of intensity $q$ and which is in a semi-infinite medium. The following boundary and initial conditions exist: $T = 0$, $z = 0$ for all $t$; and $T = 0$, $t = 0$ for all $z$. The effect of the slab can be obtained from the solution for a plane source of heat of infinitesimal thickness, placed at depth $z'$, and which starts to generate heat at $t = 0$, (Carslaw and Jaeger, 1948, p 222, equation 8), namely

$$T = q\left(\frac{t}{\pi\alpha}\right)^{\frac{1}{2}} \exp\{-(z - z')_1^2\} - \frac{q\,|z - z'|}{2\alpha} \operatorname{erfc}|z - z'|_1. \tag{24}$$

In the notation of this formula ($\rho cq$) is the rate of heat generation per unit area of the plane source, which is equivalent in the notation of this paper to $qdz'$ ($dz'$ is the thickness of the elementary slab). Formula 24 is valid for an infinite body and satisfies the initial condition $T = 0$ at $t = 0$.

The temperature produced by a slab extending from $z = h$ to $z = H$ in an infinite body is obtained by integration of the temperature produced by the elementary slab. The expression $|z - z'| \operatorname{erfc}|z - z'|_1$ is in all cases positive and is a function of the distance of the point where the temperature is measured to the elementary slab. Then, the effect of the term that contains it is symmetrical with respect to the slab. To avoid confusion of signs it is better to express the results in terms of the greatest and the smallest distances $D$ and $d$, respectively, of the plane $P$ where the temperature is measured to the faces of the slab. If $P$ is inside the

slab, $D$ is the distance to the face chosen as upper, as shown in Figure 6.

When $P$ is outside the slab, either $P_1$ or $P_3$ in Figure 6, then

$$T = \frac{2qt}{\rho c}\,(i^2\,\mathrm{erfc}\,d_1 - i^2\,\mathrm{erfc}\,D_1); \qquad (25)$$

when $P$ is inside the slab,

$$T = \frac{qt}{\rho c}\,(1 - 2i^2\,\mathrm{erfc}\,D_1 - 2i^2\,\mathrm{erfc}\,d_1), \qquad (26)$$

where $i^2$ erfc is the second repeated integral of the error function, and $D_1 = D/2(\alpha t)^{\frac{1}{2}}$, etc.

To satisfy the boundary condition at $z = 0$, a slab is added which is the image with respect to the $z = 0$ plane of the $(+q)$ slab, but of intensity $(-q)$. Therefore

$$T = \frac{2qt}{\rho c}\,\{i^2\,\mathrm{erfc}\,d_1 - i^2\,\mathrm{erfc}\,D_1 + i^2\,\mathrm{erfc}\,(h + H - d)_1 - i^2\,\mathrm{erfc}\,(h + H - D)_1\} \qquad (27)$$

for the temperature between the surface and the slab (point $P_1$, Fig. 6);

$$T = \frac{qt}{\rho c}\,\{1 - 2i^2\,\mathrm{erfc}\,D_1 - 2i^2\,\mathrm{erfc}\,d_1 + 2i^2\,\mathrm{erfc}\,(h + H + D)_1 - 2i^2\,\mathrm{erfc}\,(h + H - D)_1\} \qquad (28)$$

for the temperature inside the slab (point $P_2$, Fig. 6); and

$$T = \frac{2qt}{\rho c}\,\{i^2\,\mathrm{erfc}\,d_1 - i^2\,\mathrm{erfc}\,D_1 + i^2\,\mathrm{erfc}\,(h + H + D)_1 - i^2\,\mathrm{erfc}\,(h + H + D)_1\} \qquad (29)$$

for the temperature below the slab (point $P_3$, Fig. 6).

For large $t$, *i.e.*, small values of $u$, it is useful to expand $i^2$ erfc $u$ in the power series

$$i^2\,\mathrm{erfc}\,u = \frac{1}{4} - \frac{u}{\sqrt{\pi}} + \frac{u^2}{2} - \frac{u^3}{3\sqrt{\pi}} \cdots. \qquad (30)$$

In equations 25–29, the $i^2$ erfc terms are multiplied by $2qt/\rho c$. Hence, when $t \to \infty$, the terms in the first power of "$u$" increase without bounds. Since these terms do not cancel out in equations 25 and 26, the temperature increases indefinitely with time when the medium is infinite. However, the $u$ terms in equations 27, 28, and 29 cancel out. Therefore, for a semi-infinite medium, with the boundary condition $T = 0$ at $z = 0$, the temperature does not increase indefinitely.

The $u^2$ terms are independent of time, and they must represent the steady state. In fact, it is easy to verify that the $u^2$ terms in equations 27, 28, and 29 lead to equations 7a–7c, after allowance for changes of notation.

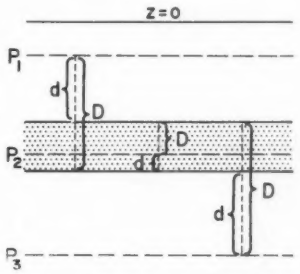


FIGURE 6.—CONVENTION ABOUT DISTANCES $D$ AND $d$

The $u^3$ terms decrease as $t^{-1}$. On separating these terms, the same value

$$T_{(3)} = -\frac{q}{k\sqrt{\pi}}\,(H^2 - h^2)z_1 \qquad (31)$$

is found for the temperatures above, inside, and below the slab. The subscript (3) denotes the part of $T$ corresponding to the $u^3$ terms. For a given time, $T_{(3)}$ varies linearly with $z$.

Since the coefficient of $u^4$ in the series of equation 30 is zero, the addition of $T_{(3)}$ to the steady state gives quite accurate values of the temperature, even for relatively large $u$. This is well illustrated in Figure 11, where the deviation from the steady state for $t = 50 \times 10^6$ yr and greater times is practically linear in $z$. The formulae derived for the radioactive slab are of course applicable to heat sources other than radioactive heat sources.

*Radiogenic heat conducted to the earth's interior.*—Inspection of the temperature build-up curves for radioactive slabs close to the earth's surface (Figs. 10, 11) demonstrates that most of the heat generated during the life of the earth must have been lost at the surface.

A layer with sources of intensity $q$, which extends from the surface to a depth $H$, may be assumed to represent the radioactive part of the crust. The heat conducted to the surface per unit of horizontal area is

$$Q(t) = \int_0^t k\left(\frac{\partial T}{\partial z}\right)_{z=0} dt. \qquad (32)$$

By introducing $\left(\frac{\partial T}{\partial z}\right)_{z=0}$, derived from equa-

tion 27, carrying out the integration, and expanding in powers of $H_1 = H/2(\alpha t)^{\frac{1}{2}}$, one can find for long times that the heat conducted to the interior, expressed as a fraction of the total heat, is

$$m = \frac{2}{\sqrt{\pi}} H_1 . \tag{33}$$

If the age of the crust is $2000 \times 10^6$ yr and $\alpha = 0.010$ cm$^2$ sec$^{-1}$ and $H = 30 \times 10^5$ cm, then $m = 0.067$. Hence, only about 7 per cent of the total heat generated in the crust has been conducted to the interior. It can readily be shown that this heat corresponds to an average temperature rise of the whole earth equal to

$$\Delta T = \frac{3qHtm}{\rho c R} . \tag{34}$$

The new symbols introduced here are $R$, the radius of the earth, and $\Delta T$, the average rise in temperature. Formula 34 assumes that the radioactive crust extends all over the surface of the earth. If the values of $H$ and $t$ are introduced, and also $m = 0.067$, $\rho = 5.52$ g cm$^{-3}$, $c = 0.20$ cal g$^{-1}$ °C$^{-1}$, and $R = 6.37 \times 10^8$ cm, then $\Delta T = 22$°C. The average increase of temperature throughout the earth is only one-fifteenth of the maximum increase (which is attained at the base of the crust).

Therefore, the heating produced by the radioactive crust is practically negligible at the central zone of the earth even after 2000 million years. This indicates that, as far as the heat produced in the crust is concerned, the error arising from the assumption that the earth's surface is a plane and that the earth extends to infinity in one direction is not serious.

## Application of Rapid-Subsidence Theory to a Geosyncline

### *General Considerations*

As an application of the rapid-subsidence theory, the temperature variations for specific subsidences of 6 and 13 km are calculated on the assumption that initially there is a layer of 2 km of sediments resting on a crystalline crust 30 km thick (Fig. 1). The same value, 0.010 cm$^2$ sec$^{-1}$, is taken for the thermal diffusivities of the three layers. The assumed values of the different parameters are summarized in Table 1. The temperature variations are calculated at times of 0.1, 1, 5, 20, 50, 100, and 300 million years after the subsidence. For comparison of the results for the two models, both are assumed to produce the same geothermal gradient at the surface.

Table 1.—Values of Principal Parameters

| Parameter | Case 1 | Case 2 |
|---|---|---|
| Subsidence, $s$ | $6 \times 10^5$ cm | $13 \times 10^5$ cm |
| Initial thickness of sediments, $h_0$ | $2 \times 10^5$ cm | $2 \times 10^5$ cm |
| Initial depth of base of crust, $H_0$ | $32 \times 10^5$ cm | $32 \times 10^5$ cm |
| Thermal diffusivity, $\alpha$ | 0.010 cm$^2$ sec$^{-1}$ | 0.010 cm$^2$ sec$^{-1}$ |
| Thermal conductivity, $k$ | 0.006 cgs | 0.006 cgs |
| Depth-attenuation coefficient of the subsidence, $a$ | $0.23 \times 10^{-6}$ cm$^{-1}$ | $0.23 \times 10^{-6}$ cm$^{-1}$ |

### *Components of Temperature Deviation when the Heat Comes from the Deep Interior*

It has been shown that when the heat comes from the deep interior the subsidence produces a temperature deviation from the final steady state which is

$$\Delta T_a = \Delta T^{\mathrm{I}} + \Delta T^{\mathrm{II}} + \Delta T^{\mathrm{III}} . \tag{35}$$

The term $\Delta T^{\mathrm{I}}(z, t)$ at $t = 0$ has the constant value $-T_1$ from $z = 0$ to $z = \infty$. The term $\Delta T^{\mathrm{II}}(z, t)$ at $t = 0$ is linear in $z$ and extends from $z = 0$ where it has a value $T_1$ to $z = s$ where it is 0. Finally, the term $\Delta T^{\mathrm{III}}(z, t)$ is produced by the deformation of the substratum. These temperature variations have been expressed in terms of $T_1 = Es$ as unit, where $E$ is the steady-state gradient and $s$ is the subsidence. The temperature $T_1$ is the ultimate temperature increase throughout the crust.

The variation $\Delta T_a$, written in full, is

$$\Delta T_a = -T_1 + \{i^1 \operatorname{erfc}(z - s)_1 - i^1 \operatorname{erfc}(z + s)_1\} \cdot T_1/2s_1 + \{\theta(h + z, t) - \theta(h - z, t)\}T_1 , \tag{36}$$

where $i^1$ erfc is the first integral of the error function, $\theta$ is a function defined under Determination of $\Delta T^{\mathrm{III}}$, $z_1 = z/2(\alpha t)^{\frac{1}{2}}$, and $s_1 = s/2(\alpha t)^{\frac{1}{2}}$. The depth $z$ is measured from the surface; $H$ is the depth of the base of the crust.

For long times, the asymptotic value of $\Delta T_a$ is

$$\Delta T_a = -\frac{Es(6H + 3aH^2 - as^2)}{12a\sqrt{\pi}(\alpha t)^{3/2}}. \qquad (37)$$

Thus, after a long time, the temperature variation behaves as $t^{-3/2}$. The factor $a$ is an attenuation coefficient of the subsidence; $a$ is taken as $0.23 \times 10^{-6}$ cm$^{-1}$, which corresponds to an attenuation of the subsidence at 100 km below the crust to one-tenth of its value. When $t$ and $a$ are large, the temperature variation becomes independent of $a$. When $a$ is small, the variation increases as $1/a$.

The propagation of temperature disturbances in the earth is clarified by examination of the components of $\Delta T_a$. For this discussion, $T_1$ is taken as 1.

The disturbance produced by the surface is represented by $(\Delta T^{\mathrm{I}} + \Delta T^{\mathrm{II}})$. Initially, this term increases linearly from 0 at the surface to 1 at a depth equal to the subsidence. Below this depth, it is equal to 1. The decay of this surface perturbation is illustrated in Figure 7 for subsidences of 6 and 13 km. The initial break in the gradient is smoothed out very quickly. In fact, in only 100,000 years, it is smoothed throughout a depth range of about 10 km. After about 5 million years, the difference between the curves for the two subsidences has practically disappeared. In 50 million years, the gradient is practically uniform down to 50 km. The disturbance $(\Delta T^{\mathrm{I}} + \Delta T^{\mathrm{II}})$ tends to zero very slowly. Even after 300 million years the temperature down to the depth of the base of the crust, 35 km, is still as high as 20 per cent of its initial value.

The term $\Delta T^{\mathrm{III}}$ is given by equation 17 in terms of the function $\theta(z, t)$. The latter function represents the effect of the distortion of the substratum when the zero-temperature surface is at $z = -\infty$. The term $\Delta T^{\mathrm{III}}$ is shown in Figure 8 for $s = 6$ and $s = 13$ km.

The heat-flow equation

$$\frac{\partial T}{\partial t} = \alpha \frac{\partial^2 T}{\partial z^2} \qquad (38)$$

indicates that the rate of change of the temperature is approximately inversely proportional to the radius of curvature of the temperature profile, and that the sign of $\partial T/\partial t$ is such that this profile tends to become straight. This equation of one-dimensional heat flow can be compared with the equation

$$M = EI \frac{d^2y}{dz^2} \qquad (39)$$

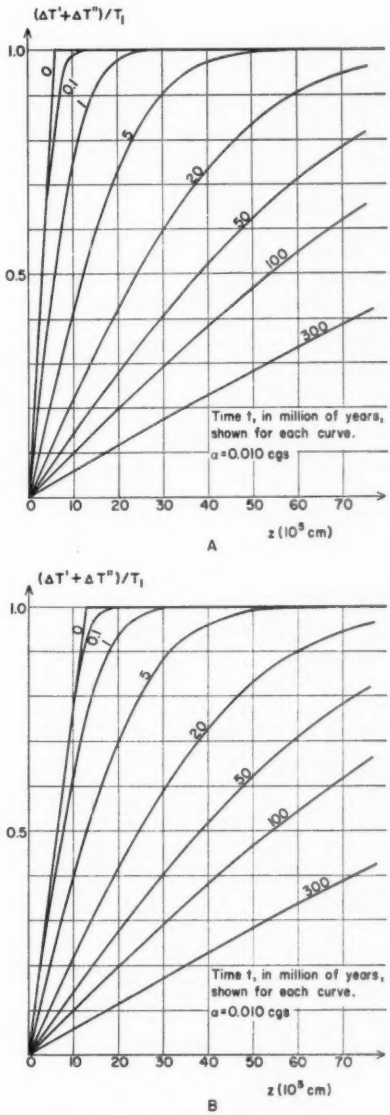


FIGURE 7.—DECAY OF SURFACE DISTURBANCE $(\Delta T^{\mathrm{I}} + \Delta T^{\mathrm{II}})$

In A, for $t = 0$, it has value 1 at $z = 6$ km; in B, for $t = 0$, it has value 1 at $z = 13$ km.

of bending of a beam. The moment $M$ is in a certain way equivalent to $\partial T/\partial t$. Also $M$ acts in a direction that would straighten up the beam and is proportional to the radius of curvature.

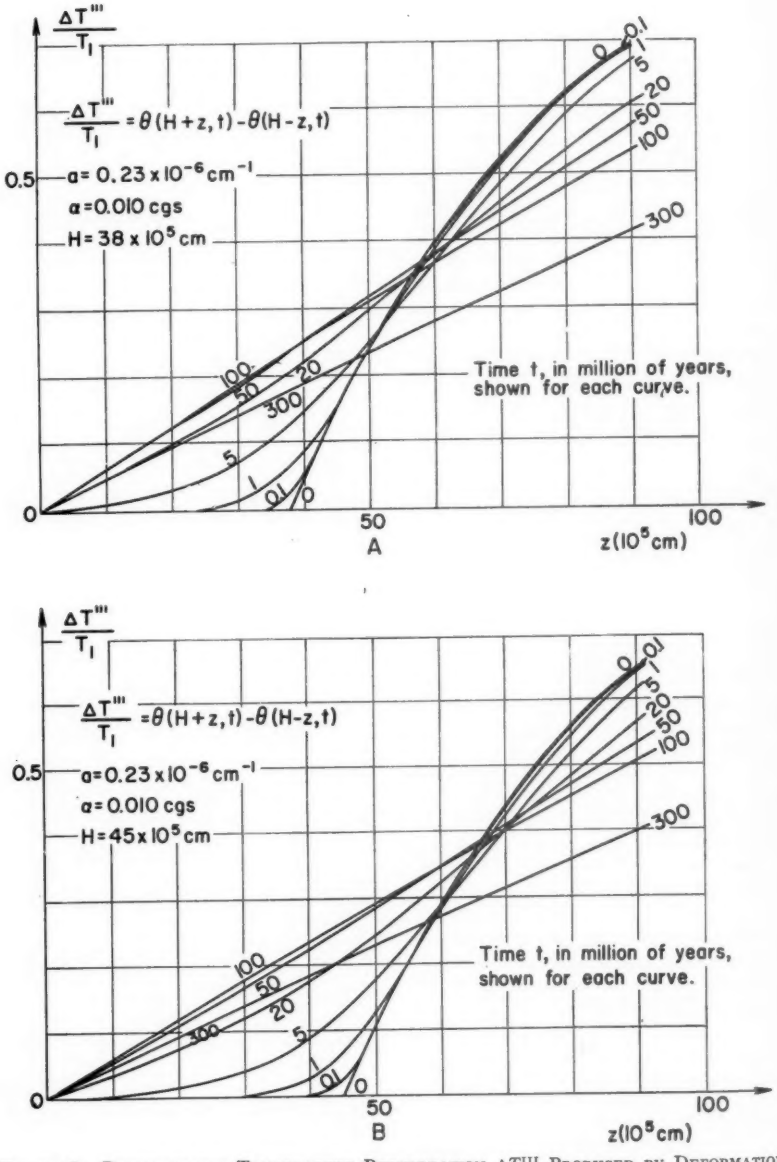


FIGURE 8.—DECAY OF THE TEMPERATURE PERTURBATION $\Delta T^{III}$ PRODUCED BY DEFORMATION OF THE SUBSTRATUM BY A RAPID SUBSIDENCE

A, for a subsidence of 6 km; B, for a subsidence of 13 km

The tendency of a temperature profile, in the absence of heat sources, is to become straight.

Initially, the temperature distribution $\Delta T^{III}/T_1$ presents two bends, a sharp bend at the base of the crust and a smooth one in the substratum. The smooth bend in the substratum gradually straightens up, feeding heat to the sharp bend at the base of the crust. The substratum bend

becomes straight later than that at the base of the crust because its straightening involves the change in temperature of a greater volume of material. In about $50 \times 10^6$ yr, the distribution becomes practically a straight line from the surface to more than 90-km depth (Fig. 8), *i.e.*, the surface gradient increases with time from zero to a maximum value. Afterward, the deficiency in the heat supply from the interior causes the gradient to decrease. The time at which the maximum gradient is reached can be determined by equation 19 by making $d/dt\,(\Delta T^{III})_{z=0} = 0$, whereby

$$t = \frac{3}{4}\frac{H(2 + aH)}{a\alpha}. \tag{40}$$

If it is assumed that $a = 0.23 \times 10^{-6}$ cm$^{-1}$ and $\alpha = 0.010$ cm$^2$ sec$^{-1}$, then $t = 113 \times 10^6$ yr for $H = 38 \times 10^5$ cm, and $t = 141 \times 10^6$ yr for $H = 45 \times 10^5$ cm. When $a$ is very large, *i.e.*, when the deformation is limited to a narrow zone at the base of the crust, formula (40) reduces to

$$t = 3H^2/4\alpha. \tag{41}$$

It gives $t = 48 \times 10^6$ yr for $H = 45 \times 10^5$ cm and $t = 34 \times 10^6$ yr for $H = 38 \times 10^5$ cm. Hence, even if the subsidence would form a sharp front at the base of the crust, the maximum gradient would be felt at the surface only after $35 \times 10^6$ yr.

The three components—$\Delta T^{I}$, $\Delta T^{II}$, and $\Delta T^{III}$—of the total deviation $\Delta T_a$ from the final steady state have been determined. Since the temperature variation which occurs after the subsidence is of interest, the initial state is taken as datum. Hence, what is wanted is

$$\begin{aligned}\Delta T_A &= |\,\Delta T_a(z, t)\,|_0^t \\ &= \Delta T_a(z, t) - \Delta T_a(z, 0).\end{aligned} \tag{42}$$

This variation is shown in Figure 12 for the subsidences of 6 and 13 km, but it will be discussed hereafter.

### *Components of Temperature Deviation When the Heat Is Generated in the Crust*

When the heat is generated in the crust, the subsidence produces a temperature deviation, from the final steady state, which is

$$\Delta T_b = -\Delta T_b^{I}(z, t) - |\,\Delta T_b^{II}(z, t)\,|_t^{\infty}. \tag{43}$$

The term $\Delta T_b^{I}$ represents the decay of the deviation from the initial steady state, and $\Delta T_b^{II}$ is the temperature build-up produced by the new radioactive-heat sources. The distribution of sources after the subsidence and the sedimentation is considered as the sum of the initial sources and of additional sources. Thus the initial steady state can be considered as being maintained by the initial sources. The additional sources consist of two slab distributions, as shown in Figure 5. The temperature deviations are expressed in terms of $T_2$ as unit, which is the ultimate temperature increase in the substratum.

For long times, it is enough to consider $\Delta T_b^{II}$, because the deviation of $\Delta T_b^{II}$ from its ultimate value varies less rapidly than the decay of $\Delta T_b^{I}$, namely as $t^{-1}$ as against $t^{-3/2}$. For long times an asymptotic value of $\Delta T_b$ is obtained, namely

$$\Delta T_b = -\frac{z}{\sqrt{\pi\alpha t}}\,(T_2^{\text{upper}} + T_2^{\text{lower}}), \tag{44}$$

where $T_2^{\text{upper}}$ and $T_2^{\text{lower}}$ are the $T_2$'s for the upper and lower radioactive slabs, respectively.

The term $\Delta T_b^{I}$ is given by

$$\begin{aligned}\Delta T_b^{I} = T_2\{&i^1 \operatorname{erfc}(z - H_0 - s/2)_1 - i^1 \operatorname{erfc} \\ &(z + H_0 + s/2)_1\}/2(H_0 + s/2)_1 - T_2 \operatorname{erfc} \\ &(H_0 + s/2)_1 - T_2\{i^1 \operatorname{erfc}(z - s)_1 - i^1 \operatorname{erfc} \\ &(z + s)_1\}/2s_1 + T_2 i^1 \operatorname{erfc} s_1,\end{aligned} \tag{45}$$

where $i^1$ erfc is the first integral of the error function, $(z - H_0 - s/2)_1 = (z - H_0 - s/2)/2(\alpha t)^{\frac{1}{2}}$, etc.

The decay of $\Delta T_b^{I}$ is shown in Figure 9 for subsidences of 6 and 13 km. Initially, $\Delta T_b^{I}$ is a triangular temperature distribution which has value zero at $z = 0$, its maximum value at $z = s$, and is zero at $z = H_0 + s/2$. In $5 \times 10^6$ yr the maximum value of $\Delta T_b^{I}$ is reduced to less than one-third its initial value, and in $50 \times 10^6$ yr, it has practically disappeared.

The term $\Delta T_b^{II}$ is the sum of two parts, one for each of the radioactive slabs which represent the change from the initial condition. The temperatures produced by each of these slabs are obtained from equations 27, 28, and 29. When the heat-source intensities in the sediments and in the crust are equal, *i.e.*, $q_1 = q_2$, only the lower slab is left. Table 2 gives the dimensions of the slabs for the two values of the subsidence considered.

The temperature build-up produced by the radioactivity of the slabs is shown in Figures 10 and 11. The linearity of the deviation from the steady state from about 100 million years justifies the use of the asymptotic formula for large $t$. This has been used for 1000, 2000, and 3000 million years.

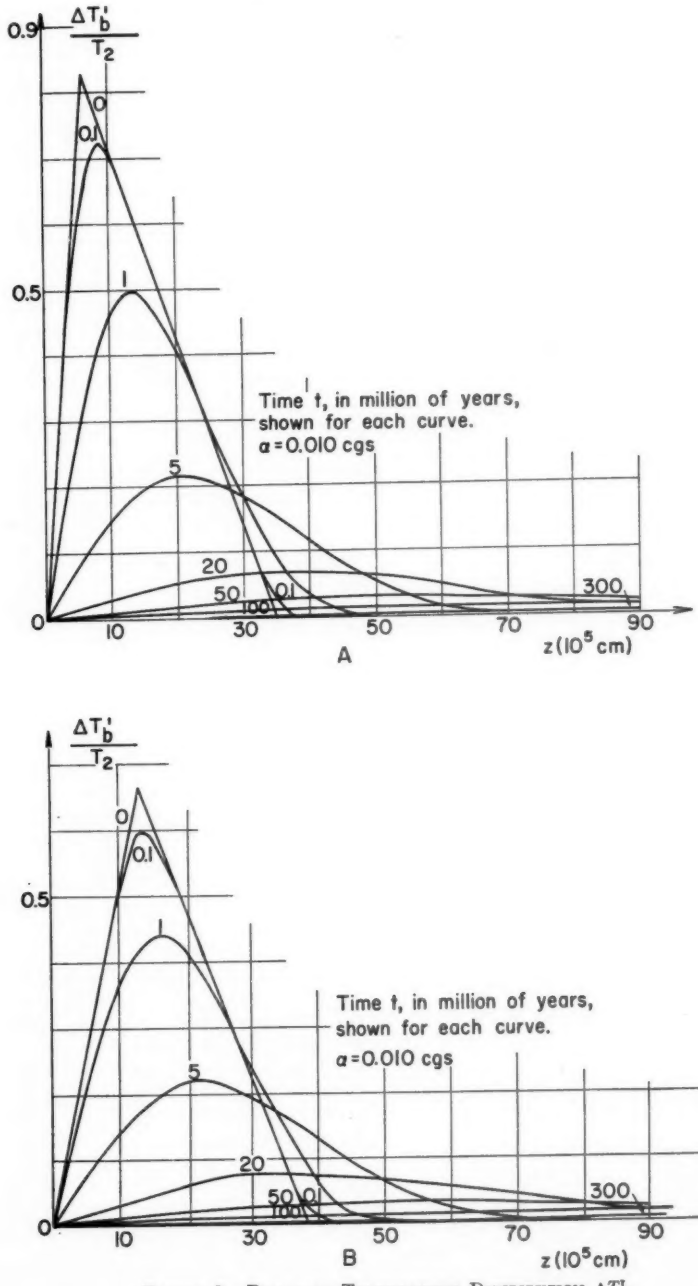


FIGURE 9.—DECAY OF TEMPERATURE DISTRIBUTION $\Delta T'_b$
In A, it initially extends from the surface down to 35 km; in B, it initially extends from the surface down to 38.5 km

Because of their relative proximity to the surface, the effect of the two upper slabs is felt rather rapidly at the surface. One million years is enough for the gradient at the surface to almost reach its steady-state value. In about $20 \times 10^6$ yr, the temperatures above these slabs have practically reached the steady state. Only after 1 million years is there any perceptible increase in the temperature at the depth of the base of the crust; even after $50 \times 10^6$ yr, this temperature is only half its steady-state value.

Because of the greater depth of the two lower slabs, it takes longer for their effect to be felt at the surface. About $5 \times 10^6$ yr are required for a detectable increase of the surface gradient. After about $20 \times 10^6$ yr, the gradient is practically uniform between the surface and the top of the slab. But even after $50 \times 10^6$ yr, it is only slightly more than half its steady-state value, and still after $300 \times 10^6$ yr, the deviation from the steady state is significant.

The components $\Delta T_b^{\mathrm{I}}$ and $\Delta T_b^{\mathrm{II}}$ of the deviation $\Delta T_b$ from the final steady state have been obtained. To determine the variation with respect to the initial state, one takes instead

$$\Delta T_B = |\Delta T_b(z, t)|_0^t = -\Delta T_b^{\mathrm{I}}(z, t) + \Delta T_b^{\mathrm{I}}(z, 0) + \Delta T_b^{\mathrm{II}}. \quad (46)$$

This variation is shown in Figure 13 for the subsidences of 6 and 13 km. It will be discussed hereafter.

*Discussion of Rapid-Subsidence Assumption*

The suitability of the rapid-subsidence model can be judged only if the order of magnitude of the subsidence velocity in actual geosynclines is known. The only direct indication of subsidence throughout geologic time at present is the thickness of sediments. Present-day rates of deposition are not suitable to estimate subsidence, because they are controlled by other factors besides rate of subsidence. For the Cenozoic—an era with a fairly complete record—the average rate of deposition has been estimated to be 0.67 km per million years (Schuchert, 1931, p. 44). Because of erosion, compaction, and periods of no deposition, this rate is likely to be smaller than the subsidence velocity. Present rates of subsidence in some geosynclines are larger than the figure mentioned. Kidwell and Hunt (1958) estimate that the average rate in Eastern Venezuela is 10 km per million years. Moore (1955) found that the present rate is 2.1 km per million years. The subsidence during one orogenic cycle is equal to at least twice the thickness of the sediments which is later found in the geosyncline. Thus, the subsidence velocity may be of the order of 1.3 km per million years. The subsidence of 6 km would require about 5 million years, and that of 13 km about 10 million years.

TABLE 2.—DIMENSIONS OF RADIOACTIVE SLABS

(In $10^5$ cm)

| Dimension | Subsidence of 6 km | Subsidence of 13 km |
|---|---|---|
| $h_0$, upper slab | 2 | 2 |
| $h$, upper slab | 8 | 15 |
| $H_0$, lower slab | 32 | 32 |
| $H$, lower slab | 38 | 45 |

The term $\alpha \partial^2 T/\partial z^2$ in the heat equation, equation 1, has been neglected in the consideration of the subsidence. The only change of temperature during rapid subsidence is produced by the displacement of the medium. The question is how large is the change due to diffusion, which occurs during the subsidence, in the initial steady state. This effect can be estimated by comparing it with the effect of diffusion upon the rapid-subsidence model after an interval of time equal to that required by the subsidence. In one case there is diffusion and subsidence, and in the other, first only subsidence and then only diffusion.

The surface perturbation is represented by the sum $(\Delta T^{\mathrm{I}} + \Delta T^{\mathrm{II}})$ in Figure 7. The surface gradient of $(\Delta T^{\mathrm{I}} + \Delta T^{\mathrm{II}})$ has lost 75 per cent of its initial value in 5 million years for the subsidence of 6 km and 62 per cent in 10 million years for the subsidence of 13 km. The times mentioned here are equal to the times required by the respective subsidences. The perturbations $(\Delta T^{\mathrm{I}} + \Delta T^{\mathrm{II}})$ for the subsidences of 6 and of 13 km, expressed in terms of $T_2$, become practically equal after 5 million years. These times are comparable to the times required by the subsidence. Thus, these two observations indicate that the surface gradient and the temperatures in the sedimentary layer given by the rapid-subsidence model are too low. But for the subsidence velocity considered herein, 1.3 km per million years, the discrepancy with respect to the rapid-subsidence model disappears in about 5 million years.

In the model in which the heat comes from the deep interior, because of the deformation of

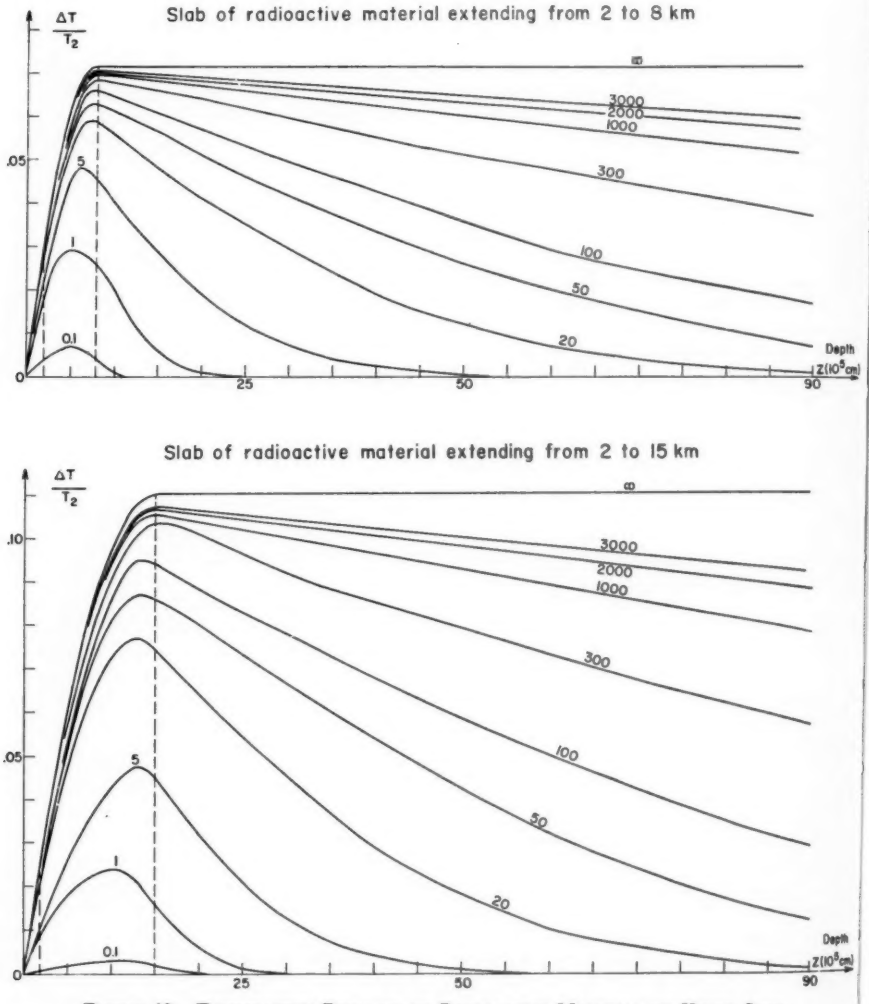


FIGURE 10.—TEMPERATURE BUILD-UP BY RADIOACTIVE MATERIAL OF UPPER SLAB
(Time interval after subsidence in $10^6$ years)

the substratum, $\partial^2 T/\partial z^2 \neq 0$ in the substratum. The adjustment of this perturbation is shown in Figure 8 for the subsidences of 6 and 13 km. This perturbation is practically unchanged in the zone of the substratum even after 5 and 10 million years for the 6- and 13-km subsidences, respectively. Hence there is no appreciable error here because of the assumption of rapid subsidence.

However, the effect of rapid subsidence in the lower part of the crust is yet to be considered. If the subsidence had taken place gradually, instead of instantaneously, the temperature rise in the lower part of the crust would have been smaller than shown in Figure 8. This is because the thermal gradient in the substratum builds up gradually during the subsidence. In Figure 8A, which corresponds to the 6-km subsidence, the area between the curves for $t = 5 \times 10^6$ yr and for $t = 0$ and which lies above the base of the crust is of interest. This area represents the heat conducted during 5

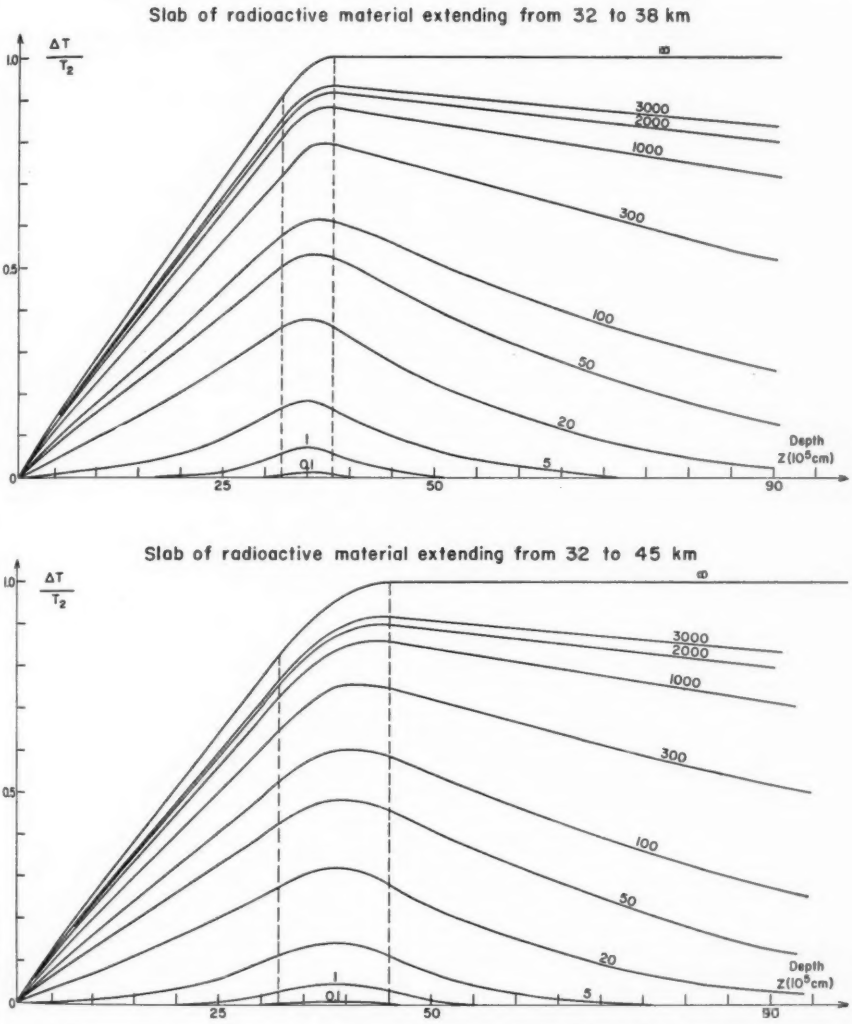


FIGURE 11.—TEMPERATURE BUILD-UP BY RADIOACTIVE MATERIAL OF LOWER SLAB
(Time interval after subsidence in $10^6$ years)

million years from the substratum into the crust. After 5 million years the heat escape at the surface is still negligible. It is easy to show, from equation 15, that the excess gradient increases proportionally to the subsidence. Thus, its average value is half its ultimate value. Accordingly, the area referred to would be at most equal to half what is shown in Figure 8. Allowing for this factor, the error is greatest at the base of the crust, but even there it is not serious. For a subsidence of 6 km occurring in 5 million years, the error on the temperature variation can be estimated to be less than 10 per cent of the ultimate temperature variation, and for the subsidence of 13 km occurring in 10 million years to be less than 12 per cent.

When the heat is generated in the crust, the surface perturbation $\Delta T_b^{\mathrm{I}}$ and the temperature build-up $\Delta T_b^{\mathrm{II}}$ produced by the additional radioactive slabs must be considered.

The peak value of $\Delta T_b^{\mathrm{I}}$ is reduced in about 5 and 10 million years to 26 and 24 per cent, respectively, of its initial value for the subsidences of 6 and 13 km, respectively (Fig. 9). Hence, this term cannot introduce too large an error even in the sedimentary layer, where it has its greatest value. As for $\Delta T_b^{\mathrm{II}}$, only the lower slab need be considered, since it can be assumed that $(q_1 - q_2) \ll q_2$. The temperature build-up produced by the lower slab is shown in Figure 11 for the subsidences of 6 and 13 km. In 5 and 10 million years, respectively, the disturbance has barely reached the surface. Hence, for the subsidence velocity considered, $\Delta T_b^{\mathrm{II}}$ is quite suitable as given by the rapid-subsidence model.

The rapid-subsidence assumption introduces practically no error in the substratum. In the lower part of the crust the maximum error is about 10 and about 12 per cent for the subsidences of 6 and 13 km, respectively. If the subsidence velocity were of the order of 1.3 km per million years, the rapid-subsidence model would give too low temperatures in the sedimentary layer for the first 5 million years. But after a time equal to that required for the subsidence, the rapid-subsidence model becomes more and more suitable. The finite subsidence velocity introduces an uncertainty in the time origin of the rapid-subsidence model. For the study of events which occur long after subsidence, the instantaneous assumption is adequate. Moreover, its effect is always unimportant in the lower part of the crust and substratum.

### *Temperature Variations after Subsidence of a Geosyncline*

To determine the temperature variations produced by subsidence, two different models have been investigated. In model 1 the heat comes from the deep interior; in model 2, the heat is generated in the earth's crust.

Numerical calculations were performed for two cases; namely, when the subsidence is 6 and 13 km. The results for the hypothesis that the heat comes from the deep interior are shown in Figure 12, and for the hypothesis that it is generated in the crust, in Figure 13.

A number of general observations can be made about these temperature variations after a subsidence. The temperature increases much more rapidly in the sediments than in the lower part of the crust. For instance, the temperature variations in the new layer of sediments, for the subsidence of 6 km, have reached 74 per cent of their ultimate values after 5 million years in both models, whereas at the base of the crust they have reached only 15 and 3 per cent in models 1 and 2, respectively. A similar observation can be made for the 13-km subsidence. When the heat comes from the deep interior, there is, for a certain length of time, a zone of cooling in the substratum. For instance, after 20 million years the cooling at 90 km is about 0.08 $T_1$. After about 20 million years, the deviation from the final equilibrium condition in the crust is a reasonably linear function of the depth. For large times, the deviation varies as $t^{-3/2}$ when the heat comes from the interior and as $t^{-1}$ when it is generated in the crust.

In general, the results for the two hypotheses about the origin of the heat are similar. In the sedimentary layer and upper part of the crust, they are practically the same up to about 5 million years. But afterward the temperature increases more rapidly when the heat comes from the deep interior. The rates of increase differ more in the lower part of the crust. The temperature increases more rapidly in the model in which the heat comes from the deep interior. The contrast is even greater in the substratum.

The evolution of the temperature profiles which exist at any time after the subsidence is illustrated for the two models in Figure 14. The rapid subsidence and sedimentation sets a perturbation at the level of the original surface and another which extends into the substratum from the base of the crust. When the heat is generated in the crust and the subsidence is instantaneous, only the first of these perturbations has to be considered. The subsequent evolution of the temperature profile can be described as a gradual adjustment of this perturbation. The temperature adjustment progresses gradually from the presubsidence surface downward. When the heat comes from the deep interior, both perturbations are present, and the temperature increases more rapidly, particularly in the lower part of the crust. The times required for the adjustment of the temperature profile are large enough to be of significance in geological processes.

The increases of the temperature with time at the base of the sedimentary layer and at the base of the crust are shown in Figure 15 for the subsidences of 6 and 13 km. The continuous-line curves correspond to heat generated in the crust, and the broken-line curves to heat coming from the deep interior. Since heat may be

derived from both these sources, the actual curves may lie between these two curves.

An important feature of these curves is the large and rapid increase of temperature which takes place during the first 20 million years or so. Thereafter, the temperature increases at a much smaller rate. A similar observation is valid for any intermediate depth in the crust. The sharp bend in the temperature curves is more apparent in the case of heat generated in the crust and for the smaller subsidence.

The conditions represented by the continuous-line curves of Figure 15A, which correspond to the subsidence of 6 km and to the heat being generated in the crust, are probably nearer to the actual conditions in a geosyncline than for the other cases considered here.

The actual values in degrees centigrade of the temperature increase are obtained by multiplying the relative variations, shown in Figures 12 and 13, by the factor $T_1$ or $T_2$, as the case may be. If all the heat reaching the earth's surface is derived from the radioactivity of the crust, only $T_2$, which is given by equation 22, is needed. The quantities which enter in this formula are taken as: $q = 4 \times 10^{-13}$ cal cm$^{-3}$ sec$^{-1}$, $H = 32 \times 10^5$ cm, $k = 0.006$ cgs, and $s = 6 \times 10^5$ cm. The values thus obtained for $T_2$ are indicated in the first line of Table 3.

The solution obtained for the temperature variations after subsidence is based on the assumption that the thermal conductivity is constant. However, it decreases with the temperature. If this decrease were taken into account, the temperature variations would be greater than those obtained. Assuming $k = 0.008\ T_0/T$ cgs, where $T_0 = 290$°K., I have calculated the ultimate temperature at the base of the crust (Grossling, 1951, PhD thesis, London Univ.). The temperature increases which result for subsidences of 6 and 13 km are shown in the second line of Table 3. Clearly, the decrease of conductivity with temperature leads to much greater temperature variations than would be the case if the conductivity were constant and equal to that of the surface rocks. However, in both cases the temperature variations are geologically significant.

## Significance of Temperature Variations

### *Significance for Lithification*

The sediments of a geosyncline gradually become lithified as a result of burial. This lithification depends mainly on the temperature and on the confining and differential stresses. Although it is not completely understood how the temperature affects the lithification, some experimental evidence indicates the importance of the temperature. Fairbairn (1950) found that the strength of quartz and quartzite decreases markedly at 150°–315°C. Maxwell and Verrall (1954) showed experimentally that in sands the degree of grain shattering and orientation and the degree of cementation increase with the temperature. Their results suggest that certain temperature thresholds exist below which cementation does not occur.

As for the effect of the stresses, if the sediments accumulate on a horizontal subsiding basement and the deformation in the horizontal direction is zero, one of the principal stresses is vertical, and the other two are horizontal. The state of stress on a small cube of sediments can be resolved in a hydrostatic stress plus a deviatoric stress. The normal force acting on a small plane interface is partly taken by the solid matrix of the sediment and partly by the interstitial fluid. The load on the solid matrix, when expressed as normal stress over the total area of the interface, is called contact effective stress. This is the stress directly responsible for the compression of the solid matrix. The part of the hydrostatic stress taken up by the solid matrix may be called confining stress. Obviously, the entire tangential stresses are supported by the solid matrix.

Most of the compaction of a sediment occurs at shallow depths and consists of compression of the grain matrix and squeezing out of the interstitial fluids. This stage usually extends in the pressure range from 0 to about 300 psi. Because of viscous fluid-flow resistances, the fluid pressure is greater than the hydrostatic fluid pressure corresponding to the height of the fluid column. As the compaction progresses, the excess pressure is gradually transferred to the solid matrix.

For this kind of consolidation, in a one-dimensional system, Terzaghi (1925) established the equation

$$\frac{\partial e}{\partial t} = C\frac{\partial^2 e}{\partial z^2}, \tag{47}$$

where $e$ = void ratio = volume of voids/volume of solids, and $C$ = consolidation coefficient. In mathematical sense, this equation is the same as the one-dimensional heat-flow equation (equation 38). Furthermore, the coefficients in these two equations have the same dimenssoni, namely $L^2T^{-1}$. Hence, if the dimensions and boundary conditions are the same, the

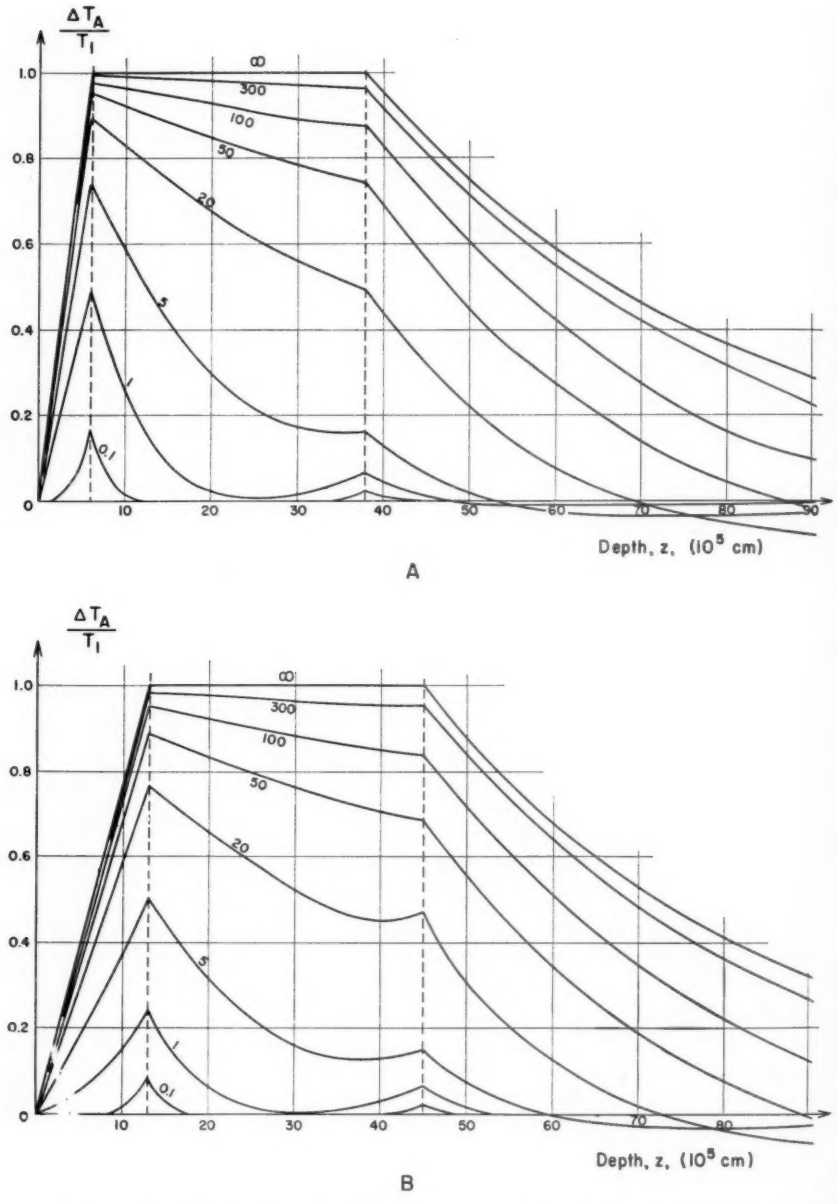


FIGURE 12.—TEMPERATURE INCREASE AFTER RAPID SUBSIDENCE AND SEDIMENTATION WHEN THE HEAT COMES FROM THE EARTH'S DEEP INTERIOR

A, for a subsidence of 6 km; B, for a subsidence of 13 km. Thickness of crust is equal to 30 km, initial thickness of sediments is equal to 2 km. Deformation of substratum assumed to decrease to one-tenth at 100 km below the crust. Time intervals after subsidence in $10^6$ years. Ultimate temperature in the crust taken as unity.

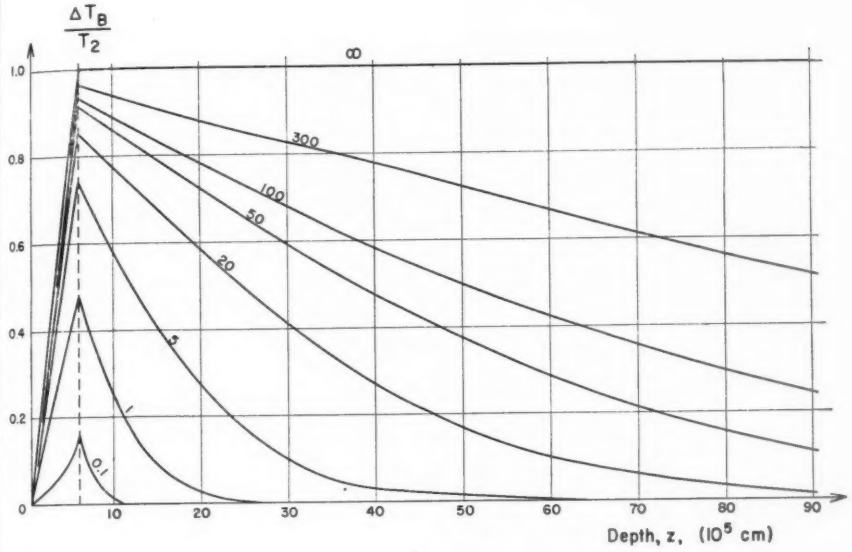


A

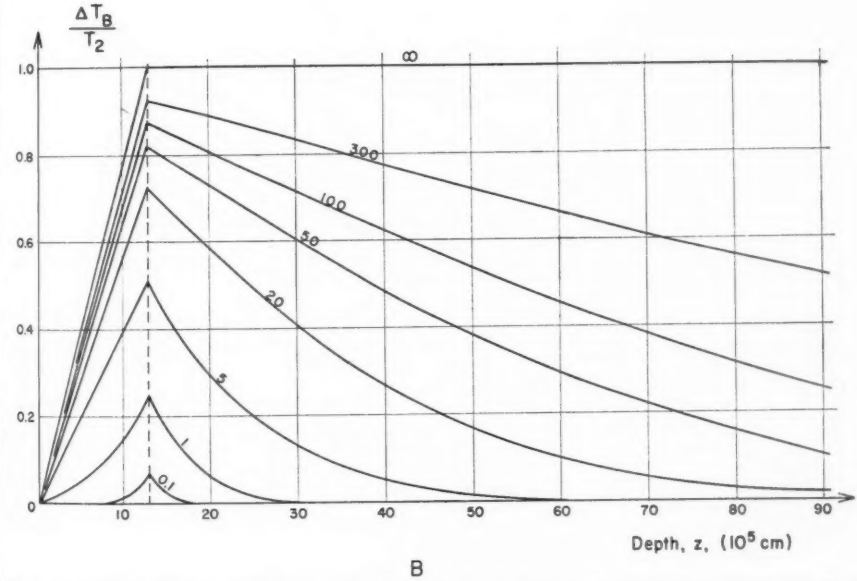


B

FIGURE 13.—TEMPERATURE INCREASE AFTER RAPID SUBSIDENCE AND SEDIMENTATION WHEN THE HEAT IS PRODUCED BY THE RADIOACTIVITY OF THE CRUST AND SEDIMENTARY LAYER

A, for a subsidence of 6 km; B, for a subsidence of 13 km. Thickness of crust is equal to 30 km, initial thickness of sediments is equal to 2 km, $q_1 = q_2$. Time intervals after subsidence in $10^6$ years. Ultimate temperature increase in the crust taken as unity.

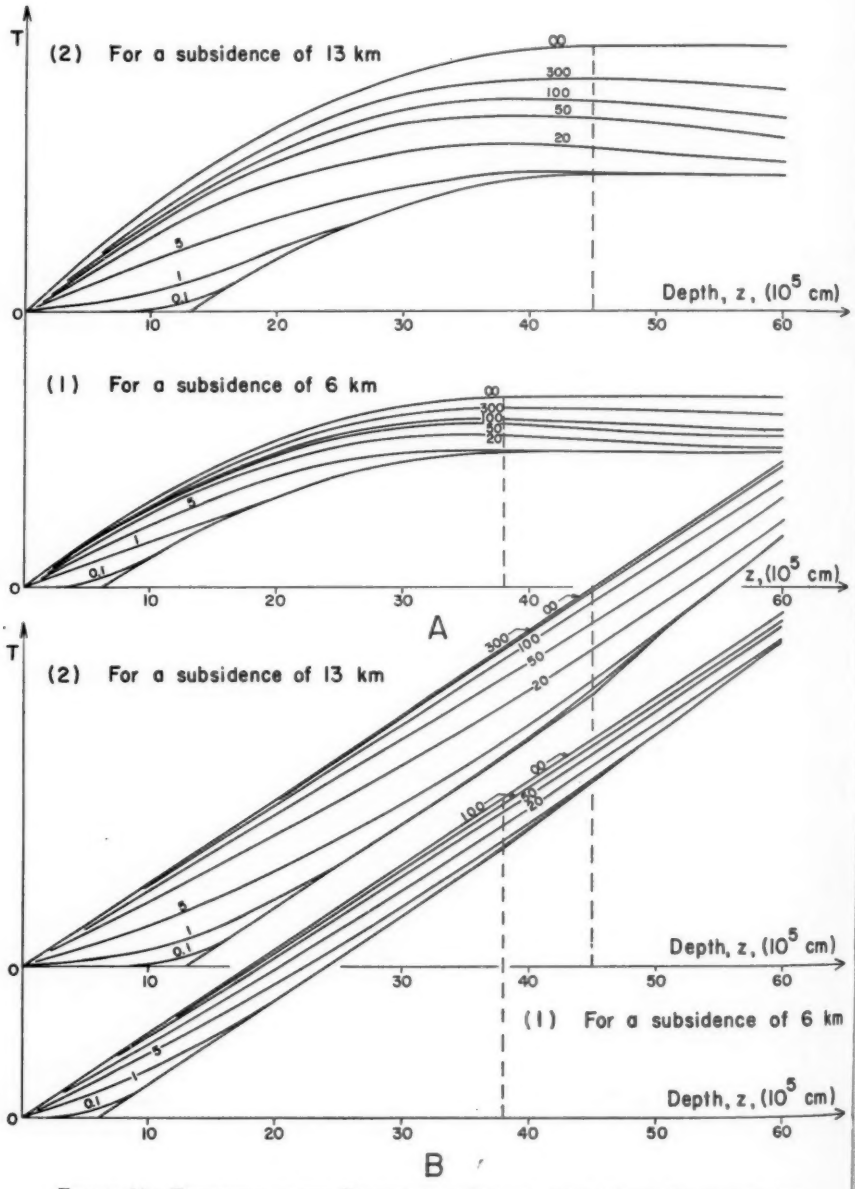


FIGURE 14.—EVOLUTION OF THE TEMPERATURE PROFILE AFTER RAPID SUBSIDENCE AND SEDIMENTATION

In A, the heat is produced by the radioactivity of the crust and sediments; in B, the heat comes from the earth's deep interior.

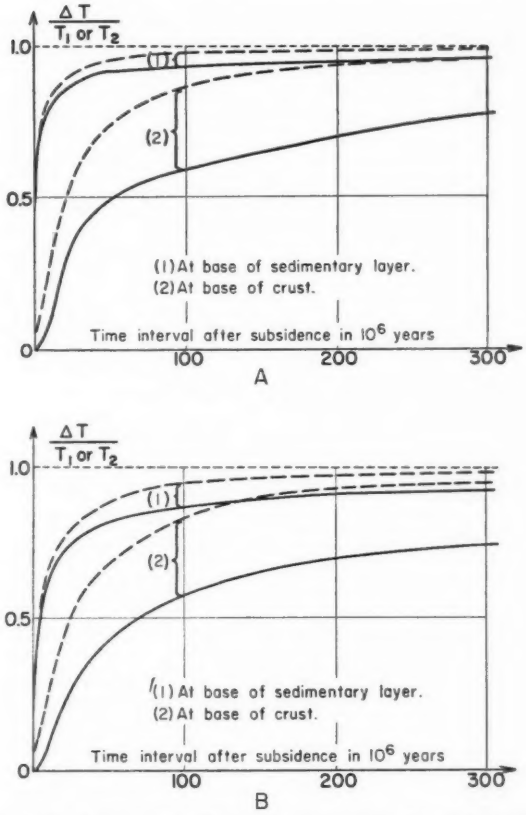


FIGURE 15.—INCREASE OF TEMPERATURE AFTER A RAPID SUBSIDENCE

A, for a subsidence of 6 km; B, for a subsidence of 13 km. Continuous-line curves correspond to heat generated in the crust, and broken-line curves to heat coming from the deep interior.

TABLE 3.—ULTIMATE TEMPERATURE INCREASE $T_2$ AT BASE OF CRUST

| | For subsidence $6 \times 10^5$ cm | For subsidence $13 \times 10^5$ cm |
|---|---|---|
| $k = 0.006$ cgs | 140°C | 333°C |
| $k = 0.008 \frac{T_0}{T}$ cgs | 289°C | 907°C |

relative rates of change in the two processes depend on the relative value of these coefficients. For ordinary sediments, the consolidation coefficient is of the order of (2-10) $\times$ $10^{-4}$ cm$^2$ sec$^{-1}$, whereas the thermal diffusivity is of the order of $10^{-2}$cm$^2$ sec$^{-1}$. Hence, up to depths of a few hundred feet, the adjustment of the stresses lags behind the adjustment of the temperature, so that the progress of the consolidation depends on the adjustment of these stresses.

When the mere squeezing of the fluids has been nearly completed, the fluid pressure affects the subsequent compaction very little (Taylor and Merchant, 1940). Thereafter the grains begin to bend, crush, and shear. Resistance to further volume compression is provided mainly by the solid matrix. This stage may extend to about 6000 psi. At larger pressures, a number of other things occur: melting at grain contacts, solidification at unstressed parts, stress-induced solution, and recrystallization. Hence, below

depths of a few hundred feet, the lag in the adjustment of the confining stress is negligible.

Both the stresses and the temperature of a certain portion of sediment increase with the subsidence. Below a few hundred feet the solid matrix is constantly subject to confining stresses

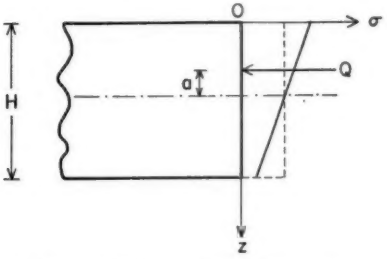


FIGURE 16.—STRESS DISTRIBUTION IN THE CRUST PRODUCED BY A COMPRESSIONAL FORCE $Q$

which correspond to the current depth. On the other hand, this investigation shows that the lag in the adjustment of the temperature is appreciable. Thus, the lithification may not be completed, at certain depths, because the temperature is still too far below its steady value. This seems to be corroborated by the existence of soft sediments at relatively great depths in basins such as the Gulf Coast.

This paper has shown that in the sedimentary layer, 70–80 per cent of the ultimate temperature increase occurs within the first 15 million years after the subsidence. It seems likely, therefore, that lithification is completed during that time interval.

### *Significance for Evolution of Geosynclines*

A geosyncline begins by subsidence of the earth's crust along an elongated trough. Some time later comes a period of increased compression. This is the folding stage, in which the sediments and the crust are folded or fractured, or both. During this stage, probably no true rupture of the crustal material occurs, but rather the rate of shearing of the crustal rocks increases markedly. Under differential stresses, the crustal rocks can flow continuously, although at a very small rate. This flow can be described in terms of a solid viscosity. Whatever the ultimate cause of the crustal compression, the forces responsible for it work against the compressional strength of the crust. Therefore, crustal strength must be a relevant factor in the evolution of a geosyncline.

Of particular interest is whether the position of the lower boundary of the crust, the Mohorovičič discontinuity, depends on the temperature. The crustal viscosity appears to decrease markedly at the depth where the temperature reaches a certain value. The value of this temperature is not needed herein; it is sufficient to assume that it is the temperature at the base of an undisturbed crust.

The solid viscosity of the crustal material is assumed to decrease when the temperature reaches the value it has at the base of an undisturbed crust. In consequence, the compressional strength of the crust will vary as the thickness of the crust which is at temperature smaller than that value. The temperature increase, which occurs after the subsidence, progressively reduces the crustal strength by decreasing the crustal thickness.

At the start, there is assumed to be a homogeneous and isotropic crust, of constant thickness, parallel to the geoid, and under no tectonic stress. Thus, one of the principal stresses is vertical and the other two are equal and horizontal. These stresses are assumed to vary linearly with depth. Whether the vertical stress is the maximum or the minimum or whether the three are equal depends on how the system came into being and also on the long-time strength of the crustal materials. If this stress system has acted for a long time, then the absolute values of the three stress differences are equal to or smaller than twice the yield shear stress. Tresca's maximum-shear yield criterion has been assumed for simplicity.

It is assumed now that a tectonic force, $Q$, per unit length is applied in the $x$ direction (Fig. 16). If the part of the crust subject to this force is a long belt, such as a geosyncline, there is no strain relief in the direction of the long axis of the belt. For the tectonic force $Q$ to produce plastic deformation in planes perpendicular to the axis, the difference of principal stresses in this plane must be equal or larger than twice the yield shear stress.

Smoluchowski (1909) has shown that the crust cannot be buckled elastically, because the buckling compressional stress is much larger than the elastic limit. When the maximum differential stress equals the yield limit, the crust thickens plastically. Vening-Meinesz and Heiskanen (1958, p. 326–343), following Bijlaard (1935; 1936), show that the crust buckles as a result.

It will be supposed that a part of the crust has begun to downbuckle; therefore, the tectonic force $Q$ is applied above the middle plane of the crust, as shown in Figure 16. Such a force is equivalent to a force of magnitude $Q$ acting

on the middle plane, plus a bending moment $Qa$. The stresses produced by the bending moment contribute to accentuate the bending of the crust, whereas the force on the middle plane merely thickens the crust without bending. The bending stress $\sigma$ at depth $z$ is

$$\sigma = \frac{12Qa(H/2 - z)}{EH^3}, \qquad (48)$$

where $E$ = Young's modulus and the other symbols designate the quantities shown in Figure 16. The deformation rate $\dot{\epsilon}_z$ is

$$\dot{\epsilon}_z = \frac{\sigma}{2\eta} = \frac{6Qa(H/2 - z)}{E\eta H^3}, \qquad (49)$$

where $\eta$ is the solid viscosity. The rate of the relative angular rotation, $\dot{\gamma}$, of two sections a unit distance apart is

$$\dot{\gamma} = \frac{6Qa}{E\eta H^3}. \qquad (50)$$

The progressive decrease of crustal strength, assuming that the strength varies as the inverse power of the thickness, is shown in Figure 17 for the subsidences of 6 and 13 km and for the two hypotheses about the nature of the heat. The several curves of variation of the crustal strength with time exhibit, at a certain time, well-defined bends. The strength decreases relatively quickly up to about 20 million years and thereafter much more slowly. This observation is valid whether the heat comes from the deep interior or is generated in the crust. But the bend is more pronounced if the heat is generated in the crust. Moreover, the bends would be even more pronounced if the relative rate of angular rotation $\dot{\gamma}$ (equation 50) had been considered. This varies with the inverse third power of the thickness.

Another thermal effect of the subsidence which may affect the evolution of a geosyncline

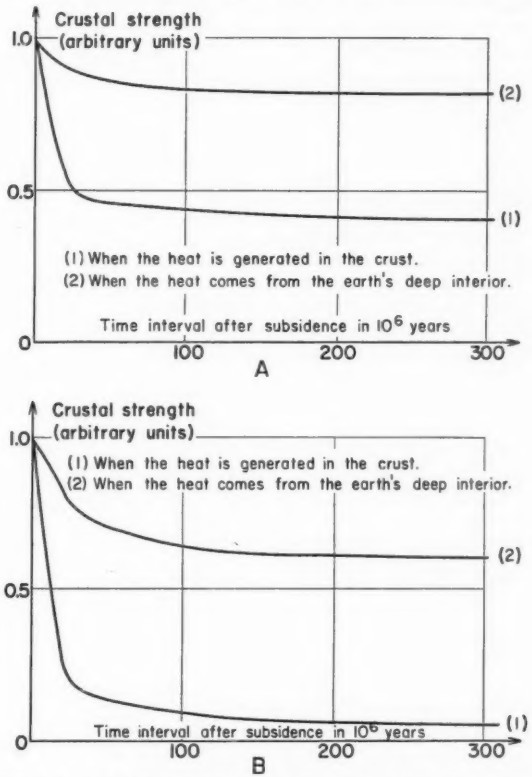


FIGURE 17.—VARIATION OF THE CRUSTAL STRENGTH BECAUSE OF THE INCREASE OF TEMPERATURE WHICH FOLLOWS A RAPID SUBSIDENCE
A, for a subsidence of 6 km; B, for a subsidence of 13 km

is the temporary cooling of the substratum if the heat comes from the deep interior. During the subsidence, a given layer is displaced to greater depths, practically maintaining its temperature. Thereafter, its temperature actually decreases for a certain length of time because it conducts more heat to shallower layers than it receives from deeper ones. This zone of cooling in the substratum may effectively lock, for a certain time, the subsequent uplift of the crust.

## Conclusions

Subsidence and sedimentation produce important temperature variations in the earth's outer layers. Similar results are obtained for the two hypotheses as to the origin of the heat: (1) heat comes from the deep interior, and (2) heat is generated in the crust. The variations are practically the same up to about 5 million years in the sedimentary layer and upper part of the crust. After about 5 million years, the increase becomes more rapid when the heat comes from the deep interior. But in the lower part of the crust, when the heat comes from the deep interior, the temperatures are built up more rapidly from the beginning. During the first 20 million years or so, the temperature increases rapidly; thereafter the rate of increase is much smaller. For large times, the deviation from the steady state is a linear function of the depth and varies as $t^{-3/2}$ if the heat comes from the deep interior and as $t^{-1}$ if it is generated in the crust.

The times required for the adjustment of the temperature are large enough to be of significance in geological processes. Thus, the temperature variations here determined should interest other investigators.

The gradual increase of temperature after subsidence should affect the lithification of the sediments and should decrease the crustal strength. Lithification is likely to be completed within the first 15 million years after the subsidence. The crustal strength decreases relatively quickly up to about 20 million years and thereafter much more slowly. This decrease of crustal strength after the subsiding stage in the evolution of a geosyncline may control the time at which the folding stage begins, thus acting as a trigger effect. The folding stage would take place 15–20 million years after the subsidence. When heat comes from the deep interior, the temperature in the substratum below a certain depth, which varies with the temperature, actually decreases for a time. This cooling may retard the subsequent uplift of the geosyncline by increasing the solid viscosity of the substratum.

## References Cited


Benfield, A. E., 1949, The effect of uplift and denudation on underground temperatures: Jour. Appl. Physics, v. 20, p. 66–70

Bijlaard, P. P., 1935, Beschouwingen over de Knikzekerheid en de plastische vervormingen van de aardkorst in verband met de geologie van de Indische Archipel: Ingr. Nedert.-Indie, v. 11, p. 135–156

—— 1936, Théorie des deformations plastiques et locales par rapport aux anomalies négatives de la gravité, aux fosses océaniques, aux géosynclinaux, au volcanisme, à l'orogénie et à la géologie de l'Océan Pacifique Occidental: Assoc. Internat Geologie v. Trav., 13, no. 12, 23 p.

Birch, Francis, 1950, Flow of heat in the Front Range, Colorado: Geol. Soc. America Bull., v. 61, p. 567–630

Bullard, E. C., 1938, The disturbance of the temperature gradient in the earth's crust by inequalities of height: Royal Astron. Soc. Monthly Notices, Geophys. Supp., v. 4, p. 360–362

Carslaw, H. S., and Jaeger, J. C., 1948, Conduction of heat in solids: Oxford Univ. Press, 386 p.

Coster, H. P., 1947, Terrestrial heat flow in Persia: Royal Astron. Soc. Monthly Notices, Geophys. Supp., v. 5, p. 131–145

Fairbairn, H. W., 1950, Synthetic quartzite: Am. Mineralogist, v. 35, p. 735–748

Gutenberg, Beno, 1951, Internal constitution of the earth: N. Y., Dover Publications, Inc., 439 p.

Hartree, D. R., 1935, Properties and applications of the repeated integrals of the error function: Manchester Philos. Soc., Mem. 80, p. 85–102

Jeffreys, Harold, 1931, The thermal effects of blanketing by sediments: Royal Astron. Soc. Monthly Notices, Geophys. Supp., v. 2, p. 323–329

—— 1938, The disturbance of the temperature gradient in the earth's crust by inequalities in height: Royal Astron. Soc. Monthly Notices, Geophys. Supp., v. 4, p. 309–312

Kidwell, A. L., and Hunt, J. M., 1958, Migration of oil in recent sediments of Pedernales, Venezuela, p. 790–817 *in* Weeks, L. G., *Editor*, Habitat of oil: Am. Assoc. Petroleum Geologists, 1384 p.

Maxwell, J. C., and Verrall, Peter, 1954, Low porosity may limit oil in deep sands: World Oil, v. 138, no. 5, p. 106–113; v. 138, no. 6, p. 102–104

Moore, D. G., 1955, Rate of deposition shown by relative abundance of foraminifera: Am. Assoc. Petroleum Geologists Bull., v. 39, p. 1594–1600

Schuchert, C., 1931, Geochronology, or the age of the earth on the basis of sediments and life: Natl. Research Council Bull. no. 80, p. 10–64

Smoluchowski, M., 1909, Versuche über Faltungsercheinungen schwimmender elasticher Platten: Anz. d. Akad. d. W. Krakaw, Math.-naturw. Kl., v. 2, p. 3ff

Taylor, D. W., and Merchant, J. C., 1940, A theory of clay consolidation accounting for secondary compressions: Jour. Math. and Physics, 19, p. 167–185

Terzaghi, Karl, 1925, Erdbaumechanik: Vienna, Deuticke, 399 p.

Vening-Meinesz, F. A., and Heiskanen, W. A., 1958, The earth and its gravity field: N. Y., McGraw-Hill Book Co., Inc., 470 p.

THE CALIFORNIA RESEARCH CORPORATION, LA HABRA, CALIF.

MANUSCRIPT RECEIVED BY THE SECRETARY OF THE SOCIETY, FEBRUARY 6, 1958

BULLETIN OF THE GEOLOGICAL SOCIETY OF AMERICA
VOL. 70, PP. 1283–1292, 1 PL. OCTOBER 1959

# INSPISSATION OF POST-OLIGOCENE SEDIMENTS IN SOUTHERN LOUISIANA

BY ROBERT W. CROUCH

## ABSTRACT

The aggregate thickness between stratigraphic markers of post-Oligocene sediments in southern Louisiana, established from records of several thousand wells, is at least 62,000 feet.

The sediments along the Texas-Louisiana coast accumulated rapidly in rim synclines and in an area of "hinge-line" faults. Composite thicknesses are as follows: Miocene, 48,000 feet; Pliocene, 6000 feet; Pleistocene (including Recent and modern), 8000 feet. An additional 7100 feet of sediment is present in areas where no basal markers were found.

Because the unconsolidated beds in southern Louisiana reflect poorly, the geophysical data give an erroneous regional picture. Foraminiferal data and electric-log correlations together can give an adequate regional interpretation.

No valid evidence supporting the suggested regional reversal of dip or regional thinning of section can be found in any of the deep wells drilled in southern Louisiana. In spite of this, most workers in the area believe that a geosyncline of some type exists. No single center of deposition for post-Oligocene sediments can be established in a given geographic position. Each geologic subdivision possesses its own depositional axis at some unknown geographic point offshore.

## CONTENTS

### TEXT

| | Page |
|---|---|
| Introduction | 1283 |
| Acknowledgments | 1284 |
| Previous work | 1284 |
| Stratigraphy | 1284 |
| Miocene | 1285 |
| Lower Miocene | 1285 |
| Middle Miocene | 1285 |
| Upper Miocene | 1286 |
| Pliocene | 1286 |
| Pleistocene | 1286 |
| Total inspissation | 1288 |
| Geophysics | 1288 |
| Regional paleontology | 1289 |
| Gulf Coast geosyncline | 1290 |
| Conclusions | 1291 |
| References cited | 1291 |

### ILLUSTRATIONS

| Plate | Facing page |
|---|---|
| 1. Contour map of southern Louisiana and offshore area | 1292 |

### TABLE

| Table | Page |
|---|---|
| 1. Post-Oligocene inspissation table | 1287 |

## INTRODUCTION

A tremendous thickness of post-Oligocene sediments has been deposited in the southern Louisiana area. The total thickness of the Miocene sediments may exceed that of any geologic period. The aggregate thickness was derived by piecing together stratigraphic data from wells that penetrated the thickest sections known between each set of foraminiferal markers. This method does not give the absolute maximum inspissation, as the thickening continues down-dip beyond the range of controlled study. There is no valid evidence of a regional reversal of dip or of a regional thinning of section in any of the deep wells drilled in southern Louisiana. Paleontologic information from several thousand wells has been considered in this report. Most of the specific data from individual wells have been omitted because the petroleum companies wish to restrict them. However, sufficient information from restricted wells can be cited to demonstrate the great thickness of post-Oligocene sediments and the rapidity with which they were deposited.

## Acknowledgments

The author wishes to thank T. W. Campbell, A. D. Ellis Jr., and C. W. Stuckey for making available many data on wells in critical areas. Grateful acknowledgment is made to T. M. Burke and O. R. Gammon for advice on the geophysical aspects of this paper. Special thanks go to S. L. Mason, who read the manuscript while it was in preparation. The writer is indebted to J. B. Garrett and M. L. Natland, the critical readers.

## Previous Work

Barton, Ritz, and Hickey (1933) first suggested that a geosyncline lies along the Gulf Coast of Louisiana and Texas and that a regional trough of gravity minimum lies axially along the Gulf Coast. They interpreted the trough as a geosyncline on the basement; they believed that the basement changes progressively from granitic under land to basaltic under the Gulf of Mexico. They also stated that more than 30,000 feet of section is present south of New Orleans. Fisk (1944) in a north-south cross section (Plate 33) shows a Pliocene-Miocene depositional axis in the Gulf Coast geosyncline passing near Houma, Louisiana, with reversal of dip in that vicinity. He established the top of the Miocene on the basis of the mollusk *Rangia microjohnsoni* and the top of the lower Miocene on the basis of the *Heterostegina* zone. Carsey (1950, Fig. 2) shows a north-south cross section from Washington Parish south to Grand Isle off Plaquemines Parish, Louisiana. He assigned 30,000 feet of sediment to the Tertiary; of this he assigned approximately 15,000 feet to undifferentiated Pliocene and Miocene. The gravity data suggest that the deepest part of the Gulf Coast geosyncline is just inland from the Louisiana coast. Weaver (1951, p. 395) postulates that more than 20,000 feet of Tertiary sediment lie off the Louisiana coast. He states that no regional thinning of the Tertiary has been demonstrated to a depth of 14,000 feet along the Louisiana coast. He believes that with greater distance from the shore lines, formations should thin for lack of material available for sedimentation. Formations, therefore, should thin farther out on the Continental Shelf. Murray (1952) believes the Gulf Coast geosyncline (Miocene to Recent) axis intersects Plaquemines Parish on the east about 5 miles north of Potash Field (Pl. 1), extends westerly to near Lake Hermitage, passes slightly south of Houma in Terrebonne Parish, and crosses the western boundary of Terrebonne Parish near the mouth of the Atchafalaya River. From this point he believes it continues offshore on the same course until it intersects the present shore line at Galveston, Texas. He also shows (1952, Table 5) the rate of sedimentation in the submerged part of the central Gulf Coastal Plain. Murray assigns the Tertiary sediments a thickness of 26,700 feet and the Neogene (Miocene to Recent) a maximum thickness of 15,900 feet. He also states (1952, p. 1188) that offshore drilling proves that Miocene sediments exist at a depth of 13,000 feet. The wells do not show any thinning or upturning of strata for at least 30 miles offshore. His studies would show that sediments accumulated in "depocenters" (areas of maximum thickness) up to a maximum of about 3000 feet. The centers then shifted to a new area of deposition. These "depocenters" are not known to occur vertically above the older ones. Nettleton (1952, p. 1228) concludes that geophysical methods indicate that the regional dip in the Gulf Coast of Texas and Louisiana extends to the coast line without any synclinal axis at or immediately beyond the coast. The thickest sediments at the coast line are about 40,000 feet thick. Stuckey (1953, p. 29) notes that a 5000-foot Miocene section in the vicinity of Houston, Texas, thickens to about 20,000 feet in the Mississippi Delta region. He further states that "... the rate of seaward thickening in the Miocene of Louisiana is noteworthy". This thickening is depicted on his delta cross-section chart. Stuckey (Personal communication) states that the wells in the delta section were selected for geographic position rather than for maximum thickness, and because of this much of the stratigraphic section is not pictured. In recent years many workers have speculated that the post-Oligocene sediments in the Gulf Coast range in thickness from 15,000 to 30,000 feet.

## Stratigraphy

The great thicknesses of sediment are believed to have been deposited rapidly (1) in areas of salt withdrawal or rim synclines, and (2) on the downthrown side of regional faults commonly called "hinge-line faults" by geologists in the coastal area. These faults are downthrown to the south. Some have a throw of nearly 5000 feet and can be traced laterally, at least as zones, for about 100 miles. These faults are believed to be caused by sedimentary

overload and are loci of accelerated seaward thickening.

It is not possible to establish a subsurface stratigraphic type section based solely on lithology for Miocene units in Louisiana because the lithology changes abruptly along the depositional strike, and new sedimentary units appear down-dip. The down-dip wedges are not recognizable in the updip section.

The maximum thickness of post-Oligocene sediments was established by piecing together the thickest sections between reliable foraminiferal zones. The foraminiferal nomenclature used in this report was taken from Akers (1954) and from the New Orleans Geological Society (1954). Unfortunately in some instances the generic and specific names from which the zones have been named are incorrect.

Topotype specimens of *Bigenerina floridana* Cushman from the Florida Miocene were loaned to the author by Mr. A. D. Ellis, Jr. The forms referred to as *B. floridana* in this report from the Louisiana Miocene do not conform to the topotype specimens. *Spiroplectammina barrowi* Cushman and Ellisor is not synonymous with the forms commonly referred to as *S. barrowi* in this report. This discrepancy was pointed out to the author by Mr. J. B. Garrett, who showed the author topotype specimens from a well core from which the species was described. The interval from which the species is described is identical with the *Bigenerina directa* zone. Two zones, the *Robulus* "43" and the Amphistegina "B", are based upon undescribed species.

The Miocene is subdivided herein for convenience into an upper part, a middle part, and a lower part of the lower, middle, and upper Miocene, although this may not agree with other published reports.

## Miocene

### *Lower Miocene*

The greatest thickness of lower Miocene sediments is in Cameron and Vermilion parishes. The lower Miocene aggregate section approximates 15,000 feet. The top of the lower Miocene is marked by the appearance of *Robulus* "43" or *Amphistegina* "B" zones. Information about this part of the Miocene is most incomplete because of the lack of deep wells (17,000 + feet). The greatest thickness recorded for the upper part of the lower Miocene comes from a well drilled in the vicinity of Fresh Water Bayou, Vermilion Parish, where about 3500 feet of section was noted. The middle part of the lower Miocene is marked by the appearance of the *Discorbis bolivarensis* zone. About 4500 feet of section is represented in a well drilled in block 40, West Cameron area (Pl. 1), offshore from Cameron Parish. *Siphonina davisi* marks the top of the lower part of the lower Miocene. The thickest section (7000 feet) between *S. davisi* and the *Heterostegina* sp.-*Bolivina perca* zones is in the vicinity of Second Bayou, Cameron Parish.

### *Middle Miocene*

The top of the middle Miocene is established by the first occurrence of the *Bigenerina directa* zone. About 15,500 feet of sediments have been dated as middle Miocene. Actually 20,500 feet were penetrated in drilling operations; however, the basal foraminiferal markers were not encountered, as the wells were not drilled deep enough.

Northeast of the Lake Washington area is a thick section between the *Bigenerina directa* and *Bigenerina humblei* zones. In several deep wells as much as 7000 feet of section has been recorded. A thicker section must exist nearby, because nearly 8000 feet were drilled without penetrating the *Bigenerina humblei* zone. Crouch (1955) pointed out that *Bigenerina humblei* is a particularly good time indicator, because this species lived in almost all marine environments from near shore to the deepest recognizable paleoecologic zones and died out in all the ecologic zones at approximately the same time. It is concluded, therefore, that *B. humblei* was not encountered because wells drilled were not sufficiently deep.

Near Bourg, Terrebonne Parish, the *Bigenerina humblei* zone contributes 5500 feet of section to the middle Miocene before the *Cibicides opimus* zone is encountered. At Hollywood, southwest of Bourg, an even thicker section is present. Here 8000 feet was drilled from the *B. humblei* zone, and the *C. opimus* zone was not reached. This well contained fossils that indicated a relatively shallow-water environment from *B. humblei* to the total depth of the well. This would be favorable for the appearance of *C. opimus*. The thickest section of the lower part of the middle Miocene is in the vicinity of Second Bayou, Cameron Parish. About 3000 feet of section is between the *C. opimus* zone and the *Robulus* "43" zone. Nearly 4500 feet of section has been observed at Lafourche Crossing, Lafourche Parish; there the *Robulus* "43" zone has not been

encountered. The thickness of the lower part of the middle Miocene is doubtful because no wells have been drilled in areas where the section is presumed to attain great thickness.

### *Upper Miocene*

The upper Miocene as designated herein is marked by the first occurrence of the *Bigenerina floridana* zone.

Another fauna stratigraphically higher in the section shows some aspects of a Miocene assemblage; it is not used at the present time to mark the top of the Miocene because the fauna is not as widespread or reliable as the *B. floridana* zone. It was more affected by adverse ecologic conditions and does not traverse as many ecologic zones. This assemblage is represented in about 3000 feet of sediment offshore from Terrebonne Parish. This thickness, however, is included in the total Miocene thickness.

Over 14,000 feet of upper Miocene sediments have been penetrated to date—actually 17,000 feet including the probable Miocene assemblage. Ecologic interpretations of the faunas in the outer reaches of the Eugene Island area indicate that much more inspissation can be expected. The *B. floridana* zone has not heretofore been recognized by paleontologists because it is found at great water depth (Crouch, 1955, paleoecologic zones 5–6). A well drilled far offshore did not reach this zone at a drilling depth of 15,000 feet. The foraminiferal assemblages, however, indicate that it approached within approximately 1000 feet of the *B. floridana* zone.

The greatest thickness (6000 feet) between the *B. floridana* zone and the *Buccella mansfieldi* zone was found in a deep well northeast of Coon Point, offshore from Terrebonne Parish. Nearly 4500 feet of sediments occurs between the *Bucella mansfieldi* and the *Spiroplectammina barrowi* zones in a well drilled near Grand Bay Field, Plaquemines Parish. However, on the northeast flank of Venice Field, Plaquemines Parish, a well drilled to approximately 5200 feet below the *Buccella mansfieldi* zone did not reach the *Spiroplectammina* zone.

A composite of 48,000 feet of section is recorded for the Miocene. This total is well defined between marker zones. A thicker section (55,000 feet) is known where the basal markers were not reached (Table 1).

### Pliocene

Wells drilled in the outer reaches of the Eugene Island area had not reached the top of the Miocene at a depth of 15,000 feet; only approximately 6000 feet of Pliocene sediments had been penetrated. This section is relatively thin partly because most of the Pliocene sediments were deposited farther from shore than the overlying Pleistocene. The ecologic interpretation of the Foraminifera in the Pliocene deposits substantiates this theory. The Pliocene sections drilled encountered Foraminifera with recent counterparts presently living on the Continental Shelf. Few fossils had been observed that indicate a relatively steep-slope environment for the deposition of the Pliocene except in the South Pass area, off the tip of the present delta. This area covers drilling operations closest to the break in the Continental Shelf. Another factor relating to the thinness of the Pliocene is that wells have not yet been drilled on the flanks of the large offshore structures. When this phase of exploration begins, a much thicker Pliocene section will probably be found.

In the updip section, the top of the Pliocene is difficult to place because it is mostly nonmarine. The top of the Pliocene is established in this report by a foraminifer that shows affinity to *Buliminella curta* Cushman var. *basispinata* R. E. and K. C. Stewart. Younger faunas higher in the section suggest a possible Pliocene affiinity; however, no reliable marker zone has been observed.

Until deeper wells are drilled on the Continental Slope and off the flanks of the large offshore structures, the extent and thickness of the Pliocene sediments will not be adequately known.

### Pleistocene

Pleistocene, as used in this report, includes Recent and modern sediments. No satisfactory paleontological marker has been found for Recent sediments.

In southern Louisiana, Pleistocene seas transgressed much farther inland than Pliocene seas, especially in southeastern Louisiana. Consequently, most of the Pleistocene sediments overlapped the Pliocene and were deposited in much deeper water than the underlying Pliocene. Akers and Holck (1957) have discussed the southeastern Louisiana Pleistocene sediments thoroughly.

The thickest section of Pleistocene sediments encountered to date is in the offshore areas of Eugene Island, Ship Shoal, and South Timbalier. Wells drilled in the outer reaches of these areas have penetrated nearly 8000 feet of Pleistocene sediments.

TABLE 1.—POST-OLIGOCENE INSPISSATION TABLE
(All measurements in feet)

TABLE 1.—POST OLIGOCENE INSPISSATION TABLE
(All measurements in feet)

| | | Paleontologic Zone | Definite Interval | Vicinity | Indefinite Interval | Vicinity |
|---|---|---|---|---|---|---|
| Pleistocene | | Pleistocene assemblage | 8000 | Outer Eugene Island<br>Ship Shoal<br>S. Timbalier area | | |
| Pliocene | | *Buliminella* aff. *curta. var. basispinata* | 6000 | Outer Eugene Island<br>Ship Shoal<br>S. Timbalier area | | |
| Miocene | Upper | (Miocene ?) assemblage | 3000 | Outer Eugene Island | | |
| | upper | *Bigenerina floridana* | 6000 | Coon Point, Ship Shoal area | | |
| | middle | *Buccella mansfeldi* | 4500 | Grand Bay, Plaquemines Parish | 5200 | Venice, Plaquemines Parish |
| | lower | *Spiropleclammina barrowi* | 4000 | Four League Bay, Terrebonne Parish | 5400 | Southeast of Lake Washington, Plaquemines Parish |
| | Middle | | | | | |
| | upper | *Bigenerina directa* | 7000 | Lake Washington, Plaquemines Parish | 8000 | Northeast of Lake Washington, Plaquemines Parish |
| | middle | *Bigenerina humblei* | 5500 | Bourg, Terrebonne Parish | 8000 | Hollywood, Terrebonne Parish |
| | lower | *Cibicides opimus* | 3000 | Second Bayou, Cameron Parish | 4500 | Lafourche Crossing, Lafourche Parish |
| | Lower | | | | | |
| | upper | *Robulus* "43" *Amphistegina* "B" | 3500 | Fresh Water Bayou, Vermilion Parish | | |
| | middle | *Discorbis bolivarensis* | 4500 | Block 40, West Cameron area | | |
| | lower | *Siphonina davisi* | 7000 | Second Bayou, Cameron Parish | | |
| Oligocene | upper | *Heterostegina* sp.<br>*Bolivina perca* | | | | |
| | | *Total* | 62,000 | | 69,100 | |

Lowman (1949) has shown that the base of the "Upper Marine Beds" in southeastern Louisiana may be mapped (presumably by electric logs and paleontological data) over a wide area. Akers and Holck (1957) have pointed out that the base of the "Upper Marine Beds" does not correspond to the base of the Pleistocene. The datum, nevertheless, as used by Lowman, is equivalent to a regional "time horizon"; this is substantiated by Foraminifera and electric logs. Electric logs are difficult to use for this horizon west of the western half of Terrebonne Parish and adjacent offshore areas because the "Upper Marine Beds", which largely consist of shale in the east, rapidly grade to sand in the west.

South-central Louisiana is best mapped on marker Foraminifera used in the southeastern part of Louisiana. The unreliability of the electric-log correlations makes a rapid detailed study impossible. Akers and Holck (1957) have pointed out that most paleontologists have not been interested in the Pleistocene sediments, and therefore cuttings have been preserved only from the older sections. Even when samples are caught in the Pleistocene interval, it is extremely difficult and time-consuming to locate the marker Foraminifera, owing to the sandy nature of the samples. Close space control is not possible owing to the lack of sufficient wells having shallow samples.

The determination of the total thickness of Pleistocene sediments in southern Louisiana will have to await drilling operations farther out from shore.

## Total Inspissation

The aggregate thickness for the post-Oligocene sediments is 62,000 feet. An additional 7100 feet should be considered even though basal markers were not observed in the wells containing the thickest section (Table 1).

Stuckey (1953, p. 27) states that Louisiana paleontologists establish the top of the Oligocene on the basis of the foraminifer *Textularia warreni*. In this report, *Heterostegina* sp. and its down-dip equivalent, *Bolivina perca*, are used to establish the top of the Oligocene. If the Louisiana teminology were used, an additional 20,000–25,000 feet of sediment would be added to the total accumulation for the post-Oligocene in the Gulf Coast area.

The total vertical section of post-Oligocene sediments at one geographic locality in the down-dip position in southern Louisiana is unknown. The deepest well to date is the Richardson and Bass, John W. Mecom *et al.*, Humble-Louisiana Land #1 St. Lse. 2414, Sec. 35, T. 19 S., R. 25 E. This well was drilled to 22,564 feet northeast of the Lake Washington dome. The top of the Pliocene was reached at 3000 feet, the top of the Miocene at about 6000 feet. At total depth this well was still drilling in sediments equivalent to the upper part of the lower Miocene. Comparison with nearby wells indicates that 2000–3000 feet or more of middle Miocene section is missing in the #1-L well. The adjacent wells indicate that the #1-L well was drilled on a deep structural high and therefore encountered a much thinner section than would normally be expected in this position. West of the #1-L well John W. Mecom and Freeport Oil Company drilled a 18,466-foot test well. This well did not reach the middle part of middle Miocene and had a considerably thicker upper Miocene section than the #1-L well. John W. Mecom drilled the Louisiana Land Exploration, Bayou Chalaud #2, in Sec. 22, T. 20 S., R. 27 E. to a depth of 16,029 feet. This well is approximately 8 miles south of the #1-L. The Bayou Chalaud #2 did not reach sediments equivalent to the upper part of the middle Miocene. This well indicated a thickening of section of more than 6000 feet in relation to the #1-L on this datum. Wire-line cores taken from a depth of 14,000 feet in this well indicate that the lower part of the upper Miocene dips less than 5°. Farther south and east the upper Miocene thickens considerably, indicating that the thickening is regional.

Geophysical data have indicated good reflections from strata at 35,000 feet. The reflections probably come from Miocene strata and may not be older than the middle part of the lower Miocene. By extrapolating data between known points in this general area and by assuming rates of thickening as indicated in the wells one can postulate a depth of between 25,000 and 30,000 feet to the top of the middle part of the middle Miocene in the John W. Mecom Bayou Chalaud #2.

## Geophysics

Regional geophysical traverses do not support the thickening indicated by the Foraminifera. Mr. T. M. Bruke, the geophysical co-ordinator for John W. Mecom, feels that this is because of the poor reflecting quality of the unconsolidated beds in southern Louisiana. Massive sand bodies grade into shales down-dip, causing reflections to shift to younger and

unger sands. The absence of a regional reflecting medium means that the reflections cannot be traced down the true regional dip. Because there is no good regional reflecting stratum, the geophysical data appear to progress upward in the section as the traverse progresses down-dip. A better regional geophysical picture can be presented along the strike. The same problems are present here as in the down-dip section but to a much lesser extent.

Nettleton (1952, p. 1221) arrived at a similar conclusion, stating that "... geophysical data are of limited use in adding information between, beyond, and below direct observations from deep wells and thereby contributing to our understanding of the general configuration of the Gulf Coast embayment and the volume of sediments which it contains". He further states that commercial geophysical exploration in the Gulf Coast is intended to find local structures rather than for regional interpretation. Gravity and magnetic surveys also have limited regional value.

If the general regional geophysical picture were correct, it would be possible to correlate electric logs regionally. This is definitely not possible. With foraminiferal data and electric-log correlations, however, the regional picture can be ascertained.

## Regional Paleontology

Contours on Plate 1 depict the regional interpretation of the paleontologic subdivisions for the Pliocene, upper Miocene, middle part of the middle Miocene, lower part of the middle Miocene, and the upper Oligocene. Local low or high areas were discounted in order to present a regional expression of the paleontological data. Considerable data were available onshore for locating the contour intervals. Data for the offshore contours were relatively limited. Care was taken to use only data from wells on the flanks of structures onshore. Offshore, it was not possible in all cases to make a regional interpretation of the paleontological data owing to the lack of wells drilled on the flanks of salt domes or off local structures. Almost all offshore wells examined were drilled on large high structures; the paleontological data support this. The information available from the offshore area now is similar to the data available onshore in the early 1940's. Future flank-drilling operations will undoubtedly prove the offshore contours are very conservative, especially the Pliocene contours. Thinning of section as wells are drilled higher on structures can be demonstrated for all the salt domes in the Gulf Coastal area. In the Lake Washington area, Plaquemines Parish, a section displaced because of uplift on the dome showed a difference of 7000 feet as compared with the same section on the flank. Where only one well has been drilled on a structure, faults are not easily detected. A shortened section, therefore, can exist without being recognized. These examples point out the difficulties of contouring the offshore area at the present stage of exploration.

Depth contours depicting water depths from 300–600 feet were sketched on Plate 1 from charts drawn by Gealy (1955). They show the position of the offshore area in relation to the present shelf. Several wells have been drilled in water depths of 120 feet in the West Delta and South Pass areas.

A single 12,000-foot contour is shown on Plate 1 for the approximate down-dip extent of the *Heterostegina-Bolivina perca* (Oligocene top) zone. The regional expression of the zone has not been located farther to the south for two reasons. One is that sand rapidly grades to shale and therefore has not been conducive to exploration. The other is that the dip of the late Oligocene sediments increases markedly beyond the 12,000-foot contour, and deep wells drilled a few miles south of the datum have not reached the equivalent zone.

The 14,000-foot contour (Pl. 1) is based on the top of the *Siphonina davisi* zone, designated as the upper part of the lower Miocene. Data for 15,000- and 16,000-foot contours will probably be available in later years when deeper down-dip drilling is accomplished.

Contour intervals between the uppermost dip position and the lowest down-dip position are depicted on Plate 1 for the *Bigenerina humblei* zone (the top of the middle part of the middle Miocene). The 6000-foot contour represents the extreme updip occurrence of *Bigenerina humblei*. This zone is very thin and represents a marginal, shallow-water environment. Excellent samples are necessary to permit detection of its presence along this contour. The 15,000-foot contour is the last that can be pictured with regional control. A 20,000-foot contour has been proposed, and the data used to determine its location were extrapolated from a few wells that have penetrated this zone to a depth of 17,000 feet. Ecologic conditions in this down-dip position are similar to those of the deep-water paleoecologic zones 5 and 6 of Crouch (1955). Oil-bearing sands in the *B. humblei* zone have been commercially remark-

able in isolated localities, even in relatively deep water. However, present production history indicates that these sands have little areal extent. The validity for the 20,000-foot contour may be supported by future exploration.

The *Bigenerina floridana* zone (the top of the upper Miocene) traverses nearly as many ecologic zones as the *Bigenerina humblei* zone. The accuracy of the uppermost contour is also governed by the same conditions as those applied to the *Bigenerina humblei* zone. The down-dip contours are located far offshore, and the data obtained from wells there show that they were drilled on structurally high areas and may fail to reflect the regional trend accurately. Future drilling on the flanks may add nearly 5000 feet to some of the outer contour depths.

Sufficient data were available in the delta region for the Pliocene contours to show a ridge or nose effect. The ridge strongly suggests that this area was high during at least part of Pliocene time. Contours follow the general configuration of the present shore line in the southeastern offshore area. It is uncertain whether the Pliocene contours follow the present shore line in the area west of the delta area.

## Gulf Coast Geosyncline

The hypothesis of the Gulf Coast geosyncline has been based on the assumption that a regional reversal of dip exists. The assumption depends on the existence of a large gravity minimum in southern Louisiana.

Barton, Ritz, and Hickey (1933) contend that the regional variation of gravity suggests the existence of a geosyncline on the basement of the Texas-Louisiana Gulf coast. The large gravity minimum extends from Orange, Texas, to the Mississippi River near Baton Rouge, Louisiana. Nettleton (1952, p. 1223) points out that the large minimum is not supported by magnetic data, and wells drilled across this feature indicate a monoclinal coastward dip with the dip increasing with depth. He further explains that the gravity anomaly is great enough to be accounted for by the density contrasts deep within in the basement rock. Fisk (1944, Pl. 33) has used gravity-minima data and the mollusk *Rangia microjohnsoni* Gardner to support the theory of a regional reversal of dip.

Examination of Foraminifera associated with *R. microjohnsoni* indicates that this small mollusk lived in and is restricted to a brackish-to near-brackish-water environment. It is commonly found with the foraminifer *Eponidella* sp. and oyster fragments. The rapid change in the environmental conditions traversing the regional dip from shoal to deep water makes *R. microjohnsoni* invalid as a regional marker fossil. Crouch (1955) pointed out that regional fossil-correlation work in the Gulf Coast area must depend on marker species that traverse several ecologic conditions and die out quickly. The more ecologic zones that the fossil may traverse, the more widespread and reliable the regional correlation. Fossils confined to brackish water commonly appear to extend upward in the section and make it appear as though the beds thin down-dip.

Weaver (1951, p. 395) feels that the sediments must thin at some point on the Continental Shelf owing to the lack of sediment source far offshore.

None of the requirements for a geosyncline can be substantiated at this time—that is, no regional reversal of dip and no regional thinning of beds can be demonstrated. Most workers feel that a geosyncline of some type exists even though evidence is lacking. This author feels that under the miles of sediment offshore the units begin to thin, the geographic position differing for each of the geologic subdivisions. There have been many relatively minor eustatic changes in sea level in the Gulf Coastal area of Louisiana since the end of Oligocene time. A few major changes have been noted. Since the beginning of Miocene time, the main depositional area has migrated seaward. This seaward shift continued to the close of Pliocene time. At the beginning of the Pleistocene the depositional area shifted temporarily shoreward, and Pleistocene sediments completely overlapped the marine Pliocene. Near the close of the Pleistocene the main depositional area resumed its migration seaward; it continues to migrate seaward to the present. The shoreward shift of the depositional area during the Pleistocene would not have assumed as great an importance in the over-all picture if no change in the nomenclature from Pliocene to Pleistocene had been made. In the final analysis, there can be no single depositional axis for post-Oligocene sediments in a given geographic position. The main center of deposition has migrated seaward since the beginning of Cretaceous time. Without a doubt the sediments thin and the beds flatten somewhere offshore. This satisfies the broader definition of a geosyncline. The location and depth of the depositional axis of each of the

subdivisions is still unknown. This report supports the contention that the post-Oligocene sediments are thicker than was supposed and that the depositional axes are located farther from the ancient shore lines than was formerly supposed.

## Conclusions

The writer has attempted to show the magnitude of the post-Oligocene sediment inspissation in southern Louisiana. Present data are insufficient to establish the extent and maximum thickness of these sediments with any certainty. The following conclusions are based upon the data from several thousand wells drilled in southern Louisiana:

(1) An assemblage presumed to be Miocene is nearer to the top of the marine Miocene than the *Bigenerina floridana* zone. This assemblage loses part of its value as a regional marker because it is not as widespread as the *B. floridana* zone and did not traverse as many ecologic zones.

(2) Little is known about the thickness of the Pliocene. Most of the Pliocene sediment was deposited far from shore; also, wells drilled far out on the Continental Shelf have been located on high areas. The section in these high areas is materially shortened in comparison with the same section on the flanks.

(3) Regional paleontologic contours indicate that the present delta area was high during part of the Pliocene. The Pliocene contours in the delta region generally follow the present shore line. Control is insufficient to determine whether these contours follow the configuration for the entire coast line.

(4) The marine Pleistocene sediments have completely overlapped the marine Pliocene and were deposited in much deeper water than the underlying Pliocene.

(5) None of the wells examined given any indication of a regional reversal of dip or of regional thinning. This makes it impossible to establish any depositional axes for the subdivisions of the post-Oligocene sediments.

(6) Areas of salt withdrawal (rim synclines) and areas on the down-thrown side of large regional "hinge-line" faults are conducive to rapid sedimentation. The latter, being downthrown seaward, account for the rapid thickening of sediment in that direction.

(7) A stratigraphic type section for the post-Oligocene sediments cannot be established owing to the rapid changes in facies both along the strike and down the regional dip. No lithologic differences exist in the upper, middle, or lower Miocene beds.

(8) The main depositional trend has been seaward since Oligocene time, except briefly during the Pleistocene. This trend has probably continued since Cretaceous time.

(9) Down-dip regional geophysical profiles extend upward in section because massive sand bodies grade to shales down-dip and cause reflections to shift to younger and younger sands.

(10) Nearly 70,000 feet of post-Oligocene sediments have been recorded by using aggregate thicknesses mainly from wells drilled off the flanks of salt domes. This procedure was not applicable to the offshore area because exploration has not entered the flank-drilling stage. A complete evaluation of the total inspissation of post-Oligocene sediments will have to await deeper drilling operations on the Continental Slope as well as on shore in southern Louisiana.

## References Cited


Akers, W. H., 1954, Planktonic foraminifers, suggested means of correlating Gulf coastal and West Indian neogene sediments: Gulf Coast Assoc. Geol. Soc. Trans., v. 4, p. 169–180

Akers, W. H., and Holck, A. J. J., 1957, Pleistocene beds near the edge of the Continental Shelf, southeastern Louisiana: Geol. Soc. America Bull., v. 68, p. 983–992

Barton, Donald C., Ritz, C. H., and Hickey, Maude, 1933, Gulf Coast geosyncline: Am. Assoc. Petroleum Geologists Bull., v. 17, p. 1446–1458

Carsey, Ben J., 1950, Geology of the Gulf Coastal area and Continental Shelf: Am. Assoc. Petroleum Geologists Bull., v. 34, p. 361–385

Crouch, R. W., 1955, Pragmatic approach to correlation of Miocene strata in southern Louisiana: Am. Assoc. Petroleum Geologists Bull., v. 39, p. 2321–2328

Fisk, Harold N., 1944, Geological investigation of the alluvial valley of the lower Mississippi River: Vicksburg, Miss., Miss. River Comm., December 1, 1944, p. 78.

Gealy, B. L., 1955, Topography of the Continental Slope in northwest Gulf of Mexico: Geol. Soc. America Bull., v. 66, p. 203–228

Lowman, S. W., 1949, Sedimentary facies in Gulf Coast: Am. Assoc. Petroleum Geologists Bull., v. 33, p. 1939–1997

Murray, G. E., 1952, Sedimentary volumes in Gulf Coastal Plain of the United States and Mexico, Part III, Volume of Mesozoic and Cenozoic sediments in central Gulf Coast Plain of United States: Geol. Soc. America Bull., v. 63, p. 1177–1192

New Orleans Geological Society, 1954, Cross-section study maps

Nettleton, L. L., 1952, Sedimentary volumes in

Gulf Coastal Plain of the United States and Mexico, Part VI, Geophysical aspects: Geol. Soc. America Bull., v. 63, p. 1221–1228

Stuckey, C. W., 1953, Tertiary stratigraphy of the Texas Gulf Coast: Houston Geological Soc. Guidebook, Joint Annual Meeting of A.A.P.G., S.E.P.M., and S.E.G., p. 25–29

Weaver, Paul, 1951, Continental Shelf of the Gulf of Mexico: Am. Assoc. Petroleum Geologists Bull., v. 35, p. 393–398

℅ JOHN W. MECOM, BOX 2566, HOUSTON, TEXAS

MANUSCRIPT RECEIVED BY THE SECRETARY OF THE SOCIETY, AUGUST 25, 1958

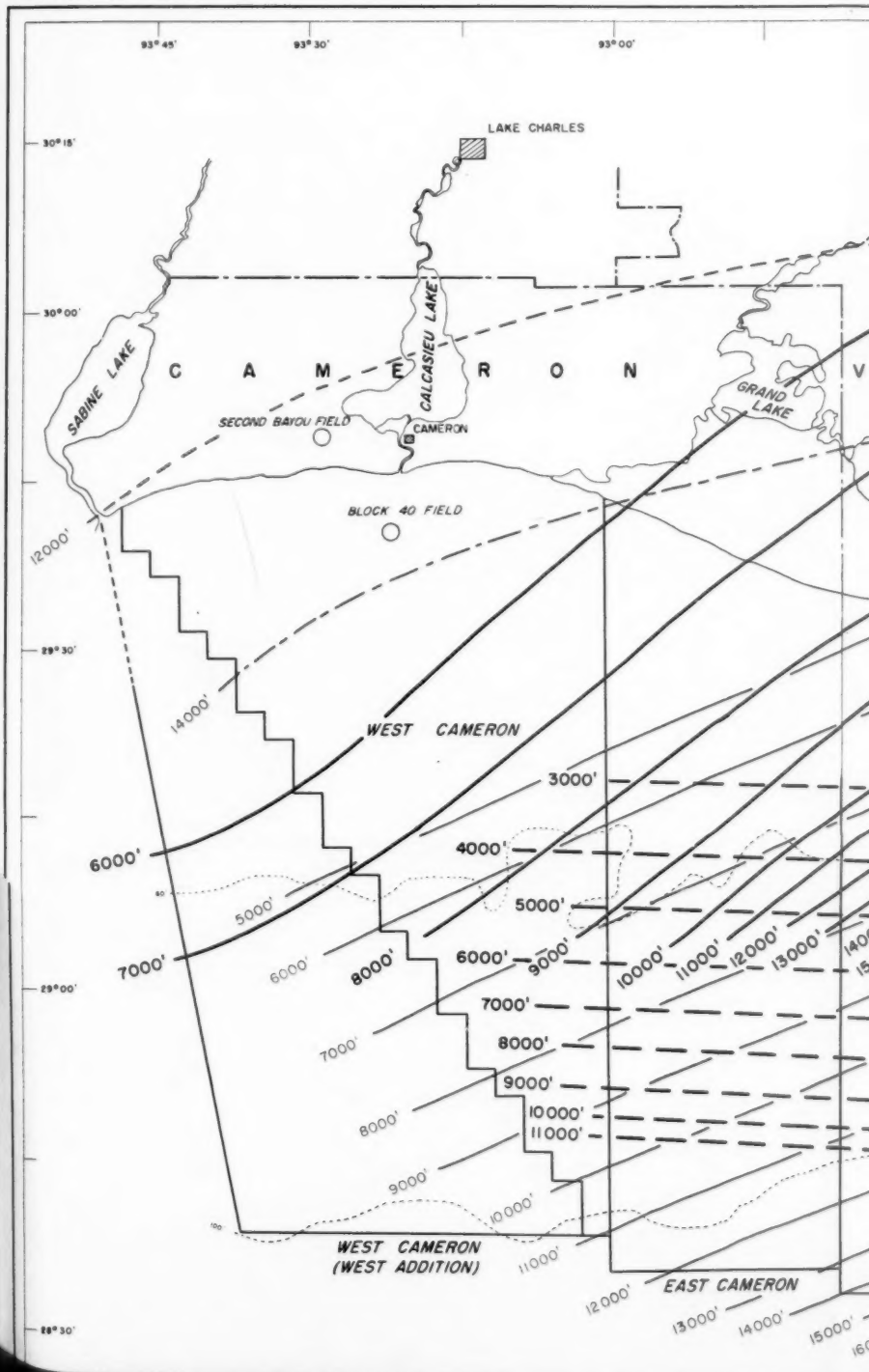
93°45'
93°30'
93°00'
30°15'
30°00'
29°30'
29°00'
LAKE CHARLES
SABINE LAKE
CALCASIEU LAKE
C A M E R O N
GRAND LAKE
SECOND BAYOU FIELD
CAMERON
BLOCK 40 FIELD
12000'
14000'
WEST CAMERON
3000'
4000'
5000'
6000'
7000'
8000'
9000'
10000'
11000'
12000'
13000'
6000'
5000'
7000'
6000'
8000'
7000'
9000'
8000'
10000'
11000'
9000'
10000'
WEST CAMERON
(WEST ADDITION)
11000'
12000'
EAST CAMERON
13000'
14000'
15000'

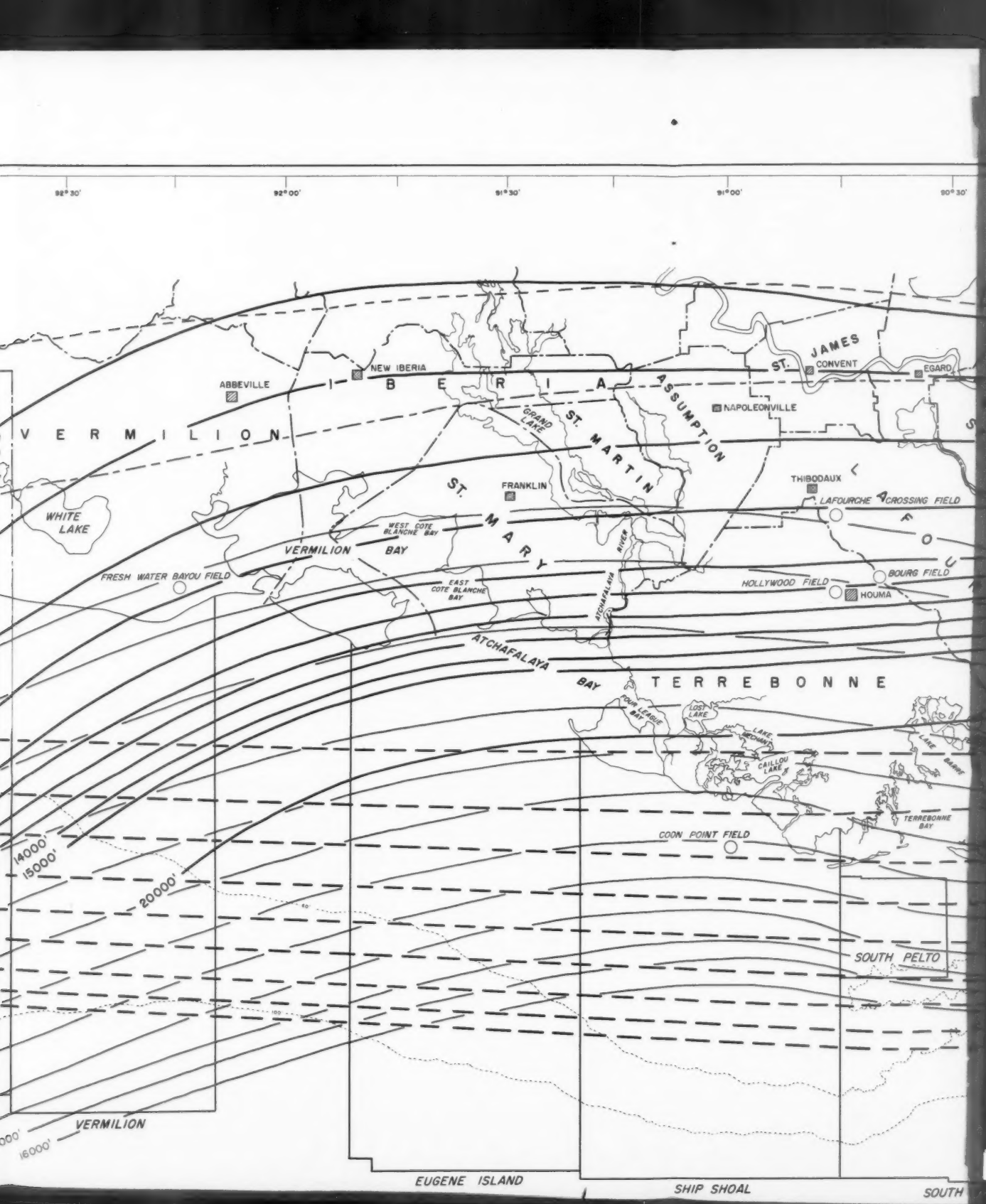
92° 30'
92° 00'
91° 30'
91° 00'
90° 30'
VERMILION
IBERIA
ST. MARY
ST. MARTIN
ASSUMPTION
ST. JAMES
LAFOURCHE
TERREBONNE
ABBEVILLE
NEW IBERIA
NAPOLEONVILLE
CONVENT
EGARD
FRANKLIN
THIBODAUX
LAFOURCHE CROSSING FIELD
WHITE LAKE
GRAND LAKE
WEST COTE BLANCHE BAY
VERMILION BAY
EAST COTE BLANCHE BAY
ATCHAFALAYA RIVER
FRESH WATER BAYOU FIELD
HOLLYWOOD FIELD
BOURG FIELD
HOUMA
ATCHAFALAYA BAY
FOUR LEAGUE BAY
LOST LAKE
LAKE BARRE
CAILLOU LAKE
TERREBONNE BAY
COON POINT FIELD
SOUTH PELTO
14000'
15000'
20000'
16000'
VERMILION
EUGENE ISLAND
SHIP SHOAL
SOUTH

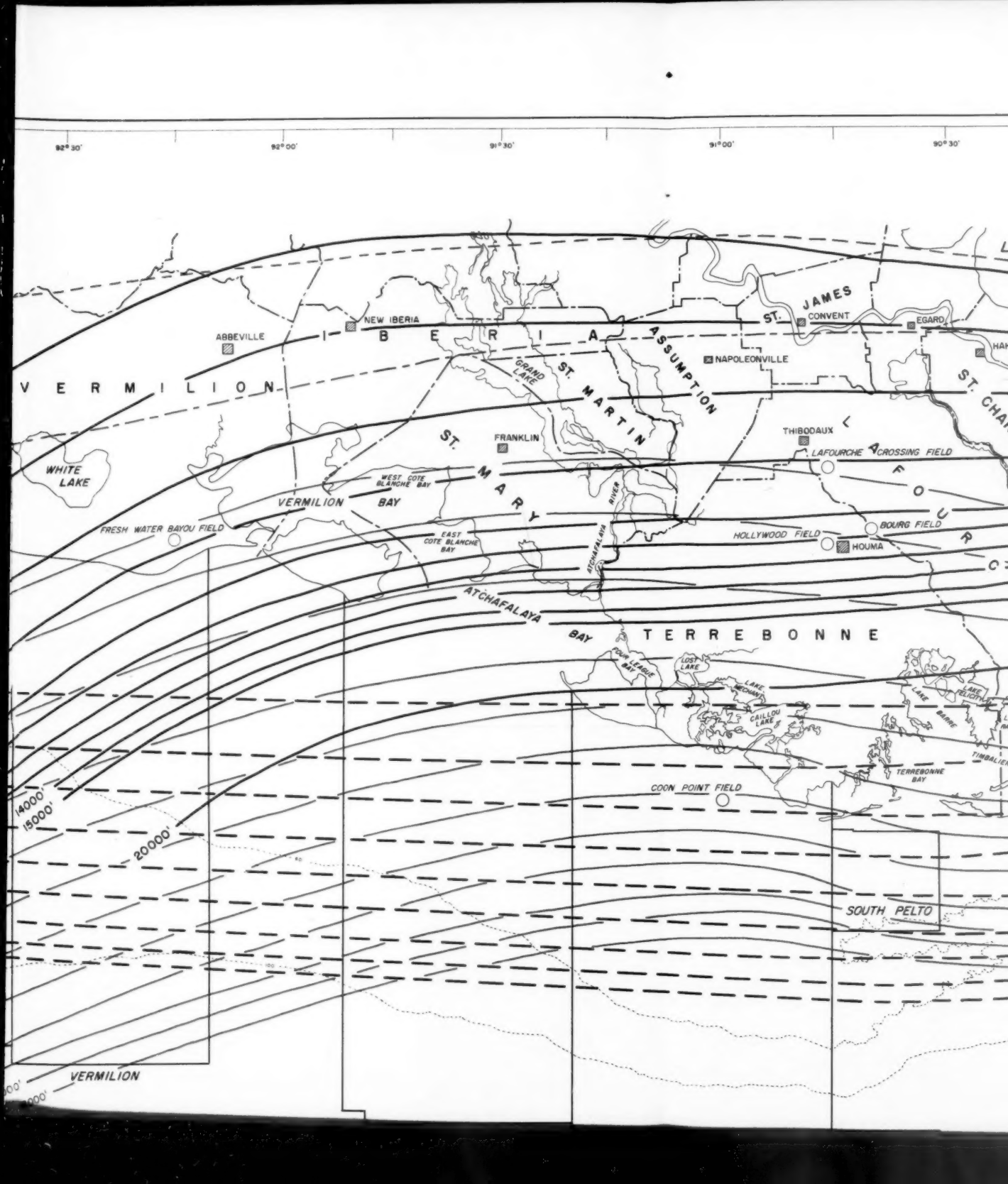
92° 30'
92° 00'
91° 30'
91° 00'
90° 30'
ABBEVILLE
NEW IBERIA
I B E R I A
ST. JAMES
CONVENT
EGARD
NAPOLEONVILLE
ASSUMPTION
V E R M I L I O N
GRAND LAKE
ST. MARTIN
ST. MARY
FRANKLIN
THIBODAUX
LAFOURCHE CROSSING FIELD
L A F O U R C H E
WHITE LAKE
WEST COTE BLANCHE BAY
VERMILION BAY
FRESH WATER BAYOU FIELD
EAST COTE BLANCHE BAY
ATCHAFALAYA RIVER
HOLLYWOOD FIELD
BOURG FIELD
HOUMA
ATCHAFALAYA BAY
T E R R E B O N N E
POINT LEAGUE BAY
LOST LAKE
LAKE MECHANT
CAILLOU LAKE
LAKE BARRE
LAKE PELTO
TERREBONNE BAY
COON POINT FIELD
SOUTH PELTO
14000'
15000'
20000'
VERMILION

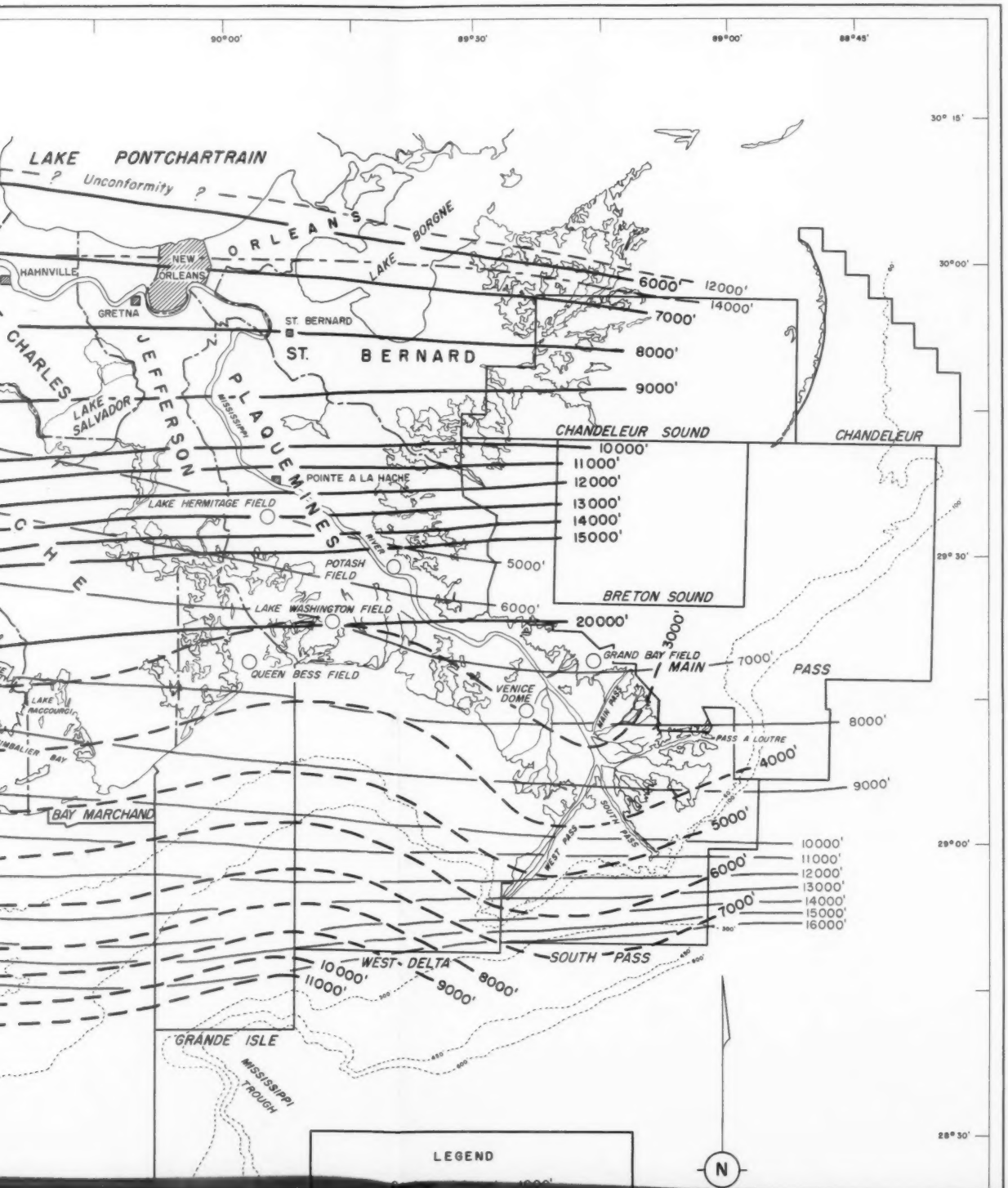
90°00'
89°30'
89°00'
88°45'
30° 15'
30°00'
29° 30'
29°00'
28° 30'
LAKE PONTCHARTRAIN
? Unconformity ?
ORLEANS
LAKE BORGNE
NEW ORLEANS
HAHNVILLE
GRETNA
ST. BERNARD
ST. BERNARD
JEFFERSON
PLAQUEMINES
CHARLES
LAKE SALVADOR
MISSISSIPPI RIVER
CHANDELEUR SOUND
CHANDELEUR
POINTE A LA HACHE
LAKE HERMITAGE FIELD
POTASH FIELD
LAKE WASHINGTON FIELD
QUEEN BESS FIELD
BRETON SOUND
GRAND BAY FIELD
MAIN PASS
VENICE DOME
PASS A LOUTRE
LAKE MACCOURO
BAY MARCHAND
WEST PASS
SOUTH PASS
WEST DELTA
SOUTH PASS
GRANDE ISLE
MISSISSIPPI TROUGH
6000'
12000'
14000'
7000'
8000'
9000'
10000'
11000'
12000'
13000'
14000'
15000'
5000'
6000'
20000'
3000'
7000'
8000'
4000'
9000'
5000'
10000'
11000'
6000'
12000'
13000'
7000'
14000'
15000'
16000'
10000'
11000'
9000'
8000'
LEGEND
N

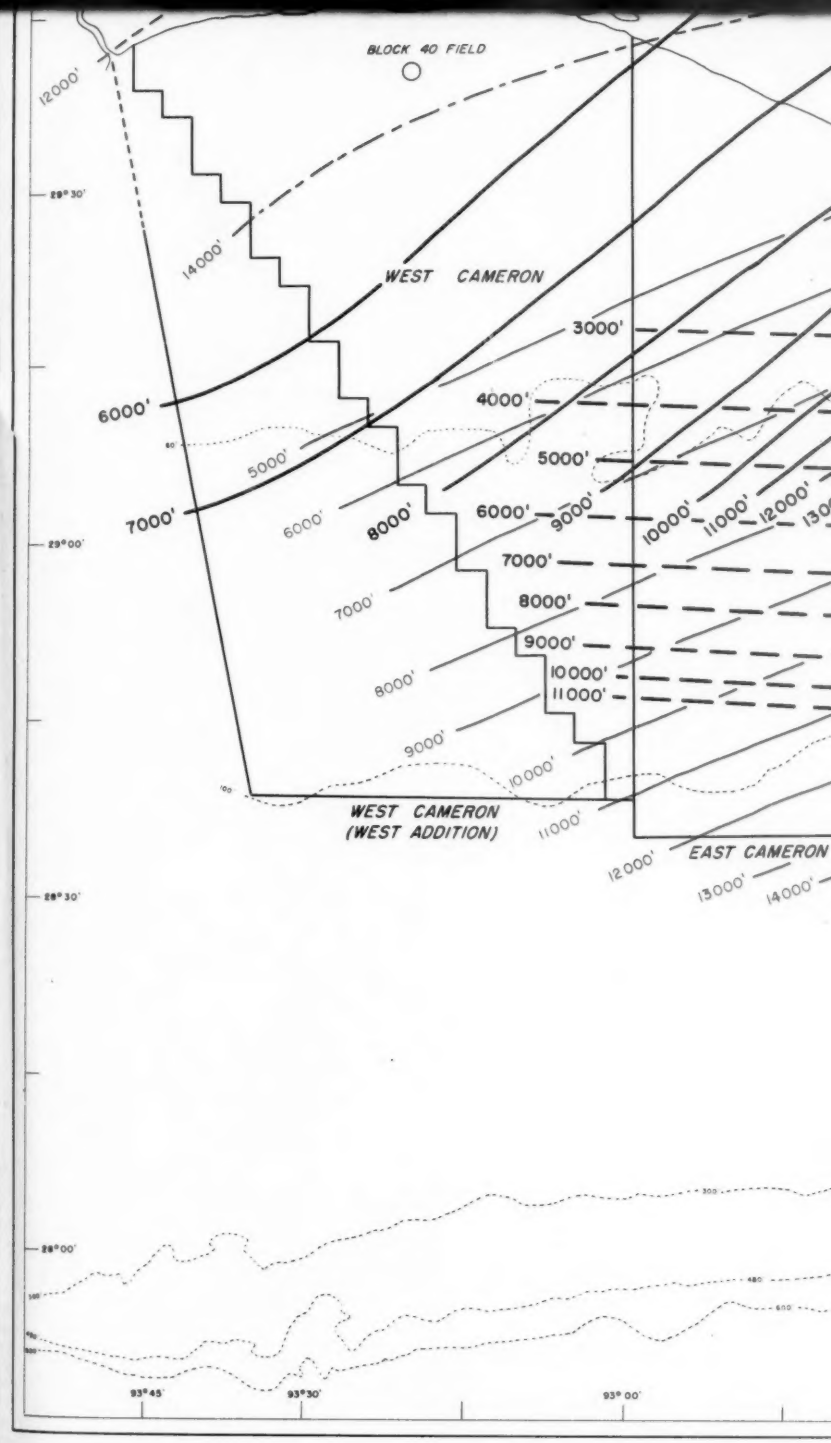
BLOCK 40 FIELD
12000'
29° 30'
14000'
WEST CAMERON
3000'
4000'
6000'
5000'
7000'
6000'
8000'
6000'
9000'
10000'
11000'
12000'
13000'
7000'
8000'
7000'
9000'
8000'
10000'
11000'
9000'
10000'
29°00'
WEST CAMERON
(WEST ADDITION)
11000'
12000'
EAST CAMERON
13000'
14000'
28° 30'
29°00'
93°45'
93°30'
93° 00'

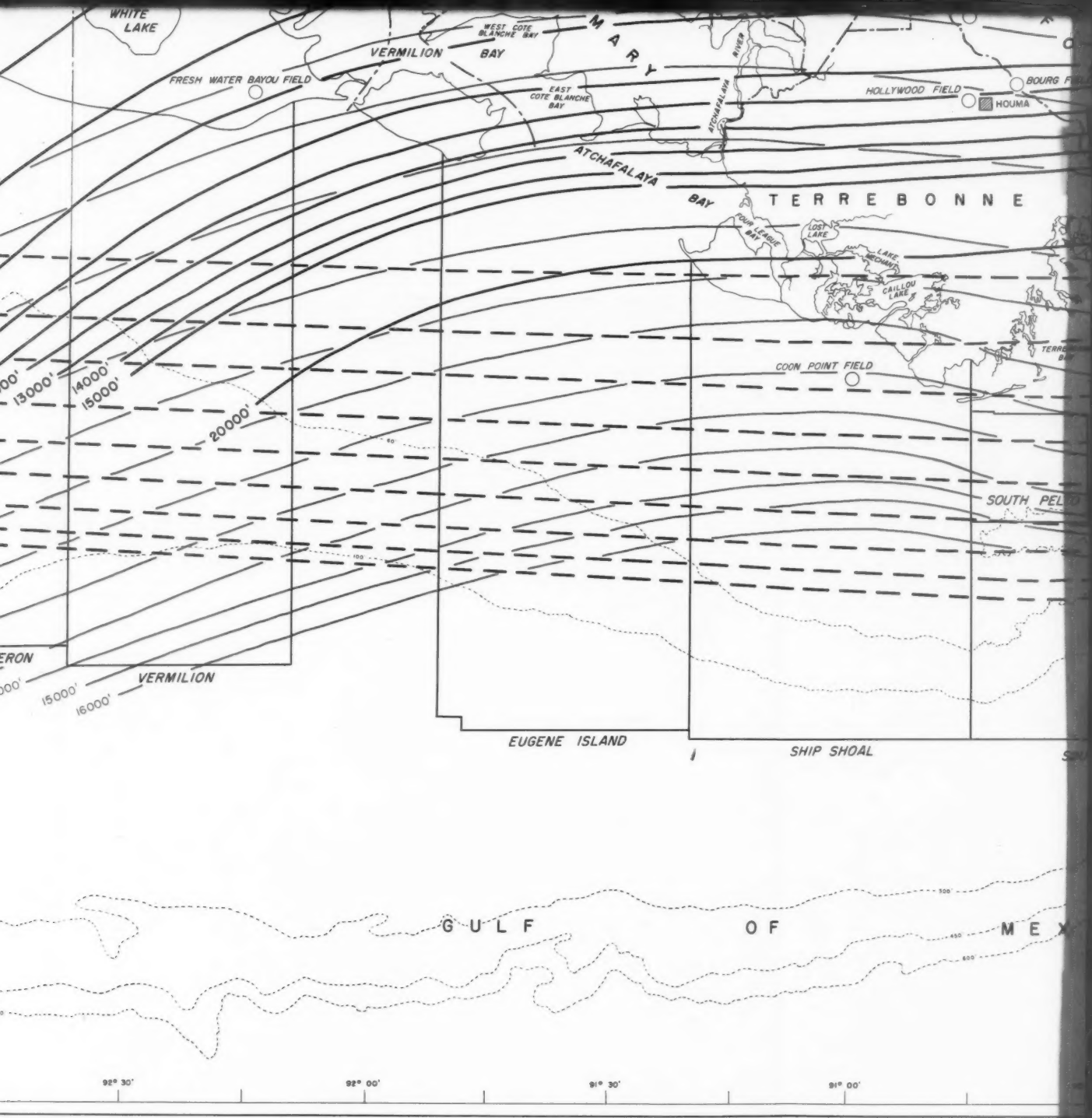


CONTOUR MAP OF SOUTHERN LOUISIANA AND OFFSHO

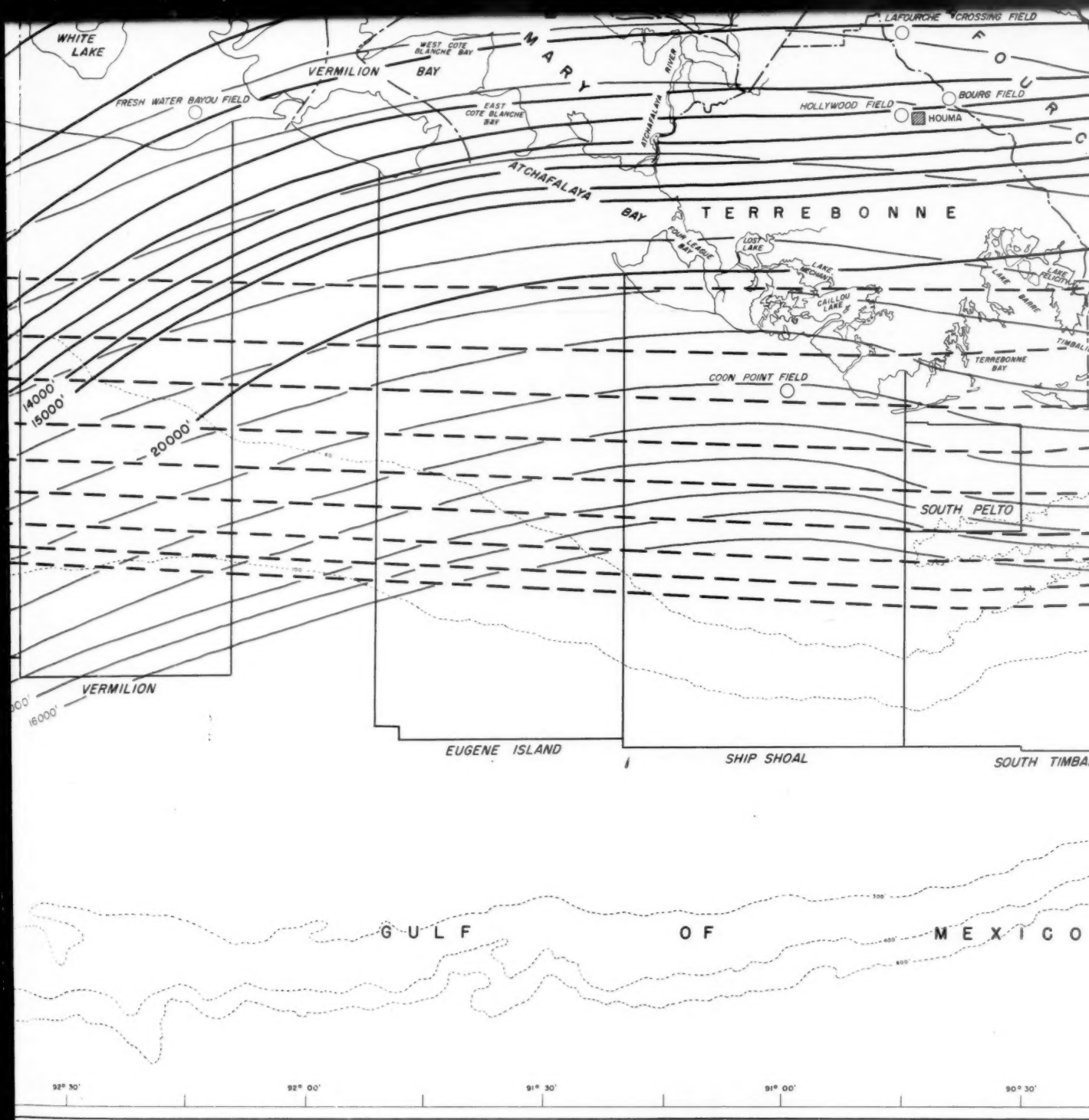


CONTOUR MAP OF SOUTHERN LOUISIANA AND OFFSHORE AR

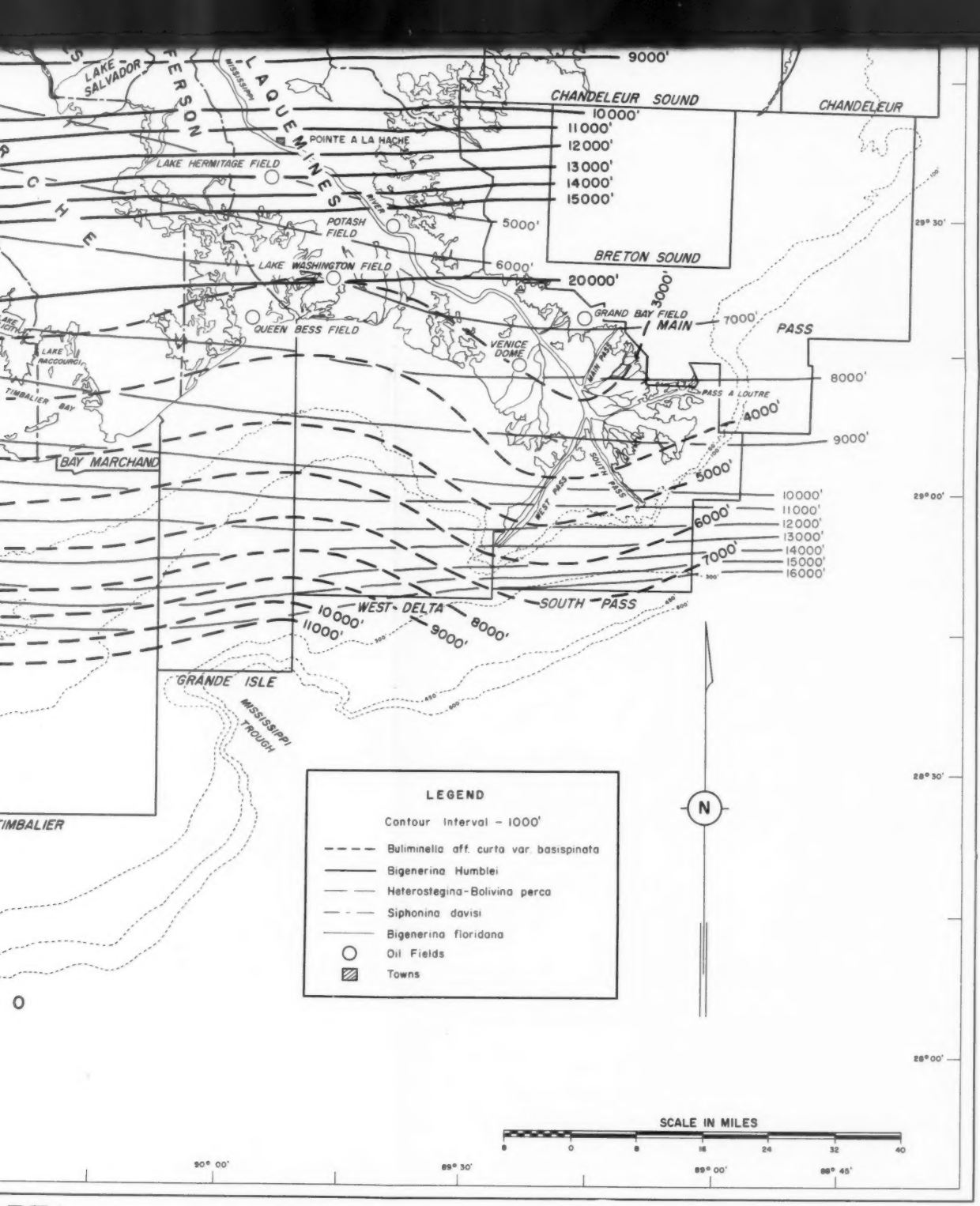
LAKE SALVADOR
LAQUEMINES
POINTE A LA HACHE
LAKE HERMITAGE FIELD
POTASH FIELD
LAKE WASHINGTON FIELD
QUEEN BESS FIELD
CHANDELEUR SOUND
CHANDELEUR
BRETON SOUND
GRAND BAY FIELD
MAIN PASS
VENICE DOME
PASS A LOUTRE
SOUTH PASS
WEST PASS
BAY MARCHAND
WEST DELTA
SOUTH PASS
GRANDE ISLE
MISSISSIPPI TROUGH
LAKE MACCOURGI
TIMBALIER BAY
9000'
10000'
11000'
12000'
13000'
14000'
15000'
5000'
6000'
20000'
3000'
7000'
8000'
4000'
16000'
29° 30'
28° 00'
28° 30'
90° 00'
89° 30'
89° 00'
88° 45'
N
LEGEND
Contour Interval – 1000'
Buliminella aff. curta var. basispinata
Bigenerina Humblei
Heterostegina-Bolivina perca
Siphonina davisi
Bigenerina floridana
Oil Fields
Towns
SCALE IN MILES
0 0 8 16 24 32 40

AREA

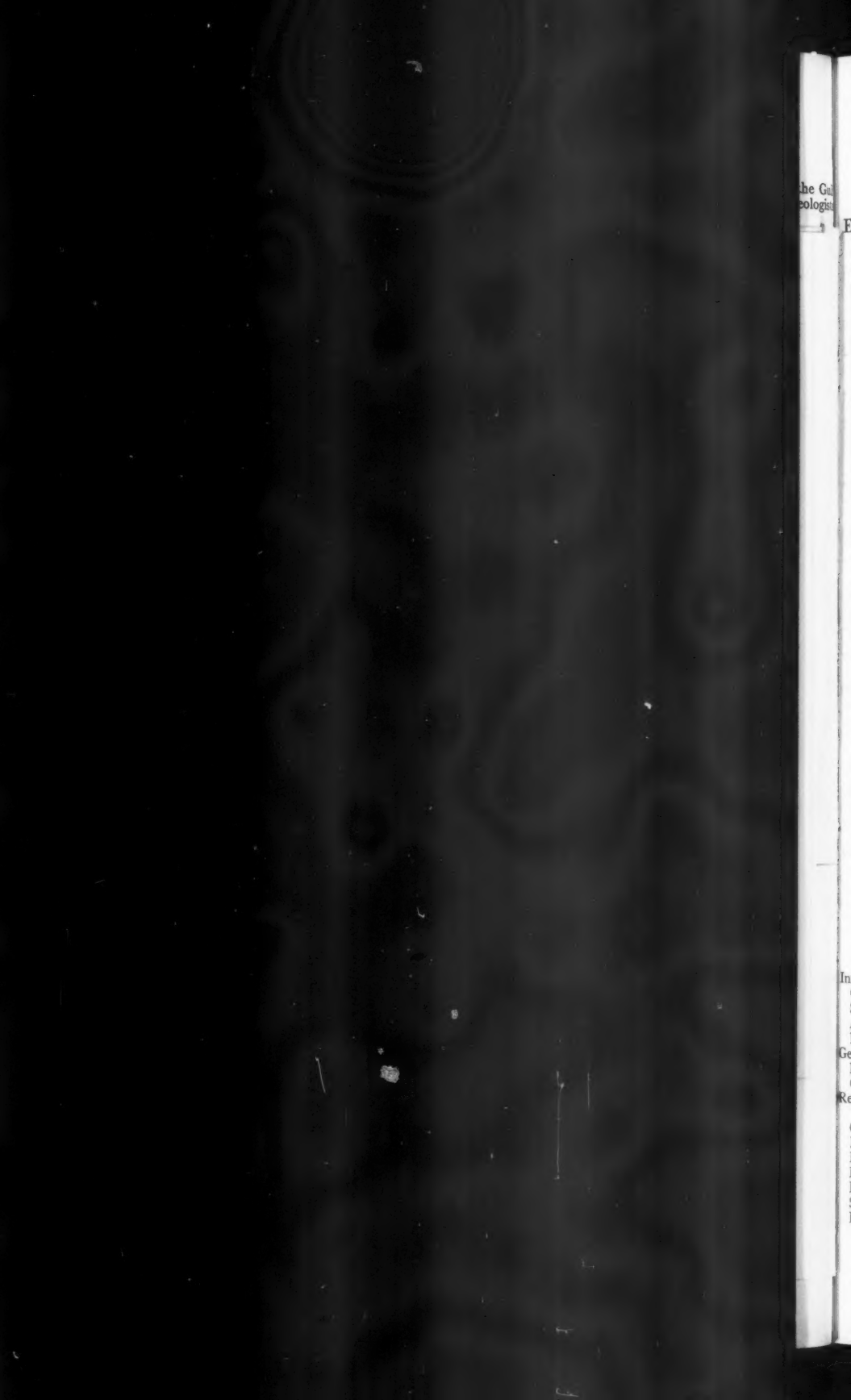

BULLETIN OF THE GEOLOGICAL SOCIETY OF AMERICA
VOL. 70, PP. 1293–1326, 21 FIGS. OCTOBER 1959

# EMPLACEMENT OF THREE GRANITIC PLUTONS IN SOUTHEASTERN ONTARIO, CANADA

BY AJIT KUMAR SAHA

## ABSTRACT

The manner and history of emplacement of three post-tectonic granitic plutons in Hastings and Peterborough counties, Ontario, were studied using lithological and structural mapping, petrographic studies (including modal analyses, chemical analyses, radiometric and decrepitometric studies), and petrofabric studies. The country rocks consist of Grenville metasedimentary rocks which were folded in two stages along northeast- and east-southeast-trending axes respectively, before emplacement of the plutons. The elliptical (5 by 3 miles) Chandos Lake pluton is made up of a central body of foliated syenite-monzonite, surrounded by later foliated biotite granite grading to a granodiorite. Both components are steep-dipping, crosscutting, funnel-shaped bodies emplaced by forceful intrusion at the site of a pre-existing structural basin. The elongated body of the foliated Wollaston biotite-hornblende granite (6 by 1.5 miles) was forcefully intruded along the eastern flank of a regional anticline as several steep, east-dipping bodies of granite, separated by narrow screens of paragneissic country rocks, parts of which were granitized to a granite gneiss. The composite Deloro pluton (20 square miles) consists of an earlier crescent-shaped (on plan), forceful intrusion of perthite granite grading to syenite along the western border, followed closely by the intrusion of a smaller body of granophyric granite in the east.

The biotite granite-granodiorite of Chandos Lake pluton and the Wollaston biotite-hornblende granite show unsystematic variations of the modal quartz (Q)–feldspars (F)–mafic minerals (M) and the quartz (Q)–potassium feldspar (Kf)–plagioclase (Pl) proportions and of the $\alpha$ activity; assimilation of varied rock types by the granite magmas accounts for such variations. In the Deloro pluton assimilation of gabbro-diabase by the granite magma accounts for the syenitic western border, but magmatic differentiation by fractional crystallization caused a systematic trend of acidification toward the central and eastern parts of the pluton and the location of the Q-Pl-Kf plots of the perthite granites within the thermal valley of Bowen. The cooling of the plutonic rocks was accompanied by extensive recrystallization of quartz in all the plutons, formation of myrmekite and of albite rims on plagioclase in the Chandos Lake and Wollaston plutons, and segregation of albite from the perthites in the Deloro pluton.

## CONTENTS

### TEXT

| | Page |
|---|---|
| Introduction | 1294 |
| General statement | 1294 |
| Scope of the work | 1294 |
| Acknowledgments | 1295 |
| Previous work | 1296 |
| General geology | 1296 |
| Regional setting | 1296 |
| General characters of the plutons | 1297 |
| Regional structure around Chandos Lake and Wollaston plutons | 1297 |
| General statement | 1297 |
| Principles of reconstruction | 1297 |
| Folding | 1298 |
| Lineation | 1298 |
| Relative ages of the cross folds | 1298 |
| Structural setting of the plutons | 1299 |
| Fold movements earlier than the emplacement of the plutons | 1299 |
| Regional structure around the Deloro pluton | 1300 |
| Internal structures of the plutons | 1300 |
| Chandos Lake pluton | 1300 |
| Foliation and lineation | 1300 |
| Shape of the pluton | 1301 |
| Joints | 1303 |
| Syenite-granite relationship | 1303 |
| Wollaston pluton | 1304 |
| Foliation | 1304 |
| Lineation | 1304 |
| Inclusions and roof pendants | 1304 |
| Joints | 1306 |
| Granite offshoots | 1306 |
| Shape of the pluton | 1306 |
| Deloro pluton | 1307 |
| General relations | 1307 |
| Joints | 1307 |
| Mineralogical and chemical variations in the plutons | 1309 |

| | Page |
|---|---|
| General statement | 1309 |
| Variations in the Chandos Lake pluton | 1309 |
| Variations in the Wollaston pluton | 1313 |
| Variations in the Deloro pluton | 1316 |
| Petrogenic implications of the data on the $\alpha$ activity of the plutons | 1318 |
| Recrystallization in the granitic plutons | 1319 |
| General statement | 1319 |
| Recrystallization in Chandos Lake and Wollaston plutons | 1319 |
| Recrystallization in the Deloro pluton | 1323 |
| Outline history of emplacement of the granitic plutons | 1323 |
| References cited | 1324 |


## ILLUSTRATIONS


| Figure | Page |
|---|---|
| 1. Location map | 1295 |
| 2. Regional structure map of the country between Apsley and Coe Hill, Ontario | 1297 |
| 3. Axes of girdles in the quartz orientation diagrams for samples of biotite paragneiss | 1299 |
| 4. Equal-area projection of the measured lineations | 1300 |
| 5. Regional structure map of the area around the Deloro pluton | 1301 |
| 6. Geological and structural map of the Chandos Lake pluton | 1302 |
| 7. Diagrammatic cross section across the Chandos Lake pluton | 1303 |
| 8. Orientation of 85 pegmatite and granite dikes around the Chandos Lake pluton | 1304 |
| 9. Geological and structural map of the Wollaston pluton | 1305 |
| 10. Sketch of an outcrop showing an aplite vein across the foliation of Wollaston biotite-hornblende granite | 1306 |
| 11. Sketch plan showing an elongated inclusion of biotite paragneiss in Wollaston pluton | 1306 |
| 12. Diagrammatic cross section across the Wollaston pluton | 1307 |
| 13. Diagrammatic sections illustrating the effect of intrusion of Wollaston pluton | 1307 |
| 14. Geological and structural map of the Deloro pluton | 1308 |
| 15. Variation in modal composition with respect to distance from margin in Chandos Lake syenite | 1311 |
| 16. Q-F-M and Q-Pl-Kf diagrams for rocks of the Chandos Lake pluton | 1312 |
| 17. Mineralogical variations in samples of the gabbro-diorite inclusions in Chandos Lake pluton | 1312 |
| 18. Q-F-M and Q-Pl-Kf diagrams for rocks of the Wollaston pluton | 1313 |
| 19. Variations in mineralogical composition across the Deloro pluton | 1317 |
| 20. Q-F-M and Q-Pl-Kf diagrams for rocks of the Deloro pluton | 1319 |
| 21. Orientation diagrams of quartz optic axes in granite, paragneiss, and granitized paragneiss | 1320 |


## TABLES


| Table | Page |
|---|---|
| 1. Joints in the Chandos Lake pluton | 1308 |
| 2. Joints in the Wollaston pluton | 1309 |
| 3. Mineralogical composition of the Chandos Lake pluton | 1309 |
| 4. Chemical analyses of representative samples of the granitic plutons | 1310 |
| 5. Color ratio of gabbro-diorite | 1313 |
| 6. Average modal composition of the biotite-hornblende granite, Wollaston pluton | 1314 |
| 7. Average modal composition of gray granite gneiss | 1316 |
| 8. Gradation of biotite-hornblende paragneiss to granite gneiss | 1316 |
| 9. Mineralogical composition of the Deloro pluton | 1317 |
| 10. Correlation among the minerals of perthite granite-syenite, Deloro pluton | 1318 |


## Introduction

### *General Statement*

A detailed structural and petrological study of three granitic plutons in the Grenville subprovince of Ontario was undertaken with the object of determining the manner and history of their emplacement. The three plutons are: (1) Chandos Lake pluton: area, 14 square miles, Chandos township, Peterborough County; (2) Wollaston pluton: area, 8 square miles, Wollaston township, Hastings County; (3) Deloro pluton: area, 20 square miles, Marmora and Madoc townships, Hastings County.

These plutons lie near the southern fringe of the Canadian Shield; the nearest important towns are Peterborough to the southwest, Bancroft to the north, and Madoc to the southeast (Fig. 1).

### *Scope of the Work*

The problem of emplacement of these bodies has been considered in two specific aspects:

(1) To determine whether these granitic bodies were produced *in situ* by metasomatic replacement of pre-existing country rocks, or whether they crystallized from an intrusive magma. The author is not immediately concerned with the origin of the magma or with the source of the solutions that might cause replacement. As will be shown in the following pages, the plutons under consideration originated essentially from intrusive magma.

(2) Having determined the magmatic origin

of the rocks, the second part of the problem is to find out as much as possible regarding the manner and history of emplacement of the magma. The following considerations are involved: (a) whether the pluton resulted from forceful emplacement, magmatic stoping, or cauldron subsidence; (b) whether the various parts of the pluton were emplaced simultaneously or successively; (c) determination of the direction of intrusion and the shape of the intrusive body; (d) the causes of the broad mineralogical and textural variations in the plutons; (e) determination of the temperature of formation of the granitic rocks.

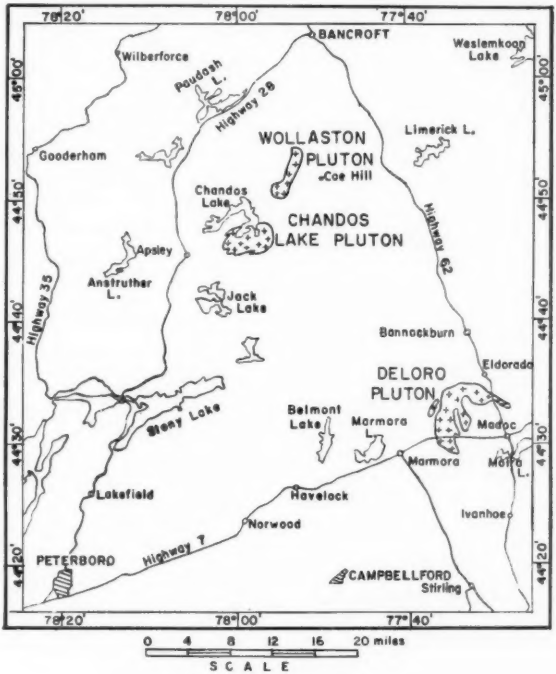


FIGURE 1.—LOCATION MAP

These problems were followed up, using as many diverse methods as possible, such as: (1) detailed geological mapping with special reference to the structures (foliation, lineation, and joints) of the plutons and the surrounding country rocks, on the scale of 4 inches equals 1 mile, using the air photographs of the Ontario Department of Lands and Forests; references to the locations of specific outcrops are given here according to the grid system used on the Department of National Defense topographical sheets; (2) detailed petrographic study of the samples collected to determine mineralogical and chemical variations; study of feldspar composition and of textures and structures; determination of $\alpha$ activity in a large number of samples of the pluton; chemical analyses of a few representative samples of rocks; (3) petrofabric study of the lattice orientation of quartz in the granite, inclusions, and country rocks; (4) geothermometric studies using the electronic decrepitation method; the results of such studies will be communicated in a separate paper.

A period of about 18 weeks during the summer of 1956 was spent in field work. Laboratory investigation of the samples took more than a year for completion.

*Acknowledgments*

The work embodied in this article was carried out in the Department of Geological Sciences, University of Toronto, with the financial assistance of the Government of Canada. Funds for

chemical analyses were provided by the Advisory Board on Research, University of Toronto. Profs. W. W. Moorhouse, F. G. Smith, and R. E. Deane provided valuable suggestions and criticisms in the course of this work. Sincere thanks are also due Dr. D. F. Hewitt, Messrs. D. A. Moddle, and R. Smith of the Ontario Department of Mines for assistance in various ways.

Professors Moorhouse and Smith, Drs. O. F. Tuttle and C. H. Stockwell were kind enough to review the manuscript critically.

### *Previous Work*

A good, concise summary of the previous geological work in the Grenville region of Ontario has been given by Hewitt (1956). Fairly intensive geological mapping and economic minerals investigations have been carried out in this region during the last 100 years. The recent compilation of the geological map of Haliburton-Bancroft region on the scale of 1 inch equals 2 miles (Hewitt *et al.*, 1957), includes all the three plutons under consideration; the excellent geological maps by Wilson (1940a; 1940b) show the Deloro pluton and the associated metasedimentary and volcanic rocks.

The classic memoir of Adams and Barlow (1910) gives a good account of the regional geology, including some interesting general observations on the structure and mode of emplacement of the granitic bodies in the Hastings and Peterborough counties. According to them, the granitic bodies in this region are projections from a huge batholith underlying the metasedimentary and volcanic rocks. With regard to the Chandos Lake pluton and the adjacent Methuen batholith, they observed that the surrounding rocks ". . . are found in almost all cases to dip inward toward the invading granite-gneiss. . . . These masses have evidently eaten their way up into downward sagging portions of the overlying sedimentary series."

From a brief study of the structures in the Chandos Lake pluton, Cloos (1934) found that it is a funnel-shaped body with inward-dipping contacts. In view of the systematic orientation of the wall-rock fragments with the magma stream, Cloos ruled out the probability of a foundering roof over a larger batholithic mass. He observed that ". . . the granite-filled funnel is not part of a batholith underneath, but one of the many openings through which the magma has reached higher levels, in close relation with the surrounding wall-rock structure."

Tuttle (1952) described a sample of Deloro granite as a typical perthite granite, in which no recrystallization has taken place.

No other published report on the three granitic plutons under consideration is available. Within recent years, however, a few granitic plutons in the Grenville region of Ontario have been studied in detail, *viz.*, the Burleigh, Anstruther, Cheddar, and Cardiff "batholiths" (Hewitt, 1957, unpub. ms.), the granitic rocks around the Clair River syncline (Ambrose and Burns, 1956), the Westport pluton near Kingston (Wynne-Edwards, 1957), and the granitic and pegmatitic rocks of Monteagle township (Peach, 1950, Ph.D. thesis, Univ. Toronto).

## General Geology

### *Regional Setting*

The Chandos Lake and Wollaston plutons are situated on what Hewitt (1956) calls the Methuen "segment" of the Haliburton Highland zone, which is an area of relatively high-grade metamorphism (amphibolite facies); the Deloro pluton lies in the Hastings basin, which is an area of low-grade metamorphism (greenschist facies).

The main geological units in the areas studied by the present author are as follows:

Paleozoic limestones and shales
Unconformity
Granite and syenite
Gabbro-diabase-diorite
Grenville series
2. Bluish crystalline limestone and dolomite, conglomerate, slates with interbanded acid and intermediate volcanic rocks.
1. Crystalline limestone, calcareous paragneiss, biotite paragneiss (including rusty-brown paragneiss)

The bluish limestone, conglomerate, and slate (around the Deloro pluton), shown here in the upper part of the Grenville series, were considered by Miller and Knight (1914) and Wilson (1940a) as belonging to the "Hastings series", which was supposed to overlie the volcanic rocks of the Grenville series with a conglomerate zone at the base. According to Miller and Knight, certain granites intruding the Grenville series underlie the Hastings series; Wilson, however, found that these granites actually intrude the Hastings series.

Subsequent work in parts of Eastern Ontario

by Harding (1942), Smith (1951), and Ambrose and Burns (1956) has indicated that grade of metamorphism and lithology are not valid criteria for distinguishing the Hastings from the Grenville series. Important conglomerate members are found in the Hastings-Grenville sequence at least at three horizons. Granitized sedimentary rocks of high metamorphic grade lie stratigraphically above the "Hastings-type" conglomerate and blue limestone. A number of acid to intermediate volcanic bands in the typical "Hastings-type" blue limestones have been noted by the present author for the first time in the areas west of the Deloro pluton (Fig. 14).

The Grenville metasedimentary and volcanic rocks are strongly folded, in some places isoclinally, along a northeast-trending axis, but another northwest-southeast fold axis also is discernible at places. The gabbroic bodies were intruded into the folded sequence, probably at a late stage of metamorphism, for they are metamorphosed to a low degree. Most of the gabbroic bodies within the present area occur as narrow sills or small patches in the metasedimentary rocks or as inclusions in the Chandos Lake and Deloro plutons. Evidence presented below indicates that the granitic bodies were emplaced somewhat later than the basic intrusions.

### *General Characters of the Plutons*

The Chandos Lake and Wollaston plutons consist of foliated granites and syenites, whereas the Deloro pluton is made up of relatively massive rocks.

The Chandos Lake pluton (Fig. 6) is roughly elliptical in shape; its east-west diameter is 5 miles, and its north-south diameter is 3 miles. It consists of a central body of syenite-monzonite, several large inclusions of diorite-gabbro, and an outer complex of biotite granite grading into granodiorite.

The Wollaston body (Fig. 9) of gneissic biotite-hornblende granite extends 6 miles in a north-northeast direction and is about 1½ miles in width. A series of roof pendants, partly biotite-hornblende paragneiss and crystalline limestone and partly a gray granite gneiss, divides the pluton into roughly equal halves. There are a number of offshooting dikes and sills of granite; one of the dikes has been traced for more than 1½ miles.

The Deloro pluton (Fig. 14) is a composite body, made up of (1) a north-south elongated body of perthite granite and syenite, about 6 miles by 2 miles, with an east-southeast projection from the north end, and (2) an oval body of granophyric granite, covering about 4 square miles in the eastern part of the pluton.

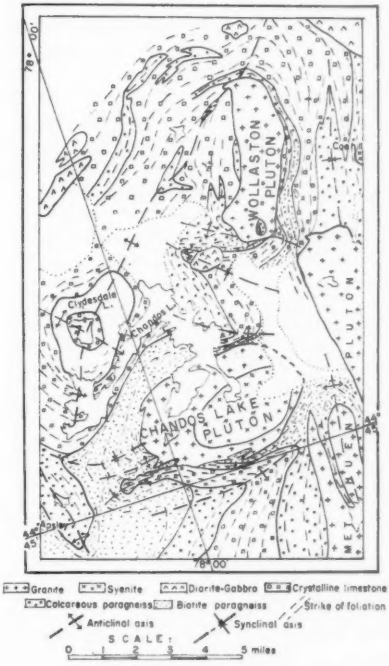


FIGURE 2.—REGIONAL STRUCTURE MAP OF THE COUNTRY BETWEEN APSLEY AND COE HILL, ONTARIO

A cross-folded pattern of the metamorphic rocks is characteristic.

## REGIONAL STRUCTURE AROUND CHANDOS LAKE AND WOLLASTON PLUTONS

### *General Statement*

The country rocks of this area (Fig. 2) are mainly crystalline limestones, together with biotite paragneisses, calcareous paragneisses, and several isolated gabbro-diorite intrusions. Pronounced sedimentary or structural facies changes are common; gradations between the calcareous paragneiss and the biotite paragneiss are particularly common.

### *Principles of Reconstruction*

Figure 2 is the result of an attempt to reconstruct the broad fold axes in the area on the basis of the following data and assumptions:

(1) Foliation data collected by the present author were supplemented by data from the North Hastings sheet by Adams and Barlow (1905) and also from the new map of the Haliburton-Bancroft area (Hewitt *et al.*, 1957).

(2) With rare exceptions, schistosity or foliation parallels the bedding as inferred from the compositional bands and the broad stratigraphic contacts. Even in the crestal regions of the major folds, foliations in the crystalline limestone and the paragneiss alike are parallel to the bedding. Foliation may thus be regarded as approximately parallel to bedding.

(3) Configuration of the stratigraphic units on the map has helped delineation of the fold axes.

### *Folding*

The regional structure map in Figure 2 shows two major sets of fold axes:

(1) The main set trends north-northeast or northeast. A major anticline belonging to this set runs across the Clydesdale Lake and intersects the northwest corner of the Wollaston pluton and can be traced for at least 14 miles; north of Clydesdale Lake, it has a gentle to moderate plunge to the north, and south of it, the plunge is to the south. Intersection of this anticline with a minor northwest-trending anticline has produced a dome structure at the site of Clydesdale Lake.

(2) The other set of relatively nonpersistent folds with moderate to steep plunges trends east-west to southeast-northwest. Individual fold axes of this set do not generally persist for more than 3 miles.

Some of the complex crumplings (overfolds in most cases) seen in the crystalline limestones appear to be in part due to the compression caused by the intrusion of the plutons; the frequency and complexity of such folds increase toward the contacts of the plutons. Trends of such fold axes are rather irregular and bear little or no relationship to the major fold axes.

### *Lineation*

Lineations parallel to the two sets of fold axes have been found. Those parallel to the major northeasterly folds are relatively rare. They consist of minor crinkles that plunge gently south-southwest or northeast (up to 30°); in some places the crinkles in the paragneiss are accompanied by a mineral lineation due to parallelism of biotite flakes. Lineation parallel to the fold axes that trend southeast-northwest is more prominent. It is best developed near Owenbrook, where prominent puckers and drag folds in calcareous paragneiss plunge 30°–60° S.-SE., parallel to the axis of the anticline there.

### *Relative Ages of the Cross Folds*

Lineation with an east-west bearing continues across the major north-northeast–south-southwest anticlinal axis, east of Lasswade (Fig. 2). This lineation is not related to the major fold here, because it is neither parallel nor perpendicular to that fold axis; in other words, it could be regarded neither as *a* lineation, nor as *b* lineation with respect to the north-northeast-trending fold. Although presence of lineation oblique to the fabric axes has been claimed by Kvale (1953) from the Caledonides of Norway, the mechanism of formation of such lineation is not properly understood. In the present case, however, the lineation can be explained by assuming that it is parallel to the fold axes belonging to the second set. In fact there is such an east-west anticlinal axis about a mile southwest of this locality.

This evidence of the continuation of the lineation parallel to the second set of folds across the nose of the first suggests that the second set formed later than the first set. The same inference is suggested also by the fact that the more prominent fold axes of the first set are parallel to the regional trend of the strike and appear to be related to the same period of movement that produced the foliation in the metasedimentary rocks. The second set of folds represents shortening of the strata in a northeast-southwest direction and appears to have involved local rotation of the already existing northeast-trending folds around steeply plunging northwest-southeast or east-west axes.

This idea of the northeast-trending major fold movements being succeeded by a second stage of east-west to northwest-southeast folding is supported also by the statistical study of quartz orientation in the paragneiss. Orientation diagrams of quartz c axes in four samples of paragneiss are given in Figure 21 A–D. All these diagrams show two girdles; one of the girdles (*ac*) is peripheral to the megascopic *b* lineation, and the other one makes an angle of 5°–35° with the *bc* plane. The second girdle is progressively better developed in L 111 A, L 500 A, and W 908; in W 11, it is more prominent than the *ac* girdle. The visible *b* lineation in these samples corresponds to the axis of the folds trending northwest-southeast, with moderate to steep plunges; the axes of the second girdle corre-

spond to those of the gently plunging northeast-southwest folds (Fig. 3).

Quartz fabric diagrams with intersecting girdles (also called B ∧ B′ tectonite) have been

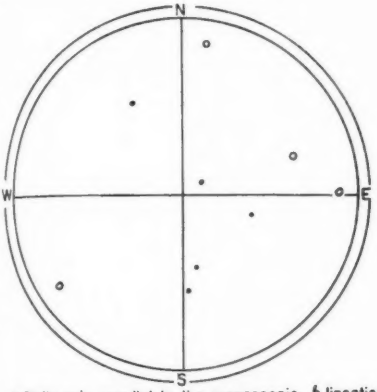


FIGURE 3.—AXES OF GIRDLES IN THE QUARTZ ORIENTATION DIAGRAMS FOR SAMPLES OF BIOTITE PARAGNEISS

Girdle axes parallel to the megascopic *b* lineation correspond to the axes of northwest- to southeast-trending folds; axes of the second girdle correspond to the regional northeast-southwest folds.

interpreted in some cases as due to movements in a single period of deformation. But in such cases, either two girdles would be developed in all the samples to the same extent, or the angle between the two would always approximate 90° (Turner and Verhoogen, 1951, p. 555–556). In the present case, the angle between the two girdles is variable and is never 90°; the second girdle has an extremely variable degree of prominence, which suggests that it is possibly a relict feature. Apparently, during the later stage of fold movements with northwest-southeast axis, the fabric of quartz was partially reconstituted, so that the earlier fabric pattern is still recognizable.

Similar conclusions on two successive directions of fold movements have been made recently for certain other areas in the Grenville subprovince, *viz.*, in the Westport area near Kingston, Ontario (Wynne-Edwards, 1957), and in the Balmat-Edwards district of New York (Brown and Engel, 1956).

### *Structural Setting of the Plutons*

The result of these successive fold movements has been to produce a number of structural domes (or culminations) and basins (or depressions) in this region. The Chandos Lake pluton occupies the site of a basin, bounded by two major northeast-trending anticlines to the northwest and southeast respectively and two relatively minor east-west and northwest- to southeast-trending anticlines (belonging to the second set of fold axes) to the south and northeast respectively. The country rocks dip from all sides toward the pluton, and the amount of dip increases as the granite margin is approached. The foliation in the granite dips away from the contact, except in the southwestern part. Although the strike of foliation in the granite is invariably parallel to the contact, its dip is generally much higher than that of the country rocks. The granite boundary intersects the strike of foliation of the country rocks at numerous places. Therefore this pluton is not concordant.

The Wollaston pluton occupies the flank of a major northeast-trending anticline, whose axis is intersected by the northwestern tip of the pluton. The structures of the country rock, broadly parallel to the granite boundary, tend to bend around the southern and northern ends of this elongated body. This pluton (Fig. 9), also, is not strictly concordant, as seen from (1) the discordances in strike along the southeastern border of the pluton, and (2) dips of the country rocks (20°–45° E.) considerably lower than those of the granite foliation (55°–80° E.) along the western contact of the pluton.

### *Fold Movements Earlier Than the Emplacement of the Plutons*

The following evidences suggest that the plutons under consideration were emplaced subsequent to both stages of folding that affected the country rocks: (1) The Chandos Lake pluton crosscuts a few fold axes belonging to the second set at its western border. These fold axes do not show any tendency to continue into the pluton; (2) the patterns of foliation and lineation in both the plutons are distinctly different from those of the country rocks. Figure 4 indicates clearly the independence in attitude between the lineations in the two plutons and those in the adjacent country rocks. As shown below, foliation and lineation in these plutons are of primary origin; there is no evidence of any foliation or lineation of secondary origin.

This idea of the post-tectonic origin of the present plutons contradicts that of Adams and

Barlow (1910, p. 50), who regarded the granitic bodies in this region as having been emplaced contemporaneously with the regional northeast-trending folding.

toward north and south is also clearly indicated. Along the southwest and south border of the Deloro pluton, there is a tight syncline, overturned in places to the southwest. This fold

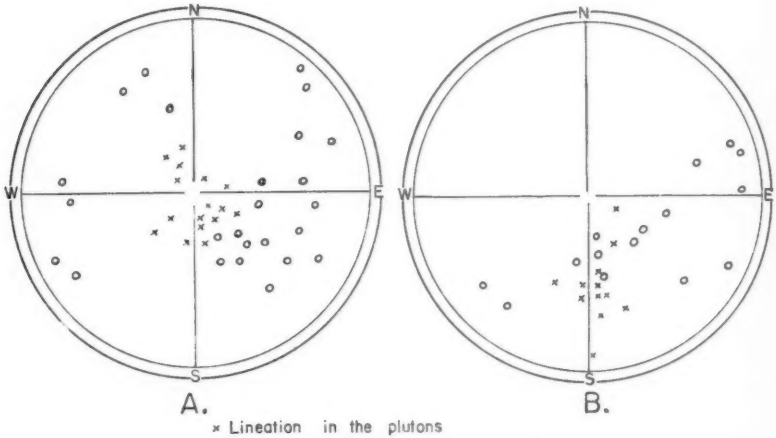


FIGURE 4.—EQUAL-AREA PROJECTION OF THE MEASURED LINEATIONS
A. Chandos Lake granite and adjacent metamorphic rocks
B. Wollaston granite and adjacent metamorphic rocks
The data indicate independence in attitude between the lineations in the plutons and those in the adjacent rocks.

## REGIONAL STRUCTURE AROUND THE DELORO PLUTON

On the basis of the excellent geological maps by Wilson (1940a; 1940b), supplemented by personal observations and measurements of the attitudes of bedding and foliation in the country rocks around the Deloro pluton, an attempt has been made to interpret the regional structure of this area (Fig. 5).

The country rocks consist of fine-grained crystalline limestone, slate, phyllite, conglomerate, and patches of metavolcanic rocks (trachytic-andesitic in composition). They show recognizable bedding in most outcrops. It is recognized in the conglomerate by the arrangement of pebbles, in the volcanic rocks by well-defined color bands and locally by the arrangement of vesicles, and in the limestones by color bands and the chloritic partings parallel to them.

Figure 5 shows a number of east or east-northeast folds, some of which are overturned, usually toward the north. The tendency of the Deloro pluton to push aside these fold axes could be due to the compression generated by the intrusion of the pluton.

## INTERNAL STRUCTURES OF THE PLUTONS

### *Chandos Lake Pluton*

*Foliation and lineation.*—Foliation in the rocks of this pluton (Fig. 6) consists of the following: (1) Planar arrangement of streaky patches of biotite and hornblende, of tabular crystals of perthitic microcline, and of granular quartz aggregates; (2) arrangement of small inclusions (biotite paragneiss and amphibolite) in parallel planes. Foliation is seen practically all over the pluton, except in some areas of the central syenite, where the rock is massive. A rude downdip lineation, caused by the linear arrangement of mineral patches and inclusions on the foliation planes, can be made out in some outcrops; usually such lineation is indistinct, and measurement of it is often subject to personal bias. In this respect, the present author cannot agree with Cloos (1934), who found lineation to be very prominent throughout this pluton. As already indicated (Fig. 4A), the

trends of lineation in this pluton are distinct from those in the associated paragneiss.

The primary origin of the foliation and lineation is indicated by:

The above evidence suggests that the foliation and lineation within the pluton are due to some sort of fluidal movement, but one could still argue from the transformist point of view

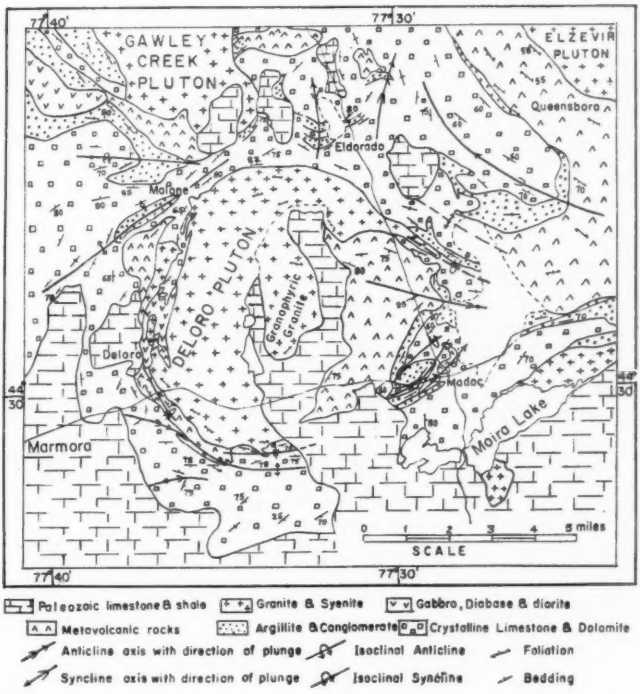


FIGURE 5.—REGIONAL STRUCTURE MAP OF THE AREA AROUND THE DELORO PLUTON
The Deloro pluton appears to have pushed aside the regional east-northeast folds

(1) Parallelism of foliation with the margin of the pluton, even where the contact is transverse to the foliation in the country rocks, such as in the southwestern part of the pluton.

(2) Clear evidence of fluidal flow is indicated by the numerous instances of the foliation in granite and syenite sweeping around the inclusions of biotite paragneiss and amphibolite. Rotation of some of the inclusions in a fluidal environment is indicated by the fact that the foliation in them is at an angle (in places, at about one right angle) with the foliation in the surrounding granite.

(3) The foliation varies in trend and dip within short distances, in many cases within the same outcrop; it is always irregularly wavy and never so sharp and straight as in a metamorphic gneiss.

that, during granitization by pegmatitic and hydrothermal solutions, the replaced country rocks might have become partially mobile from the heat consequent on intense granitization. Such mobile materials could flow around the unreplaced remnants and also parallel to the margins of the granitized body. This appears unlikely, because in that case, (1) one would not expect the regular pattern of foliation (funnel-shaped with two centers), as seen in the Chandos Lake pluton; (2) the generally sharp contacts between the pluton and the country rocks would be unlikely.

*Shape of the pluton.*—As the foliation and lineation in this pluton are of primary origin, an idea of its shape and direction of intrusion may be obtained from the pattern of foliation and lineation.

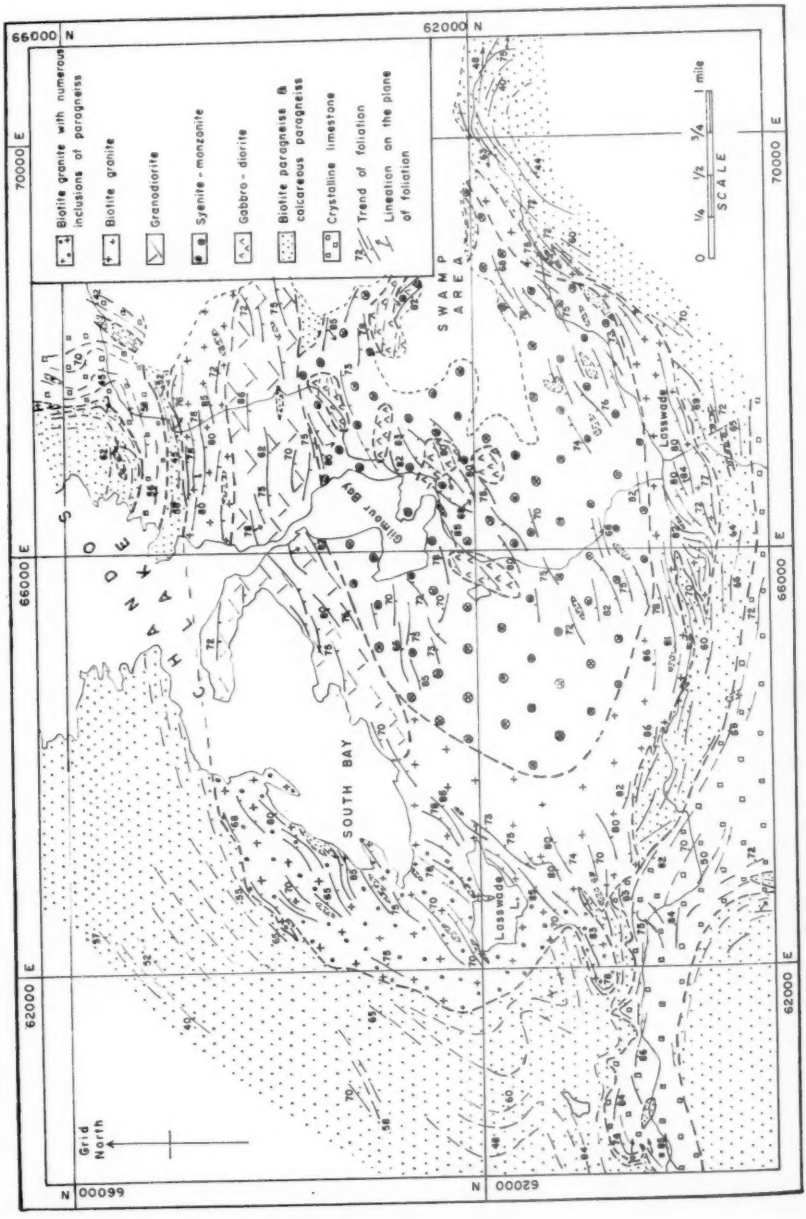


FIGURE 6.—GEOLOGICAL AND STRUCTURAL MAP OF THE CHANDOS LAKE PLUTON

The shape of the pluton so inferred is that of a funnel with the walls dipping inward from all sides at angles of 70°–82° (Fig. 7), except in the southwestern side, where the southern wall apparently dips outward. The central body of syenite-monzonite also appears to be funnel-shaped.

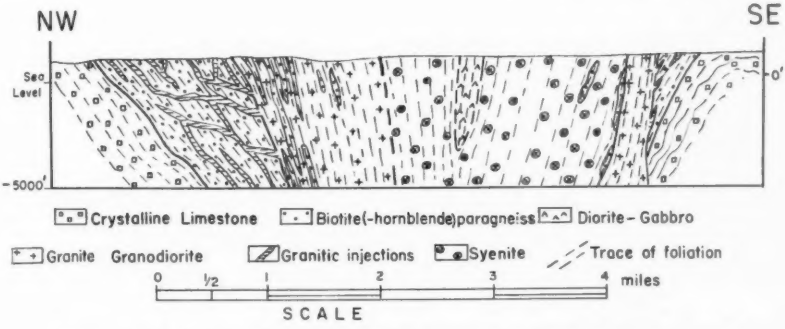


FIGURE 7.—DIAGRAMMATIC CROSS SECTION ACROSS THE CHANDOS LAKE PLUTON

The inward-dipping foliation planes form two centers or loops. One of these centers is occupied by an inclusion of gabbro, southeast of Gilmour Bay; the other center lies off the southwestern inlet of the same bay. These centers might represent the centers of upwelling of the magmatic mush, and possibly the downward extension of their positions represents the locations of the vents through which the magma came up and extended outward.

The northwestern part of the pluton contains a large proportion of paragneissic inclusions of various dimensions, all of which strike northeast and dip southeast. This region consists of a network of sills and dikes crisscrossing through the biotite paragneiss; the ratio of granite to paragneiss is approximately 2:1. The larger paragneissic remnants do not appear to have been displaced, however, and may be considered as roof pendants, as pictured in the diagrammatic cross section across the pluton (Fig. 7).

*Joints.*—A statistical study of the joints in a large number of outcrops of the pluton indicates that the pattern of jointing all over the intrusion tends to have similar azimuthal trends; the presence of five sets of joints is indicated. These, in order of abundance, are as shown in Table 1.

None of these joints has a symmetrical relationship with the foliation and lineation, as would be expected in the case of primary joints. Most of the joints are open, except for thin veneers of chlorite and sericite on some of the joint surfaces. Thin pegmatite and aplite veins occur in a few places along the joints of sets I, II, and IV, but pegmatites along any of these sets of joints may be cut across by joints of the other sets. No distinct age differences between the joint sets could be established.

TABLE 1.—JOINTS IN THE CHANDOS LAKE PLUTON

(In order of abundance)

| Set no. | Average strike | Average dip |
|---|---|---|
| I | N. 18° E. | Vertical |
| II | S. 60° E. | Vertical |
| III | S. 85° E. | Vertical |
| IV | S. 30° E. | Vertical |
| V | N. 60° E. | 82° SE. |

The most important set of joints in the country rocks within half a mile to 1 mile from the pluton is the north-northeast set, whose trend is fairly constant throughout the area; the other sets do not appear to have any regional trend. A large number of pegmatite and granite dikes lie along the north-northeast joint planes (Fig. 8).

Cloos (1934) observed that the joints in this pluton are "problematical" and that they do not resemble the joints related to flow structure in other regions. The present study indicates that although these joints are not of primary origin, their formation took place in part during the separation of the pegmatitic and aplitic phases from the magma. By this time the stresses due to the magma movements were replaced largely by regional stresses.

*Syenite-granite relationship.*—The contact be-

FIGURE 6.—GEOLOGICAL AND STRUCTURAL MAP OF THE CHANDOS LAKE PLUTON

tween the syenite-monzonite core and the marginal granodiorite-granite appears to be sharp. Although the exact contact between the two has not been observed, sharp variations in lithology have been noticed between outcrops, barely 200 feet apart. Several patches of paragneiss intervene between the outcrops of granite and syenite in the vicinity of Lasswade; apparently they represent remnants of the country rock along the border of the syenite. Veins of granite in syenite were observed east of Gilmour Bay at grids 63400 N.: 67100 E. and also in the roadside outcrops at 61500 N.: 65800 E.; the syenite therefore formed earlier than the granite.

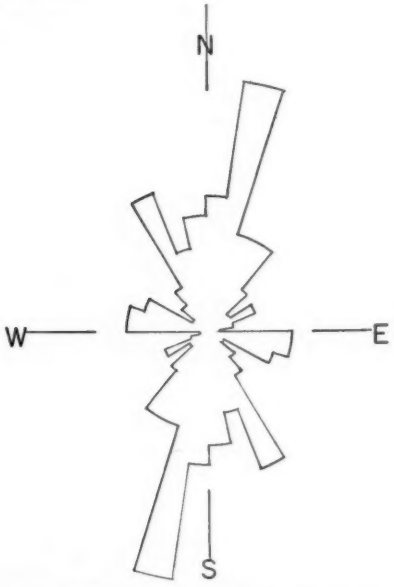


FIGURE 8.—ORIENTATION OF 85 PEGMATITE AND GRANITE DIKES AROUND THE CHANDOS LAKE PLUTON

### *Wollaston Pluton*

*Foliation.*—The character of the foliation in Wollaston pluton (Fig. 9) is similar to that in the Chandos Lake pluton and is considered primary for similar reasons. In addition, one special line of evidence is available here, as exemplified by an outcrop of granite near the southern border of the pluton. At this place, an aplite vein 4 inches wide cuts across the foliation in coarse-grained, gneissic biotite-hornblende granite (Fig. 10); within the vein is a narrow inclusion 6 inches long of the same type of gneissic granite. The inference is that the coarse granite must have been already foliated when the aplites, which represent the late phase of the granite magma, cut across the granite; in other words, the foliation is of primary origin.

A predominant north-northeast trend of the foliation with a steep easterly dip is characteristic of this pluton. The foliation, which is parallel to the granite border, is less steep along the western border (55°–75°E.) than along the eastern border (75°–85°E. or vertical); steep westerly dips are also found in a few places near the eastern border.

*Lineation.*—Linear arrangement of biotite-hornblende aggregates on the plane of foliation has given rise in places to linear structures with moderate to gentle south or south-southeast plunge; this suggests a probable south to north movement of the magma inclined at about 45° with the horizontal. Figure 4 indicates that the attitudes of the lineations in the pluton are different from those in the surrounding country rocks.

*Inclusions and roof pendants.*—Inclusions of paragneiss and crystalline limestone arranged subparallel to the foliation in the granite are locally common. Some of these inclusions are abnormally long; most spectacular of these is an inclusion of biotite paragneiss 5–8 feet wide extending north-northwest and traceable for more than 200 feet (Fig. 11). A series of three roof pendants along the length of the pluton divides it into two nearly equal areas of outcrop (Fig. 9). The two northerly roof pendants are made up of gray granite-gneiss, which, on evidence presented below, represents granitized biotite-hornblende paragneiss. The southern patch consists of crystalline limestone, overlain by calcareous paragneiss, all dipping steeply eastward.

Several lines of evidence indicate that at least at the present level of erosion, Wollaston pluton was emplaced as two bodies of granite magma, separated by a screen of country rocks, only parts of which are preserved as the three above-mentioned roof pendants; the rest became engulfed in the magma:

(1) The foliation in granite forms two sweeping loops at the southern end of the pluton, one to the west and the other to the east of the roof pendant (Fig. 9).

(2) Assuming that the gaps along the line of roof pendants represent country rocks engulfed

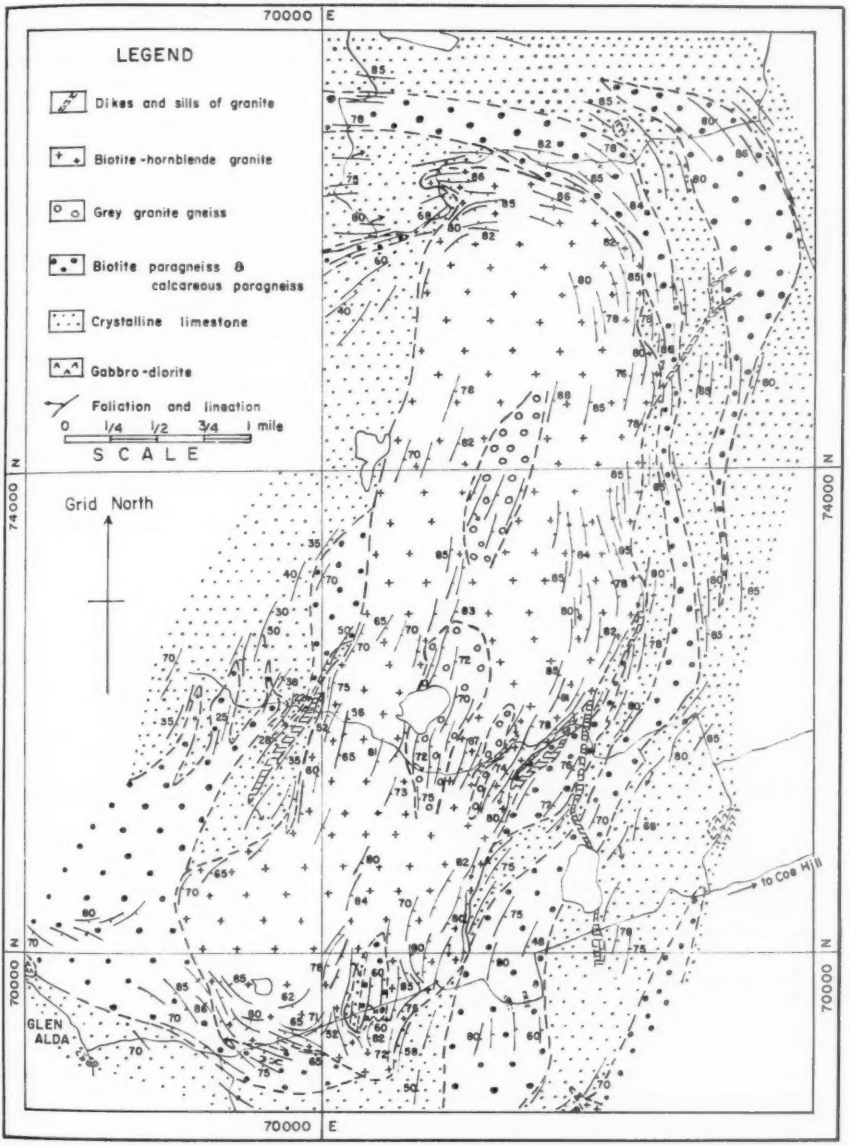


FIGURE 9.—GEOLOGICAL AND STRUCTURAL MAP OF THE WOLLASTON PLUTON

in the magma, one can visualize a screen of country rocks extending from the south end of the pluton to about a mile south of the north end of the pluton.

(3) As described in the section on petrology, the granitic rocks of this pluton tend to be more sodic and less mafic toward the borders; the same tendency has been noted in places also with respect to the contacts with the central granitized patch.

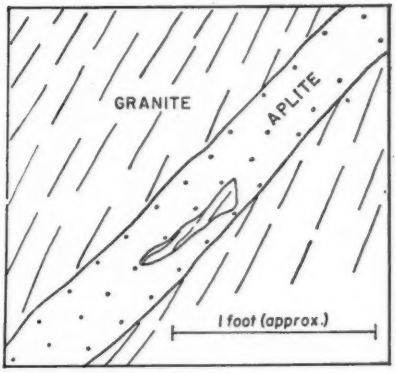


FIGURE 10.—SKETCH OF AN OUTCROP SHOWING AN APLITE VEIN ACROSS THE FOLIATION OF WOLLASTON BIOTITE-HORNBLENDE GRANITE
Near southern border of the Wollaston pluton (tracing from a photograph)

and lineation suggests that this pluton is a steep, east-dipping body; the western wall dips more gently than the eastern wall. At least at the present level of erosion, the body tends to become narrower in depth (Fig. 12).

It appears that the granite magma producing this pluton cut through the flank of a major northeast-trending anticline, slightly oblique to the foliation of the rocks. As the magma moved upward and northward toward the crest of the anticline it also expanded slightly outward. Consequent on such expansion, the east-dipping country rocks along the western border of the pluton were dragged up, and the rocks along the eastern wall were pushed eastward and upward, producing the steeper dips and in a few places overturning along the contact zone (Fig. 13). The effect of forceful intrusion also broadened the crest area of the anticline at the northern end of the pluton. The tendency of the upward

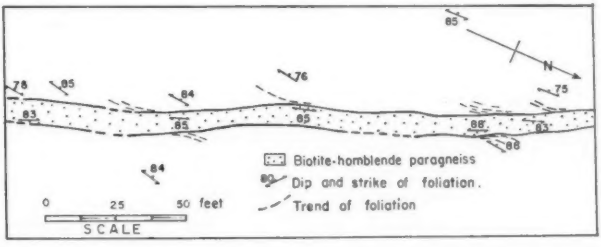


FIGURE 11.—SKETCH PLAN SHOWING AN ELONGATED INCLUSION OF BIOTITE PARAGNEISS IN THE BIOTITE-HORNBLENDE GRANITE, WOLLASTON PLUTON

*Joints.*—As in the Chandos Lake pluton, the joints in Wollaston pluton show no correlation with foliation and lineation and seem to have a general pattern all over the pluton. Altogether six sets of joints can be made out (Table 2).

As in the case of the Chandos Lake pluton, the most prominent joint, in many cases filled with pegmatite and aplite, is a north-northeast set.

*Granite offshoots.*—The presence of four dikes of granite projecting from the eastern border and one sill 60–100 feet thick branching from the western border of the pluton is of particular interest. The longest of these is the dike 50–100 feet wide projecting from the main body at grids 72000 N.: 72100 E. and extending southward obliquely across the paragneiss-crystalline limestone sequence for more than 1½ miles.

*Shape of the pluton.*—The pattern of foliation

TABLE 2.—JOINTS IN THE WOLLASTON PLUTON
(In order of abundance)

| Set no. | Average strike | Average dip |
|---|---|---|
| I | N. 14° E. | 86° E. |
| IIIa | N. 88° E. | Vertical |
| IIIb | S. 72° E. | Vertical |
| II | N. 42° E. | 87° SE. |
| V | S. 15° E. | Vertical |
| IV | S. 50° E. | Vertical |

expansion of the magma could be explained partly by dilatational distortions of the strata toward the crest of the anticline, which would facilitate the intrusion of the magma as it moved upward.

*Deloro Pluton*

*General relations.*—Unlike the Chandos Lake and Wollaston plutons, the granites and syenites of the Deloro pluton (Fig. 14) are essentially massive rocks with practically no foliation or lineation. In a few places one observes foliation due to a parallel arrangement of small clots of inclusions with steep dip and approximately parallel in trend to that of the nearest granite border. From such data nothing conclusive can be said regarding the dip of the granite walls, except that they appear to dip steeply either inward or outward.

The body of granophyric granite, occupying 4 square miles in the eastern part of the pluton, is younger than the perthite granite and syenite, which make up the bulk of the pluton. The evidence is:

(1) The perthite granite is injected by thin veins, irregular injections, and dikes of granophyric granite. Such injections become more and more common as the main body of granophyric granite is approached.

(2) The granophyric granite is generally very fine-grained at the contact with perthite granite and tends to become coarser away from the contact.

*Joints.*—A pattern of intersecting lineaments, represented by bushy and swampy low ground between the blocks of bare rocky areas, shows up nicely in the air photographs. The frequency distribution of the orientation of these lineaments (in terms of length) indicates the follow-

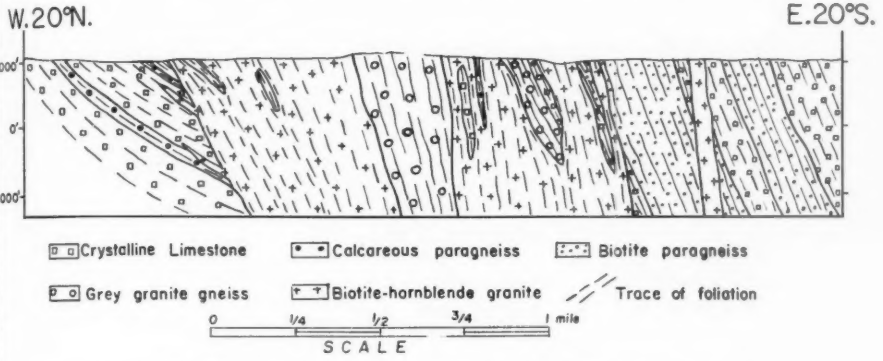


FIGURE 12.—DIAGRAMMATIC CROSS SECTION ACROSS THE WOLLASTON PLUTON

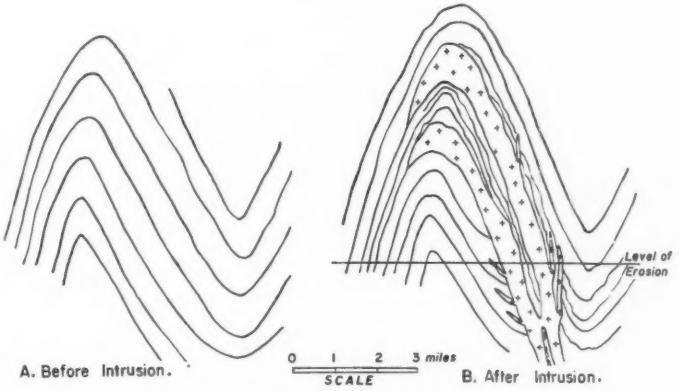


FIGURE 13.—DIAGRAMMATIC SECTIONS ILLUSTRATING THE EFFECT OF INTRUSION OF THE WOLLASTON PLUTON

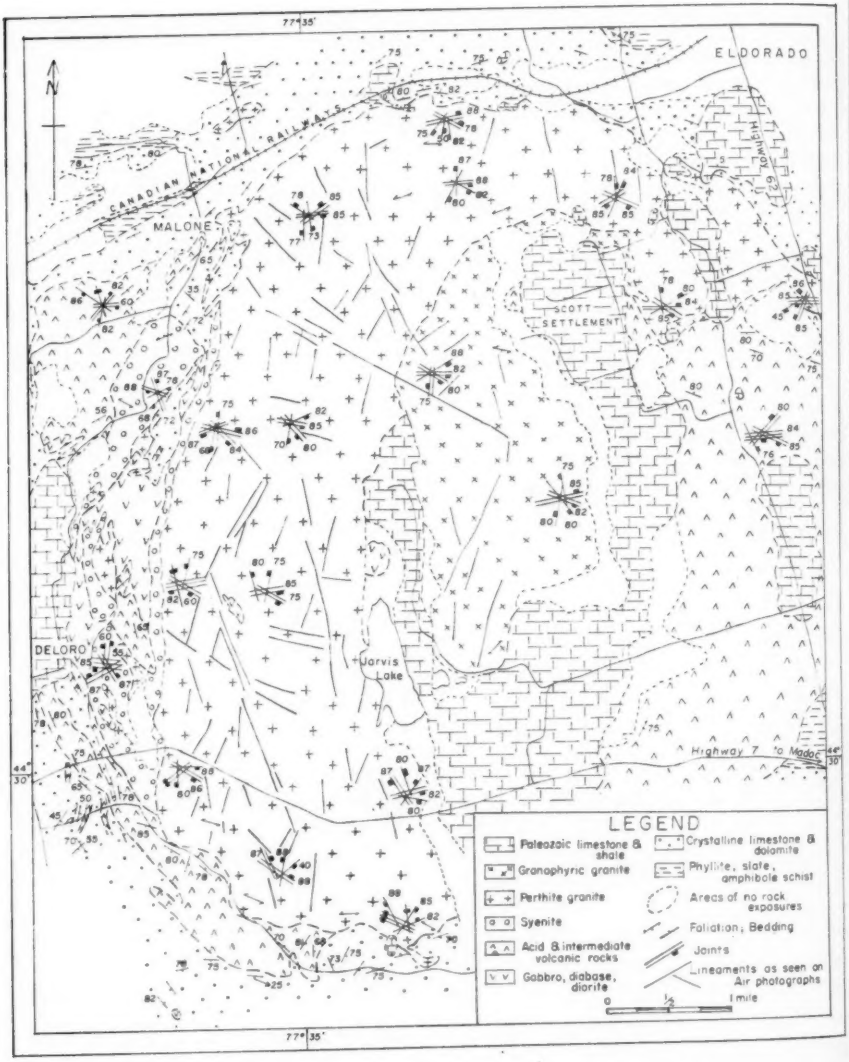


FIGURE 14.—GEOLOGICAL AND STRUCTURAL MAP OF THE DELORO PLUTON

ing maxima (in order of abundance): N. 15° E., S. 10° E., S. 25° E., S. 80° E., S. 65° E.

The north-northeast lineament is by far the most prominent. Systematic measurements of joints in the pluton indicate, however, that two east-trending sets of joints are by far the most prominent and that the north-northeast set is not prominent (Fig. 14). Dominance of north-northeast lineaments, as seen on the air photos, is to be ascribed to the effects of Pleistocene glaciation; a south-southwest movement of the ice is indicated on the numerous striated pavements in the area.

As in the other two plutons, a general uniformity in the pattern of joints in the different parts of the pluton is also evident in this pluton. All these joints appear to be essentially shear joints and originated later than the injection of

the granophyric granites but earlier than or simultaneously with the hydrothermal alteration of the granites (chloritization, hematitization), because materials so altered occur along these joint planes.

in such a body. Assimilation of varied rock types by an intrusive magma would, in general, produce unsystematic variations, giving rise to poor correlation among the constituents of the rock.

TABLE 3.—MINERALOGICAL COMPOSITION OF THE CHANDOS LAKE PLUTON
(All values in volume per cent)

| Minerals | Syenite (15 samples) | | Biotite granite (18 samples) | | Granodiorite (9 samples) | |
|---|---|---|---|---|---|---|
| | Average composition | Standard deviation | Average composition | Standard deviation | Average composition | Standard deviation |
| Quartz | 2.1 | 2.2 | 25.1 | 6.7 | 24.0 | 5.5 |
| Plagioclase | 40.6 | 6.1 | 32.2 | 7.6 | 50.3 | 5.9 |
| Microcline-microperthite | 45.9 | 10.4 | 36.5 | 7.7 | 12.8 | 6.1 |
| Biotite + chlorite + hornblende | 8.1 | 6.3 | 3.7 | 1.9 | 11.4 | 2.8 |
| Magnetite | 1.6 | ..... | 0.8 | — | 0.2 | — |
| Rest | 1.7 | ..... | 1.7 | — | 1.3 | — |

## MINERALOGICAL AND CHEMICAL VARIATIONS IN THE PLUTONS

### *General Statement*

Petrological work on the samples from the plutons and the associated country rocks was directed toward obtaining as full a picture as possible of the history of emplacement of the plutons. In addition to the usual qualitative study of the textures and microstructures of these rocks, an attempt was made to find out the quantitative variations in the different parts of the plutons, through modal analyses (using a point counter), optical determinations of the feldspar compositions, determinations of $\alpha$ activity (using an $\alpha$-scintillation counter on powdered samples), and a few chemical analyses. For each of the plutons, compositions of the modally analyzed samples were plotted on quartz (Q)-feldspar(F)-mafic minerals (M), and quartz(Q)-plagioclase(Pl)-potassium feldspar (Kf) diagrams.

The correlation coefficients between the various mineral constituents in particular plutons were made use of in making petrogenic inferences. Thus, for example, good correlations among the various constituents of samples from an igneous rock body should support magmatic differentiation as the prime cause of variation

### *Variations in the Chandos Lake Pluton*

As already stated, the Chandos Lake pluton is made up of a central body of syenite-monzonite (with several large inclusions of gabbrodiorite) and an outer complex of biotite granite grading to granodiorite.

SYENITE-MONZONITE: The rock is a medium- to coarse-grained aggregate of oligoclase ($An_{18}$–$An_{22}$), microcline-microperthite, and biotite, together with a very small proportion of quartz and also a little hornblende, muscovite, and calcite. Oligoclase is typically in the form of granular aggregates, whereas microcline occurs as coarser well-crystallized grains. The average modal composition of the rock, as calculated from the modal analyses of 15 specimens, is given in Table 3. The $\alpha$ activity of the rock is low and ranges 0.1–0.7 $\alpha/cm^2$/hour.

Chemical analysis of a typical sample of the rock (L668) and its molecular norm (Barth, 1952, p. 76–81) and modal analysis are given in Table 4.

The syenites tend to become more acidic from the center toward the margin of the body (Fig. 15). The changes involved are: (1) potassium increases and (2) decreases of mafic minerals, plagioclase, and anorthite content of plagioclase. In addition, good correlations exist among the proportions of the different minerals, as

TABLE 4.—CHEMICAL ANALYSES OF REPRESENTATIVE SAMPLES OF THE GRANITIC PLUTONS

| | L 219 Granodiorite, Chandos Lake | L 668 Syenite, Chandos Lake | W 608 Granite, Wollaston | W 487 Gray granite gneiss, Wollaston | D 59 Syenite, Deloro | D 1100 Perthite granite, Deloro | D 968 Granophyric granite, Deloro |
|---|---|---|---|---|---|---|---|
| **Chemical Analyses*** | | | | | | | |
| $SiO_2$ | 68.48 | 59.88 | 71.88 | 70.68 | 65.16 | 75.45 | 75.88 |
| $TiO_2$ | 0.45 | 1.07 | 0.37 | 0.48 | 0.37 | 0.23 | 0.19 |
| $Al_2O_3$ | 15.80 | 18.27 | 11.66 | 14.07 | 14.67 | 11.34 | 11.92 |
| $Fe_2O_3$ | 1.35 | 2.46 | 1.34 | 0.69 | 2.24 | 1.82 | 2.14 |
| FeO | 2.42 | 1.99 | 2.63 | 2.65 | 3.48 | 1.21 | 0.64 |
| MnO | 0.06 | 0.08 | 0.06 | 0.05 | 0.04 | 0.03 | 0.01 |
| MgO | 0.91 | 1.26 | 0.72 | 0.57 | 0.33 | 0.42 | 0.07 |
| CaO | 2.53 | 2.35 | 1.13 | 1.90 | 1.61 | 0.42 | 0.60 |
| $Na_2O$ | 4.38 | 4.54 | 3.92 | 4.13 | 5.77 | 4.04 | 4.28 |
| $K_2O$ | 3.83 | 6.78 | 4.18 | 3.88 | 4.06 | 4.20 | 4.18 |
| $P_2O_5$ | 0.19 | 0.25 | 0.10 | 0.12 | 0.06 | 0.02 | 0.01 |
| $H_2O+$ | 0.40 | 0.76 | 0.71 | 0.57 | 0.70 | 0.69 | 0.47 |
| $H_2O-$ | 0.00 | 0.02 | 0.02 | 0.00 | 0.02 | 0.05 | 0.00 |
| $CO_2$ | 0.00 | 0.00 | 0.57 | 0.45 | 1.22 | 0.00 | 0.00 |
| | 100.80 | 99.71 | 99.29 | 100.24 | 99.73 | 99.92 | 100.39 |
| **Molecular Norms** | | | | | | | |
| q | 19.3 | 1.5 | 28.6 | 25.2 | 12.5 | 32.5 | 31.8 |
| or | 22.5 | 40.0 | 25.5 | 23.0 | 24.0 | 25.5 | 25.0 |
| ab | 39.0 | 40.5 | 36.0 | 37.5 | 52.0 | 37.0 | 39.0 |
| an | 11.5 | 9.5 | 1.0 | 5.5 | 1.0 | 0.3 | 1.0 |
| hy | 5.0 | 3.8 | 4.8 | 4.8 | 4.2 | 1.6 | 0.2 |
| wo | .... | 0.2 | .... | .... | .... | 0.8 | 0.8 |
| c | 0.3 | .... | 0.4 | 1.2 | 0.5 | .... | .... |
| mt | 1.4 | 2.6 | 1.5 | 0.8 | 2.4 | 1.9 | 1.5 |
| il | 0.6 | 1.4 | 0.6 | 0.6 | 0.6 | 0.4 | 0.2 |
| cc | .... | .... | 1.4 | 1.2 | 2.8 | .... | 0.5 (hm) |
| ap | 0.5 | 0.5 | 0.3 | 0.3 | .... | .... | .... |
| | 100.1 | 100.0 | 100.1 | 100.1 | 100.0 | 100.0 | 100.0 |
| **Modes** | | | | | | | |
| Quartz | 23.0 | 0.4 | 30.4 | 29.3 | 8.8 | 31.3 | 32.9 |
| Microcline (usually perthitic) | 21.1 | 48.4 | 26.4 | 19.2 | 80.8 | 63.7 | 63.1 |
| Plagioclase | 46.0 | 42.5 | 29.4 | 39.8 | | | |
| Biotite + chlorite | 5.0 | 6.5 | 7.4 | 10.4 | 7.8 | 1.4 | 1.8 |
| Hornblende | 4.2 | 0.7 | 4.2 | .... | .... | 1.9 | .... |
| Magnetite | .... | 0.8 | 0.4 | .... | 1.7 | 1.2 | 2.1 |
| Calcite | .... | .... | 1.0 | 0.8 | 0.7 | 0.2 | .... |
| Non-opaque accessories | 0.7 | 0.8 | 0.8 | 0.5 | 0.2 | 0.3 | .... |
| | 100.0 | 100.1 | 100.0 | 100.0 | 100.0 | 100.0 | 99.9 |

* Analyst, H. B. Wiik, Finland.

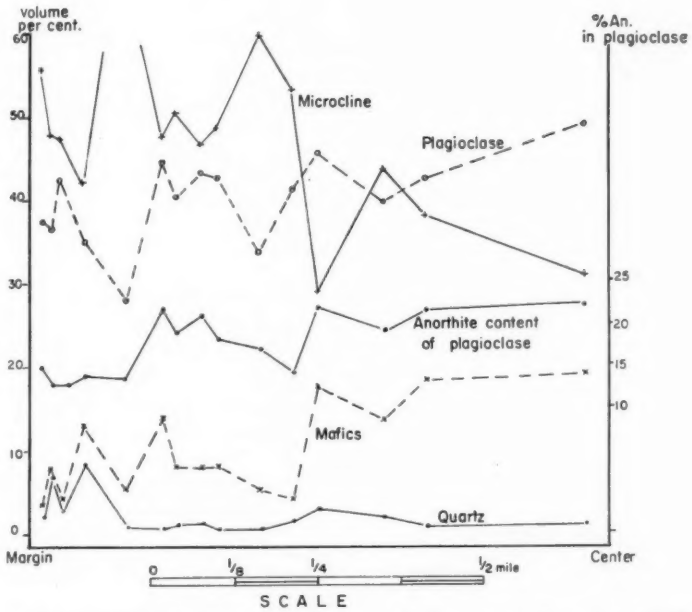


FIGURE 15.—VARIATION IN MODAL COMPOSITION WITH RESPECT TO THE DISTANCE FROM MARGIN IN CHANDOS LAKE SYENITE

Note the systematic tendency of the syenite to become more acidic from center toward margin

would be indicated by the following values of the correlation coefficients:

| | |
|---|---|
| Plagioclase %–microcline % | −0.86 |
| Plagioclase %–anorthite content of plagioclase | +0.66 |
| Plagioclase %–mafic minerals % | +0.49 |
| Mafic minerals %–anorthite content of plagioclase | +0.734 |
| Mafic minerals %–$\alpha$ activity | −0.56 |

All these correlations are statistically significant, except the one between plagioclase and mafic minerals per cent, which is slightly below the 5 per cent probability level ($P_{.05}$—0.514, $P_{.01}$—0.641; d.f. 13). The rather low positive correlation between plagioclase and mafic minerals per cent is perhaps also significant, because the two variates are from closed tables (tables with a fixed sum, in this case 100). As pointed out by Chayes (1948), for variates from closed tables, there is *a priori* 87 per cent chance that a given correlation will be negative, so that even a rather low positive correlation between the two variates would be considered significant.

These systematic variations in composition favor a magmatic origin of the syenites. The variations might have been due to one of the following causes: (1) crystallization of the magma started near the center of the body, and the residual parts crystallized later, presumably along with the expansion of the magma chamber; or (2) assimilation of gabbro-diorite inclusions produced the more basic central part of the body, and the relatively uncontaminated portions crystallized toward the outer parts. Significant assimilation of limestone or paragneiss is not favored, as in such a case the systematic variations observed are unlikely.

The relative abundance of gabbro-diorite inclusions in the basic central part of the syenite body and their absence in the acidic marginal parts support the idea of their assimilation being one of the causes of variation; but the systematic variations of composition of the syenite with respect to the distance from border would be unlikely, had assimilation been the sole cause. That there has been a certain amount of assimilation of gabbro-diorite inclusions is undoubted; whether this is the major factor in producing the observed variations cannot be decided with the data at hand.

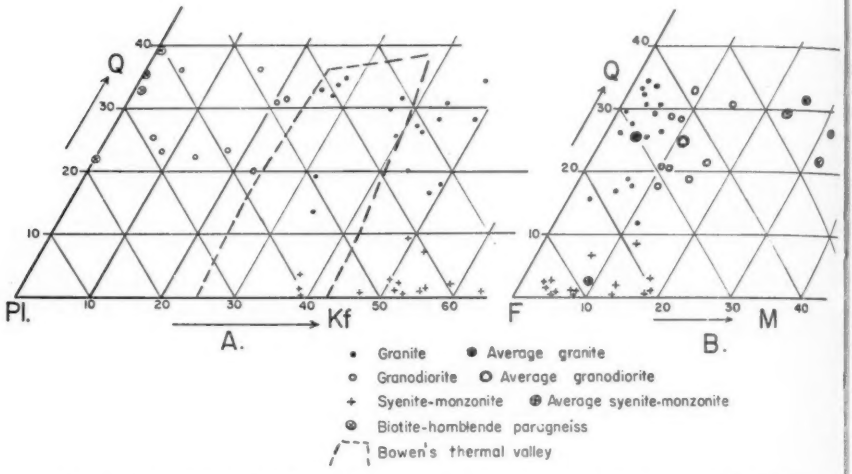


FIGURE 16.—Q-F-M AND Q-PL-KF DIAGRAMS FOR ROCKS OF THE CHANDOS LAKE PLUTON

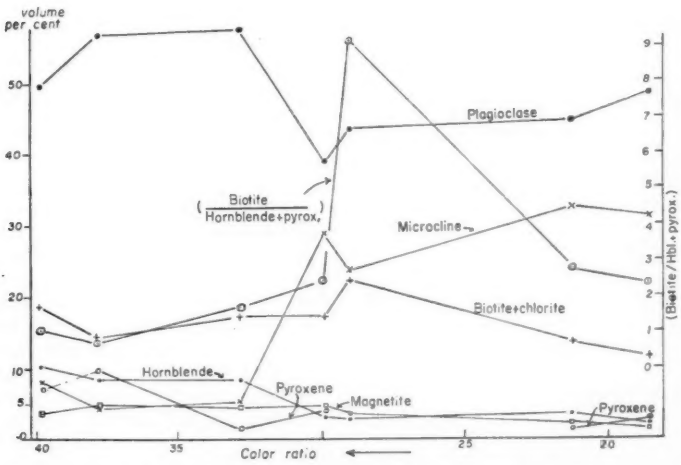


FIGURE 17.—MINERALOGICAL VARIATIONS IN SAMPLES OF THE GABBRO-DIORITE INCLUSIONS IN CHANDOS LAKE PLUTON

GRANITE-GRANODIORITE: Biotite granite is the dominant rock type in the pluton and consists of a medium- to coarse-grained aggregate of quartz, oligoclase-albite ($An_8$–$An_{16.5}$), microcline (usually microperthitic), biotite, magnetite, and a little hornblende. The rock is appreciably finer-grained toward the border of the pluton, where it is aplitic in many places. The granodiorite grades from the biotite granite and is developed chiefly along a zone in the central part of the pluton (Fig. 6). It consists of plagioclase ($An_{15}$–$An_{25}$), quartz, microcline (usually nonperthitic), biotite, hornblende, magnetite, and a little calcite. Hornblende in many cases alters to a granular epidote.

The average mineral compositions of the biotite granite and the granodiorite are given in Table 3; chemical analysis of a typical sample of the granodiorite and its mode and molecular norm are shown in Table 4.

Considerable variations in mineral composition characterize both the granite and the granodiorite (Fig. 16). The variations in space are not very regular, although a few of the samples close to the north and the south border of the pluton are more potassium-rich, less mafic, and lower in anorthite content of plagioclase than the average granite. The only significant aspect of variation within the biotite granite is the positive correlation between the mafic minerals per cent and the anorthite content of plagioclase ($r = +0.47$; d.f.—16).

The values of $\alpha$ activity within the granite-granodiorite group are generally between 0.5 and 2.2 $\alpha/cm^2/hr$, except for some abnormally high values (more than 4.0) in the inclusion-rich northwestern part of the pluton. Excluding these high values, the correlation coefficients between the $\alpha$ activity and the proportions of the different minerals are all very low.

The granodiorite is intermediate in composition between the granite and the biotite-hornblende paragneiss (Fig. 16). Inclusions of the latter in the granodiorite are very abundant. Such inclusions are in many cases elongated parallel to the lineation; most contacts are sharp, although a considerable amount of little stringers, veins, and dikes of granodiorite material have penetrated the inclusions. These facts suggest that assimilation of the paragneiss by the granitic magma has been an important factor in the genesis of the granodiorite.

The reason for the rather unsystematic variations within the biotite granite is not clear. Possibly incorporation of considerable amounts of the potassium-rich biotite paragneiss has had something to do with such variations.

INCLUSIONS OF GABBRO-DIORITE: Seven fairly large inclusions (roof pendants?) of gabbroid diorite have been mapped within this pluton; six of these are within the syenites. These rocks are typically dark gray, slightly foliated, granulitic, medium-grain aggregates of plagioclase ($An_{24}$ — $An_{33}$), hornblende, pyroxene, and biotite with varying proportions of perthitic microcline, magnetite, quartz, and calcite. A few small dikes of granite and pegmatite cut across the dioritic rocks.

The textural and mineralogical similarity between these rocks and the gabbro-diorite intrusions in the surrounding country rocks is striking. Both groups of rocks have the same range of plagioclase composition, similar diopsidic pyroxene, similar sieve-textured hornblende altering from pyroxene. The differences are: (1) Absence of microcline in the gabbro-diorites outside the pluton. Adams and Barlow (1910, p. 153), however, note a little microcline in some of the diorite intrusions. (2) Higher values of the ratio biotite:(pyroxene + hornblende) in the inclusions. As potassium feldspar increases, the ratio tends to increase (Fig. 17).

TABLE 5.—COLOR RATIO OF GABBRO-DIORITE

| Sample | Color ratio | Color ratio, excluding microcline |
|---|---|---|
| L 236 | 39.9 | 43.3 |
| L 154 | 37.8 | 39.4 |
| L 422 | 32.8 | 34.6 |
| L 201 | 29.8 | 41.8 |
| L 178 | 29.0 | 37.9 |
| L 158 | 21.2 | 31.3 |
| L 155 | 18.1 | 26.2 |

The perthitic microcline in the gabbroid inclusions replaces plagioclase; irregular small patches of microcline are scattered within the larger, strained crystals of plagioclase. With increasing microcline content, the color ratio decreases. The specimen-to-specimen variation in color ratio is greatly reduced when it is recalculated, neglecting the microcline content (Table 5). The recalculated color ratios are well within the range of those of the gabbro-diorite intrusions outside the pluton.

It appears then that the gabbro-diorite patches within the Chandos Lake pluton represent inclusions of slightly metamorphosed gabbro-diorite, modified by the potassic contributions from the syenitic magma, which brought about replacement of some plagioclase by perthitic microcline and facilitated alteration of pyroxene and hornblende to biotite.

### *Variations in the Wollaston Pluton*

The Wollaston pluton, as already stated, consists chiefly of biotite-hornblende granites with a number of roof pendants of biotite-hornblende paragneiss and crystalline limestone; the former are granitized partly to a gray granite gneiss.

BIOTITE-HORNBLENDE GRANITE: The rock is essentially a medium- to coarse-grained aggregate of plagioclase ($An_3$ — $An_{16}$), microcline

(usually perthitic), quartz, biotite, and hornblende; magnetite, apatite, sphene, and a little calcite are accessories. Hornblende may be absent locally from the border region

soda and silica in the biotite paragneiss tend to decrease, and those of $K_2O$ and mafic minerals rise, as the granite is approached; both these tendencies are approximately exponential

TABLE 6.—AVERAGE MODAL COMPOSITION OF THE BIOTITE-HORNBLENDE GRANITE, WOLLASTON PLUTON

| Minerals | Border group (13 samples) | | Central group (21 samples) | | Average for the whole body |
|---|---|---|---|---|---|
| | Volume per cent | Standard deviation | Volume per cent | Standard deviation | Volume per cent |
| Quartz | 31.8 | 6.65 | 27.9 | 5.70 | 28.5 |
| Plagioclase | 41.7 | 9.05 | 30.8 | 6.65 | 32.6 |
| Microcline | 22.1 | 10.12 | 32.8 | 4.04 | 31.1 |
| Biotite + chlorite | 3.6 | 2.94 | 5.6 | 3.04 | 5.3 |
| Hornblende | 0.3 | | 2.2 | | 1.9 |
| Magnetite | 0.1 | ..... | 0.1 | ..... | 0.1 |
| Rest | 0.4 | ..... | 0.6 | ..... | 0.5 |
| Average An per cent in plagioclase | $An_{9.5}$ | ..... | $An_{12.5}$ | ..... | $An_{11.5}$ |
| Average $\frac{Kf \times 100}{\text{Total feldspar}}$ | 34.6 | ..... | 51.6 | ..... | 48.8 |

of the pluton. The mafic minerals characteristically tend to aggregate. The rock is appreciably finer-grained toward the margin, where it is aplitic in many places.

Within 100 yards of the border of the pluton the rock is more sodic and silicic and poorer in mafic minerals and potassium than the rest of the body. The average modal compositions of the two groups of rocks are given in columns 2 and 4 of Table 6. Since the border type represents only 15–20 per cent of the total area of the granite, the central and the border compositions were weighted in the ratio of 21:4 respectively in computing the average composition of the granite (Table 6, column 6).

Chemical analysis of a sample of the central rocks and its observed mode and calculated norm are given in Table 4.

The changes in composition from the center toward the border are gradual, becoming more and more marked as the border is approached; in fact, the variations of composition are approximately exponential *vs.* distance from contact. A similar soda- and silica-rich zone 3 feet wide was found along the border of a dike of granite branching from the main body. Along the contact of this dike, the contents of

*vs.* distance from contact. Details of these studies have been reported in a separate paper (Saha, 1958), wherein a process of aqueous diffusion of silica and alkalies from the heated paragneiss into the adjacent granite magma (after Kennedy, 1955) has been suggested as the explanation of the various features of variation in this pluton (Fig. 18).

The $\alpha$ activities of the border and central groups of the biotite-hornblende granite are 2.1 and 1.3 $\alpha$/cm²/hour respectively. The variation is rather unsystematic, and some of the samples show abnormally high values (more than 6.0 $\alpha$/cm²/hour). The offshooting granite dikes have relatively higher activities (average 2.5 $\alpha$/cm²/hour) than the main body, although proportions of the major constituents are approximately the same in both.

GRAY GRANITE GNEISS: The gray medium-grained biotite-hornblende granite gneiss, showing all gradations to biotite-hornblende paragneiss, occurs in the form of several large elongated patches, at least three of which are mappable. The rock consists of a more or less equigranular aggregate of plagioclase ($An_{16}$ – $An_{18}$), microcline, quartz, biotite, and horn-

blende (partially altered to chlorite), and a little calcite, epidote-zoisite, and almandine garnet; zircon, apatite, and sphene are the accessories.

This rock (Table 7) has a crystalloblastic texture. The mafic minerals are distributed rather uniformly within the quartz-feldspar aggregate. This is in sharp contrast to the general tendency of the mafic minerals and the accessories to aggregate in the biotite-hornblende granites and suggests a parametamorphic origin of the gray granite gneiss (Moorhouse, 1956). Plagioclase and microcline tend to be porphyroblastic in habit.

Chemical analysis, observed mode, and molecular normal of a typical sample (W 487) are given in Table 4.

These gneissic rocks apparently resulted from recrystallization of the biotite-hornblende paragneiss, along with the introduction of some silica and alkalies from the surrounding granite magma and perhaps also partial removal of some of the mafic elements. The following are some of the evidences which suggest such a mode of origin:

(1) Mineralogical gradation between the granite gneiss and the biotite-hornblende paragneiss is distinct (Table 8).

(2) Fresh, unaltered microcline occurs as irregular patches (veinlike in a few places) within more altered (sericitized) and strained grains of plagioclase; this suggests later introduction of much of the microcline.

(3) Although most of the quartz grains occur in the equigranular quartz-feldspar mosaic, a second generation of quartz occurs as elongated, relatively coarse grains crosscutting the boundaries of other grains.

(4) Some reddish, microcline-rich aplite veins cut across these rocks with replacement types of contact; where such veins cut across the foliation, the parallel alignment of hornblende and biotite extends from the gneiss for a few centimeters into the vein. Such veins probably represent the granitizing materials, and those that are seen now were introduced into an already granitized paragneiss toward the closing stages of the granitizing episode.

(5) The petrofabric characters of the gray granit gneiss, as described in a later section of this report, are different from those of the Wollaston granite and the paragneiss. The fabric pattern of the gray granite gneiss can be

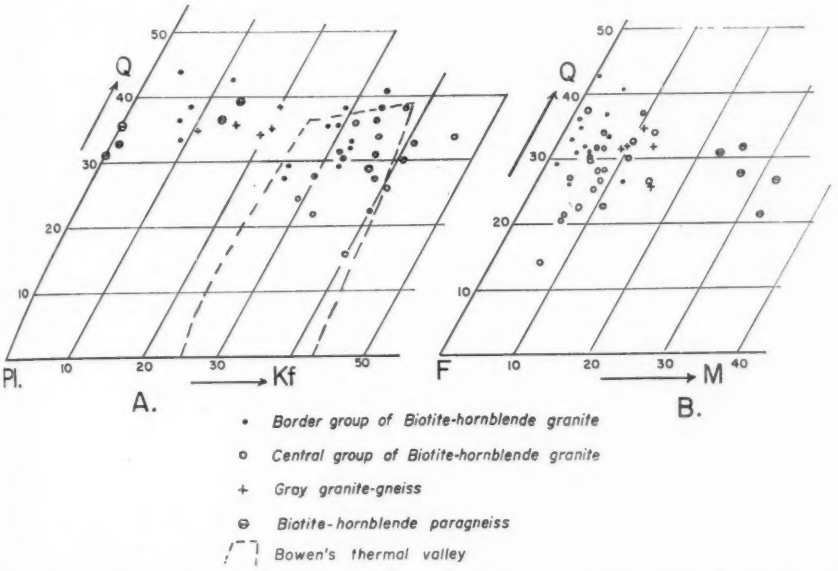


FIGURE 18.—Q-F-M AND Q-Pl-Kf DIAGRAMS FOR ROCKS OF THE WOLLASTON PLUTON

explained satisfactorily by assuming introduction of granitic material during the recrystallization of the biotite-hornblende paragneiss.

TABLE 7.—AVERAGE MODAL COMPOSITION OF GRAY GRANITE GNEISS

| Minerals | Per cent (by volume) |
|---|---|
| Quartz | 30.6 |
| Plagioclase | 39.5 |
| Microcline | 17.8 |
| Biotite + chlorite | 9.8 |
| Hornblende | 1.5 |
| Magnetite | 0.1 |
| Rest | 0.8 |
| | 100.1 |

TABLE 8.—GRADATION OF BIOTITE-HORNBLENDE PARAGNEISS TO GRANITE GNEISS

(All compositions in volume per cent)

| Sample no. | Quartz | Plagioclase | Microline | Biotite + chlorite | Hornblende | Opaque accessories | Nonopaque accessories |
|---|---|---|---|---|---|---|---|
| Paragneiss | | | | | | | |
| W 581 | 21.1 | 45.0 | 0.7 | 20.5 | 11.8 | — | 0.9 |
| W 321 | 30.3 | 35.5 | 10.9 | 20.8 | 1.6 | 0.2 | 0.6 |
| W 305 | 27.0 | 31.1 | 12.9 | 19.0 | 7.1 | 0.1 | 2.9 |
| Granitic gneiss | | | | | | | |
| W 475 | 24.9 | 41.2 | 17.0 | 12.1 | 3.7 | — | 1.1 |
| W 487 | 29.3 | 39.8 | 19.2 | 10.4 | — | — | 1.3 |

### *Variations in the Deloro Pluton*

The Deloro pluton, as already stated, consists of the main body of perthite granite grading to syenite along the western rim and a smaller body of granophyric granite in the east.

PERTHITE GRANITE-SYENITE: The perthite granite is a coarse-grained, hypidiomorphic aggregate composed chiefly of perthite and quartz, some albite, an alkali amphibole (riebeckite-crossite), biotite, magnetite, and various accessories such as calcite, zircon, sphene, pyrite, and fluorite. Varying proportions of granular albite sheath many of the subhedral grains of perthite. Magnetite and sphene are predominantly associated with the patches of amphibole-biotite aggregates. Quartz occurs both as highly strained, coarse, anhedral grains and as fine granular aggregates interstitial to the perthites; the latter type of quartz is associated in many places with granular secondary albite. Inclusions of volcanic rocks of intermediate composition are locally abundant in the granite.

The average mineral composition of the perthite granite, as determined from the modal analysis of 40 samples collected from all over the body, is shown in column 2 of Table 9. The values of $\alpha$ activity have a rather limited range (0.8–2.3 $\alpha$/cm²/hour). Chemical analysis of a typical sample (D 1100) is given in Table 4. In most of the modally analyzed samples, the relative proportions of albite and microcline components in the perthite could be determined by point counting with close spacing (0.2 mm) along closely spaced lines (0.5 mm apart) in a number of perthite grains, sectioned approximately perpendicular to the plane of intergrowth. This procedure could not be adopted for perthites with very fine intergrowths, whose Ab and Or components have been calculated from the chemical determinations of $K_2O$ and $Na_2O$ per cent in the (perthite + quartz) aggregates of the rock. Check determinations in four samples revealed fairly good agreement between the chemically determined Or per cent and modal Kf per cent in perthites.

The syenites, which show all gradations to perthite granite, are medium-grained rocks containing lath-shaped crystals of antiperthitic albite, a small proportion of fine-grained clear secondary albite, a fair proportion of biotite, chlorite, alkali-amphibole (riebeckite), magnetite, and a small proportion of interstitial quartz. The average modal composition of the rock is shown in column 4 of Table 9; chemical analysis of a typical sample is given in Table 4. The values of $\alpha$ activity (0.2–0.9 $\alpha$/cm²/hour) are lower than in the perthite granite.

Some systematic trends of variation are evident within the body of perthite granite-syenite:

(1) There is a trend of progressive acidification from the west, north, and south borders toward the central and eastern part of the pluton, as shown by increasing quartz and the ratio Kf/Naf in the feldspars and decreasing mafic minerals toward the center. A profile of modal composition east-west across the pluton indicates this trend (Fig. 19). The variations relatively sharp up to about a quarter of a mile from the dividing line between syenite

TABLE 9.—MINERALOGICAL COMPOSITION OF THE DELORO PLUTON
(All values in volume per cent)

| Minerals | Perthite granite (40 samples) | | Syenite (8 samples) | | Granophyric granite (7 samples) | |
|---|---|---|---|---|---|---|
| | Average composition | Standard deviation | Average composition | Standard deviation | Average composition | Standard deviation |
| Quartz | 27.1 | 5.61 | 7.0 | 2.83 | 29.9 | 3.9 |
| Perthite | 62.4 | 5.34 | 75.2 | 3.45 | 66.7 | 3.4 |
| "Free" albite | 5.2 | — | 2.0 | — | | |
| Biotite + chlorite + alkali-amphibole | 3.7 | — | 12.8 | 4.84 | 1.5 | — |
| Magnetite | 1.1 | — | 2.0 | | 1.5 | — |
| Rest | 0.5 | — | 1.0 | — | 0.5 | — |
| Kf × 100 / Total feldspar | 44.6 | — | — | — | — | — |
| $\alpha$ activity ($\alpha$/cm²/hour) | 1.36 (average of 50) | ..... | 0.55 (average of 13) | ..... | 1.28 (average of 8) | ..... |

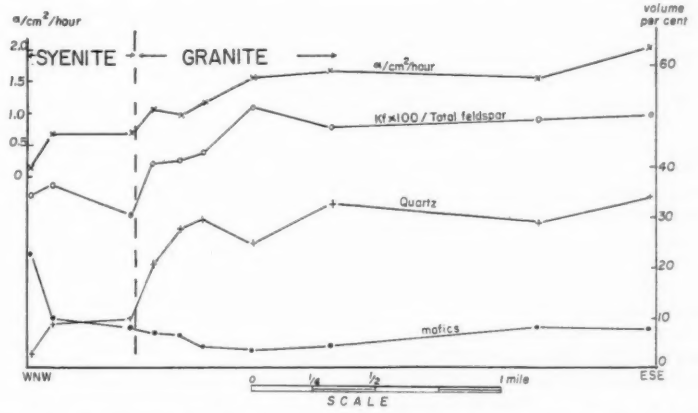


FIGURE 19.—VARIATIONS IN MINERALOGICAL COMPOSITION ACROSS THE DELORO PLUTON
Along a line approximately parallel to Highway 7. Note the tendency of the rocks to become richer eastward in quartz, potassium feldspar ratio, and $\alpha$ activity.

and granite, flatten out farther east. The most acidic part of the pluton is the narrow northeasterly projection.

(2) Certain systematic correlations of relative proportions exist among the different minerals (Table 10).

(3) The Q-Pl-Kf plots of these rocks lie mostly within the thermal valley of the diagram (Fig. 20).

The syenites owe their origin, at least in part, to the assimilation of gabbro-diabases, as shown by: (1) abundance of inclusions of diabase and intermediate volcanic rocks within the syenite along the western border of the pluton, the diabases are locally injected by syenite in an intimate fashion; (2) many irregular gradations of syenite to perthite granite in numerous small patches; (3) location of the

syenites in an area where the pluton is in contact with gabbro-diabase intrusions into the country rocks; (4) their absence from the northern and southern borders of the pluton, where basic rocks are absent.

TABLE 10.—CORRELATION AMONG THE MINERALS OF PERTHITE GRANITE-SYENITE, DELORO PLUTON

| Mineral pairs | Values of r | Degree of freedom | $P_{.05}$ | $P_{.01}$ |
|---|---|---|---|---|
| Quartz–(Kf × 100 / total feldspars) | +0.553 | 36 | 0.32 | 0.41 |
| Quartz–mafic minerals | −0.77 | 36 | 0.32 | 0.41 |
| Quartz–$\alpha$ activity | +0.84 | 32 | 0.34 | 0.44 |
| (Kf × 100 / Total feldspar)–$\alpha$ activity | +0.63 | 32 | 0.34 | 0.44 |

Thus, apart from the effect of assimilation in producing the syenites, magmatic differentiation by fractional crystallization was the main factor in causing the variations in this body, as suggested by the systematic trends of variation mentioned above. According to Bowen (1937), fractional crystallization of a liquid of basaltic composition would generate liquids lying in or near the thermal valley of the system $SiO_2$-$NaAlSi_2O_6$-$KalSi_2O_6$. The fact that almost all the samples in the present case have compositions within the thermal valley would indicate crystallization under magmatic conditions. One would not expect such regularity if assimilation of rocks of heterogeneous composition (such as those found around this pluton) were important.

The significant correlation data in Table 10 suggest that with the progress of crystallization, the ratio $K_2O$ to $Na_2O$ increased, the proportion of the mafic elements decreased, and that of the radioactive elements increased in the residual liquid.

GRANOPHYRIC GRANITE: These are fine- to medium-grained leucocratic rocks, characterized by graphic intergrowth between microcline-microperthite and quartz. Euhedral to subhedral phenocrysts of cryptoperthitic albite (-acid oligoclase) stand out against the groundmass made up of the graphic intergrowth, scattered grains of magnetite and pyrite, few short flakes of biotite, and accessories such as fluorite and zircon. Many of the albite euhedra are replaced by quartz, tongues of which penetrate into them from the surrounding graphic intergrowth.

The average mineral composition of this rock is shown in Table 9; chemical analysis of a typical sample (D 968) is given in Table 4. The values of $\alpha$ activity (0.6–2.4 $\alpha$/cm²/hour) have about the same range as in the perthite granite.

Compared with the perthite granite, this rock is significantly less mafic, more alkaline, and has a generally higher $Na_2O/K_2O$ ratio. The low standard deviations of the quartz and feldspar contents (Table 9) show that no significant variation exists between the different parts of the body.

### *Petrogenic Implications of the Data on the $\alpha$ Activity of the Plutons*

The distribution of $\alpha$ activity in the Deloro pluton differs from that in the other two plutons in two important respects: (1) a good correlation of the $\alpha$ activity with the major mineral constituents and a tendency of the $\alpha$ activity to concentrate in the siliceous and hence presumably later fractions of the magma—a tendency not well marked in the other two plutons; (2) rather limited range of values in all the rock types—no values are higher than 2.4 $\alpha$/cm²/hour; this is in marked contrast with the abnormally high values (more than 6.0) seen in many places in the Wollaston and Chandos Lake plutons.

Petrological studies, as already described, have indicated that in the Chandos Lake and Wollaston plutons, assimilation of varied rock types has been important in causing the mineralogical and chemical variations, but assimilation has been relatively unimportant in the Deloro pluton except locally. A good correlation between the $\alpha$ activity and the major mineral constituents in a pluton may thus be indicative of magmatic crystallization without appreciable assimilation. Extensive assimilation would tend to obliterate such correlation.

Several abnormally high values of $\alpha$ activity in the Chandos Lake and Wollaston plutons are found in the areas of abundant inclusions of calcareous paragneiss, which seem to have facilitated the precipitation of radioactive minerals near them. This could happen in one of two ways: (1) radioactive elements could be leached out of the heated inclusions or country rocks into the magma, or (2) presence of inclusions of particular composition could exer

some sort of chemical influence causing precipitation of the radioactive elements. The former possibility is unlikely, as the amount of radioactivity in the paragneiss (average, 0.5 /cm²/hour) is much less than in the granite. Precipitation of radioactive minerals in pegmatite dikes is known to be controlled by the country rocks, which they cut across. Thus in the uranium mines around the Cheddar batholith, Ontario, concentrations of uranium in pegmatite occur where the pegmatite cuts across crystalline limestone or calcareous paragneiss (Hewitt, 1957, oral communication).

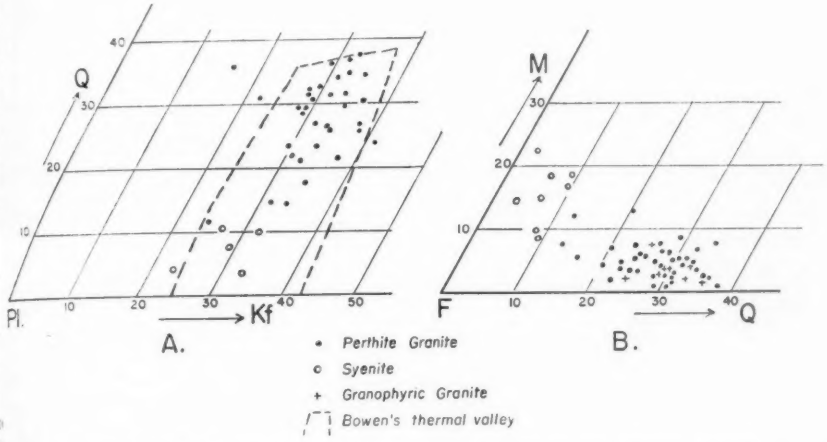


FIGURE 20.—Q-F-M AND Q-PL-KF DIAGRAMS FOR ROCKS OF THE DELORO PLUTON

## RECRYSTALLIZATION IN THE GRANITIC PLUTONS

### *General Statement*

A critical study of the textures of the granitic rocks of all the three plutons indicates evidences of recrystallization during the cooling and consolidation of the rocks.

### *Recrystallization in Chandos Lake and Wollaston plutons*

Textures of the granitic rocks of these plutons suggest that the earliest mineral to crystallize in them was plagioclase. Later, quartz joined plagioclase, and after most of the plagioclase (excluding the albite rims) had already crystallized out, potassium-rich feldspar started to crystallize with quartz and plagioclase. In the syenites, quartz crystallized at the end.

Recrystallization of the granites and syenites is indicated in the following ways: (1) presence of thin rims of clear, untwinned albite around plagioclase; (2) myrmekites seen in varying amount in almost every sample; (3) recrystallization of quartz, as indicated by petrofabric studies.

ALBITE RIMS: Thin rims of clear, untwinned albite occur around microcline in most samples of granite, granodiorite, and syenite. A statistical study of the nature of the grain boundary associated with the albite rims, on the same lines as that by Tuttle (1952, p. 115–116), indicated that the albite rims are overwhelmingly associated with the plagioclase-microcline contacts. The association of such rims with myrmekitic plagioclase is in about the same proportion as that with nonmyrmekitic plagioclase. In the former type, rims of clear albite truncate the quartz intergrown with plagioclase. These facts suggest that the albite rims were probably derived from the potassium-rich feldspar after the formation of the myrmekites.

MYRMEKITES: Myrmekites are common in the granite and granodiorite of the two plutons and in the gray granite gneiss of the Wollaston pluton. Some of the salient features of the myrmekite grains are: (1) proportion of quartz from grain to grain ranges from 10 to 50 per cent; (2) subhedral outlines are common; (3) myrmekitic plagioclase is always enclosed (partially or wholly) in microcline microperthite;

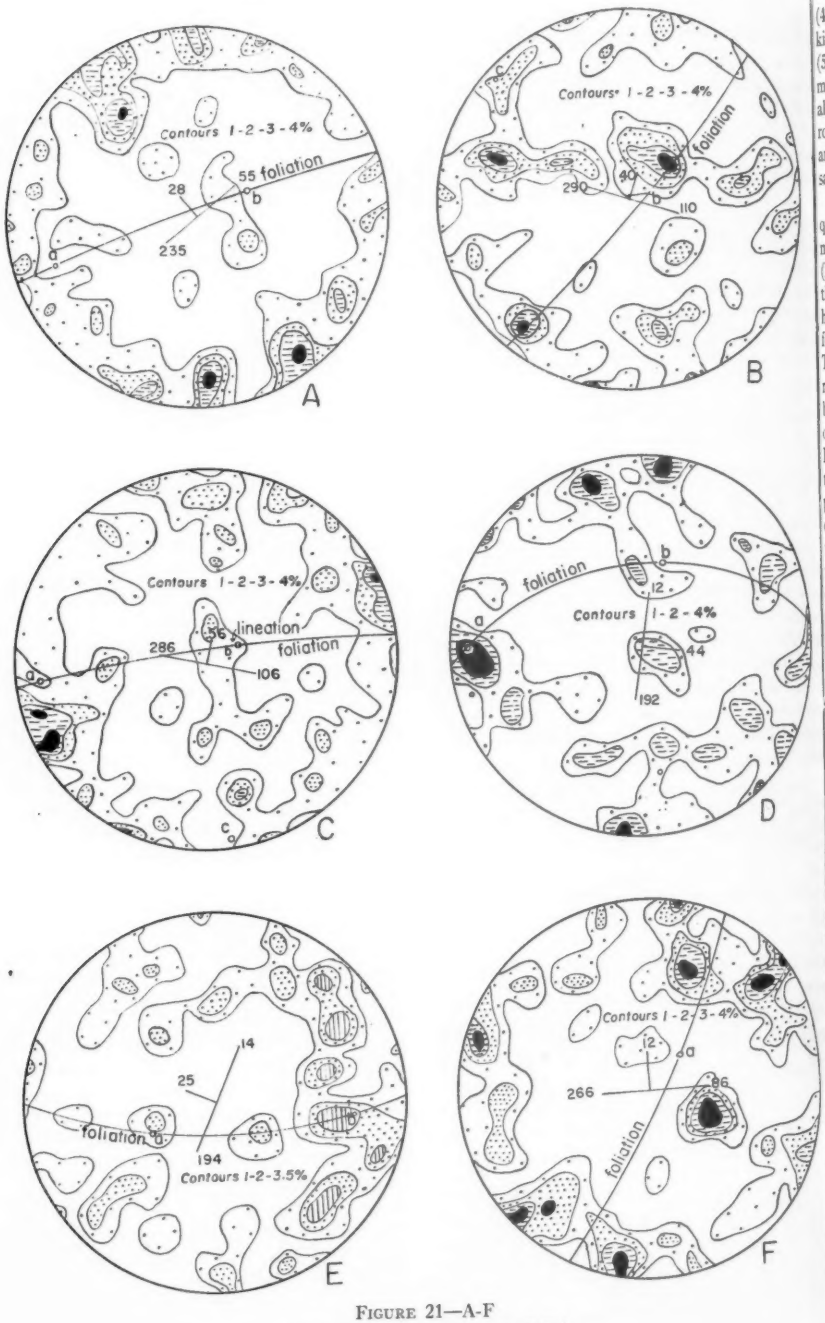


FIGURE 21—A-F

(*See* page 1322 for diagrams G-K.)

(4) in many cases a plagioclase grain is myrmekitic only in the part adjacent to microcline; (5) in the same rock identity with the nonmyrmekitic grains in composition, sericitic alterations, presence of albite rims, and corroded borders against microcline; myrmekitic and nonmyrmekitic plagioclase belong to the same generation.

These characters cannot be explained adequately by the hypothesis of magmatic replacement of potassium feldspar by plagioclase (Becke, 1908), nor on the assumption of exsolution and rearrangement of materials formerly held in solution within the potassium-rich feldspar (Schwantke, 1909; Spencer, 1945). The myrmekites under consideration strongly resemble the type I myrmekites, as described by Drescher-Kaden (1948), and a similar mode of origin is likely. According to Drescher-Kaden, myrmekites originate in one of the two ways: (1) siliceous solutions carried with potassium feldspars replace the adjacent or enclosed earlier formed plagioclase (myrmekite type I), or (2) sodic solutions left over after the crystallization of microcline replace parts of the microcline metasomatically, forming myrmekites (myrmekite type II). Drescher-Kaden assumes that potassium- and silica-rich solutions responsible for the formation of type I myrmekite came from outside the rock. No evidence in the present case suggests, however, that microcline-forming solutions, with excess silica, came from outside the magma.

The best explanation of the observed features of the albite rim and myrmekite in the two plutons appears to be as follows: During the closing stages of magmatic crystallization, when the potassium-rich feldspars and quartz were crystallizing, the magma possessed a high concentration of volatiles in which silica was more soluble than the components of the feldspars. The resulting silica-rich solution replaced the plagioclase grains adjacent to or enclosed in the potassium-rich feldspars, producing the myrmekites. Later, albite lamellae began to exsolve out of the potassium-rich feldspar. During this process some of the exsolved albite tended to segregate out of the perthite grains and produced the albite rims on the adjacent minerals, particularly on plagioclase.

RECRYSTALLIZATION OF QUARTZ: Statistical study of quartz orientation in a few samples of Chandos Lake and Wollaston granites (Fig. 21E-H) provides evidences of recrystallization of quartz during the cooling of the rock.

The diagrams show that the quartz c axes are arranged in nearly complete peripheral girdles around the visible lineations (which, as indicated by field evidence, represent the directions of flow of magma, *i.e.*, the *a* fabric axis). In addition, a small-circle girdle occurs 25°–35° from the lineation; this girdle consists of a series of four or five maxima rather than a wide scatter of points as in a normal girdle.

A comparison of the quartz fabric diagrams of the associated paragneisses (Fig. 21A–D) shows that although peripheral girdles around the visible lineation occur in both, the small-circle girdle around lineation is characteristic of the granites. As already shown, lineation in these granites is independent of that in the associated country rocks (Fig. 4).

Following Sander (1950, p. 307–310), the writer suggests that during the later stages of consolidation of the magma, the forces that caused flowage in the magma also deformed and rotated the already crystallized materials in the same way as would tectonic deformation of solid rocks.

QUARTZ FABRIC OF THE GRAY GRANITE GNEISS: Quartz fabric of the gray granite gneiss of the Wollaston pluton (Fig. 21 J–K) differs from those of the granites and the paragneisses in two important points:

(1) Preferred orientation of quartz in these rocks is very weak; the *r* test (after Chayes, 1949) applied on the point diagrams indicates that the preferred orientation is "not significant" statistically. This does not mean that the parent fabric of the rocks is necessarily isotropic (Chayes, 1949, p. 325). All that the tests indicate is that the probability of the null hypothesis being true is sufficiently high to be

FIGURE 21.—ORIENTATION DIAGRAMS OF QUARTZ OPTIC AXES IN GRANITE, PARAGNEISS, AND GRANITIZED PARAGNEISS

A. Biotite paragneiss (W 908), 200 quartz c axes; contours 1-2-3-4% (maximum 5.5%)
B. Biotite paragneiss (W11), 150 quartz c axes; contours 1-2-3-4% (maximum 5.5%)
C. Biotite-hornblende paragneiss (L 111A), 200 quartz c axes; contours 1-2-3-4% (maximum 6%)
D. Biotite-hornblende paragneiss (L 500A), 200 quartz c axes; contours 1-2-4% (maximum 6.5%)
E. Biotite granite, Chandos Lake pluton (L 65), 200 quartz c axes; contours 1-2-3.5% (maximum 5%)
F. Biotite granite, Chandos Lake pluton (L 27), 150 quartz c axes; contours 1-2-3-4% (maximum 5.6%)

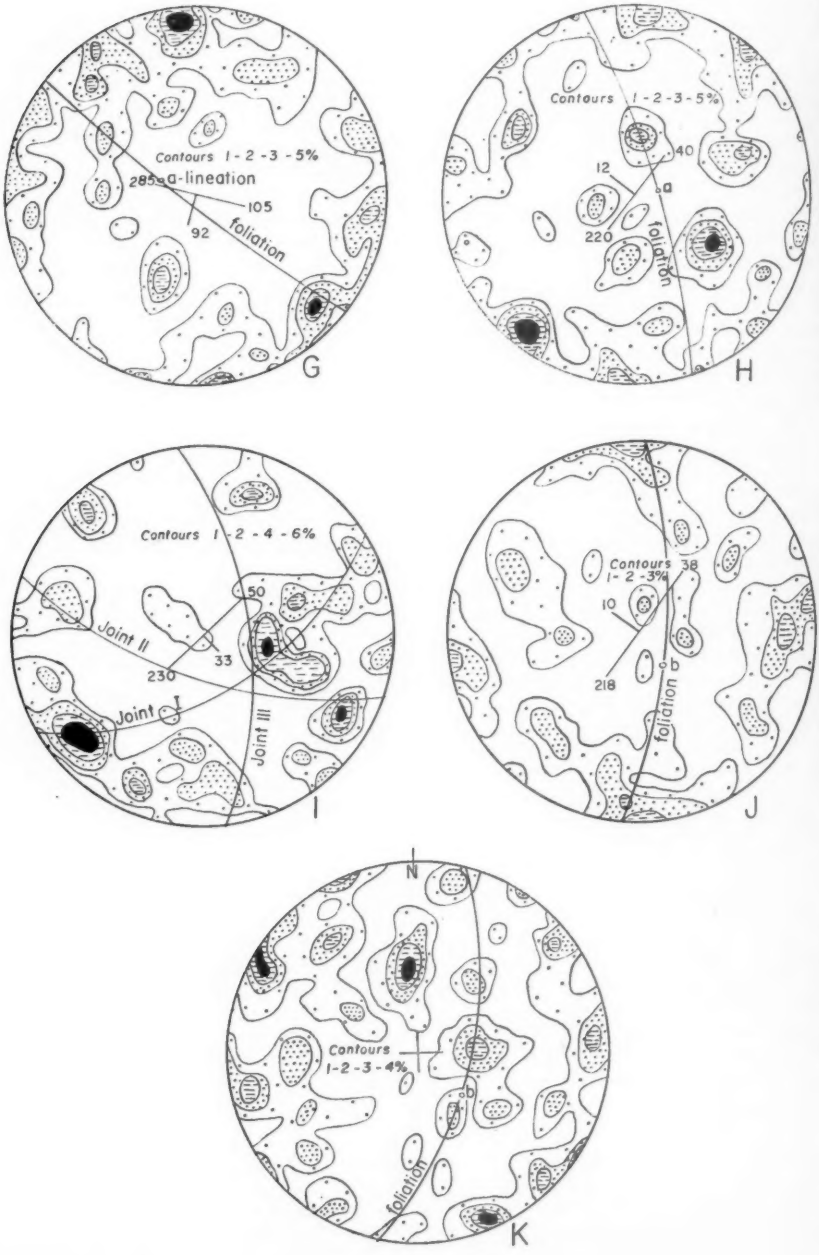
Contours 1-2-3-5%
285 a-lineation
105
92
foliation
G
Contours 1-2-3-5%
40
12
a
220
foliation
H
Contours 1-2-4-6%
50
Joint II
33
230
Joint I
Joint III
I
Contours 1-2-3%
38
10
218
b
foliation
J
N
Contours 1-2-3-4%
b
foliation
K

FIGURE 21—G-K

not negligible. The symmetry of the diagrams is triclinic.

(2) Another special feature of these diagrams is the tendency to show a weak *ab* girdle, in addition to a weak *ac* girdle. The former is generally considered to suggest influence of mimetic crystallization along the *s* plane in which particular direction of grain growth predominates (Knopf and Ingerson, 1938, p. 125–126). Such an influence is not unlikely in the present case, for the crystallization of the introduced quartz might have been controlled by the already existing foliation of the paragneiss.

The process of recrystallization during metasomatic introduction of the alkaline and siliceous fluids into these rocks has probably so modified the original paragneiss fabric that the net result is to show such a weak preferred orientation.

### *Recrystallization in the Deloro Pluton*

Two interesting types of recrystallization effects are seen in the perthite granite and syenite: segregation of secondary albite from perthite and recrystallization of quartz.

SEGREGATION OF SECONDARY ALBITE FROM PERTHITE: There are all gradations between perthites without any albite rim to the coarse crystals (up to 1 mm in size) of secondary albite adjacent to a perthite grain. One can observe several stages in such gradation:

(1) In most perthite grains, one finds a thin albitic margin in optical continuity with the albite components of the perthite. This albite, however, has the same composition ($An_8$–$An_{12}$) as the rest of the grain.

(2) At the next stage, one notices fine, granular, clear albite, extinguishing differently from the plagioclase component of perthite; the albite here is much more sodic in composition ($An_{3-5}$); in some cases, between two adjacent grains of perthite, one finds two such rows of albite granules.

(3) At the next stage the small granules tend to coalesce to form bigger, elongated crystals with incipient twinning along the margins of the perthite grain. Belonging to about this stage are some veins of secondary albite (and a little quartz) cutting across perthite, in the relatively more sheared types of granite.

(4) The last stage is the development of well-twinned, coarser crystals of albite well outside the outlines of the original perthite but always adjacent to it.

Secondary albite is more abundant in the relatively more granulated and deformed rocks than in the less strained samples. This suggests that during exsolution, the segregation of albite from perthite was aided by stresses.

RECRYSTALLIZATION OF QUARTZ: In the coarse perthite granites, much of the quartz occurs in large nests; each nest consists of a large number of equidimensional quartz grains (0.1–0.4 mm). All stages leading to the formation of such aggregates by progressive marginal granulation of the originally single, large crystals of quartz and partial recrystallization of the granulated materials can be seen.

Quartz orientation in a few specimens of the perthite granite was studied. The orientation diagram of 150 quartz c axes of the sample D 131 (Fig. 21 I) is a typical example. There is no girdle pattern, but the preferred orientation is strong; there are two prominent maxima (8.5 and 7.5 per cent respectively). The maxima do not have any symmetrical relationship with the joints in the rock, but the tendency of the poles to cluster into two prominent maxima suggests the activity of shearing movements.

## Outline History of Emplacement of the Granitic Plutons

The principal facts and inferences presented in the previous sections may now be synthesized to build up a connected outline of geological history of emplacement of the three granitic plutons.

(1) The Chandos Lake and the Wollaston plutons were emplaced approximately at the same time and under similar conditions of temperature and pressure at a fairly deep level in the crust; the Deloro pluton was emplaced

FIGURE 21—(*Continued*)

G. Biotite granite, Wollaston pluton (W 819), 150 quartz c axes; contours 1-2-3-5% (maximum 6%)
H. Biotite-hornblende granite, Wollaston pluton (W 47), 200 quartz c axes; contours 1-2-3-5% (maximum 7.5%)
I. Perthite granite, Deloro pluton (D 131), 150 quartz c axes; contours 1-2-4-6% (maximum 8.5%)
J. Gray granite gneiss, Wollaston pluton (W 487), 150 quartz c axes; contours 1-2-3% (maximum 4%)
K. Gray granite gneiss, Wollaston pluton (W 1164), 150 quartz c axes; contours 1-2-3-4% (maximum 4.5%)

higher up in the crust. In the absence of age-determination data, nothing definite can be said regarding the relative age of the Deloro pluton.

(2) The Chandos Lake and Wollaston plutons were emplaced at the close of the earth movements which folded and metamorphosed the Grenville sediments. The regional northeast-trending folding with gentle plunges was followed by the local westnorthwest folding with moderate to steep plunges. Toward the close of the fold movements a large number of small isolated intrusions of gabbro-diorite cut across the metasediments throughout the area. The granitic plutons were emplaced following a low-grade metamorphism of the gabbro-diorite intrusions.

(3) The composite Chandos Lake pluton was emplaced in a structural basin formed as a result of the configuration of folds belonging to the two sets of folds mentioned above. Both components of the pluton—the central elliptical syenite-monzonite body and the surrounding granite-granodiorite—are steep-dipping, cross-cutting, funnel-shaped intrusions emplaced by forceful upward and outward injection and locally also by intimate injections along the foliation planes of the paragneiss, such as in the northwestern part of the pluton.

The earlier syenite-monzonite intrusion developed a more basic central part and more acidic outer parts by a process of fractional crystallization, aided by the partial assimilation of several large inclusions of gabbro-diorite. Shortly after the consolidation of the syenite the body of biotite granite was emplaced around it. Although forceful injection was important, assimilation of varied rock types caused widespread rather unsystematic variations in the body of biotite granite; widespread assimilation of the biotite-hornblende paragneiss along a zone in the north-central part of the pluton gave rise to granodiorite.

Recrystallization processes during the cooling of the granitic and syenitic rocks gave rise to extensive myrmekitic intergrowths and albite rims on plagioclase. At this stage, the country rocks as well as the pluton were subjected to regional stresses, causing widespread jointing; many joints were filled by the residual fractions (pegmatitic) of the granite magma.

(4) The Wollaston pluton was emplaced along the eastern flank of a regional anticline as two major parallel bodies of granite separated by a screen of country rocks a quarter of a mile to half a mile wide. The body, as a whole, is east-dipping, the magma stream having moved south to north at approximately 45° to the horizontal, mainly by forceful injection tending to widen upward toward the crest of the anticline, and sending out narrow, offshooting granite dikes and sills. Parts of the screen of country rock have been incorporated by the granite, and parts of it were granitized to a granite gneiss. Aqueous diffusion of soda and silica from heated country rocks at an early stage of emplacement of the magma perhaps accounts for the remarkable soda-rich, silicic, potassium-poor border phase of the granite.

As in the case of the Chandos Lake pluton, regional stress following solidification of the magma caused widespread jointing in the pluton and in the country rocks; some of the joints were filled with pegmatitic and aplitic injections. This postconsolidation stress, characterized by the production of a prominent north-northeast joint set, was perhaps simultaneous in both areas.

(5) The Deloro pluton was emplaced in two distinct stages: (a) An earlier, crescent-shaped (on plan), forceful intrusion of perthite granite which grades to syenite along the western border because of assimilation of the gabbro-diabase country rock. Fractional crystallization starting from the northern, western, and southern borders of the body caused relative enrichment in the central and eastern parts of the pluton in silica and potassium. The steep-dipping intrusion pushed aside the country rocks on all sides, maintaining a largely concordant relationship with them. (b) While the main body of perthite granite was already solid but still fairly hot, more sodic and less mafic granophyric granite was intruded in the east. Intrusion of the granophyric granite delayed the cooling of the perthite granite body, as a result of which segregation of secondary albite from the perthites by migration of materials in the solid state was possible.

During this stage of cooling, regional stresses caused widespread fracturing and jointing and recrystallization of quartz; this was followed by the invasion of the fractured granite, syenite, and granophyric granite by hydrothermal solutions from depth, causing widespread chloritization and hematitization.

## References Cited

Adams, F. D., and Barlow, A. E., 1905, North Hastings sheet: Geol. Survey Canada Map 770, scale 1:126,720

— 1910, Geology of the Haliburton and Bancroft areas, Province of Ontario; Geol. Survey Canada Mem. 6, 419 p.

Ambrose, J. W., and Burns, C. A., 1956, Structures in the Clair River syncline: a demonstration in granitization: Royal Soc. Canada Special Pub. 1, p. 42–53

Barth, T.F.W., 1952, Theoretical petrology: N. Y., John Wiley & Sons, Inc., 387 p.

Becke, F., 1908, Über Myrmekit: Tscherm. Min. Petr. Mitt., v. 27, p. 377–390

Bowen, N. L., 1937, Recent high-temperature research on silicates and its significance in igneous geology: Am. Jour. Sci., v. 33, p. 1–21

Brown, J. S., and Engel, A.E.J., 1956, Grenville stratigraphy and structure in the Balmat-Edwards district, New York: Geol. Soc. America Bull., v. 67, p. 1599–1622

Chayes, F., 1948, A petrographic criterion for the possible replacement origin of rocks: Am. Jour. Sci., v. 246, p. 413–425

— 1949, Statistical analysis of fabric diagrams, p. 297–326 *in* Fairbairn, H. W., Structural petrology of deformed rocks: Cambridge, Mass., Addison-Wesley Press, 344 p.

Cloos, E., 1934, The Loon Lake pluton, Bancroft area, Ontario: Jour. Geology, v. 42, p. 393–399

Drescher-Kaden, F. K., 1948, Die Feldspat-Quarz-Reaktionsgefuge der Granit und Gneise: Berlin, Springer-Verlag, 259 p.

Harding, W. D., 1942, Geology of Kaladar and Kennebec townships: Ont. Dept. Mines, v. 51, pt. 4, p. 51–74

Hewitt, D. F., 1956, The Grenville region of Ontario: Royal Soc. Canada Special Pub. 1, p. 22–41

Hewitt, D. F., *et. al.*, 1957, Haliburton-Bancroft area: Ont. Dept. Mines Map 1957b, scale 1:126,720

Kennedy, G. C., 1955, Some aspects of the role of water in rock melts, p. 489–503 *in* Poldervaart, Arie, *Editor*, Crust of the earth: Geol. Soc. America Special Paper 62, 762 p.

Knopf, E. B., and Ingerson, E., 1938, Structural petrology: Geol. Soc. America Mem. 6, 278 p.

Kvale, A., 1953, Linear structures and their relation to movements in the Caledonides of Scandinavia and Scotland: Geol. Soc. London Quart. Jour., v. 109, p. 51–73

Miller, W. G., and Knight, C. W., 1914, Correlation of the Precambrian rocks of Ontario: Ont. Bur. Mines Rept. 22, p. 123–138

Moorhouse, W. W., 1956, The paragenesis of accessory minerals: Econ. Geology, v. 51, p. 248–261

Saha, A. K., 1958, Mineralogical and chemical variations in the Wollaston granitic pluton, Hastings County, Ontario: Am. Jour. Sci., v. 256, p. 609–619

Sander, B., 1950, Einführung in die Gefügekunde der geologischen Körper, Teil 2: Vienna, Springer, 409 p.

Schwantke, A., 1909, Die Beimischung von Ca im Kalifeldspat und die Myrmekitbildung: Centralbl. Min., p. 311–316

Spencer, E., 1945, Myrmekite in graphic granite and in vein perthite: Min. Mag., v. 27, p. 79–98

Turner, F. J., and Verhoogen, J., 1951, Igneous and metamorphic petrology: N. Y., McGraw-Hill Book Co., 602 p.

Tuttle, O. F., 1952, Origin of the contrasting mineralogy of extrusive and plutonic salic rocks: Jour. Geology, v. 60, p 107–124

Wilson, M. E., 1940a, Madoc-Hastings, Lennox, and Addington counties, Ontario: Canada Geol. Survey Map 559A, scale 1:63,360

—— 1940b, Marmora-Hastings, Peterborough, and Northumberland counties, Ontario: Canada Geol. Survey Map 560A, scale 1:63,360

Wynne-Edwards, H. R., 1957, Structure of the Westport concordant pluton in the Grenville, Ontario: Jour. Geology, v. 65, p. 639–649

Department of Geology, Presidency College, Calcutta, India

Manuscript Received by the Secretary of the Society, August 5, 1958

BULLETIN OF THE GEOLOGICAL SOCIETY OF AMERICA
VOL. 70, PP. 1327–1368, 20 FIGS. OCTOBER 1959

# STRATIGRAPHIC-SEDIMENTARY SIGNIFICANCE OF CONTEMPORARY CLIMATE AND RELIEF IN FOUR REGIONS OF THE ANDES MOUNTAINS

By H. F. Garner

## Abstract

Portions of the Andes Mountains of South America close to sub-base-level depositional sites currently yield a wide variety of clastic material in suites ranging from dominant clay with sand to coarse boulder-clay composites, which indicates that present concepts, associating source-area tectonic intensity as expressed through relief with control of clastic size, require revision. Relief and source-deposit distance do not alone determine depositional clastic-size range in the Andes, because, of four source areas examined, all are extremely high, and three are very close to depositional sites. The element controlling clastic size of sediments is capable of producing differing results where relief and distance of transport remain relatively constant and country rock suites are varied. Evidence presented indicates that the governing element is climate.

Humid weathering, as a dominantly chemical process, generates fine clastic material which is protected from fluvial or eolian erosion by vegetation and forms soil. Arid weathering, as a dominantly mechanical process, generates a high per cent of coarse alluvium which tends to accumulate within arid regions due to eolian removal of fine fractions and absence of perennial runoff.

Evidence presented shows that climate shifts can bring erosional and weathering processes of a given climate into contact with features previously developed by basically different processes. Regolith in a source and sediments yielded therefrom can reflect a single and prevailing climatic genesis (humid, Cordillera de la Costa, Venezuela; arid, Crodillera Occidental and coastal desert, Peru) or multiclimatic genesis where weathering and erosion have failed to eliminate inherited climatic effects (arid-humid transitions, Cordillera Oriental, Peru and Cordillera Occidental, Ecuador).

Clastic size being yielded by the four Andes regions correlates directly with vegetal cover, regolith, nature and/or competency of agents of transportation, and, therefore, climate. Sediments moved following a climate change tend to be weathering mixtures of a coarseness reflecting inherited regolith and progressing weathering and erosion.

The delay between the generation of a quantity of weathered material and its eventual delivery to a deposit by agents of subsequent climate(s) is designated sedimentary lag. Because movement of essentially all clastic material to sub-base-level deposits is characterized by sedimentary lag, the principle is important in tectonic-sedimentary relations and marine-nonmarine correlation.

## CONTENTS

### TEXT

| | Page |
|---|---|
| Introduction and acknowledgments | 1328 |
| Regional descriptions | 1333 |
| North Coastal Range of Venezuela | 1333 |
| Orography and structure | 1333 |
| Physiography | 1333 |
| Climate | 1334 |
| Bedrock and weathering | 1335 |
| Erosion | 1336 |
| Discussion | 1339 |
| Eastern Peruvian Sierra | 1339 |
| General information | 1339 |
| Climate | 1339 |
| Bedrock, weathering, and erosion | 1339 |
| Origin of residual alluvium | 1341 |
| Eastern geomorphic history | 1348 |
| Discussion | 1349 |
| Western Ecuadorian Sierra | 1349 |
| General information | 1349 |
| Alluvial accumulations | 1350 |
| Erosion | 1351 |
| Significance of alluvium | 1351 |
| Discussion | 1352 |
| Western Peruvian Desert | 1352 |
| General information | 1352 |
| Climate | 1353 |
| Drainage | 1355 |
| Vegetation | 1355 |
| Erosion | 1355 |
| Arid residual accumulations | 1356 |
| Through-flowing rivers | 1358 |
| Significance of alluvium | 1359 |
| Western geomorphic history | 1359 |

Page
Discussion ..... 1361
Comparative geomorphic events in the Peruvian Andes ..... 1362
Sequence of events ..... 1362
Theory of alternating Andean climates ..... 1363
Sedimentary and stratigraphic implications ..... 1364
General statement ..... 1364
Principle of sedimentary lag ..... 1365
References cited ..... 1367

## ILLUSTRATIONS

Figure Page
1. Index map of South America ..... 1329
2. River and strand-line relationships of the Cordillera de la Costa, Venezuela ..... 1334
3. Diagrammatic cross section of the Cordillera de la Costa north of Caracas, Venezuela ..... 1335
4. Schematic block diagram of the Cordillera de la Costa north of Caracas, Venezuela ..... 1336
5. Strand line and slide scar of the Cordillera de la Costa, Venezuela ..... 1337
6. Landslide scars and slide debris of the Cordillera de la Costa, Venezuela ..... 1338
7. Diagrammatic cross section of the Cordillera Oriental of Peru east of Mount Huascarán ..... 1340
8. Diagrammatic cross profiles of the Urubamba River Valley in Peru at four distinct valley-floor elevations ..... 1341
9. High-level alluvial fill along the Urubamba River Valley, Cordillera Oriental, Peru ..... 1342
10. Intermediate-level alluvial fill along the Urubamba River, Cordillera Oriental, Peru ..... 1343
11. Block diagram of the typical physiographic relations of the Cordillera Oriental, Peru ..... 1346
12. Schematic cross-section profiles of the geomorphic sequence and development in the Cordillera Oriental, Peru ..... 1346
13. Drainage and alluvium of the Cordillera Occidental, Ecuador ..... 1350
14. Diagrammatic multiple cross sections of the Cordillera Occidental, Ecuador ..... 1351
15. Schematic block diagram of the western slopes of the Cordillera Occidental southeast of Guayaquil, Ecuador ..... 1352
16. Diagrammatic northeast-southwest cross section of the Cordillera Occidental and Coastal Desert through Mount Coropuna, Peru ..... 1353
17. Arid topography and alluvium of the lower coastal desert, Peru ..... 1354
18. Schematic block diagram of the Cordillera Occidental and Coastal Desert, Peru ..... 1355
19. Arid alluvium and sparse vegetation of the Cordillera Occidental, Peru ..... 1356
20. Schematic cross-section profiles of the geomorphic sequence and development in the Cordillera Occidental, Peru ..... 1360

Table Page
1. Comparative developmental events in the Andes Mountains of eastern and western Peru ..... 1362

### Introduction and Acknowledgments

The Cordillera de la Costa of Venezuela near Caracas, the Cordillera Oriental of Peru, and the Cordillera Occidental of western Ecuador and Peru are areas of very high relief, and, with the exception of the Cordillera Oriental of Peru, all are very close to sub-base-level sites of deposition (Fig. 1). These areas are examined and data recorded with regard to country-rock suites, type of climate, major weathering processes, nature of clastic material currently being generated, active erosional agents, and type of clastic material being yielded to adjacent depositional sites.

The limitation of an erosional study to a single mountain range establishes the very general contemporaneity of elevation and slope of the separate montane segments with respect to orogenic activity. The spatial arrangement of these mountain provinces requires that any mechanism to explain sedimentary processes in one area must also be applicable in adjacent areas. The cases cited include three distinct source environments and the local development of a fourth (high-elevation mechanical weathering)—the Cordillera Occidental of Ecuador is very similar to the Cordillera Oriental of Peru but is included because proximity of base level closely parallels that of Venezuela and western Peru.

All four of the source areas considered have exceedingly high relief, and each displays a varied bedrock lithologic assemblage, yet they separately yield clastic material ranging from suites in which sands and clays dominate to boulder-clay composites. These relations depart drastically from the general assumption of tectonic or bedrock control of derivative clastic grain-size range. Moreover, the absolute elevation attained is not the determining factor. Comparison of the four areas discloses that the coarse materials formed in the zone of high-elevation frost action (where it is present) are almost invariably subjected to the climatic environment(s) which prevail at lower elevations before deposition at base level. As such high-elevation clastic fragments are commonly (1) incorporated into intermediate- or low-elevation arid coarse clastic residuals, sub-

FIGURE 1.—INDEX MAP OF SOUTH AMERICA

The four environmental regions discussed relative to the major physiographic trends are (1) Cordillera de la Costa of Venezuela, (2) Cordillera Oriental of Peru, (3) Cordillera Occidental of Ecuador, (4) Cordillera Occidental and Coastal Desert of Peru.

jected to arid environments, and are only potentially available to base level as sediments or (2) descend into intermediate- or low-elevation humid environments to be chemically decomposed together with the underlying bedrock; some fraction is introduced directly into perennial drainage systems and carried to base level. The fraction immediately yielded as a relatively coarse clastic element invariably has the greatest possible vertical distance and most commonly the greatest possible horizontal distance of movement to base level. The former is axiomatic to the definition of the zone in question, and the latter holds since the area of the zone usually constitutes or coincides with drainage divides. The initially coarse material is therefore potentially subject to greater grain-size reduction during transport than that from lower-elevation mechanical-weathering environments, and in deposits the former should be finer than the latter.

Further consideration of the influences of high-elevation mechanical weathering is eliminated from the present study also on the following counts: (1) it is a nonvegetated regimen paralleling the effects of aridity in terms of weathering; (2) its occurrence requires uplift extremes in excess of 11,000–16,000 feet within 35° lat. on either side of the equator; (3) for about 60° lat. on either side of the equator the appearance of derivative materials in a sediment would mark neither emergence of land nor rate of orogenic uplift; (4) the high-elevation coarse clastic material is not, to date, demonstrably distinguishable from other types of mechanically weathered clastic material although the potentially greater distance of movement to base level suggests that the former would not be extremely coarse; (5) if eventually distinguished in sediments the materials can signify only a particular degree of emergence or uplift and not necessarily initial emergence or orogenic beginnings except possibly in very high latitudes; (6) the high-elevation zone does not develop at all in many mountain ranges, such as the Sierra de la Costa of Venezuela, which attain great but not extreme elevations; (7) former adjustments in the vertical and/or geographic position of the high-elevation environment could alter the present limits of such developments but would not free the derivative materials from the marked influences of the various lower-elevation climates.

A standard element of tectonic and stratigraphic reports is the casual association of certain clastic sizes in marine deposits with particular conditions of relief, elevation, and/or proximity of source. Coarse materials are nominally attributed to some combination of high relief, high elevation, nearness and rapidity of uplift of source. Conversely, most argillites are traced to sources which are low, distant, and stable.

Transportation of clastic material will in general reduce the size of the fragments moved. However, the evidence presented shows that the association of orogenic activity (expressed in elevation and relief) with particular clastic sedimentary counterparts is in many cases unwarranted. The amount of movement and the nature of the parent bedrock are not the principal factors governing clastic size in many cases. This is shown by the distinctive clastic suites yielded by the separate Andes Mountains areas studied where the critical phases are close and essentially equidistant from base level, and source bedrock suites are of a similar varied nature. (*Compare* Figs. 3, 7, 16.) Because all four of the source areas considered are high and three are immediately adjacent to basins of deposition, the factor controlling clastic size must be a variable in a sedimentary clastic formula in which relief, complex bedrock suites and source-deposit distance are relative constants.

In the humid areas considered, where rivers are carrying appreciable amounts of coarse clastic materials, the loads are largely derived from high-elevation alluvial-valley fills emplaced under conditions different from those of the present. The presence of such alluvial fills and accumulations in the Andes Mountains has been discussed by a number of workers. Jenks *et al.* (1956, p. 246) with regard to the Peruvian Andes state that lateral valleys were choked with debris to a high level along the Mantaro, Huallaga, and Marañon rivers. In his studies made on the Yale Peruvian Expedition of 1911 Bowman (1916) makes repeated reference to a widespread alluviation which he attributed, with reservations, to glacial activity. Bowman (1916, Fig. 43, Caption) states that the Urubamba River aggraded its floor to a depth of several hundred feet. Elsewhere (p. 269) he adds, "... fluvial deposits [exist] as valley fill throughout the entire Andean realm." Vast alluviation versus limited glaciation cause Bowman's astonishment (p. 271) that,

"... deposits are everywhere important in amount, distinctive in topographic form and of amazing

wide extent. . . . They reach far into and possibly across the Amazon basin [*see also* Garner (1958)], they form a distinct though small piedmont fringe along the eastern base of the Andes and they are universal through the Andean valleys."

Logically enough, the humid area considered that yields dominantly fine material is the north slope of the Cordillera de la Costa in Venezuela in its wettest and most elevated portions immediately north of Caracas. The valleys on these slopes lack alluvial fills. The only area of the four that is generating coarse clastic detritus through weathering processes is arid, yields dominantly eolian-transported clastic material, and retains most of the coarse clastic material as residual accumulations. This statement refers to the western Peruvian desert, of which Bowman (1916, p. 232) observes that arid aggradation is now in progress. In the northernmost portion of the same desert Bosworth (1922, p. 284) notes that current processes are filling each valley and gully with alluvial material, and similar conditions prevail in the regions near Talara and Lima, Peru.

Standard textbooks and technical papers ascribe coarse alluvial valley fills to eustatic and/or tectonic causes. In the instances cited herein the alluvium occurs on both landward and seaward sides of a single mountain system at essentially all elevations. Moreover, many of the valley fills at elevations of more than 10,000 feet are now in early stages of dissection and are far removed from the nearest marine deposits. These factors eliminate the possibility that the alluvium was emplaced at or near sea level and subsequently elevated. In this connection Jenks *et al.* (1956, p. 246) makes a similar observation about the slight degree of dissection of the alluvium, as does Bowman (1916, p. 195). On these bases eustatic controls must be eliminated from consideration.

In the Andean region there are also serious objections to tectonic and tectonic-eustatic theories for the development of alluvial deposits. Coarse alluvial accumulations several hundred feet thick occur in western Ecuadorian mountain valleys at elevations exceeding 8000 feet and at even higher levels in eastern Peru. Bosworth (1922, p. 245) cites fills 150 feet thick in the northern Peruvian desert. Bowman mentions similar accumulations in the southern part of the same desert several hundred feet thick (1916, p. 230, 267, 273), and he cites high-elevation residuals in eastern Andean valleys (p. 272, 273) more than 400 feet thick. If these deposits, which have been assigned Pleistocene to Recent ages by (Bowman, 1916; Fenner, 1948b; Newell, 1949, and Jenks *et al.*, 1956) are due to tectonics, then the direction of movement was downward, as pointed out by Quinn (1957, p. 152) with regard to similar associations in Texas. However, according to Newell (1949, p. 13, 93), Bowman (1916, p. 267), Jenks *et al.*, (1956, p. 245, 246), Bucher (1952, p. 60), and Bosworth (1922, p. 267) the entire Andean system has been undergoing uplift during Pleistocene to Recent time and is probably continuing to do so. Jenks (April 14, 1958, personal communication) notes that faulting in coastal Peru has recently raised some surfaces 500–600 feet, tilted down others, and left still others relatively unmoved. (*See also* Newell (1956, p. 14).) Thus, emplacement of high-level alluvial-valley fills has taken place without regard to orogenic uplift and beyond the influence of combined tectonic-eustatic controls.

Newell, working in the Lake Titicaca area, did not deal with alluvial valley fills, though he (1949, p. 13) mentions intermontane basin fillings in structural depressions on the elevated plateaus of the Central Andes and further (p. 93) notes pediment surfaces having ". . . a veneer (up to 2 meters thick) of coarse stream gravel," in the vicinity of Lake Titicaca. Bowman and Jenks both recognized that the alluvium in the lateral mountain valleys could not be explained in terms of tectonic adjustments. Both of these workers regarded the deposits as of glacio-fluvial origin in spite of certain clearcut inconsistencies. Jenks (*in* Jenks *et al.*, 1956, p. 246) notes these inconsistencies but offers no explanation when he says,

"Throughout Peru there has been a deepening of stream channels in youthful valleys. Remarkably enough, however, many valleys have not yet been cut down to the depth they had before they were choked by overloaded glacial melt waters."

The valley fill, recent slight incision in the east, and youthfulness are a matter of record. However, with reference to the principles outlined by Gilbert (1880, p. 105, 108), Quinn (1957, p. 154) points out, ". . . that a stream increasing in volume in the downstream direction is capable of degrading its channel and cannot become overloaded, regardless of the quantity of sediment supplied." It is here

suggested that this relation be termed Gilbert's law of stream capacity. The eastern rivers in question not only increase in volume through the normal additions of tributaries but, as pointed out in the section dealing with eastern Peru, rainfall also increases downslope. (*See also* Ogilvie, 1922.)

Bowman's descriptions (1916, p. 186, 195, 196, 232, 257, 267, 268) are very detailed with regard to the alluvial fill and his ideas of its origin. He states,

"The Pleistocene deposits fall into three well-defined groups; (1) glacial accumulations at the valley heads, (2) alluvial deposits in the valleys, and (3) lacustrine deposits formed on the floors of temporary lakes in inclosed basins."

The third group has no direct bearing on the present problem, as was recognized by Bowman (1916, p. 269) and has been discussed, in many of its phases, by Newell (1949). In group (1) Bowman includes relatively recent terminal moraines, ground moraines, and recessional moraines, which according to Jenks (*in* Jenks *et al.*, 1956, p. 246) do not occur below an elevation of 3800–4000 meters. The deposits of group (2) extend many miles down the mountain valleys. Apparently because the glacial outwash below the terminal moraines has some of the lithologic characters of the valley fill Bowman felt compelled to attribute the entire alluvial complex to glaciation; but he emphasizes,

"... that a deposit of such volume—many times greater than all the material accumulated in the form of high-level alluvial fans or terminal moraines—should originate in a topical land in a region that suffered but limited Alpine glaciation vastly increases its importance.

"... through alluviation the valleys and basins of the Andean Cordillera, and the vast area of the great Amazon plains east of it, felt the effects of the glacial conditions of a past age" (p. 271).

In an effort to reconcile relatively restricted glacial activity with the immense amount of alluvium Bowman (1916, p. 268) offers the following explanation.

"The rock waste ground up by the ice was only a small part of that delivered to the streams in glacial times. Everywhere the *wetter* climate resulted in the partial stripping of the residual soil gathered upon the smooth mature slopes formed during the long Tertiary cycle of erosion. This moving sheet of waste as well as the rock fragments carried away from the glacier ends were strewn along the valley floors, forming a deep alluvial fill."

Bowman (1916, fig. 180) states, "... the extensive alluvial deposits of the valleys ... consist ... of confluent alluvial fans ...", and he adds (p. 270, 271),

"... where the fans were deposited in narrow valleys the effect was to increase the thickness of the deposits at the expense of their areas, to dam the drainage lines or displace them, and to so load the streams that they have not yet cleared their beds after thousands of years of work under torrential conditions."

This also is in disagreement with Gilbert's law, and it is difficult to understand how the "thousands of years of work under torrential conditions" should have differed from the "wetter" (glacial) climate which resulted in the formation of the alluvial fill according to Bowman (1916, p. 268).

Of the other writers who favor the idea of relatively recent elevation of the Andean region, Bucher (1952) had no occasion to refer to alluvial deposits. Bosworth (1922), working in northwestern Peru in the Tumbes Desert, repeatedly refers to Pleistocene and Recent alluviation of the mountain valleys and uplifted marine terraces. He attributes the aggraded channels and terraces to heavily loaded desert flash floods which lose wates and hence volume by absorption and evaporation which would in turn cause them to deposit. The ideas expressed by Bosworth were earlier stated by Johnson (1901).

The evidence in eastern Peru demonstrates that the humid conditions there, which are essentially duplicated in the coastal ranges of Ecuador and Venezuela, have associated weathering processes which generate fine clastic material. Coarse alluvium cannot be deposited if it is not being formed. Therefore, why are the residual deposits dominantly coarse? Conditions of aggradation differ materially from those of incision, just as weathering processes that yield fine clastic material differ from those that form dominantly coarse material.

All the data available from the Andean region lend clear support to the contention that climate is the factor that controls clastic fragment-size generation and accumulation on land. The mechanism as it functions in this regard has been outlined by Quinn (1957, p. 158–161). The geologic evidence presented here seems more than sufficient to establish climate as the mode of control over movement of material to basins of deposition.

Demonstrable climatic fluctuations automatically eliminate the usual assumption that there is a continuous removal of all sedimentary types from source to deposit. These principles should clarify the relations between marine and nonmarine sedimentary facies and the significance of such facies as expressions of tectonic activity through climate.

All four of the Andes Mountains areas discussed are rather difficult of access away from the few main routes of travel. In most cases the areas are only rarely visited by geologists and those largely in search for petroleum indications and mineral wealth. The available literature dealing with the specific regions in question ranges from general treatments (Bowman, 1916; Bosworth, 1922; Liddle, 1928; 1946; Sheppard, 1937; Jenks, 1948; Jenks *et al.*, 1956; Newell, 1956) to specific structural, paleontologic, or stratigraphic studies (Fenner, 1948a; 1948b; Newell, 1949; Bucher, 1952; Newell, Chronic, and Roberts, 1953). Consequently, reference material dealing specifically with the relations of contemporary erosion, weathering, relief, and climate are limited and widely disseminated. Bowman's data (1916) are pertinent and detailed with regard to Peru. The relations disclosed by the present study were to some extent anticipated in theory by Twenhofel *et al.* (1926, p. 87–108; 1932, p. 141–142; 1939, p. 19). Some of these ideas were modified and applied with excellent results by Quinn (1957). The field work, which is the basis for the report, was done intermittently during the years 1951–1956.

The writer is indebted to many people who knowingly and unknowingly assisted him in his observations. Some of these are private residents of the various South American countries, whereas others are or were oil-company employees. Particular thanks are due Dr. Walter L. Youngquist of the University of Oregon and formerly of the International Petroleum Company at Talara, Peru, Dr. K. C. Jackson of the University of Arkansas who read and criticized the manuscript, and Dr. J. H. Quinn of the same institution, whose basic work, suggestions, and assistance are fundamental to the present report. Thanks are also due Dr. W. F. Jenks of the University of Cincinnati and Dr. N. D. Newell of the American Museum of National History who read the manuscript and offered many valuable comments and suggestions.

Illustrations for the present paper were prepared by Mr. L. E. Pool working with the writer. The drawings shown in Figures 2, 5, 6, 9, 10, 13, 17, 19 were obtained by tracing details on illuminated projections, 6 inches by 10 inches, of 35 mm Kodachrome color slides. Acknowledgment is also due the College of Arts and Sciences of the University of Arkansas, which made the completion of this report financially possible.

## Regional Descriptions

### *North Coastal Range of Venezuela*

*Orography and structure.*—The North Coastal Range of Venezuela is also known as the Sierra del Norte and the Sierra or Cordillera de la Costa. It bounds Venezuela on the north and lies immediately adjacent to the Caribbean Sea, trending east-west at lat. 10° N. As pointed out by Liddle (1928, p. 48) these mountains attain their greatest elevations in the Caracas region. The Serrañia del Interior or Inner Range comprises foothills which lie immediately south of the Coast Range proper. The present study is confined to the seaward slopes of the higher portion of the Cordillera de la Costa near Caracas (Fig. 1).

This area has been treated in a rather general way by Liddle (1928; 1946), later by others including Aguerrevere and Zuloaga (1937), and more recently from a structural standpoint by Bucher (1952). Liddle (1928, p. 48) regards the Cordillera de la Costa as an eastward continuation of the Venezuelan Andes. Bucher (1952) does not include the area in his discussion of the Venezuelan Andes and appears to regard the coastal mountain system as being structurally associated with the Caribbean complex. All workers seem to consider the main Andean Mountains and the North Coastal Range of Venezuela as being of generally similar age tectonically and therefore physiographically.

*Physiography.*—Sea cliffs occur for many miles along the Caribbean border of these mountains, and the coastal plain, where present, rarely exceeds 1 mile wide (Figs. 2A, 5A). The range attains maximum elevations just north of Caracas where the peaks of La Sila and Naguata are nearly 10,000 feet high. The Serrañia del Interior is lower and the maximum relief is less than that of the Coast Range, for many of the more southern valleys have thick alluvial fills like that found in the Valle de Caracas. The northern slope of the Cordillera de la Costa is steep and descends

A

B

FIGURE 2.—RIVER AND STRAND-LINE RELATIONSHIPS OF THE CORDILLERA DE LA COSTA, VENEZUELA

A. Aerial view of north slope of coast range east of La Guaira. Light areas are cultivated ridge crests from which jungle cover has been cut. The stream is the Rio Tuy which empties into the Caribbean Sea in the foreground.

B. Mountain valley on north slope of range looking north and downstream. Channel is inclined away from viewer about 15° at this point. Vegetation and soil cover extend down steep valley sides to channel margins. Channel floor is bare bedrock containing pockets of medium-grained garnet-rich sand and surficial patches of slide debris composed of vegetal fragments and partially weathered bedrock cobbles. Seventy-five feet directly behind viewer is near-vertical face of a slide scar which merges with the channel in a pile of varied plant and rock rubble.

from an altitude of slightly less than 2 miles to sea level in a horizontal distance of about 6 miles (Fig. 3).

*Climate.*—The northern slopes of the Cordillera de la Costa in the area of maximum altitude receive 40–50 inches of rainfall annually. The precipitation is distributed throughout the year but is considerably accentuated in the months of November and December. Evaporation is much reduced by cloud cover resulting from daily condensation of moisture carried by winds rising from the warm Carib-

bean Sea. The slopes support a tropical rain forest from near sea level to more than 8000 feet, and thick growths of bamboo and fern were observed at elevations of more than 9000 feet. The average temperature is 20° C.; it

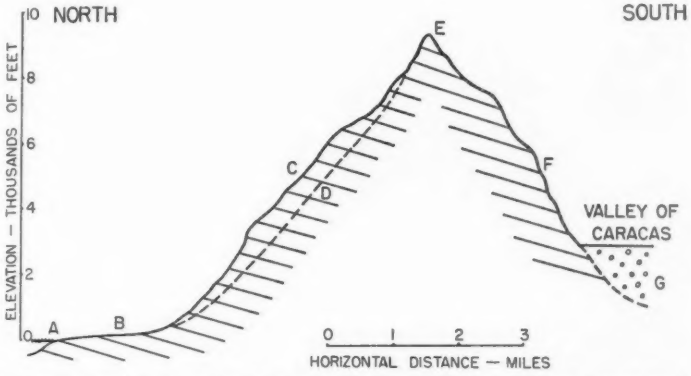


FIGURE 3.—DIAGRAMMATIC CROSS SECTION OF THE CORDILLERA DE LA COSTA NORTH OF CARACAS, VENEZUELA

Illustrated are (A) south Caribbean shore, (B) narrow Coastal Plain, (C) humid, steep northern slopes (D) generalized stream profile paralleling direction of greatest slope, (E) Pico de Naguata—highest mountain in the coast range, (F) relatively dry southern slopes, (G) alluvial valley fill of the Valle de Caracas—also common to the other valleys of the Serraña del Interior.

is somewhat cooler along the crest of the range and warmer at sea level.

South of the Coast Range the climate is generally subarid, and rainfall is between 20 and 30 inches annually. Vegetal cover is patchy and commonly confined to watercourses. Moisture capable of supporting a rain forest on the south slopes of the Coast Range proper is apparently related to crestal rainstorms on the higher peaks. A rare and violent electrical storm with considerable precipitation was observed from the peak of La Silla. The storm was caused by a strong southerly wind which developed at sundown, ascended the landward slopes, particularly the valleys, and met a similar current of air rising from the Carribbean Sea. The rainfall centered on the crest of the range, but some moisture gained the south slopes directly or by runoff.

*Bedrock and weathering.*—The rocks of the coastal mountains are predominantly metamorphosed and intruded sedimentary rocks. They include "greenstones," talc and garnet schists ("eclogites"), quartzites, and limestones. Bucher (1952, p. 51) mentions garnet-rich rocks near the town of Antímano, and the same association occurs in several quebradas draining the north slopes along the old Spanish mule trail between Caracas and the coast (Fig. 2B). Aguerrevere and Zuloaga (1937, p. 20) noted augen gneiss along the road from Caracas to Maiquetía, and it also occurs on the peak of La Silla. These rocks belong to the lithologic suite to which Bucher (1952, p. 50) assigns a Cretaceous age.

Bedrock exposures are relatively rare on the north flank of the range considering (Bucher, 1952, p. 60) "... the tremendous gradients of the valleys in the Cordillera de la Costa and the fierce slopes of the valley sides" (Fig. 4). The rocks are obscured by dense plant cover and by thick weathered zones (Fig. 2B).

The weathered interval is as much as 40 feet thick where observed in stream cuts on the gentler slopes, about 10 feet thick on the very steep slopes, and is gradational with bedrock. Liddle (1928, p. 49) mentions talus slopes along the northern coast, but the writer failed to observe them in the range north of Caracas. Possibly Liddle was speaking of slide scars, which are discussed below. Talus accumulations probably would not form under prevailing conditions, for the weathered interval is maintained on the slopes by dense vegetation. Thickness of the weathered zone is attributable to chemical alteration of the country rock in the presence of abundant moisture, humic acids, and high temperature. In color the weathered interval ranges from light tan to brick red.

*Erosion.*—The streams that drain the north slopes of the Cordillera de la Costa range from intermittent to permanent, during normal years. They carry a solid load of principally argillaceous material, some fine to medium sand, and very little larger material. The stream loads are derived from the mantle, in part by the process of solifluction, in connection with extreme slopes. Minor amounts of material are contributed by the alluvial fills in the Serrañia del Interior, although most of the streams of this region lie in the drainage area of the Orinoco River. The Coast Range valleys are V-shaped with weathered material covering the valley slopes to the valley floor, which in most places is coincident with the stream channel (Fig. 2B).

Rainfall was unusually heavy in the more elevated parts of the Cordillera de la Costa during November and December of 1950. The north slope of the range was water-saturated to bedrock as a result. In late January and February of 1951 a series of large-scale landslides occurred at scores of sites along the range. A single air reconnaissance disclosed more than 200 major slides and countless smaller ones (Figs. 5B, 6A).

Several of the slides were examined in detail on the ground, and many of these were in excess of 100 yards wide and up to 400 yards long (Fig. 5B).

All vegetation, weathered material, and in some places sections of rotten country rock were stripped from the slide areas which appear as light-colored scars (Fig. 6A). On the slides examined the material removed measured 2–3 yards thick. Essentially all slides appear to be inclined more than 30°, and most have their bases in steep valleys (Figs. 2B, 5B).

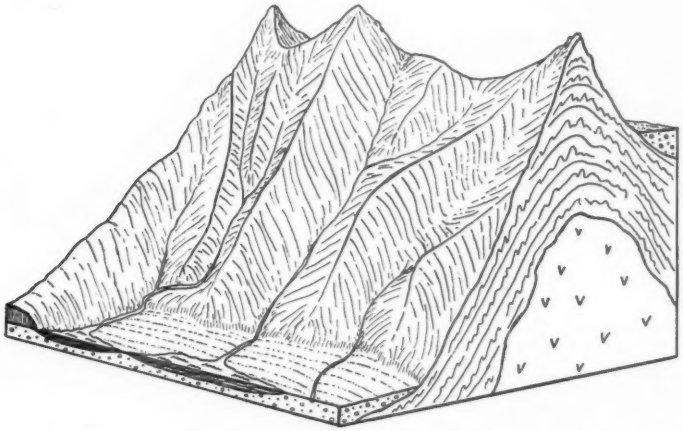

FIGURE 4.—SCHEMATIC BLOCK DIAGRAM OF THE CORDILLERA DE LA COSTA NORTH OF CARACAS, VENEZUELA

In the foreground are the narrow coastal plain and the south Caribbean shore; streams draining the north slopes flow into the sea without appreciable meander development. The mountain front illustrates the steep slopes, absence of residual valley accumulations and V-shaped valley cross profiles developed on humid slopes. Alluvial valley fills away from the coast such as in the Valley of Caracas are indicated at the far right. Vertical exaggeration × 3.

The saturated slide material quickly attained high velocity. Deposition began where the major break in slope occurred—on the coastal plain where present, otherwise in the sea. As the quantity of material supplied exceeded the capacity of the coastal-plain stream channels debris spread as a sheet over the adjacent lowland (Fig. 6B). Locally buildings, vehicles, and people were washed into the sea, and towns like La Guaira, which was in the path of the slide material, were buried to a depth of as much as 15 feet.

The deposits on the coastal lowland are poorly sorted. More than 70 per cent of the material is sand and finer. Other fractions are made up of plant material, including trees, and bedrock fragments. Most of the latter are partially decomposed by weathering. Arrangement of the sediments is random in most

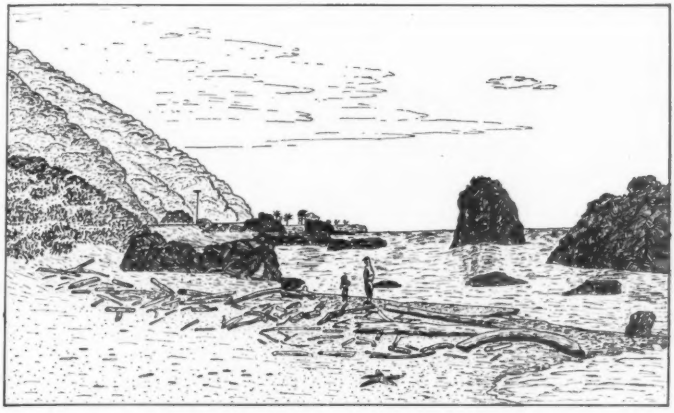

A

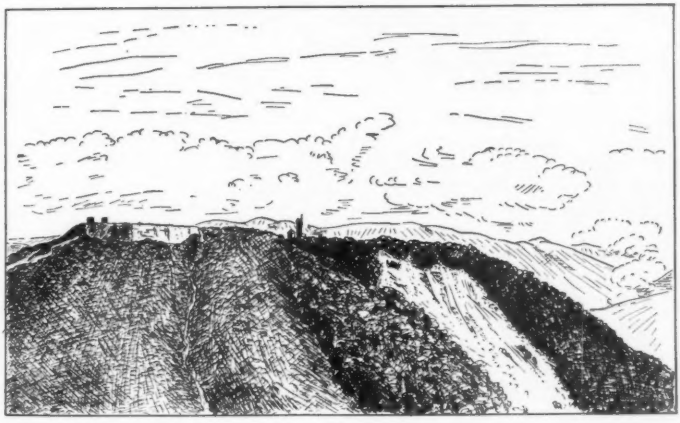

B

FIGURE 5.—STRAND LINE AND SLIDE SCAR OF THE CORDILLERA DE LA COSTA, VENEZUELA

A. Mountain-base-Caribbean Sea juncture east of La Guaira. The beach is composed primarily of medium to fine sand. The large rock masses on and near shore appear to have been cut by marine erosion from the adjacent mountain base, which is locally a cliff. No appreciable coastal plain is present, though a portion of a narrow one can be seen in the far background. The steep slopes to the left are heavily vegetated, and most of the driftwood in the foreground is landslide debris. The viewer is looking west.

B. Slide scar near Old Spanish Fort at elevation of 5400 feet. Background hills are Serraña del Interior. Foreground slopes face north. Slide scar is more than 100 yards wide and more than 1500 feet long.

places, and there is little or no bedding (Fig. 6B). The character of the deposits is so unusual that confusion with debris accumulated in a different manner is unlikely.

Estimates based on the average dimension of the slides examined suggest that a minimum of 20 million cubic yards of material was removed from the range in a very few weeks. On the basis of thickness and areal extent the coastal lowland near the towns of La Guaira and Miaquetía is estimated to have received more than 2 million cubic yards of alluvium.

A few months after the occurrence of the slides the streams draining the Cordillera de la Costa were once more carrying normal loads with only a somewhat excess coarse fraction supplied from local removal of slide debris. The material spread on the arid coastal

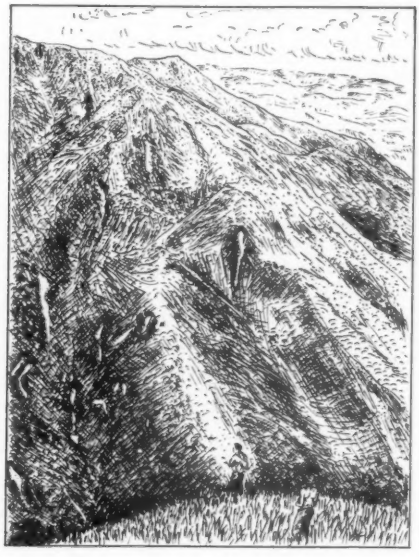

A

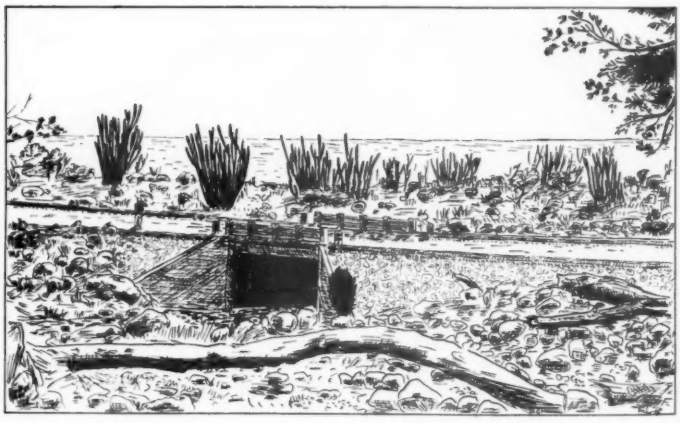

B

FIGURE 6.—LANDSLIDE SCARS AND SLIDE DEBRIS OF THE CORDILLERA DE LA COSTA, VENEZUELA

A. Slide scars of Mount Naguata. Picture taken from slopes of Mount La Silla looking northeast. Light areas in far slopes are scars at elevations between 7000 and 8000 feet. Clastic material from these particular slides was incorporated into valley fill already present in Serraña del Interior, since runoff here becomes intermittent or ephemeral to the south in the subarid-to-arid region north of the Orinoco River and the drainage lines are alluviated.

B. Slide debris on Coastal Plain. Road shown is east of La Guaira and was buried at bridge by slide debris. Excavation and subsequent erosion has removed fine material and left coarse debris on arid lowland. Caribbean sea is in background. Scene is about half a mile from base of mountains.

plain has remained as a residual. The coastal plain proper is elevated only a few feet above sea level and normally receives less than 10 inches of rain annually, as do the low offshore islands and the Peninsula of Paraguana. Sands in the coastal beaches are medium to fine-grained and incorporate much vegetal material in the form of driftwood (Figs. 5A, 6B).

*Discussion.*—On the basis of theories of tectonic control of sediment size the Cordillera de la Costa near Caracas combines a minimum distance of transport with a maximum slope and should therefore yield clastic sedimentary material of maximum coarseness. Actually, the normal solid stream load from this humid area is relatively fine—clay, silt, and sand. This detritus is a product of current weathering processes operating on steep slopes under conditions of high humidity. The valleys on the north slope of the Cordillera de la Costa contain no residual alluvial accumulations.

The landslides appear to be relatively rare occurrences in the area, are composed mainly of fine clastic material, and reach a marine depositional environment only where the base of the mountain range is approximately at the strand line. Considering the rapidity of deposition where the foot of the range meets the coastal plain, it seems certain that a coastal lowland no more than 3 miles wide would bar slide debris from direct access to the sea.

The association of large plant fragments, clay, silt, sand, and weathered bedrock debris in absence of sorting and bedding phenomena is unique. The unusual nature of the slide-debris lithologic complex should be easily recognizable in both marine and nonmarine sections if no extensive reworking has occurred. The small grain size of the normal solid stream loads and the fine material and partially decomposed bedrock in the slide debris indicate that most recent deposits in the Caribbean Sea from this area are not coarse clastic material.

Contrary to tectonic-sedimentary theory the high, steep Venezuelan north coast is not a source for gravels and conglomerates—the supposed product of high-relief source areas close to depositional sites.

### *Eastern Peruvian Sierra*

*General information.*—The Eastern Peruvian Sierra or Cordillera Oriental is the mountainous portion of the area regionally referred to as the Peruvian Oriente. The most prominent range of the region is the Cordillera Vilcapampa. The region is drained by several tributaries of the Amazon River and extends between lats. 10° and 15° S. (Fig. 1).

Probably the most detailed and inclusive study of the geologic provinces of the Peruvian Andes was made along the 73rd meridian by Bowman (1916) in connection with the Yale Peruvian Expedition of 1911 and in corollary studies (Bowman, 1914; 1924; 1938). Subsequent work such as that of Fenner (1948a; 1948b), Jenks (1948), Kummel (1948), and Newell (1949; 1956) has been more restricted and specialized though no less important.

Access to the area is very difficult beyond the main routes of travel. Slopes locally exceed those of the Cordillera de la Costa of Venezuela although their average rate of descent to sea level is somewhat less. The high plateaus of the eastern range average between 13,000 and 14,500 feet, and numerous peaks rise above this elevation; some exceed 20,000 feet. The eastern slopes descend from maximum elevations nearly to sea level in the adjacent Amazon Basin in a horizontal distance ranging between 150 and 200 miles (Fig. 7). The major streams do not parallel the direction of greatest slope, as in the Venezuelan drainage, but flow north transverse to it for many miles before joining the eastward-flowing Amazon River.

*Climate.*—Precipitation averages more than 80 inches annually in the Amazon rain forests and 40 inches or less at an elevation of about 12,000 feet on the mountains. Higher elevations receive much less rainfall. Local moisture variations on deep valley floors were described by Bowman (1916, p. 148), who also noted (p. 147), "... the belt of maximum precipitation on the eastern border of the Andean Cordillera in Peru lies between 4,000 and 10,000 feet ... the line of perpetual snow is at 15,000 feet." The distribution of moisture in the area assures stream-volume increase in a downslope direction apart from normal tributary additions. Average temperatures decrease from 20° C. on the Amazon lowland to about 10° C. at more than 12,000 feet; the greater annual variations occur in the higher altitudes.

*Bedrock, weathering, and erosion.*—Paleozoic and Mesozoic rocks are recorded by various workers including Newell (1949) and Newell,

Chronic, and Roberts (1953), and intrusions into these sediments are noted by Bowman (1916) and Jenks *et al.* (1956). Bedrock includes, therefore, a wide variety of sedimentary

Andean rivers should flow on bedrock through steep rock-walled gorges, but in most places this is not the observed relation. Rock-walled gorges are locally present, but most of the

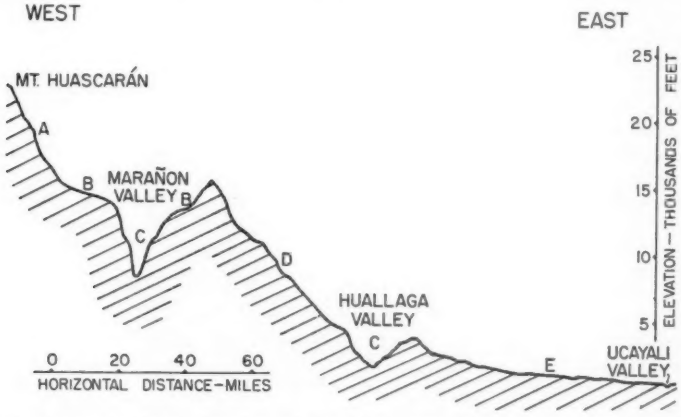


FIGURE 7.—DIAGRAMMATIC CROSS SECTION OF THE CORDILLERA ORIENTAL OF PERU EAST OF MOUNT HUASCARÁN

Illustrated are (A) rugged summit topography of high peaks, (B) more or less gently inclined elevated plateau surfaces, (C) cross profiles of northward-flowing rivers which are transverse to the direction of greatest slope, (D) steep, humid eastern slopes, (E) lowland of the Amazon drainage basin.

and igneous (intrusive and extrusive) types which fall within the range of lithologies described in Venezuela with little significant variation. This also generally applies to western Peru and Ecuador; the differences in erosionally extracted clastic material are therefore not traceable to significant bedrock differences.

Chemical weathering under humid conditions produces thick weathered intervals from the wide variety of rock types on all but nearly vertical slopes. As in Venezuela, the weathered material is anchored to the slopes by tropical rain forests which extend about 7500 feet up the mountain slopes. Heavy thorn-scrub vegetation covers most slopes from 7500 feet to more than 9000 feet, and dense grasses grow from there to more than 13,000 feet. The "cool-climate" high-altitude soils tend to be black and rich in humic material, whereas the "high-temperature" low-elevation soils are red to tan, and most are thoroughly leached. As pointed out by Bowman (1916, p. 70) some of the richest soils are developed in the valley bottoms on alluvium.

It might be supposed that alluvial soils such as those cited in the preceding paragraph would be rare in high mountain valleys. Relief and runoff seem to indicate that the eastern rivers are incised in rather flat wide alluvial-valley fills which are locally several hundred feet thick (Fig. 8). These deposits were mentioned briefly by McLaughlin (1924, p. 627) and Jenks *et al.* (1956, p. 246) and in considerable detail by Bowman (1916). Extensive alluvial accumulations extend from near the Amazon lowland up the valleys of the Apurimac and Urubamba rivers for scores of miles horizontally and thousands of feet vertically (Figs. 9A, 9B, 10A, 10B). Bowman (1916, p. 271) indicates that alluvium extends far into or possibly even across the Amazon Basin and states that such accumulations are present in almost every valley of the region (Fig. 8 B, C, D). Similar conditions are suggested for eastern Ecuador by Tschopp (1953) and on the southeast side of the Venezuelan Andes by Liddle (1946) and Mencher *et al.* (1953) and elsewhere by the writer (1958).

Most of the valley bottoms are as much as 2 miles wide at high altitudes and become narrower at lower levels (Fig. 8). The Urubamba Valley is 2½ miles wide at 11,000 feet and narrows gradually to only a few hundred yards at 7000 feet. Narrow rock-cut stream channels are best developed on the lower mountain slopes such as in the Pongo de Manseriche

of the Marañon River and the Pongo de Mainique on the Urubamba River.

The alluviated portions of the valleys have few channels incised in bedrock (Figs. 8, 9A, 9B). Bowman (1916, p. 195) remarks that the alluvial fill which lies on all the canyon and valley floors is now in the process of dissection and notes, "... since its deposition in the Pleistocene it has been eroded on the average of about 200 feet." Elsewhere (p. 272) he notes, "... at Cotahuasi ... there is a remarkable fill at least four hundred feet deep," and he emphasizes a point that the writer also noted: the rivers are still flowing on and eroding the same material into which their channels are cut (Fig. 10A).

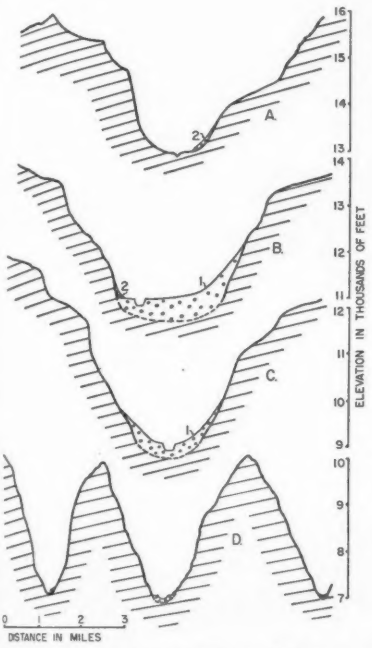


FIGURE 8.—DIAGRAMMATIC CROSS PROFILES OF THE URUBAMBA RIVER VALLEY IN PERU AT FOUR DISTINCT VALLEY-FLOOR ELEVATIONS

Illustrated are (A) glaciated source region with U-shaped valley, minor quasi-recent talus and incipient dissection of bedrock stream channel, (B) high-level alluviated valley with modified U-shaped profile showing (1) coarse valley fill from confluent talus fans and cones which predates most recent glaciation and (2) minor talus cones which postdate glaciation and predate present humidity, (C) intermediate-level alluviated valley with modified U-shaped profile inherited, as in (B), from more severe glaciation preceding the last severe aggradation, (D) intermediate-level V-shaped alluviated valley in present region of greatest rainfall; B, C, and D illustrate incomplete dissection of residual alluvium.

All observers in the area have remarked on the coarseness of the alluvial deposits (Fig. 10A). Poor sorting has also been recorded. Bowman (1916, p. 272) says, "... the material is both sand and clay with an important amount of gravel laid down with steep valleyward inclination ... elsewhere in the same deposit, running to a bowldery or stony mass". The alluvium in almost all places contains appreciable amounts of pebbles, cobbles, and boulders. Much of it is angular to subangular indicating only short distances of transport and local derivation—for example in the middle and lower valleys of the Urubamba River. Torrential deposits and scour and fill structures are common; subrounded to well-rounded fragments are mixed with angular material. As Bowman points out (1916, p. 272) "... within a given bed there may be an apparent absence of lamination." In many parts of the accumulations no bedding structures were observed, and the general size and angularity of much of the debris is indicative of normal talus accumulations.

Bowman (1916, p. 269–271) apparently wished to distinguish between alluvial accumulations that he calls valley fill and those he refers to as alluvial fans. In the currently drier high elevations it is possible to distinguish locally small alluvial fans or cones superposed on what appears to be older alluvial-valley fill (Figs. 9A, 12, stage P − 1). However, in many instances the fans appear to constitute the entire valley fill, and slopes on the alluvium are essentially continuous from the bases of scarps to the river banks (Figs. 8B, 9A). Recognizing the lack of a sharp line of distinction, Bowman (1916, p. 268–269) groups all but lacustrine and glacial sediments into "alluvial deposits in the valleys."

*Origin of residual alluvium.*—Students of stratigraphy, sedimentation, and structural geology assume that high relief in itself is sufficient to produce coarse clastic material. The amount of local relief is not a causative factor in the formation of clastic rocks in the Cordillera Oriental of Peru. Present weathering processes in the area are not contributing significant amounts of coarse debris to either the valley alluvial accumulations or directly to the rivers in spite of the high relief. Past weathering processes have generated

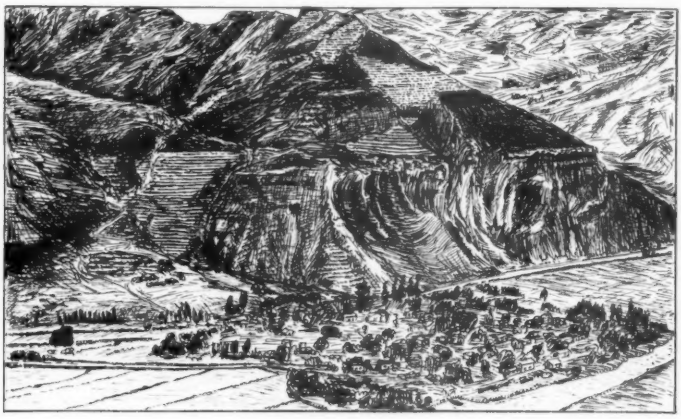

A

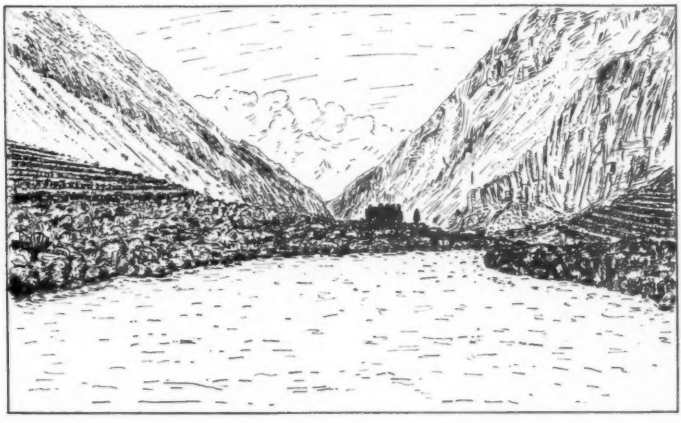

B

FIGURE 9.—HIGH-LEVEL ALLUVIAL FILL ALONG THE URUBAMBA RIVER VALLEY, CORDILLERA ORIENTAL, PERU

A. Valley of Urubamba River at 11,500 feet. Flat floor is formed on alluvial fill several hundred feet deep. Channel of river is only slightly incised (±50 feet). Alluvial cone in left background is terraced and lies on main valley fill. Upper-slope agricultural terraces are cut into weathered mantle. The valley was glaciated and formed U-shaped cross profile before most recent major alluviation. At elevations above 12,000 feet a recent glacial advance has scoured out the major fill.

B. Confluent alluvial fans in Urubamba River Valley near 10,000 feet elevation. Agricultural terraces developed on alluvium data from Inca times. Recent talus formation is slight.

coarse clastic material, when relief was essentially the same as at present. Proof is furnished by a number of related factors: (1) the nominal products of chemical rock weathering under humid conditions, (2) the development of soils, (3) the preservation of pre-Colombian agricultural terraces, and (4) the preservation of glacial physiographic forms.

CHEMICAL WEATHERING: The effects of moisture and heat on the acceleration of chemical activity and hence rock breakdown by chemical means has been amply treated by a great many workers during the past

A

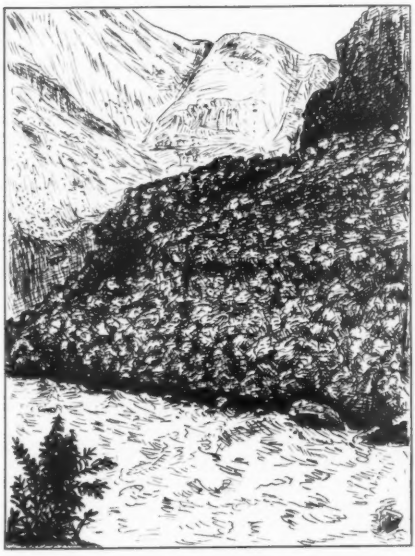

B

FIGURE 10.—INTERMEDIATE-LEVEL ALLUVIAL FILL ALONG THE URUBAMBA RIVER, CORDILLERA ORIENTAL, PERU

A. Urubamba River Valley near 9000 feet elevation. Channel is incised into coarse alluvial-valley fill from confluent alluvial fans and cones to depths of 50–175 feet. Note increased vegetal cover in comparison to Figures 9A and 9B.

B. Urubamba River Valley near 8000 feet elevation. Channel is cut into alluvium and flowing on it. Slopes are covered with dense jungle growth. Valley cross profile is nearly V-shaped and relatively narrow. Compare to Figure 8, D.

half century. Geikie (1903), Blackwelder (1925; 1927), Twenhofel *et al.* (1932), and Twenhofel (1939; 1950) pointed out many of the details of rock decomposition and generally concluded that oxidation, hydration, carbonation, and hydrolysis proceed fastest in the presence of abundant moisture and at temperatures well above freezing. Marked

solution accompanies the process where abundant moisture and the breakdown of feldspars and mafic mineral types produce clays. The plant material which is always present where adequate moisture and moderate temperatures exist heightens the weathering effect in that it adds humic components for the generation of soils (Twenhofel *et al.*, 1926, p. 17; Twenhofel, 1950, p. 33–35), aids leaching by means of humic acids (Roy, 1945, p. 393–403), maintains accumulations on slopes during the processes of decomposition, and controls amounts of runoff (Bennett, 1939, p. 147).

In the Cordillera Oriental of Peru the temperature, moisture, and vegetal associations promote principally chemical decomposition of the bedrock under present conditions at all but the highest elevations. Angular outlines are not characteristic of outcrops undergoing chemical alteration or the products they yield through chemical weathering. Therefore, the coarse, commonly angular detritus in the alluvial-valley fills is not the product of current weathering conditions.

SOIL DEVELOPMENT: The development of soils is additional proof of the effectiveness of humid chemical weathering in Cordillera Oriental of Peru. Bowman (1916, p. 70) mentions the fertile soil developed on the valley alluvium. Extensive cultivated tracts are developed on steep unterraced slopes hundreds of feet above the valley floors of the region, and thick, black humus is present on the plateau surfaces at elevations approaching 13,000 feet above Ollantaytambo where adjacent slopes support gardening plots even above 12,500 feet (Fig. 9A). These observations indicate not only weathering of bedrock by chemical means but also decomposition of the materials in the alluvial accumulations by similar processes. Bowman (1916, p. 188) also calls attention to "a deep layer of soil" on the upland slopes and notes (p. 81) that where rainfall on the valley floors is locally limited by mountainous wind and moisture barriers the soil is "thin, infertile, and dry." On the basis of this data and the recorded climatic conditions of the present the soils of the eastern Peruvian Sierra closely reflect the present humid weathering conditions.

AGRICULTURAL TERRACES: The ancient but well-preserved agricultural terrace system of the region has a direct bearing on the soil development and the source of coarse clastic debris.

Francisco Pizarro landed in Peru in 153[illegible] and shortly thereafter destroyed the Inca Empire. Detailed descriptions of this historic event are noted by Prescott (1875; 1876) and Means (1932). It is generally agreed that the Inca civilization was at an advanced stage at least 200 years before the Spanish conquest (Prescott, 1875, p. 12)—Enock (1916) suggests 400–600 years, Means (1932) 400 years, and Rowe (1944) more than 300 years. Pre-Incan cultures of considerable complexity predate the Incan climax by several hundred years according to Tschopik (1946) and Rowe (1944); Bennett and Bird (1949) indicate that an agricultural system, employing terraces and irrigation, existed before 600 A. D. or almost 1000 years before the Spanish conquest.

The extensive agricultural establishment of the early Inca civilization supported an estimated 5–8 times the 1796 population of about 700,000 which has increased to the present. According to Means (1932), Rowe (1944), and Bennett and Bird (1949) all flat land was cultivated, and since (in the mountains) this consisted largely of valley floors and cold high-altitude plateaus, expanded cultivation led to extensive terracing of the alluvial accumulations along the bases of the steeper slopes (Prescott, 1875, p. 136). The terraced clastic accumulations have the structure and form of talus cones and fans (Fig. 9A, 9B). Where debris extended far up the slopes, irrigated terrace systems were employed in many places more than 1000 feet above the valley floors (Fig. 9A), and locally terrace systems were extended to include steep slopes away from alluvial accumulations—presumably because of soil developments on bedrock. Prescott (1875, p. 136) supported this assumption. The terrace surfaces range in width from a few feet on steep slopes to several scores of feet on the more gentle inclines. (*See also* Prescott, 1875, p. 136.) Most of the terraces were man-made on alluvial accumulations and do not have erosionally beveled bedrock floors as noted by Prescott (1875, p. 137). The alluvium in the fans and cones consists of minor argillaceous material and angular to subangular sand, gravel, cobbles, and boulders upon which there is locally a considerable amount of soil. Many of the larger exposed fragments display rounding, pitting, and spalling, apparently partly in response to exfoliation. The terrace surfaces support vegetation at

present, and the terrace systems are given their outward form by man-made stone retaining walls (Fig. 9B).

An actively accumulating talus slope is characterized by the absence of soil and is hazardous to cross because of falling debris. It is hardly conceivable that the Incas and their ancestors could have stabilized actively accumulating talus by terracing or that they could have been farseeing and patient enough to wait for a soil to form after terracing had immobilized the talus slopes—a conclusion supported by Prescott (1875, p. 136–137). Thus one is forced to conclude that more than 1000 years ago no talus was accumulating on most of the slopes in the Cordillera Oriental of Peru and that it was soil that attracted the Inca farmers and their predecessors.

The destruction of the population and the disintegration of the irrigation system coincident with the Spanish conquest is well documented (Prescott, 1876, p. 230; Bennett and Bird, 1949, p. 217) and led to a 400-year interval of neglect of most of the terrace system. Nevertheless, the long interval of humid weathering on slopes commonly exceeding 30° has added very little coarse debris to the neglected terraces. Locally the hand-made retaining walls have fallen, yet most of these are surprisingly intact, and accumulating talus has not obscured or blotted out a single terrace system.

PRESERVED GLACIAL DEPOSITS: The ultimate duration of conditions of weathering similar to those of the present is indicated by the excellent state of preservation of deposits formed by the most recent significant advance and retreat of glacial ice. Bowman (1916, p. 206, 207) notes that the actual glacial deposits are marked by a variable number of morainic features, and he states,

"...at Choquetira three prominent stages in the retreat of the ice are recorded ... the lowermost one (terminal moraine) has an enormous volume, since it is oldest and was built at a time when the valley was full of waste."

Although elsewhere (p. 270) he assigns the alluvial-valley fill to the glacial interval, the present quotation indicates that the bulk of the valley-fill alluvium predates the last direct evidence of glacial conditions. This is the conclusion of the writer also, for as Bowman points out (1916, p. 207), "... the lowermost moraine is well dissected, the second is ravined and broken but topographically distinct, the third is sharp-crested and regular." Any large-scale formation of talus subsequent to the last ice retreat, with the development of cones and confluent fans such as are preserved in the valleys below the terminal moraines, would have obscured the glacial-retreat depositional features. Figure 11 illustrates the glacial, valley fill, talus, and general geomorphic relations.

McLaughlin (1924) assigns the extensive alluvial-valley fills "over 400 feet" thick of the Junin area to an earlier glaciation and states that "overloading of the streams" is probably the cause of the deposits. The inadequacy of this explanation with reference to the laws of stream behavior has already been outlined (Gilbert, 1880). McLaughlin (p. 628) emphasizes that the alluvial accumulations in the valleys are formed as "lateral filling due to the development of talus cones and fans." In regard to the most recent glaciation McLaughlin (p. 629) states,

"...postglacial erosion is practically lacking, except where narrow channels have been cut through unconsolidated moraines. Modification of the cross-profiles by talus has hardly started."

SIGNIFICANCE OF ALLUVIUM: The four independent lines of evidence just cited establish that: (1) present weathering processes under humid conditions in the Cordillera Oriental of Peru are currently generating fine rather than coarse clastic material; (2) similar or only slightly modified conditions have prevailed since the last major glacial retreat; (3) the last major aggradation of the mountain valleys predates the last significant ice advance and postdates a more intense glacial advance and period of valley incision which generated local relief of several thousand feet (Fig. 11); (4) the formation of the major alluvial-valley accumulations took place under conditions of relief essentially identical to those of the present except that mechanical breakdown of bedrock dominated over chemical decomposition (Fig. 12, stage P −3). Under present conditions of high relief and high rainfall the rivers of the Cordillera Oriental of Peru acquire their boulder-clay solid loads from the dissection of alluvial-valley fills which they are removing but could not have deposited, because (1) stream behavior, as outlined by Gilbert (1880, p. 105, 108) and Leopold and Maddock (1953), precludes the possibility of "overloading" with increasing stream volume downslope; Johnson (1901, p. 613) points out, "... in humid lands the waste

from mountain degradation . . . is carried through to the sea"; (2) the current humid weathering products of clays and solutes could not form the angular coarse clastic residual accumulations.

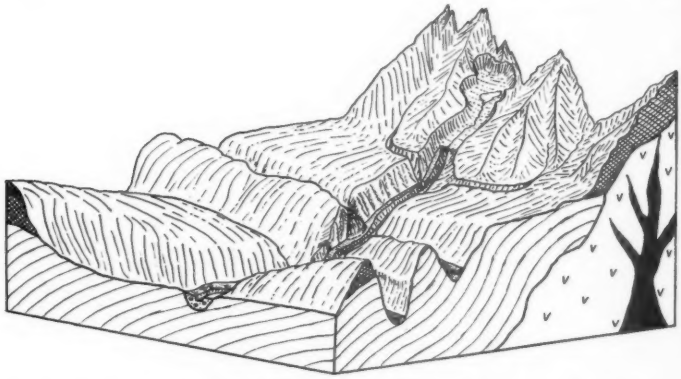

FIGURE 11.—BLOCK DIAGRAM OF THE TYPICAL PHYSIOGRAPHIC RELATIONS OF THE CORDILLERA ORIENTAL, PERU

In the background are the rugged summit glaciated peaks bordered by inclined, high-elevation plateaus which in turn form the upland margins of deeply incised lateral mountain valleys. The major streams flow transverse to the direction of greatest slope, and the valley floors are extensive alluvial fills which are currently in the process of removal. (After Bowman, 1916). Vertical exaggeration × 7.5.

The overloading of glacial streams is the only explanation that has been advanced in the literature to explain the vast residual coarse alluvium in the valleys of eastern Peru. Earlier workers must have recognized that the emplacement of continuous valley fills thousands of feet above sea level could not be attributed to eustatic fluctuations. No Pleistocene marine deposits have been reported from the area. The very slight degree of dissection of the alluvium at elevations exceeding 11,000 feet (Figs. 8B, 9A) precludes the possibility that the alluviation could have taken place before an extensive and prolonged uplift.

Gravity sliding under humid conditions similar to that described in Venezuela undoubtedly contributes material to the eastern Peruvian rivers from time to time. Such slide material, as a humid-climate phenomenon, would be continuously removed by the through-flowing rivers and therefore would not form a residual accumulation. Moreover, the slide debris would normally be composed of a high per cent of fine clastic decomposition products on the basis of the observed weathering processes. Such deposits would be localized rather than continuous and have much fine clastic material. Thus sliding cannot account for the coarse residual valley fills of great lateral extent.

The significance of the residual alluvial valley fills might remain an enigma except for the work of Quinn (1957). On the premise that the dominant type of weathering under arid conditions is mechanical, and utilizing the framework erected by workers such as Gilbert (1880), Johnson (1901), Bennett (1939), and Leopold and Maddock (1953), Quinn established that coarse clastic materials on land are to be associated with times of aridity rather than with times of humidity. The data presented with regard to Venezuela and eastern Peru are in accord with Quinn's conclusions. As Quinn points out (1957, p. 157),

"It has been repeatedly asserted and is now widely accepted that . . . varying climatic conditions existed during the Pleistocene. Times of humidity are associated with glacial stages and times of aridity with interglacial stages. Accordingly, times of stream-valley entrenchment or deepening are to be correlated with glacial stages and times of valley widening are to be associated with interglacial stages and likewise with times of major alluviation and deposition of coarse clastics in non-glaciated regions."

Application of these principles in the Cordillera Oriental of Peru has been most helpful with reference to the interpretation of the availabl

data. Most recent east Andean climatic events equal those of Guayana Shield (Garner, 1958).

COARSE CLASTIC MATERIAL AND ELEVATED SURFACES: The main significance of the principle of scarp retreat under conditions of aridity as developed by Quinn (1957) with regard to the Andes Mountains is that the process could function at essentially any elevation without regard to sea level and would accompany the generation of coarse clastic material. In instances where high-level surfaces have been attributed to peneplanation and rejuvenation as in the case of the Andes it has heretofore been necessary to elevate the surface from near sea level after base leveling. In the case in question an uplift in excess of 12,000 feet is postulated by Newell (1949, p. 13) in "relatively recent" times. Such an assumption is based on the premises that (1) the uplifted surface is the product of peneplanation, and (2) the degree of incision of mountain valleys is of the amount of and in response to tectonic uplift alone.

The elevated surfaces in the Andes Mountains of Peru are probably the product of pedimentation and associated formation of coarse clastic material rather than peneplanation; this eliminates the necessity for uplift of excessive magnitudes in the recent geologic past. The physiography of the range as a whole is largely a response to alternating arid-humid climatic conditions. In this system the incision of lateral mountain valleys reflects humidity acting on existing relief rather than tectonic uplift alone; the arid aggradation of the eastern Peruvian valleys represents a relatively recent stage of aridity in the history of the region.

Bowman (1916), McLaughlin (1924), and Newell (1949) agree that the plateau surface of the Central Andes now at an elevation of 13,000–14,500 feet is an erosional feature. In the same area many workers including the writer have observed peaks composed of Paleozoic rocks standing as much as 5000 feet above the elevated plateau (Fig. 11). A similar variety of lithologies is displayed by peaks and beveled plateau surfaces—volcanoes excepted (Jenks, 1948, p. 163, 164, 165, Figs. 6, 7; Bowman, 1916). McLaughlin (1924, p. 624) assigned to the elevated plateau the name "Puna surface." Bowman (1916, p. 185) states that the elevated surface attained a "post mature" topography, and Newell (1949), p. 13) concurs. McLaughlin (1924, p. 623) states that the surface, "hardly attained peneplaination." Puna probably equals Caldera Surface of Jenks (1948).

With regard to the Puna surface, Bowman (1916, p. 187, 188, 190) states that there are "graded slopes . . . thinly veiled with surface debris, yet so even as to appear artificially graded," and also that

> "the graded mountain slopes were not all developed (1) at the same elevation, nor (2) upon rock of the same resistance to denudation, nor (3) at the same distance from the major streams, nor (4) upon rock of the same structure."

Relative to the inclination of the graded slopes Bowman (1916, p. 190) indicates that 10-degree slopes are perhaps most common and that slopes less than and exceeding this value are not unusual.

The detailed descriptions of Bowman (1916) and the more generalized treatment of McLaughlin (1924) are in terms of a near pediplane rather than a near peneplain. King (1953) discussed pedimentation as an erosional process operating under conditions of semiaridity and outlined the physical characters of pediments. Quinn (1957, p. 158) suggests that aridity rather than subaridity would favor the development of pediment surfaces and points out (p. 160) that according to the "theory of deposition on sloping surfaces advanced by Johnson (1901), alluviation of channels likewise takes place under arid conditions."

Information concerning the Cordillera Oriental of Peru is inadequate to establish that the Puna surface is a pediplain as defined by King (1953, p. 723). Nevertheless, the available data in that area indicate that the upland slopes were formed at high elevations, are graded, and developed at various levels, beveling rocks of varying resistance and structure; most important, perhaps, they have a veneer of gravels upon which a soil has subsequently developed. This description is close to the definition of a pediment complex. In addition, Jenks (1948, p. 195) states that peaks rising above the plateau have on their flanks, "terraces or flattened spurs at levels approximating those of the majority of the [accordant] summits," in southwestern Peru.

Bowman (1916, p. 192) suggests an uplift of the Puna surface of "at least a mile" to account for the extension of the graded slopes into the foreland. Newell (1949) used the term "base leveling" to imply that the amount of uplift exceeds this figure, presumably by near peneplanation close to sea level. Bowman (1916) does not explain how a "post mature" surface

of erosion could be formed at elevations averaging 8000 feet. Pedimentation, however, controlled by climate and functioning with relation contrast to lower and more recent features attributable to climate shifts. On the basis of relations established by Quinn (1957) a number

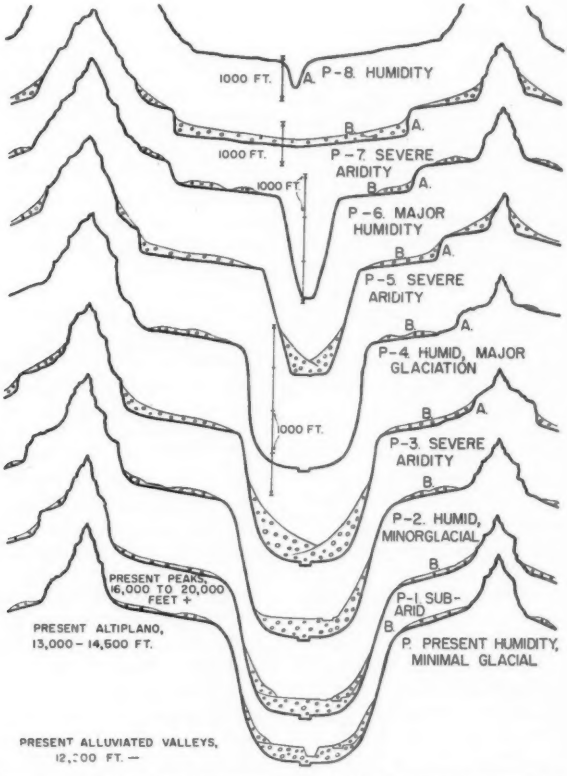


FIGURE 12.—SCHEMATIC CROSS-SECTION PROFILES OF THE GEOMORPHIC SEQUENCE AND DEVELOPMENT IN THE CORDILLERA ORIENTAL, PERU

In chronological sequence from oldest to youngest the events are: (P −8) humid dissection of an elevated surface of erosion having local topographic highs of considerable magnitude; development of scarp A (P −7) high-elevation arid pedimentation with aggradation of surfaces and retreat of scarp A forming surface B; (P −6) major humid period; valley incision to depths exceeding 2000 feet, partial removal of alluvia residuals; (P −5) severe arid period, scarp retreat, valley widening, and aggradation; (P −4) major humid glaciation, erosion of arid residuals, and development of U-shaped valley profiles to relatively low elevations (P −3) severe and widespread period of aridity and subaridity, high-level scarp retreat, mergence of scarp A with slopes of upland peaks and formation of talus cones and confluent alluvial fans in valleys; (P −2 minor humidity, high-level glacial removal of valley fills and minor lower-level erosion of arid residuals (P −1) minor subaridity, local formation of small talus cones; (P) present-day humid incision of valley residuals, glaciers confined to high peaks.

to local rather than regional base level(s) (Quinn, 1957), can occur at any elevation that will permit an arid regimen and scarp retreat.

*Eastern geomorphic history.*—The available data are insufficient to permit exact determination of the number of erosional phases represented by the Puna surface and higher peaks, in climate cycles appear to be involved. He (1957) determined that incision reflects humid conditions acting on existing relief, and that the amount of downcutting reflects (1) the duration and intensity of the humidity, and (2) the available amount of tectonically generated relief—incision to base level is the maximum

possible. In the case of erosion taking place thousands of feet above sea level, the development of low-inclination surfaces through scarp retreat would be associated with aridity.

Figure 12 shows the application of these concepts to the Cordillera Oriental of Peru, and the sequence of geomorphic events appears to involve: (1) P −8: moderate humid dissection of not more than several hundred feet of an elevated surface of erosion on the eastern Andean flank; (2) P −7: retreat of valley walls in the form of scarps, the generation of gravel veneers on graded slopes, and probably local stream aggradation under arid conditions; (3) P −6: prolonged humid dissection of the eastern mountain front and deep entrenchment of rivers; (4) P −5: arid to subarid aggradation in the deep valleys; widening of the valleys is related to decreasing humidity at higher elevations— Chacra Level of McLaughlin (1924); (5) P −4: intense glaciation of the deep valleys to relatively low elevations under conditions of humidity; the formation of U-shaped valley profiles and dissection and removal of arid residual accumulations by humid rivers and glacial scour; (6) P −3: prolonged arid to subarid aggradation of deep valleys, to a depth exceeding 400 feet, by confluent cones and fans which modified the U-shaped profiles of the previously glaciated valleys; (7) P −2: most recent glacial advance and retreat under conditions of humidity—minor talus cones suggesting a short subarid interval, P −1, between the last glacial and P, present conditions of humidity. The minor nature of the last glacial episode, its recency, and the brief subarid stage following together explain the restriction of stream incision into the widespread older residual deposits to depths of 200 feet or less.

*Discussion.*—The eastern Andean front in Peru is yielding coarse clastic material through dissection of residual deposits and minor glacial accumulations; the former is referable to the latest interglacial stage and the latter to the last relatively weak glacial advance. Prolongation of present humid conditions would result in the removal of the vast arid and minor glacial residuals now occupying the mountain valleys. Subsequently clastic size of sediments yielded by this montane source area would be drastically reduced.

### *Western Ecuadorian Sierra*

*General information.*—The Western Ecuadorian Sierra is a portion of the Andean Cordillera Occidental. The range trends generally north-south and extends 4° south of the equator in Ecuador (Fig. 1).

Most of the geologic work in Ecuador has been in petroleum exploration, mainly centered in (1) the Cordillera Oriental (Tschopp, 1953), and (2) the Coastal Lowland (Nygren, 1950; Marks, 1951). Lewis (*in* Jenks *et al.*, 1956) reviewed the data on the Cordillera Occidental from a general standpoint. Lewis (p. 269) points out that, "... our broad knowledge of the region as a whole has advanced but little during the last half-century." Nothing in the literature dealing with the physiography of the Cordillera Occidental is pertinent to the present report.

Conditions on the western slopes of the Andes Mountains north of the Peruvian Desert are comparable with those of the Cordillera Oriental of eastern Peru. The Cordillera Occidental of Ecuador lies in the equatorial doldrum belt, and wind directions are considerably more erratic than in eastern Peru. Slopes are heavily forested up to 8000 feet (Fig. 13A), and scrub brush and heavy grass cover prevail to more than 13,000 feet. Above this zone subboreal and boreal floras are common. However, in contrast with the relations in the Cordillera Vilcapampa of eastern Peru, rainfall diminishes from more than 60 inches annually near 10,000 feet to about 40 inches near the base of the mountain slopes. Rainfall is seasonal, but a heavy cloud cover reduces evaporation and maintains a relatively high level of humidity on the western slopes through most of the year, just as in the Venezuelan Cordillera de la Costa. The position of the Humboldt Current relative to the strand line has a strong influence on the distribution of moisture along this coast (Humboldt, 1801; 1826; 1837; Sheppard, 1937). Temperatures average 20° C. near sea level at Guayaquil and more than 10° C. on all but the highest peaks.

According to Lewis (*in* Jenks *et al.*, 1956, p. 271) the country rock in the Cordillera Occidental ranges in age from questionable Jurassic to late Tertiary. Lithologic types include sedimentary, igneous, and metamorphic suites with a range of variation similar to those of Venezuela and eastern Peru, though in Ecuador there are more abundant, relatively recent, high-level extrusive volcanic accumulations.

Chemical decomposition of bedrock dominates over mechanical breakdown just as in eastern Peru and on the north slopes of the

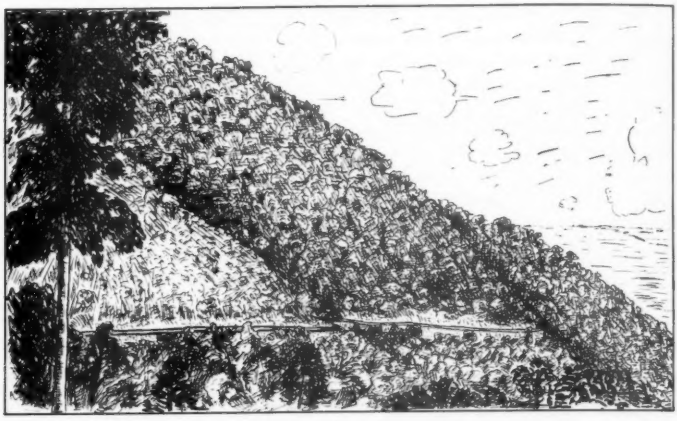

A

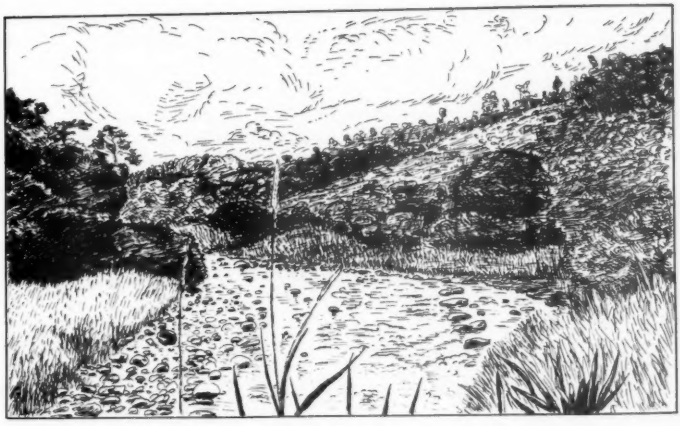

B

FIGURE 13.—DRAINAGE AND ALLUVIUM OF THE CORDILLERA OCCIDENTAL, ECUADOR

A. Western slopes of the Front Range looking south. Spurs extending into foreground valley are composed of several hundred feet of coarse alluvium covered by dense jungle. Road is at elevation near 6000 feet and extends between Duran on the coast and Tambo in the sierra. Low flat coastal plain is seen dimly through clouds in right background.

B. Valley of the Rio Yaguachi 5 miles upstream from the village of Bucáy. The channel is cut into and flows on a coarse alluvial fill which is covered by dense jungle.

Cordillera de la Costa in Venezuela. Disintegrated intervals displaying only relict bedrock structures are common.

The Daule-Guayas river system flows from north to south along the base of the Front Range. Smaller rivers drain the mountain slopes and either join the trunk streams or flow directly into the Gulf of Guayaquil through the Canal de Jambeli. Altitudes in excess of 15,000 feet in the Cordillera Occidental are encountered in horizontal distances of as little as 30 miles from the strand line (Fig. 14).

*Alluvial accumulations.*—The rivers on the western slopes of the Ecuadorian Andes flow in modified V-shaped valleys incised in thick alluvium (Fig. 13B). The material is locally very coarse, angular to rounded, and rather deeply weathered; components are cobbles and boulders and considerable pebble gravel, sand and some argillaceous material. Bedding stru

tures are confined to some channeling and scour and fill features. The alluvium occupies the bottoms of the valleys and extends up the valley walls for several hundred feet. High relief and dense jungle growth prevented ascertaining whether the main mountain spurs have alluvial caps. Nevertheless, the valley walls and smaller spurs extending into the valleys at several levels are composed of coarse, partially weathered alluvium (Fig. 13A). Within the mountain valleys alluvial spurs with flat or slightly inclined tops occur from near the mountain base to high elevations. A number of flat-topped hills 50–75 feet high on the adjacent coastal plain are composed of similar alluvial material derived from the Cordillera (Fig. 15; *see also* Sheppard, 1937). The alluvium appears to be more deeply dissected than that of eastern Peru although the streams are incised in and flowing on the same coarse detritus (Fig. 13B). Extrusive volcanic material is incorporated in the alluvium, and extensive volcanic flows and ash accumulations cover many of the upland areas. The uppermost layers of ash on the uplands closely parallel the current topography and conform closely to most slopes, which indicates the recency of the volcanic activity. Nevertheless, most of the alluvial material on the western slopes, which extends up the river channels to more than 8000 feet in elevation, was derived from the dominantly metamorphosed and intruded country rock.

*Erosion.*—The westward-flowing streams in the Cordillera Occidental carry boulder-clay solid loads derived from the weathered alluvial-valley fills. The large boulders, cobbles, pebbles, sand, and much argillaceous material currently accumulating in the Guayas Delta and in the Gulf of Guayaquil reflect not only their coarse-alluvium source but also the current chemical weathering processes. Annual tidal minima expose mixtures of cobbles and mud in the depositional area.

The current weathering processes on the western slopes of the Cordillera Occidental could not have produced the coarse, commonly angular alluvial residuals found in this area. Furthermore, present agents of transport, dominantly rivers, are carrying their loads through to the ocean.

*Significance of alluvium.*—Explanation of the emplacement of the alluvium in western Ecuador in terms of eustatic, tectonic-eustatic, and glacial factors is hampered by the same problems encountered when these concepts are applied to the Cordillera Oriental of Peru. In résumé, (1) emplacement at or near sea level fails to explain the coarseness of the material and its incomplete removal under conditions of humid runoff, (2) deposition at the main break

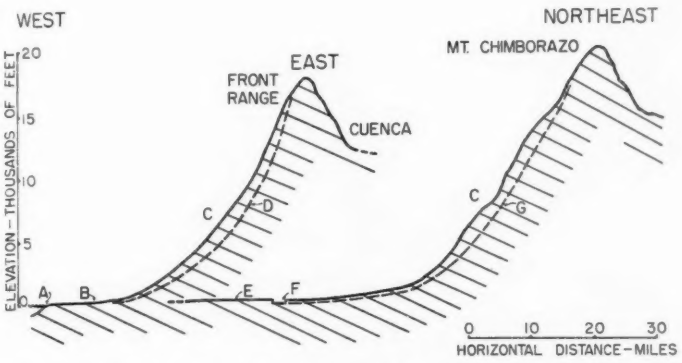


FIGURE 14.—DIAGRAMMATIC MULTIPLE CROSS SECTIONS OF THE CORDILLERA OCCIDENTAL, ECUADOR

Section on left is drawn east-west through the Front Range and the city of Guayaquil; section on right is drawn northeast-southwest through Guayaquil and Mount Chimborazo. Illustrated are (A) shore of the Gulf of Guayaquil, (B) narrow coastal plain where range fronts the Gulf of Guayaquil, (C) humid, steep western slopes of the Cordillera Occidental, (D) schematic profile of mountain streams draining west slopes directly into the Gulf of Guayaquil, (E) alluvial-filled Daule-Jipijapa Basin lying north of Guayaquil, (F) north-south flowing rivers of the Daule-Guayas river system paralleling the trend of the range in the Daule Jipijapa Basin, (G) schematic profile of mountain stream draining the humid west slopes of the range into the north-south river system represented by (F).

in slope does not account for the high-elevation slope accumulations, (3) present rivers function in the manner foreseen by Johnson (1901) and carry their loads to the sea, (4) all recognizable

ing conditions which are associated with humidity and humid through-flowing rivers. Unquestionably the coarse clastic residuals were emplaced under conditions of relief and slope

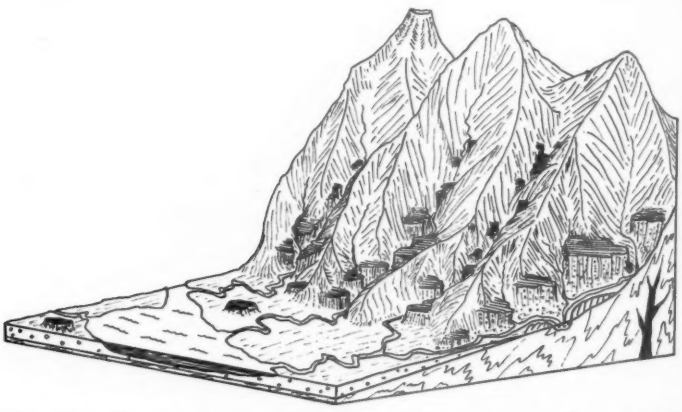

FIGURE 15.—SCHEMATIC BLOCK DIAGRAM OF THE WESTERN SLOPES OF THE CORDILLERA OCCIDENTAL SOUTHEAST OF GUAYAQUIL, ECUADOR

Illustrated as of particular importance are the Gulf of Guayaquil, left foreground; mouth of the Guayas River, left background; thick alluvial-valley fills occupying steep, modified V-shaped mountain valleys on the western slopes of the Cordillera Occidental; rather thick, generally flat-topped coarse alluvial remnants on the coastal lowland which resemble the valley-fill alluvium; meandering channels of coastal-plain streams which drain mountain front; the relations show certain striking contrasts and similarities to the Cordillera de la Costa of Venezuela. (*Cf.* Fig. 4.) Vertical exaggeration × 8.

glacial deposits are several thousand feet above and many miles removed from the valley fills, and (5) humid gravity-slide additions are presently being taken to base level rather than accumulating as residual deposits.

Although the Quito area was a center of the Inca culture as was a part of the Cordillera Vilcapampa near and in Cuzco, Peru, the terrace systems of the latter area are lacking in the former. This is presumably associated in part with the more equatorial position of the Ecuadorian Andes and the restriction of severe climatic conditions to the highest altitudes. Direct glacial deposits also are not intimately associated with the alluvial-valley accumulations, and neither the glacial nor archaeological relations aid in dating the alluviation or the sequence of physiographic events. The intense and recent volcanism of the region tends to mask development of a cyclic physiographic system.

*Discussion.*—In spite of the meager evidence it seems clear that the coarse alluvial accumulation on the western slopes of the Cordilleras Occidental in Ecuador predate present weather-

not differing greatly from those of the present and closely paralleling the associations in eastern Peru.

### *Western Peruvian Desert*

*General information.*—The Peruvian Desert is situated on the western slopes of the Andes Mountains and the adjacent coastal plain (Fig. 1). Lima, the largest city of Peru, is situated here, but otherwise the desert is sparsely populated. Desert conditions extend from southern Ecuador to northern Chile, and population density depends on availability of water.

The western or Maritime Cordillera rises to elevations in excess of 10,000 feet from sea level in horizontal distances of as little as 35 miles. The coastal area lying below 10,000 feet is no more than 40 miles wide (Fig. 16). Many of the peaks are more than 20,000 feet above sea level at only slightly greater distances from the Pacific strand line, and locally the mountain spurs extend down to the ocean.

Bedrock is similar in types and variation to

those in Venezuela, eastern Peru, and western Ecuador and includes Paleozoic and Mesozoic limestones, shales, and sandstones and their metamorphic equivalents as well as extrusive volcanic rocks covering large areas (Fenner, 1948a) and intrusive rocks of great variety. Tertiary and Pleistocene sedimentary rocks on the coastal lowland are little metamorphosed.

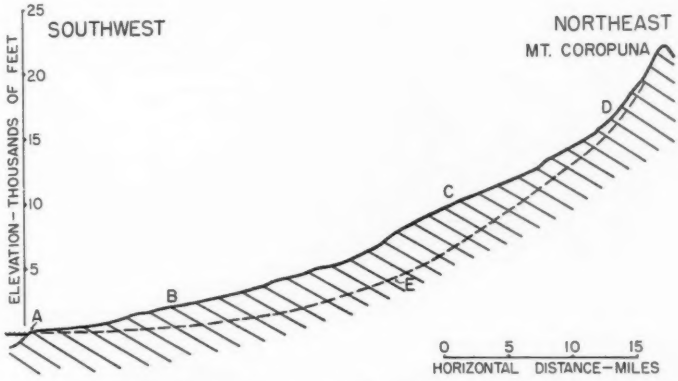


FIGURE 16.—DIAGRAMMATIC NORTHEAST-SOUTHWEST CROSS SECTION OF THE CORDILLERA OCCIDENTAL AND COASTAL DESERT THROUGH MOUNT COROPUNA, PERU

Major relations illustrated are (A) western shore of the Pacific Ocean, (B) permanently arid lower coastal desert, (C) currently arid intermediate to upper slopes in region of periodic long-term climatic variations, (D) rugged high peaks in region of seasonal rainfall and weak glacial activity, (E) schematic stream profile of the humid-source through-flowing rivers.

In recent years exploration for minerals and petroleum has added considerably to our knowledge of somewhat specialized phases of geology of the region. The regional studies of Bowman (1916) and Bosworth (1922) have been of incalculable value to the present study because of their physiographic and climatic content and regional treatments. Additional valuable contributions were made by McLaughlin (1924), Fenner (1948a; 1948b), Jenks (1948), and Newell (1949; 1956).

*Climate.*—The Peruvian desert region is one of the driest places in the world. Rainfall is far less than 10 inches annually; rain is only known at irregular intervals of many years' duration (Bowman, 1916, p. 125). A long-term periodicity in the rainfall along the west coast of South America has been noted by a number of observers (Bosworth, 1922; Sheppard, 1937) who do not agree on the length of the intervals involved. Including the slightly elevated area termed the "Coast Range" by Bowman (1916, p. 122), the western slopes of the Maritime Cordillera and the adjacent coastal lowland from lat. 5° S. to about lat. 30° S. are arid. Prevailing westerly winds in the region of Chile cause rainfall on the western slopes in that area with the result that arid and subarid conditions cross the Andean crest in southern Peru and Bolivia and occupy the eastern mountain slopes in Argentina (Bennett *et al.*, 1948, p. 4).

Aridity of the Peruvian Desert is ascribed to (1) rain-shadow effect wherein prevailing easterly winds act as evaporating agents in their descent to the Pacific (Fenner, 1948b; Bowman, 1916, p. 124); (2) adiabatic expansion of winds rising from the Pacific diurnally, with some annual variation, which causes evaporation at lower altitudes. (*See also* Bowman, 1916, p. 131.) The aridity of this region is therefore primarily a rain-shadow condition with variations in the limited precipitation on the western peaks and upper slopes caused by westerly winds. The intimate relation between the Humboldt Current of the Pacific Ocean, the diurnal westerly winds, and moisture distribution has been discussed by numerous workers. Bowman (1916, p. 127) states, ". . . under given conditions a cold current intensifies, but does not cause the aridity of the west coast desert." The corollary is implied (p. 126) that a warm or warmer current would result in increased precipitation. There appears to be a close relation between these conclusions and those of

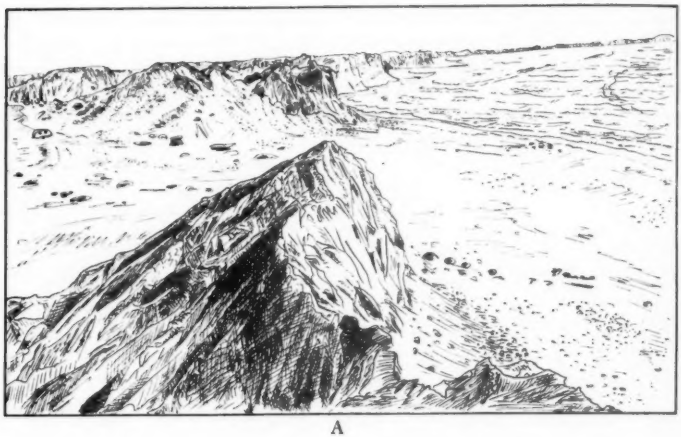

A

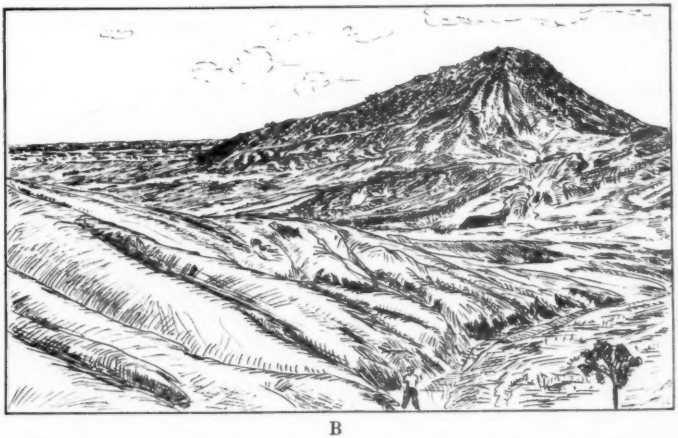

B

FIGURE 17.—ARID TOPOGRAPHY AND ALLUVIUM OF THE LOWER COASTAL DESERT, PERU

A. Sea coast and broad alluviated ephemeral stream valley near Talara, Peru. House trailer in upper left background indicates scale. Scarps are 150–200 feet high and are mantled by talus and sand-dune accumulations.

B. Badland topography developed on slightly metamorphosed Paleozoic shale near the base of the Amatope Mountains. Surface is channeled by rare sheet runoff and abraded by thin films of blowing sand. Hill in background is composed of sandstone and is buried in coarse talus accumulations.

Fenner (1948b) in connection with the Arequipa region.

Much of the high-altitude moisture on the peaks of the Maritime Cordillera falls as snow and is restricted in general to the west or southwest sides. The northeast and eastern sides of the higher peaks in the western mountains receive almost no moisture from either the east or west (Fenner, 1948b, p. 915). The period of greatest cloud cover and precipitation coincides with that of snow accumulation, although the temperatures are relatively high. The time of maximum sunshine coincides with that of lowest temperature with the result that (McLaughlin, 1924, p. 597), "... a glacier peak in this region does not possess a value for water storage comparable to snow and ice fields in western United States."

Temperatures range from 20° C. on the coast to less than 10° C. at high elevations in January. In July they decrease to about 15° C. near sea level and below 0° C. at high altitudes. The

climate is therefore seasonal, as is the rainfall, but distinctly arid.

*Drainage.*—Watercourses in the Peruvian Desert fall into two classes: (1) permanent, through-flowing rivers of the humid type that have their headwaters in high-altitude snow and ice accumulations and precipitation areas; (2) ephemeral desert arroyos that carry water only in the rare times of appreciable rainfall. Many of the larger stream valleys that carry water from time to time show evidence of long disuse with consequent accumulations of dune sand and talus piles (Fig. 17A), and nearly all the minor streams display these features (Fig. 18). Bosworth (1922, p. 282) pointed out that the hundreds of dry valleys or quebradas, in the occasional years of flood, are occupied by raging torrents of mud and stones. Bosworth also noted (p. 281) that the Rio Piura, which occupies a large valley, dries up without reaching the sea. In the Coast Range, Bowman (1916, p. 139) observed,

"...a steep-walled gorge. The bottom is clogged with waste, here boulders, there masses of both coarse and fine alluvium. The (trickle of) water in the valley was quite incapable of accomplishing any work except that associated with solution and seepage, and we saw it in the wet season of an unusually wet year. Clearly there has been a diminution in the water supply."

The writer also observed a similar situation in the Mancora Quebrada north of Talara in 1954: the stream heads in the Amatope Mountains. Thus, through-flowing rivers are in the minority and reflect the climates of their source areas rather than that of their arid lower reaches

FIGURE 18.—SCHEMATIC BLOCK DIAGRAM OF THE CORDILLERA OCCIDENTAL AND COASTAL DESERT, PERU

Illustrated in relative positions within the regional setting are the Pacific Ocean, lower coastal desert of residual gravels and "blind", double-ended arroyos which carry water only rarely and then to local base levels, large valleys of through-flowing rivers which have sources in summit region, contemporary talus accumulations at scarp bases, beveled bedrock pediment surfaces which have alluvial veneers, remnant pediment surfaces or buttes, and summit mountains—including volcanoes—moderate seasonal rainfall, weak or extinct glacial development, and waste-clad lower slopes. Vertical exaggeration × 10.

Most of them lose volume downslope through infiltration and evaporation (Fig. 18). (*See also* Jenks, 1948.)

*Vegetation.*—In sharp contrast to the three areas previously discussed, vegetation is nil from near sea level to elevations where annual moisture exceeds 20 inches and sparse grasses are developed (Figs. 17A, 17B, 19A, 19B). Moisture sufficient to support true forests occurs at altitudes that limit tree growth. Bowman (1916) and Bosworth (1922) confirm these relations and point out that the only appreciable vegetation in the coastal area is in the relatively moist valleys of the snow-fed, through-flowing streams.

*Erosion.*—As observed by the writer in the Sechura Desert, by Bosworth (1922) in the Tumbes Desert to the north, and by Bowman (1916) and Fenner (1948b) in the southern Atacama Desert area, sandstorms expressing active eolian deflation of the desert region are common (Fig. 17B). Largely as a result of these associations no true soils were observed, as they are developed in humid regions (Twenhofel, 1926, p. 17). Locally, as near the towns of Sullana and Piura, deposits resembling caliche were observed. Weathering of exposed bedrock

under the described conditions is therefore currently a dominantly mechanical process (Fig. 19A).

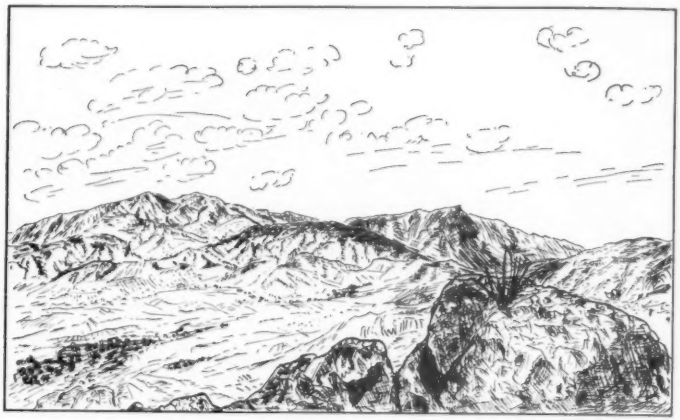

A

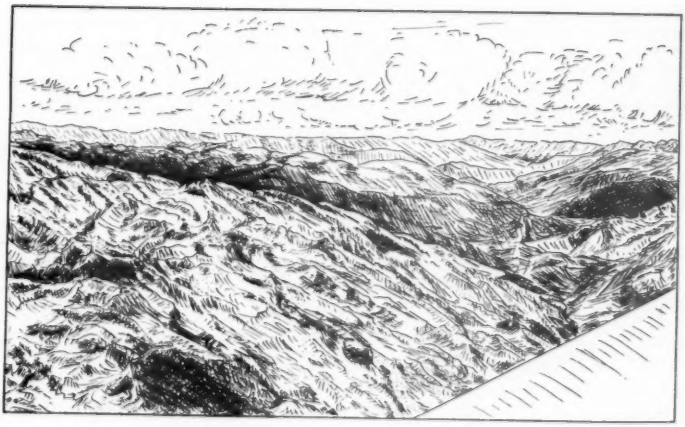

B

FIGURE 19.—ARID ALLUVIUM AND SPARSE VEGETATION OF THE CORDILLERA OCCIDENTAL, PERU

A. Amatope Mountains east of Talara, Peru. Material in immediate foreground is mechanically disintegrated Cretaceous limestone which mantles an outlying hill. Distant slopes are mantled with accumulating coarse clastic material. Vegetation is sparse and confined to channels of ephemeral streams.

B. Aerial view of upper slopes of Front Range southeast of Lima, Peru. Sharp ridge topography is softened by accumulating arid clastic material in the valleys in an almost complete absence of vegetation. Note rather even-crested summit area in background.

The excellently preserved desiccated mummies of Inca and pre-Inca peoples in the Museum of Anthropology in Lima were found in caves along the desert coast, and many were virtually exposed to the open air (Newman, 1947; Bennett and Bird, 1949). The mummies could have been preserved only by enduring and intensely arid conditions in western Peru. This indicates that the present-day desert conditions in the west persisted in historic time coincident with the humid conditions of the Cordillera Oriental in the east.

*Arid residual accumulations.*—Large amounts of coarse clastic alluvium is now being generated in the Peruvian Desert and arid western moun-

tains. This material is being retained on the land as a residual accumulation for the most part. For purposes of discussion the residual deposits can be grouped as follows: (1) in association with the essentially "waterless" lower mountain slopes and coastal lowland, (2) in association with the seasonally "wet" upper mountain slopes and peaks, and (3) relative to the major, through-flowing streams.

LOWER DESERT: In the Sechura Desert and nearby Amatope Mountains angular talus cones, fans, and rubble heaps are forming at the bases of scarps (Fig. 17A, 17B). Wind-blown sand (Fig. 17A) and desert pavements are common, as is alluvium in the ephemeral stream valleys (Fig. 17A, 19A).

Many active sand-dune areas were observed, and a wind storm in one of the more sandy regions such as in the Sechura Desert near Piura is ample evidence of current activity. Dune development in the Peruvian Desert is of far lesser magnitude than in the Sahara. Many of the dunes are barchanes which have been thought to indicate restricted quantities of sand in the source areas. In some cases bedrock seems to be the sand source, whereas in others river channels appear to furnish considerable amounts to upland surfaces. Quantities of sand are blown shoreward from beaches in the vicinity of Talara and elsewhere along the coast. It is debatable whether more sand is moved into the sea from the land or vice versa, for diurnal southwesterly winds locally have considerable force. The intensity and direction of these winds has also been noted by Bowman (1916, p. 129, 130) and Fenner (1948b, p. 916).

Talus accumulations in the dry coastal lowland and lower mountain slopes have been described by several workers. In the Amatope Mountains and adjacent desert area talus cones and confluent fans are currently forming and mantle the lower slopes of peaks, hills, and desert scarps alike in coarse, angular to subangular detritus (Figs. 17B, 19A). The lower slopes of the western mountains illustrate perfectly Johnson's statement (1901, p. 613), "... the foot slope of the desert range is a wash plain of mountain waste, burying its foot in fact." (*See also* Jenks, 1948.)

Grain size decreases generally away from the source-rock exposures. This relation was observed in Tertiary sedimentary rocks of southern Peru by Bowman (1916, p. 259). Bowman (p. 144) further speculates on the probable effects of a temperate-zone cyclonic storm on the residuals with the conclusion that, "... the alluvial valley land would be coated with infertile gravel; and mighty rivers of sand, now delicately poised on arid slopes, would inundate large tracts of fertile soil."

The alluvial accumulations in the form of large fans also impressed Bosworth (1922), who termed them "breccia cones" in the Tumbes area. He describes the material in the fans as consisting of angular cobbles of quartzite, slate of several types, and several varieties of granite. He further notes that sizes range up to more than 1 foot in length and become smaller with increase of distance from source.

The coarse residual accumulations in the Sechura and Tumbes deserts are not restricted to the more seaward slopes but are also of great extent in the valleys that cut the mountain front. They seem to be more than 100 feet thick southeast of Talara, and northward in the Tumbes area Bosworth cites a similar thickness (1922, p. 279) of 100–150 feet of alluvium near the mountains. He also notes (p. 279–286) that some of the earlier deposits extend back up the mountain valleys and their tributaries and fill them.

The process of aggradation is continuing at present under arid conditions when rare and local flash floods rapidly lose volume through evaporation and absorption and cause deposition after only relatively short distances of movement. A similar mechanism is currently operating in areas farther south, and the general coarseness of the residual accumulations emphasizes the continual removal of fine material by wind in absence of plant cover. In areas where the bedrock is argillaceous, such as some of the Paleozoic outcrops of the Amatope Mountains, deflation is extremely effective and in combination with infrequent rains produces a badland topography (Fig. 17A). Active wind deflation is also noted by Bowman (1916, p. 114) in the southern Atacama Desert.

UPPER ARID SLOPES: Aggradational processes similar to those of the lower coastal desert also function at higher elevations. Spring rains on the extreme upper slopes combined with melting snows are sufficient to cause flooding in the through-flowing streams, as pointed out by Jenks (1948) and by Fenner (1948b, p. 897) who notes,

> "... the rainfall of the season of 1939 was said to be considerably above normal, but none of the quebradas (gulches) near Arequipa showed more than a little trickle along their floors. During a considerable part of this time a swirling flood was coming down the Chili."

This emphasizes the humid character of the

through-flowing streams such as the Chili and Majes rivers which have their sources in regions of melt waters and seasonal but more adequate rainfall. Further proof of the relations are given by Fenner (1948b, p. 898, 899), where he points out that quebradas such as the Añashuaico near Arequipa are perched as much as 20 feet above the present channel of the Chili River (Fig. 18). Here at an elevation of 7550 feet rainfall is 5.4 inches per year. He notes (p. 899),

> "... large quantities of talus mantle the walls and descend to the bottom of the Quebrada Añashuaico ... evidently no torrential floods of the sort that first excavated the quebrada have flowed down its restricted channel for many years, probably centuries."

The same relations pertain to the other quebradas of the region and the bases of essentially all arid scarps and mountain slopes where accumulating talus is a feature of the present time (Fig. 19B). During the dry season the channel of the Chili River is essentially a dry "gulch" which has a bed of rubble deposited through volume loss.

RÉSUMÉ OF ARID CONDITIONS: In strong contrast to the humid regions in Venezuela, eastern Peru, and western Ecuador, the Peruvian Desert is characterized by (1) currently developing angular coarse clastic residual accumulations forming simultaneously at essentially all elevations within the arid zone; (2) dominantly mechanical disruption of bedrock associated with (a) talus accumulation, (b) retreat of scarps as outlined by Quinn (1957), and (c) the formation of pediments as described by King (1953), and as observed in the Peruvian Desert Coast Range by Bowman (1916), near Arequipa by Fenner (1948b), Jenks (1948), and Jenks (1948, personal communication *in* Fenner, 1948b), near Lake Titicaca by Newell (1949), as well as by the writer in the Sechura area; (3) efficient eolian deflation and transportation at essentially all altitudes with accompanying removal of argillaceous clastic fractions; (4) inefficient, short-distance transportation by running water of the ephemeral desert variety in which deposition normally takes place on land and only rarely reaches the ocean; (5) essential absence of soil cover; (7) accentuation of evaporation and absorption; (8) marked reduction in river volumes, capacities, and competencies downstream in association with alluviation.

Apart from eolian dust and small amounts of flash-flood debris, very little clastic material currently forming in the Peruvian Desert is moving into the adjacent Pacific Ocean. During rare intervals of significant rainfall the normally incompetent ephemeral streams carry large quantities of both coarse and fine material for short distances, and a little silt, sand, and some gravel reaches the ocean in this way. In comparison with the amount of coarse material available and continually forming the quantity delivered to base level is very small. Fine-grained eolian products in vastly greater amounts are being continuously furnished to the adjacent ocean. The total amount of material being carried to the Pacific in Peru is undoubtedly much less than that in western Ecuador, and the Peruvian marine area adjacent to the desert coast is almost certainly starved in a sedimentary sense. Newell (1949, p. 11) comes to the same conclusion: "... probably sedimentation is very slow in the Krummel Deep since it lies opposite a desert coast drained by only a few small streams...." Such associations throw doubt on conclusions that fine clastic debris or small amounts of material indicate low or distant source areas.

*Through-flowing rivers.*—The incision of valleys in the arid western Peruvian mountain front has not kept pace with that on the humid eastern slopes where the rivers are large and permanent (Bowman, 1916). The very deep valleys on the western slopes have streams with headwaters in glacial or formerly glaciated areas where rainfall is, or was appreciable (Fig. 18). The through-flowing streams therefore constitute a phenomena found in the desert region but foreign to it in the same manner as the Nile in Egypt and the Colorado of the United States. Although these waterways are called major through-flowing streams, they do not carry a large volume of water all year even in so-called "wet" years, and excessive flow is usually confined to 1 or 2 months of the year.

The westward-flowing streams at very high elevations (13,000–14,000 feet) are "raging torrents" during the rainy season, according to McLaughlin (1924, p. 595). He further observes (p. 628) that gravels emplaced in the western valleys at an earlier period have been "... completely removed and no remnants of them have as yet been recognized." At high elevations, therefore, the western streams are flowing on bedrock, have appreciable though seasonally variable volumes, and are eroding their channels.

Through-flowing streams at intermediate elevations of 7000–9000 feet have distinctly different characters from their more humid up-

stream reaches. The climate at Arequipa (elevation 7550 feet) is distinctly arid. Fenner (1948b, p. 899) states, "... it is doubtful whether erosion along the Chili (River) is going on at present," and he adds (p. 902, 903),

"At the present time Chili River, originating in a drainage basin back of the volcanoes, is subject to seasonal floods which might be thought sufficient to cause erosion under present conditions, but the flood waters bring down boulders from the upper reaches and there is no distinct evidence that either erosion or aggradation prevails."

At the observed elevation the Chili River has descended more than 10,000 feet through a region of increasing aridity. The Chili deposits a large amount of coarse material in its channel near Arequipa at the end of the rainy season. Although this same material may be removed and replaced each year much of the energy of the river is utilized in carrying its load, and volume is being lost through evaporation and absorption downstream. Jenks (1948) records aggradation downstream.

Bowman (1916), working on the Majes River about 40 miles northwest of the Chili River area, dealt with the relations in the lower reaches of a through-flowing stream. He said (1916, p. 227),

"... in the Pleistocene a great quantity of waste was swept into the Majes Valley, whereupon aggradation began; and in the middle and lower valley it has continued down to the present."

Bowman (p. 231) notes that present aggradation begins half a mile above Cosos. The elevation at that point is 2367 feet.

Although the observations of McLaughlin (1924), Fenner (1948b), Jenks (1948), and Bowman (1916) deal with high, intermediate, and lower river segments respectively, the rivers are not the same. Therefore the behavior of each of these streams is not necessarily common to all through-flowing rivers of the arid Peruvian west. Nevertheless, it is very clear that the changes of character of these streams from eroding to graded to aggrading takes place largely in response to loss in volume through evaporation and absorption, rather than breaks in slope. For these reasons much of the material carried by these rivers is prevented direct access to the Pacific Ocean.

*Significance of alluvium.*—In contrast to the northern slopes of the Cordillera de la Costa of Venezuela, the eastern Peruvian Sierra, and the Cordillera Occidental in Ecuador, the Peruvian Desert is a region currently generating great quantities of relatively coarse alluvium from bedrock, retaining the bulk of the material formed as residual accumulations, and yielding a relatively fine and dominantly eolian sedimentary product. It should be emphasized that the Peruvian Desert is an area of high relief situated a short distance from base level and is in these respects comparable to the three other regions considered. (*Compare* Figs. 3, 14, 16.)

*Western geomorphic history.*—The markedly different conditions prevailing in eastern versus western Peru are evident. It therefore seems desirable to establish the sequence of most recent events in the western Peruvian Desert for purposes of comparison with corresponding happenings in mountainous eastern Peru. Paleontologic information would be most helpful, but most of the age determinations have been very general—Pleistocene or Plio-Pleistocene (Bowman, 1916, p. 257; Fenner, 1948b, p. 910; Newell, 1949, p. 85; Jenks *et al.*, 1956, p. 288). More refined dating is lacking.

Three periods of aggradation of mountain valleys immediately preceding the conditions of the present were recorded by Bosworth (1922, p. 268). In the Sechura area at least one interval of extensive aggradation of mountain valleys and subsequent removal by incision is indicated, and Bowman (1916) cites a period of great aggradation in the Majes Valley area dating from the "Pleistocene." Because the lower and western part of the desert is a rain-shadow area, its physiography would date from the formation of the barrier responsible for the aridity. The conditions there may have been too stable to have produced a recognizable and reasonably complete sequence of events. This suggestion is substantiated to a large degree by the observations of Fenner (1948b) concerning the northeast slopes of peaks in the Cordillera Occidental in the Arequipa area.

A sequence of volcanic and erosional events took place on the southwest sides of the peaks of El Misti and Pichu Pichu. Records of these happenings are well preserved, and they are assigned by Fenner (1948b) to the, "... long glacial and preceding pluvial periods." The southwestern slopes of these peaks receive moisture from the diurnal westerly winds on a seasonal basis. The northeast slopes are in a "double" rain shadow; they receive no moisture from the southwest and likewise little from the prevailing easterly winds which have already lost most of their moisture on the eastern Andean slopes. The southwestern slope events recorded by Fenner (1948b, p. 899–903) have

no counterparts on the northeast slopes where, according to Rondón (1937, p. 53; *in* Fenner 1948b, p. 915),

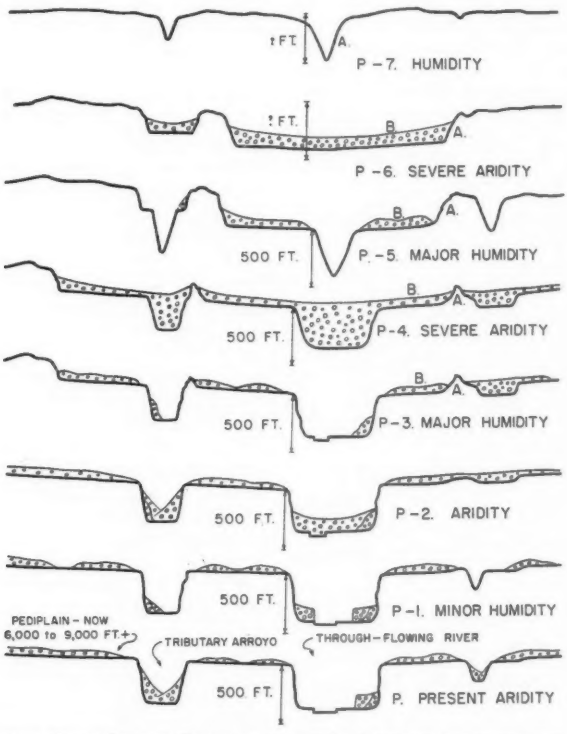


FIGURE 20.—SCHEMATIC CROSS-SECTION PROFILES OF THE GEOMORPHIC SEQUENCE AND DEVELOPMENT IN THE CORDILLERA OCCIDENTAL, PERU

In chronological sequence from oldest to youngest the events are as follows: (P −7) humid dissection of a surface of volcanic deposition; incision develops scarp A; (P −6) arid pedimentation and scarp retreat, aggradation of surfaces, and the formation of surface B; (P −5) relatively strong humid incision of stream channels to a maximum depth of 400 feet at an elevation of 7500 feet; (P −4) severe arid aggradation of all channels and interfluves, coincident destruction and retreat of scarps; (P −3) thorough humid erosion of channel deposits leaving only remnants; (P −2) minor arid aggradation of channels to a depth not exceeding 80 feet, essentially complete destruction of scarp A, development of a pediplain; (P −1) incision of channel alluvium, local development of alluvial terraces; (P) present arid aggradation of perched dry tributary arroyos; through-flowing streams are eroding at high elevations, at grade at intermediate levels, and aggrading at low elevations, through volume loss downslope.

"On the northeast and north side . . . the volcano has a more natural and less dissected declivity, presenting a regular conical form, interrupted at long distances by smooth ridges that give the impression of torrents of liquid lava that precipitated themselves down the volcano. This side is constituted in great part of sand, in some places of an intense black color. . . ."

The static climatic situation just described gives no clue to the geologic history disclosed on the opposite side of the same mountain, and in general a similar relation probably exists between the western, most severely arid portion of the Peruvian Desert and humid eastern Peru. On the basis of the preserved Inca and pre-Inca remains the present-day aridity of the west is established as being synchronous with the current humidity of the east, although other earlier events in the very dry areas are vague. For this reason the climatically variable portion of the Peruvian Desert (upper slopes with

seasonal rainfall) will be considered, as this area portrays the most detailed and understandable history of the region's physiographic development.

These events are listed as they were worked out on the upper southwest slopes of the range by Fenner (1948b, p. 899–903): (1) volcanic extrusion of extensive areas of incandescent tuff (white); (2) erosion and partial removal of white tuff; (3) volcanic extrusion of extensive areas of incandescent tuff (red); (4) pedimentation and beveling of all existing tuffaceous deposits—Laderas Pediment of Jenks (1948, p. 197); (5) minor extrusive volcanic rocks; (6) reentrenchment of Chili River into pediment surface and excavation of tributary quebradas several hundred feet deep; (7) filling of the entrenched channel of Chili River and tributary quebradas with boulder and gravel deposits more than 400 feet thick (Arequipa sediments) and aggradation of interfluvial areas with the same material—Vitor Pediment of Jenks (1948); (8) removal of coarse clastic deposits from channels; (9) deposition of 60–75 feet of coarse clastic material in the Chili River and tributaries; (10) incision and removal of a portion of the channel alluvium to form terraces; (11) recent alluviation of tributary quebradas under conditions of aridity with corresponding near-recent 20-foot channel incision of Chili River under conditions of adequate runoff from elevated areas of more rainfall.

Although Fenner (1948b, p. 903) notes the present formation of talus in the tributary quebradas, the gravel terraces in the Chili River, and the quasi-recent entrenchment of the Chili (p. 898), he groups the emplacement of the coarse clastic material of point (9) and the cutting of the terraces of point (10) under a single "stage." Moreover, although he recognized the recency of the quebrada talus he does not give the present episode a "stage" designation as such (Fig. 18). Jenks (1948) deserves credit for pediment recognition.

The sequence established by Fenner (1948b) seems to be well founded on the basis of his descriptions. He states (p. 898)

> "... it is doubtful that any great difference in the strength of the floods is indicated between the first carving out of the deep gashes, (quebradas) ... and the later filling with boulder deposits."

Following the lead of Bowman (1916), Fenner (1948b) attributes both the cutting and the aggradation of the quebrada and river channels to the overloading of torrential streams of glacial origin. The arguments applied to similar aggradations in the Cordillera Vilcapampa also apply to the Peruvian Cordillera Occidental—a much more weakly glaciated area, according to Bowman (1916), McLaughlin (1924), and Jenks *et al.* (1956). A more reasonable explanation, which is in agreement with the stream mechanics of Gilbert (1880) and deposition on slopes described by Johnson (1901), would be to attribute the periods of aggradation to conditions of aridity and scarp retreat and the periods of incision to conditions of humidity (Quinn, 1956; 1957).

Application of the principles worked out by Quinn (1956; 1957) to the data of Fenner (1948a; 1948b) and Jenks (1948) alters the result (Fig. 20) as follows: (1) P −7: dissection of volcanic deposits producing local relief—a necessary prerequisite for scarp retreat and pedimentation; (2) P −6: arid pedimentation and beveling of volcanic deposits to an "astonishingly plane surface" (Fenner, 1948b, p. 900); (3) P − 5: entrenchment of the Chili River into the pediment surface and incision of tributary quebradas several hundred feet deep under conditions of humidity; (4) P −4: aggradation of all channels and interfluvial areas—thickness in channels exceeding 400 feet—probably equivalent to the "six hundred and probably as much as eight hundred feet of alluvium" in the Majes Valley noted by Bowman (1916, p. 273); (5) P −3: removal of much of the coarse clastic arid residual channel accumulations under conditions of humid runoff; (6) P −2 aggradation of channels to a depth of 60–75 feet under conditions of aridity with some valley-wall and scarp retreat; (7) P −1: incision and removal of a portion of the channel alluvium under conditions of mild humid runoff and the cutting of alluvial terraces, possibly equal to the terraces of Bosworth (1922); (8) P: present aridity; formation of talus accumulations in tributary quebradas; volumes of through-flowing streams insufficient to erode at lower elevations.

*Discussion.*—An examination of the Peruvian Desert shows that this high-relief source area, close to a depositional site, currently yields dominantly fine clastic eolian silts; minor sands and gravels are transported by arid streams of the ephemeral type. This is in direct opposition to the idea that high-relief source areas close to depositional sites should yield coarse material as an expression of a tectonically positive and active area. Coarse clastic materials are currently accumulating as residual deposits in the desert source area. The writer thoroughly agrees with the idea that humid conditions would have a drastic effect on the arid residuals

(Bowman, 1916, p. 144). An appreciable increase in rainfall in the desert would initially greatly increase the coarseness of the clastic volcanic activity in the west has to some extent obliterated the earlier record there. Probably the most striking relation illustrated is the

TABLE 1.—COMPARISON OF EASTERN AND WESTERN PERUVIAN SEQUENCES

| Chronology | Western Andean slopes of Peru | Eastern Andean slopes of Peru |
|---|---|---|
| (P) Present | Low and intermediate- to high-level aridity with aggradation of all but seasonally through-flowing stream channels in upstream portions | Multielevation humidity with perennial stream erosion of residual and alluvium |
| P −1 | Low-level aridity (rain shadow): upper slope; minor humid erosion and terracing of residual arid channel deposits along channels of through-flowing streams | Minor subaridity with slight talus cone formation and ephemeral stream flow |
| P −2 | Minor high- and low-level arid aggradation of through-flowing stream channels and tributary quebradas | Minor alpine glaciation to 12,000-foot minimum elevation with limited lower-level beveling and erosion of arid debris |
| P −3 | Efficient humid erosion of arid residual deposits 400 feet thick from channels and partial removal of interfluvial deposits | Major arid to subarid emplacement of 400-foot thick valley fills, confluent fans, talus cones, and elevated pediment gravels |
| P −4 | Prolonged, severe aridity with high- and low-elevation aggradation of channels and interfluvial areas | Major alpine glaciation with U-shaped valley development below 12,000-foot elevation |
| P −5 | High-elevation humid incision of pediment surfaces to a depth of 400 feet; low-elevation aridity | Major arid to subarid valley aggradation and high-level scarp retreat and pedimentation |
| P −6 | Major arid aggradation and pedimentation through retreat of scarps formed during preceding humid incision | Prolonged humid entrenchment of lateral mountain valleys to depths exceeding 2000 feet |
| P −7 | High elevation, humid erosion, and incision of a surface formed by the deposition of pyroclastic material | High-elevation arid pedimentation through retreat of scarps formed during preceding humid incision |
| P −8 | Volcanic extrusion of widespread incandescent tuff deposits—sillar colorado of Fenner (1948a) | Minor humid incision of upland surfaces having local relief not to exceed 100 feet |

fragments being moved and the amount being yielded to base level in western Peru.

## COMPARATIVE GEOMORPHIC EVENTS IN THE PERUVIAN ANDES

### *Sequence of Events*

Archeological evidence indicates a synchrony of western aridity and eastern humidity extending more than 1000 years into the geologic past. From this point of departure the sequence of events on opposite sides of the Andes Mountains can be compared (Table 1).

The sequence of events discloses that the alternation of climatic conditions on opposite sides of the Andes Mountains. Such alternation would be open to question (1) if there is no reasonable control for the sequence, (2) if the sequences were shown to be out of phase, or (3) if a single major erosional feature common to both sides could be shown to be equivalent in time. Conversely, the probability of such alternating conditions would be considerably strengthened if (1) there is a reasonable method of control, (2) the events are demonstrably in phase, and (3) highly similar erosional features on opposite sides could be shown to be successive but not coincident in time.

The vast, coarse-clastic aggradation in the eastern Andes cited by Bowman (1916), McLaughlin (1924), Jenks *et al.* (1956), and the writer and the equally vast accumulations in the western Andes described by Fenner (1948b, "stage 7") and Bowman (1916) have been considered by most workers as representing the product of a single set of events. If these deposits were simultaneously emplaced during the Pleistocene as many suppose, there is no explanation for (1) their differing degrees of preservation or (2) their emplacement on the eastern side, unless that region was formerly more arid—in itself proof of changed climatic conditions on the eastern Andean front.

If the western side has always been arid and the eastern side always humid it is not possible to explain why conditions of arid runoff and minor glacial and postglacial melt would have removed the western alluvium with the exception of minor residuals, whereas the extreme humid rivers and more severe glacial and postglacial runoff of the eastern Andes has succeeded in only slightly incising the valley-floor accumulations.

Therefore, (1) the eastern accumulations are somewhat younger than the western and/or (2) humid incision in the west was formerly much greater than at present and/or (3) eastern incision was recently much less than at present. (*See also* Garner, 1958.) All three appear to be true.

Considered in reverse order the evidence indicates that conditions of humid runoff in the east have prevailed from the present back to the time of emplacement of the most widespread alluvium with only a very minor subarid interruption (Table 1, stage P −1). Humid incision in the west has clearly been more efficient several times in the past, for rivers such as the Majes and Chili are currently at grade or aggrading in places where they formerly cut valleys or removed large amounts of coarse alluvium. (Compare stages P −1 and P −3 of Figure 20.) On the basis of position in sequence, the western period of major aggradation is a phase earlier than the eastern aggradation of the same scale. (*See* Table 1, stages P −3, P −4.) On the basis of the differences in erosive powers of present eastern and western rivers, the only plausible explanation for the thoroughness of western erosion is that the western deposits are the older. Therefore, their removal took place during a humid interval long predating current western aridity, concurrent in time with the period of aggradation of the eastern mountain valleys (Fig. 12, stage P −3). It is evident that the period of greatest aggradation in eastern and western Peru is not the same although the eastern is only a phase younger than its western predecessor.

Apart from the present humid conditions in eastern Peru where glaciation is confined to the highest elevations, at least the two preceding periods of humidity coincided with times of more or less intense glaciation (Table 1, stages P −2 and P −4). The two oldest recognizable intervals of humid incision in the east as well as in the west could have been glacial also, but all direct evidence has been destroyed or masked.

The relative intensities of the chronologically equivalent climatic and erosional events are in remarkable agreement. The present humidity of the east corresponds to the aridity of the west. The last slight talus formation in the east corresponds to the development of perched tributary quebrados along the through-flowing streams in the west. The last weak glaciation in the east is commensurate with the synchronous mild aggradation in the west. The emplacement of 400-foot thick alluvial fills in the eastern valleys took place when comparably thick residual deposits were being removed in the west. The phases are much too similar in intensity to be attributed to chance although the east-west climatic conditions clearly alternate. The more recent east Andean climatic events are paralleled in type and magnitude on the eastern South American lowland (Garner, 1958).

### *Theory of Alternating Andean Climates*

A hypothesis of alternating climatic and erosional conditions on opposite sides of the Andes Mountains is suggested by the present data in connection with the observations of Bowman (1916) and Fenner (1948b). The aridity of the west coast is, in part, a product of a rain shadow on the west side of the Andes and is to that extent, therefore, as permanent as the causative barrier. The variation in rainfall on the upper western slopes must be attributed to changes in temperature of the adjacent Pacific Ocean or, more specifically, the Humboldt Current. Two basic assumptions, which appear to be fundamentally sound, must be made: (1) Intensification of Antarctic glacial conditions would cool the southern oceans—particularly currents such as the Humboldt which comes from the south. (2) Intensification of Antarctic glacial conditions

would promote alpine glaciation in Southern Hemisphere mountains where there was adequate moisture. The converse of these two assumptions is also implied.

On this basis, humid conditions and/or glaciation in the eastern Andes would correspond in time to a cold Humboldt Current which would in turn cause a relative increase in aridity in the Cordillera Occidental. The corollary is also implied—arid conditions and glacial retreat in the Cordillera Oriental would be synchronous with a warmer Humboldt Current and increased high-elevation humidity and/or glacial advances in the western Andes (*See* Bowman, 1916, p. 127).

This hypothesis is supported not only by present and past relative climatic events of eastern and western Peru, but also by the observations of Fenner (1948b, p. 917):

"The mechanism by which the southwestern sides of these volcanoes (El Misti and Pichu Pichu) receive much more precipitation than the northeastern is understandable under the climatic conditions of the present time, but the astonishing thing is that a similar meteorological mechanism was operative during the glacial period and also during the long preceding pluvial period, during both of which eras the temperature and quantity of precipitation were far different from what they are at present."

Fenner implies that not only were there climatic changes but also that high elevations were present in the Andes early in the Pleistocene and probably in the late Tertiary. This idea is supported by the data presented herein and is contrary to the current supposition that the region was reduced to base level at that time.

## Sedimentary and Stratigraphic Implications of Cyclic Climates

### *General Statement*

The geological evidence seems more than sufficient to prove that the coarse alluvial-valley fills in the mountains of western Ecuador and eastern Peru were not emplaced or formed under present conditions of humid weathering and/or runoff. Implicit in this statement is the idea that the climates in these regions are not fixed but have changed considerably from time to time in the geologic past. Explanations of alluviation by means of eustatic adjustment or overloading of streams are respectively (1) counter to the observed high-elevation association of widespread alluvial-valley fills, without associated marine deposits, on opposite sides of a single mountain system in early stages of dissection, and (2) contrary to the laws of stream mechanics and deposition on inclined surfaces.

The mountains of eastern Peru and western Ecuador are located relatively close to a desert region which is surrently generating coarse alluvium similar to that in the adjacent humid mountain valleys. Although the alluvium is presently being removed in the humid regions it is being retained as residual accumulations at almost all elevations in the desert. Arid aggradation as observed by the writer in the Peruvian Desert and as previously outlined by Quinn (1957) with regard to Central Texas appears to be the only practicable explanation of high-elevation alluvial accumulations in the humid mountains of eastern Peru and western Ecuador. The writer therefore postulates that alternating conditions of humidity and aridity have prevailed in both the Cordillera Occidental of Ecuador and the Cordillera Oriental of Peru. The available data show that a relatively recent increase in humidity of the Ecuadorian and eastern Peruvian areas is causing the removal of alluvium formed during preceding intervals of aridity.

The chronological sequence is sufficiently well established in eastern and western Peru to show that climatic conditions on opposite sides of the Peruvian Andes have alternated: one side is relatively dry when the other is relatively wet. The Ecuadorian relations are much more obscure, but present humid conditions were preceded by at least one period of extensive arid aggradation. Clear-cut indications of alternating humidity and aridity in western Peru are expressed only in the higher and relatively more "wet" portions of the Peruvian Desert. Thus the lower, more coastal desert areas have been more or less permanently arid since the formation of the Andean physiographic barrier. The upper slopes of the Peruvian Desert show evidence of alternating aridity and humidity and dominance of arid conditions. This agrees in principle with the ideas of Quinn (1956). The data also show that aridity and humidity have alternated in eastern Peru and that humid incision has dominated over arid plantation; this was also suggested in theory by Quinn (1956).

It seems doubtful that the Cordillera de la Costa of Venezuela has recently experienced an arid interval comparable in severity with that of eastern Peru and western Ecuador as

shown by the absence of residual coarse clastic material. (Compare Figs. 4, 11, 15, and 18.) However, the intermontane valleys of the Serrañia del Interior of Venezuela are currently denied moisture by the north coastal barrier and contain alluvial coarse clastic accumulations. This alluvium may therefore be due to earlier and probably more intense arid conditions, which subsequent changes have only slightly modified.

Thus, tectonically generated relief alone is not capable of controlling clastic sediment size and quantity. All four of the regions discussed are high and relatively close horizontally to base-level depositional sites except eastern Peru. Distance of transport seems important in its effect on grain size under the limits imposed. However, in the cases cited the materials that are initially coarse (arid residuals) supply a maximum quantity of coarse material to deposits relative to the distances involved. Initially fine clastics naturally tend to remain so after transport.

Climate is the only element capable of periodic fluctuations of the described nature in the four Andean regions. It governs the nature of rock breakdown and therefore initial grain size and determines when and how a weathered product will reach a base-level deposit. Therefore, climate is a variable in the sedimentary clastic formula mentioned in the Introduction; relief, kinds of bedrock, and source-deposit distance act as relative constants. Time is a second variable.

A region that is alternately humid and arid is undergoing a periodic sequence of climate changes, probably cyclic. Data for the present paper and for the Pleistocene interval as a whole make it necessary to acknowledge the existence of periodic climatic variations. There is no sound reason for supposing that such changes and associated effects have been restricted to relatively recent geologic time or to the Andes Mountains. Therefore, the sequence of events characteristic of a climatic cycle, particularly erosional and depositional events as illustrated by the regional studies of the present report, must be understood.

The Venezuelan, eastern Peruvian, and western Peruvian situations reflect distinct climatic phases; western Ecuador more or less parallels eastern Peru but is located close to a base-level depositional site. The phases illustrated are as follows: (1) the Venezuelan north coast is an area of prolonged humid conditions and is typified by (a) thorough dissection of land surfaces, high percentage of slope, and almost no flat terrain, (b) thick soils, (c) heavy vegetation, (d) dominantly chemical weathering processes, (e) no eolian activity of importance, and (f) through-flowing rivers carrying loads of fine clastic material—mainly clay, sand, carbonaceous material from land plants, solutes, and lesser amounts of coarser clastic debris; (2) the lower, western desert of Peru is an area in which arid conditions have long prevailed, and it is characterized by (a) locally and generally weakly dissected, dominantly flat land, (b) little or no soil, (c) little or no vegetal cover, (d) dominantly mechanical weathering processes, (e) accumulation of coarse clastic residual deposits, (f) ephemeral stream flow moving minor sand and gravel and no appreciable plant material or solubles, and (g) continual eolian activity which moves argillaceous fractions efficiently out of the area and locally transports sand; (3) the eastern slopes of the Peruvian Cordillera Oriental and the western slopes of the Cordillera Occidental of Ecuador are in relatively early stages of a humid cyclic phase characterized by (a) removal of coarse clastic residual arid accumulations, (b) chemical weathering processes, (c) no eolian activity of importance, (d) dense vegetal cover, (e) developing soils on bedrock and alluvium, and (f) through-flowing rivers carrying coarse clastic material derived from residual arid deposits—loads range from boulders to sand and silt and contain added solute, clay, and sand fractions reflecting current humid weathering processes—and delivering this load to base level.

### *Principle of Sedimentary Lag*

The sedimentary implications of the climatic phases outlined are clear when the phases are regarded as segments of a continuous cyclic sequence. Arid mechanical-weathering processes yield a generally coarse residual which the available agents of transport cannot efficiently move to base level. The stratigraphic-sedimentary equivalent in time of nonmarine arid coarse clastic residuals is eolian silts with sands and minor ephemeral-stream admixtures. The Peruvian Desert is a prime example of such a source.

A change from arid to humid conditions in a source area necessitates a subarid period of transition. Vegetation, rainfall, and stream flow will increase, whereas eolian activity will diminish. For example, the arid-to-humid

transition in eastern Peru and western Ecuador is promoting development of soils and removal of coarse clastic arid residuals. The marine stratigraphic equivalents in time of the developing subarid and early humid soils are river-borne coarse clastic material deposited by through-flowing streams at base level. Increasing vegetal cover nominally results in increasing amounts of plant material in derived sediments, whereas developing humid chemical weathering processes add increasing argillaceous fractions and solutes.

Prolonged humid incision and weathering in a source region as illustrated on the north slopes of the Cordillera de la Costa in Venezuela indicate the next event of the climatic sequence. Deep weathering and/or eventual removal of residuals and decomposition of bedrock result in gradual bulk clastic-size reduction; the theoretical endpoint is a dominantly clay-weathered interval plus or minus quartz sand, depending on bedrock constituents and effectiveness of silica leaching. With such source material and erosion agents the marine stratigraphic equivalent of long-term, humid-source-area decomposed mantle is fluvially transported clays, minor amounts of sand, humic additives, and solutes.

A period of transition from humid to arid produces different results from those of a transition from arid to humid, even though technically both would be subarid for a time. The South American areas considered in this report do not include an example of such a climatic phase although many of the marginal desert regions of the world illustrate the associated characters. Such a transition involves a reduction of rainfall and vegetation and the elimination of through-flowing rivers. Quinn (1957, p. 155, 156) points out the importance of plant cover in controlling the amount of sediment introduced into streams. A loss of forest and grass cover in a source area which has been humid for a long period would not only expose the humid soils to the ephemeral severity of arid runoff but, probably more significantly, would expose a vast amount of fine clastic material to eolian deflation. Under these circumstances early aridity would be characterized by the removal of the fine humid soils similar to the Dust Bowl activity in the United States during the 1930's and periodically since then. Although man destroyed the grass cover in the Dust Bowl for the most part, a climatic change would have served equally well.

Eolian deflation during early aridity would nominally free any available sand fraction and permit sand-dune formation and would expose unweathered bedrock to subsequent arid mechanical disruption. This deflated source region with possible associated dunes would therefore nominally have a stratigraphic marine counterpart—or counterpart in another vegetated land area—of eolian clays plus minor sand fractions and humic material from residual soils; abyssal marine clays may, in part, be a product of such events. Plant remains and clay components would tend to decrease, and silt (loess) fractions would increase in derived sediments as aridity becomes more pronounced and prolonged.

The first three phases of the climatic sequence are documented by examples discussed in this report. The fourth phase seems to be a logical part of the sequence and is illustrated in other parts of the world as indicated. These conclusions have a direct bearing on the problems of correlation between marine and contemporaneous nonmarine stratigraphic sections and also on the interpretations of lithologic types.

There is not, therefore, a general and continuous movement of all types of sedimentary material (via weathering and erosion) from bedrock of source areas to depositional sites. The concept of arid alluviation of the land developed by Quinn (1957) has inherent in it the idea of subsequent humid stripping and deposition in the sea. This delay in transportation here called sedimentary lag, is defined as the delayed effective removal and deposition of a sediment previously generated and held on land by the weathering and erosional effects of a particular preceding climate. Thus, the development of coarse clastic debris of the arid type, during the last interglacial stage in eastern Peru, which is currently being stripped and carried to the South Atlantic Ocean by through-flowing rivers of the present humid period, is an example of sedimentary lag. The stripping of the surficial residual soil cover by eolian deflation from the Dust Bowl in the United States during the mid-1930's drought is also an example of sedimentary lag on a small scale.

The associations in the Andes Mountains indicate that a reevaluation of stratigraphic, sedimentary, and tectonic principles is necessary and suggest a basis for a better understanding of the relationships among these phenomena. The writer hopes that the concept of climatic control of clastic size and the delivery of sediment to base level and the

principle of sedimentary lag are new tools in the approach to sedimentary, stratigraphic, and tectonic interpretations.

## References Cited


Aguerrevere, S. E., and Zuloaga, G., 1937, Geological notes on the central part of the Cordillera de la Costa, Venezuela: Geol. y Min. Bol. (Venezuela), v. 1, nos. 2–4, p. 3–22; English edition, p. 3–22

Bennett, H. H., 1939, Soil conservation: N. Y., McGraw-Hill Book Co., Inc., 993 p.

Bennett, W. C., 1948, American antiquity—A reappraisal of Peruvian archaeology: Soc. Am. Archaeology Mem., v. 13, no. 4, pt. 2, 128 p.

Bennett, W. C., and Bird, J. B., 1949, Andean culture history: Am. Mus. Nat. History Handb. 15, 319 p.

Blackwelder, Eliot, 1925, Exfoliation as a phase of rock weathering: Jour. Geology, v. 33, p. 793–806

— 1927, Desert weathering: Geol. Soc. America Bull., v. 38, p. 127–128

Bosworth, T. O., 1922, Geology of the Tertiary and Quaternary periods in the North-west part of Peru: 1st ed., London, Macmillan and Co., 434 p.

Bowman, Isaiah, 1914, Results of an expedition to the Central Andes: Am. Geog. Soc. Bull., v. 46, p. 161–183

— 1916, The Andes of southern Peru: 1st ed., N. Y., Henry Holt and Co., 336 p.

— 1924, Desert trails of Atacama: Am. Geog. Soc. Special Pub. 5, 362 p.

— 1938, Los Andes del sur del Perú: Arequipa, Peru, Editorial La Colmena, S. A., 267 p. (Trans. by Carlos Nicholson)

Bucher, W. H., 1952, Geologic structure and orogenic history of Venezuela: Geol. Soc. America Mem. 49, 113 p.

Enock, C. R., 1916, Peru: 4th ed., London, T. Fisher Unwin, Ltd., 320 p.

Fenner, C. N., 1948a, Incandescent tuff flows in southern Peru: Geol. Soc. America Bull., v. 59, p. 879–894

— 1948b, Pleistocene climate and topography of the Arequipa region, Peru: Geol. Soc. America Bull., v. 59, p. 895–917

Garner, H. F., 1958, Climatic significance of anastomosing channel patterns typified by Rio Caroni, Venezuela (Abstract): Geol. Soc. America Bull., v. 69, p. 1568–1569

Geikie, Archibald, 1903, Geological action of the atmosphere, p. 430–531 *in* Textbook of Geology, V. 1: 4th ed., London, Macmillan and Co., 637 p.

Gilbert, G. K., 1880, Report on the geology of the Henry Mountain region: 2d ed., U. S. Geog. and Geol. Survey Rocky Mtn. Region (Powell) 170 p.

Humboldt, A. von, 1801, Esquisse d'un tableau géologique del l'Amérique Méridional: Paris, Jour. Physics, t. 53, p. 30–59

— 1826, Viajes a las regiones equinocciales del nuevo continente: 1st ed., v. 1 of 6 volumes, Paris, Rosa, 364 p.

— 1837, Geognostiche und physikalische Beobachtungen über die Vulkane des Hochlands von Quito: König-Preuss-Akad. der. Wiss., N. Jahrb., p. 253–284

Jenks, W. F., 1948, Geology of the Arequipa quadrangle of the Carta Nacional del Peru: Lima, Inst. Geol. del Peru Bol. 9, 204 p.

Jenks, W. F., *et al.*, 1956, Handbook of South American geology: Geol. Soc. America Mem. 65, 378 p.

Johnson, W. D., 1901, The High Plains and their utilization: U. S. Geol. Survey Ann. Rept., v. 4, p. 601–741

King, L. C., 1953, Canons of landscape evolution: Geol. Soc. America Bull., v. 64, p. 721–752

Kummel, Bernhard, 1948, Geological reconnaissance of the Contamana region, Peru: Geol. Soc. America Bull., v. 59, p. 1217–1265

Leopold, L. B., and Maddock, Thomas, Jr., 1953, The hydraulic geometry of stream channels and some physiographic implications: U. S. Geol. Survey Prof. Paper 252, 57 p.

Liddle, R. A., 1928, The geology of Venezuela and Trinidad: 1st ed., N. Y., Little and Ives, 552 p.

—— 1946, The geology of Venezuela and Trinidad: 2d ed., N. Y., Cayuga Press, Inc., 890 p.

Marks, J. G., 1951, Miocene stratigraphy and paleontology of south-western Ecuador: Bull. Am. Paleontology, v. 33, no. 139, 144 p.

McLaughlin, D. H., 1924, Geology and physiography of the Peruvian Cordillera, Departments of Junin and Lima: Geol. Soc. America Bull., v. 35, p. 591–632

Means, P. A., 1932, Fall of the Inca Empire and the Spanish Rule in Peru; 1530–1780: N. Y., Charles Scribner's Sons, 351 p.

Mencher, E., *et al.*, 1953, Geology of Venezuela and its oilfields: Am. Assoc. Petroleum Geologists Bull., v. 37, p. 690–777

Newell, N. D., 1949, Geology of the Lake Titicaca region, Peru and Bolivia: Geol. Soc. America Mem. 36, 111 p.

—— 1956, Reconocimiento geologico de la region Pisco—Nazca: Soc. Geol. Peru Bol., t. 30, 1st Cong. Nac. Geol. Anales, pt. 1, p. 261–295

Newell, N. D., Chronic, John, and Roberts, T. G., 1953, Upper Paleozoic of Peru: Geol. Soc. America Mem. 58, 276 p.

Newman, M. T., 1947, Indian skeletal material from the Central Coast of Peru: Peabody Mus. Rept. 4, v. 27, 71 p.

Nygren, W. R., 1950, Bolivar geosyncline of northwestern South America: Am. Assoc. Petroleum Geologists Bull., v. 34, p. 1998–2006

Ogilvie, A. G., 1922, Geography of the Central Andes: Am. Geog. Soc., 240 p.

Prescott, W. H., 1875, History of the conquest of Peru with a preliminary view of the civilization of the Incas: 2d ed., v. 1 of 2 volumes, Philadelphia, J. B. Lippincott and Co., 510 p.

—— 1876, History of the conquest of Peru with a preliminary view of the civilization of the Incas: 2d ed., v. 2 of 2 volumes, Philadelphia, J. B. Lippincott and Co., 530 p.

Quinn, J. H., 1956, Origin and age of Ozark plateau surfaces in northwest Arkansas (Abstract): Geol. Soc. America Bull., v. 67, p. 1726

—— 1957, Paired river terraces and Pleistocene glaciation: Jour. Geology, v. 65, p. 149–166

Rondón, M. Enrique, 1937, Expedición Universitaria del año 1935 al crater del Volcán Misti, in a collection of papers published by the University of Arequipa, Arequipa, p. 170–188

Rowe, J. H., 1944, An introduction to the archaeology of Cuzco: Peabody Mus. Rept. 2, v. 27, 69 p.

Roy, C. J., 1945, Silica in natural waters: Am. Jour. Science, v. 243, no. 7, p. 393–403; correction, v. 243, no. 10, p. 582

Sheppard, George, 1937, The geology of Southwestern Ecuador: London, Thomas Murby Co., 375 p.

Tschopik, M. H., 1946, Some notes on the archaeology of the department of Puno, Peru: Peabody Mus. Rept. 3, v. 27, 57 p.

Tschopp, H. J., 1953, Oil explorations in the Oriente of Ecuador, 1938–1950: Am. Assoc. Petroleum Geologists Bull., v. 37, p. 2303–2347

Twenhofel, W. H., 1939, Principles of sedimentation: 1st ed., N. Y., McGraw-Hill Book Co., 610 p.

—— 1950, Principles of sedimentation: 2d ed., N. Y., McGraw-Hill Book Co., 673 p.

Twenhofel, W. H., *et al.*, 1926, Treatise on sedimentation: 1st ed., Baltimore, Williams & Wilkins Co., 661 p.

—— 1932, Treatise on sedimentation: 2d ed., Baltimore, Williams & Wilkins Co., 926 p.

Department of Geology, University of Arkansas, Fayetteville, Ark.

Manuscript Received by the Secretary of the Society, February 13, 1958

BULLETIN OF THE GEOLOGICAL SOCIETY OF AMERICA
VOL. 70, PP 1369–1394, 12 FIGS., 4 PLS. OCTOBER 1959

# GEOLOGY OF CONTINENTAL SHELF OFF LOUISIANA: ITS INFLUENCE ON OFFSHORE FOUNDATION DESIGN

BY HAROLD N. FISK AND BRAMLETTE MCCLELLAND

## ABSTRACT

Foundation problems for drilling structures offshore from Louisiana are related to the shearing strength and scour resistance of near-surface late Quaternary Continental-Shelf deposits. Over much of the shelf area, thick topstratum clays provide the foundation materials; where clays are thin, underlying substratum sands or weathered late Pleistocene deposits constitute the foundation. Study of the nature of the late Quaternary facies and of their relation to shelf topography makes it possible to map the sediment types and to date them. Compression tests on clay samples permit recognition of four categories of strength variation with depth: normally consolidated, underconsolidated approaching normal, underconsolidated, and overconsolidated clays. These tests also demonstrate that substantial time is required for clays to reach a normally consolidated condition.

## CONTENTS

### TEXT

| | Page |
|---|---|
| Introduction and acknowledgments | 1369 |
| The engineering problem | 1371 |
| General discussion | 1371 |
| Foundation types and loads | 1371 |
| Controlling engineering properties | 1372 |
| Investigational procedures | 1372 |
| Continental-Shelf deposits | 1374 |
| General description | 1374 |
| Facies of shelf deposits | 1376 |
| Age and development of the shelf deposits | 1378 |
| Foundation characteristics of the shelf deposits | 1380 |
| Engineering-geology relationships | 1383 |
| Typical strength profiles of clay sediments | 1383 |
| Effect of clay minerals on sediment strength | 1383 |
| Correlation of engineering and geological data at specific sites | 1385 |
| General statement | 1385 |
| Normally consolidated clay deposits | 1386 |
| Underconsolidated clays approaching normal state of consolidation | 1390 |
| Underconsolidated clays | 1391 |
| Overconsolidated clays | 1392 |
| Summary and conclusions | 1393 |
| References cited | 1393 |

### ILLUSTRATIONS

| Figure | Page |
|---|---|
| 1. Map of Continental Shelf off Louisiana | 1370 |
| 2. Types of foundation failures of offshore drilling structures | 1373 |
| 3. Cross section of near-surface shelf deposits along line approximately parallel to Louisiana shore | 1375 |
| 4. Positions of late Quaternary buried trenches, strand plains, and deltas off Louisiana coast | 1377 |
| 5. Areal distribution of late Quaternary topstratum units | 1382 |
| 6. Typical strength profiles for clay deposits, illustrating the effects of geologic processes | 1384 |
| 7. Relationship between plasticity index and clay-sized minerals | 1385 |
| 8. Rate of change in clay strength with increasing overburden pressure | 1386 |
| 9. Engineering and geologic data from undisturbed samples | 1387 |
| 10. Engineering and geologic data from undisturbed samples | 1388 |
| 11. Engineering and geologic data from undisturbed samples | 1388 |
| 12. Engineering and geologic data from undisturbed samples | 1389 |

| Plate | Following page |
|---|---|
| 1. Self-contained multiple-well drilling structure with helicopter platform, Grand Isle area | 1378 |
| 2. Laboratory tests for determination of the shearing strength of clays | |
| 3. Undisturbed cores of deltaic facies from late Quaternary shelf deposits | |
| 4. Undisturbed cores of shelf and prodelta facies, and the weathered zone from late Quaternary shelf deposits | |

## INTRODUCTION AND ACKNOWLEDGMENTS

Since 1944 intense construction activity on the Gulf of Mexico Continental Shelf has stimulated engineering and geologic investigation of near-surface sediments in that area. The construction illustrated by the well-drilling platform (Pl. 1) was required as part of

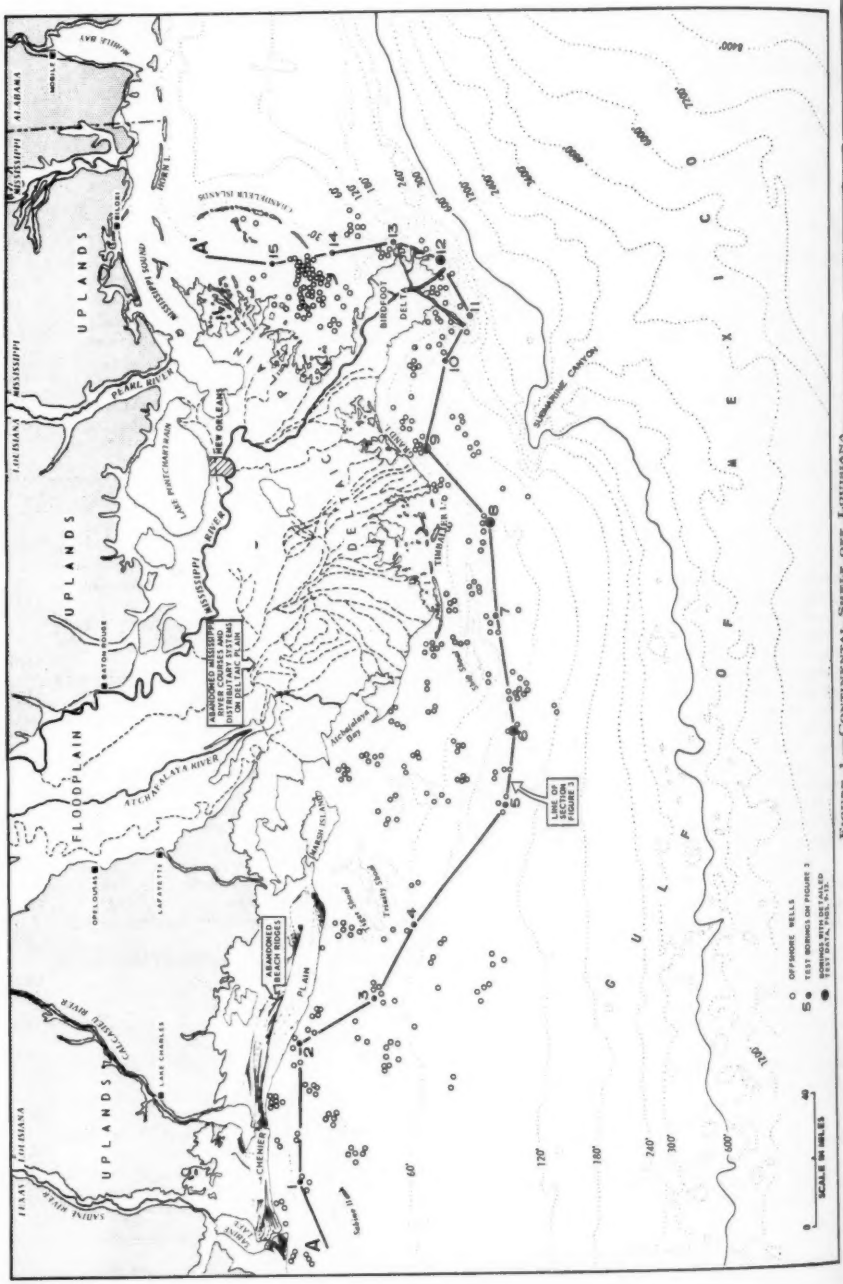


FIGURE 1. CONTINENTAL SHELF OFF LOUISIANA

the continuing search for, and production of, petroleum from beneath the waters of the gulf. As of December 1957, approximately 1200 producing oil and gas wells and 500 nonproductive wells had been drilled on the northern shelf of the gulf.

The distribution of wells drilled off the coast of Louisiana, where nearly 70 per cent of the offshore drilling in the gulf has been conducted, is shown on Figure 1. The intensity of drilling activity in this shelf region is indicated by the fact that 120 drilling rigs were operating there in August 1957, more than 25 per cent of the world's offshore rigs. Seventy-nine of these were on fixed, pile-supported platforms, and 43 were on mobile platforms capable of working in maximum water depths ranging from 15 to 150 feet.

Each type of drilling platform, whether fixed or movable, must transfer all structural loads, drilling loads, and storm forces to the deposits of the gulf floor. The safety of these structures against overturning, shifting, or subsiding is dependent upon the physical characteristics of the shelf deposits, especially their strength and resistance to scour. Clay is the dominant sediment type on the shelf, and clay deposits exhibit wide variations in strength depending on type and abundance of clay minerals, rate of deposition, and amount of overburden. Strength patterns of certain shelf clays have also been affected by erosion and desiccation. Sand bodies have consistent strength characteristics but are highly erodable; they are of particular interest from the standpoint of their location and thickness.

The shelf deposits are of late Quaternary age, and their nature, distribution, and thickness reflect the effects of the last Quaternary cycle of changing sea level and of their proximity to the Mississippi River. This fluctuation in sea level controlled depositional and erosional processes, which in turn affected engineering properties and produced patterns in the types of foundation material on the shelf. These patterns can be recognized by relating geologic characteristics and engineering properties and can be used to predict local foundation conditions.

The writers wish to acknowledge the assistance of the Humble Oil & Refining Company and of the Shell Oil Company for making available logs and samples of borings used in this study. Soil-mechanics tests to determine engineering properties were conducted in the laboratories of McClelland Engineers, Inc. Clay-mineral identifications were made by A. D. Kaiser, Jr., and M. S. Taggart, Jr., Humble Oil & Refining Company. Assemblages of Foraminifera in the samples were identified by D. O. LeRoy and S. A. Levinson, Humble Oil & Refining Company.

## The Engineering Problem

### *General Discussion*

Structures for drilling offshore oil wells may be either fixed or movable. The fixed structures are divided into two classes: self-contained platforms and tender-type platforms. Self-contained platforms (Pl. 1) are built with enough deck area to accommodate all equipment required for drilling, testing, and completing a well, and usually include arrangements for the drilling of 6 to 10 wells. The tender-type unit is smaller with little more than the derrick and drawworks on the platform; the balance of the required equipment and facilities is carried on a floating vessel or "tender" securely moored alongside. These platforms are usually arranged for drilling up to 6 wells. Substructures of the fixed platforms are prefabricated on shore, in one or more pieces; the deck structure is also prefabricated and is erected 40 feet or more above sea level to provide clean passage beneath it for hurricane waves.

Many well-drilling structures have been designed to permit their movement from one location to another and are usually called "mobile platforms." These units are self-contained and, when on location, support the drilling equipment on a deck 40 feet or more above sea level. The form of these structures varies widely; many different mechanical systems are employed to convert a floating unit to one firmly supported on the gulf bottom and, subsequently, to float it again for transportation to the next drilling site (Howe, 1954).

### *Foundation Types and Loads*

The wide variety of foundations in use for offshore drilling structures can be broadly divided into two familiar groups:

(1) ***spread footings***, which transfer loads through bearing areas at or near the ground surface, and

(2) ***piles***, which penetrate significant depths into the foundation sediments, transferring loads by skin friction to the sediments they pass through and by end bearing to sediments at their tips.

Total vertical loads of great magnitude are placed on these foundations by the combined weights of massive structures and heavy equipment and by large drilling loads. Winds, waves, and ocean currents produce large horizontal loads which tend to cause sliding or overturning of the structures. Vertical and horizontal loads carried by foundations of offshore structures frequently far exceed loads normally encountered in land construction.

In practice, foundations of the spread-footing type are used principally for mobile structures. In many, the foundation element consists of a large pontoon or barge hull which also provides flotation while moving the structure between locations. In such cases the bearing pressure when on location is quite low, usually less than 800 pounds per square foot. Some footing elements, however, have been designed for offshore use which require bearing pressures as high as 3500 pounds per square foot.

Fixed platforms are erected almost exclusively on driven piles. Tubular steel piles up to 3 feet in diameter are the most common type. Larger piles of 4-foot to 12-foot diameters, sometimes called caissons or piers, are used in the foundations of several mobile platforms. A typical vertical design load on a single 30-inch pile is 300 tons, and horizontal loads of 50–60 tons are commonplace. Such loads are virtually unknown to onshore construction. Even larger loads, of course, are sustained by the caissons or piers of larger diameter.

### *Controlling Engineering Properties*

In foundation problems offshore, as elsewhere, many physical characteristics of the near-surface sediments are of interest. Of these, shearing strength and scour resistance probably are most critical. All known cases of foundation failure in the Gulf of Mexico are attributable to one or both of these factors.

Some examples of types of failure are diagrammed in Figure 2. Although the manner of movement is different in each case, all failures illustrated are shearing failures. In Figure 2a, the combined effect of vertical and horizontal forces has caused a mobile platform to tilt; the foundation material beneath it sheared along the dotted path and heaved upward on one side. In Figure 2b, horizontal wind and wave forces have caused a mobile platform to slide horizontally; the frictional or shear resistance between the underside of the foundation barge and the sea floor was insufficient to resist these forces. This is probably the most common type of foundation problem, and movements ranging from several inches to 50 feet have been reported for the type of foundation illustrated (Rechtin, Steele, and Scales, 1957). Failure of a fixed platform by sinking or vertical displacement is illustrated in Figure 2c. A failure of this type results from inadequate skin friction between the piles and the supporting sediments; pile tests have shown that the unit skin-friction capacity of a sediment is approximately equal to its shearing strength.

In each case illustrated, particularly in the first two, failure would be encouraged and accelerated by scour or erosion of the near-surface foundation material. Significant ocean currents prevail at some offshore locations, and wave velocities at the ocean bottom are frequently high. Removal of supporting foundation material by these currents can occur at critical points, and this action frequently coincides with heavy storm loads on the structure. Shearing stresses in the remaining foundation sediments increase sharply as erosion progresses. Many occurrences of severe scour have been observed, and several have been associated with sliding or overturning of important structures.

The above examples illustrate the controlling influence of shearing strength and scour resistance of foundation materials on structural stability. Foundation investigations offshore are therefore directed toward the discovery of erodable and therefore objectionable near-surface sediments and toward the determination of the shear strength of sediments throughout the possible foundation depth range.

### *Investigational Procedures*

The physical properties of shelf deposits are investigated by conventional procedures, adapted from methods used on land. Relatively undisturbed samples are obtained with a thin-wall Shelby tube or piston sampler and tested intensively. The thickness of the section to be sampled ranges from 60 to 400 feet and is determined by the type of platform to be used, as well as the nature of the foundation.

Shear strength is, of course, one of the prime concerns of the laboratory investigations. Numerous procedures are used, each attempting to duplicate a condition in the field. For clays, the simplest and most common procedure is the unconfined compression test in which a cylindrical specimen is subjected to an increasing axial load until failure (Pl. 2, fig. 2

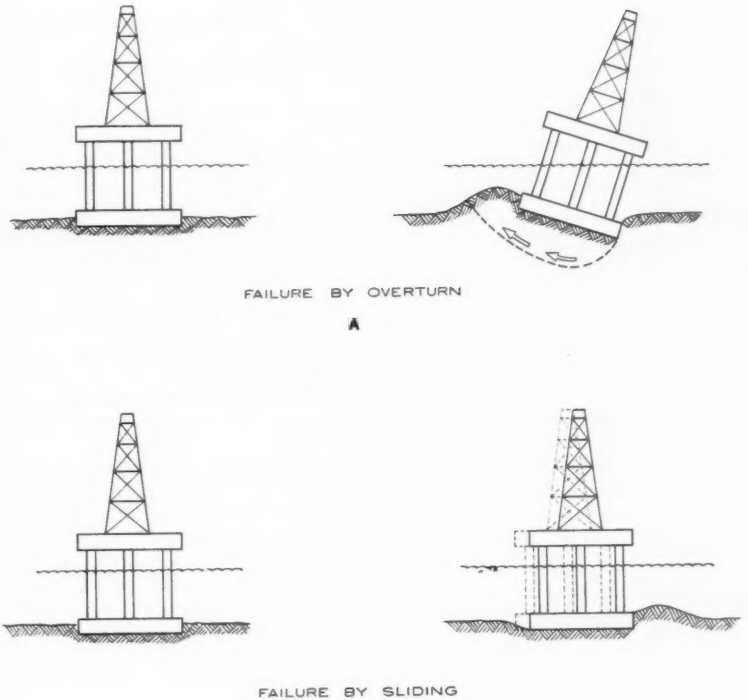


FIGURE 2.—TYPES OF FOUNDATION FAILURES OF OFFSHORE DRILLING STRUCTURES

The shear strength, or cohesion, of the specimen is half its observed compressive strength. In another compression test, called triaxial shear, similar specimens are confined laterally by controlled pressures applied through a rubber membrane to simulate stresses *in situ* (Pl. 2, fig. 1). Strength characteristics for near-surface samples too soft for satisfactory performance in the unconfined or triaxial compression tests are obtained by testing with a small vane. In this test, a four-blade vane, about ¾ inch long and ¾ inch in diameter, is inserted into the sample in the sampling tube. The vane is then rotated by a small shaft attached at its axis. The average shear strength over the cylindrical surface ruptured by the rotating vane is computed from the observed torque required to produce rotation.

In each type of shear test, specimens may be undisturbed or may be completely remolded at natural water content, depending on the purpose of the test. For simplicity, results only of unconfined compression tests on undisturbed samples are presented in this paper. Supplementary tests to interpret results of shear-strength tests, and which also help to relate strength variations to geologic history, include determinations of water content, density, grain-size distribution, and plastic and liquid limits.

Direct tests to determine scour resistance or to aid in predicting the amount of scour are not made. It is known, of course, that sands and other cohesionless materials erode more easily than do clay sediments, and that some general relationship exists between the particle size and the minimum water velocity that will "float" and transport sediment. No quantitative test or design procedures have been established, however, to cope with the many variables that relate to this problem. Conservative design must assume that either sand or soft clay at the ocean floor will be scoured severely by high water velocities, particularly around obstructions to water flow such as foundation hulls or piles. This requires that the presence of erodable materials be anticipated on the basis of geological data or be discovered by exploratory borings. The most promising design approach with respect to this hazard is the accumulation of field experience, correlated with adequate description of sediments involved.

## Continental-Shelf Deposits

### *General Description*

Near-surface deposits underlying the Continental Shelf off Louisiana form a gulfward thickening wedge which rests upon a deeply eroded and weathered surface. The wedge deposits are a gradational sequence having a topstratum of relatively unconsolidated silts and clays, with local incorporated sand bodies, and a substratum of sands and gravels. The sequence of deposits is well known onshore, and many data are available for the near-shore shelf area. Information from areas covered with more than 100 feet of water is limited to data from scattered borings and gulf-floor samples and from local seismic and sonic surveys.

The principal foundation for offshore structures is the topstratum, but where this upper layer is thin the foundation is provided by the substratum or, in its absence, by the firm materials of the weathered older deposits (Fig. 3). The topstratum clays are divided into soft, firm, and stiff zones by lines of equal cohesive shear strength. These divisions (Fig. 3) are generalizations based upon hundreds of strength tests on undisturbed samples from the cross-section borings.

Variations in thickness of the shelf deposits reflect irregularities in the underlying erosional surface and the effects of structural downwarping of the shelf. Entrenched valley systems of the Mississippi River and of minor streams have been mapped on the buried erosion surface. The Mississippi Trench has been traced from its onshore position near Timbalier Island across the shelf to the Submarine Canyon by geophysical means (Osterhoudt, 1946) and by borings (Fisk and McFarlan, 1955); minor stream trenches on the shelf are known only in near-shore areas. The axis of the buried Mississippi Trench is followed closely by the axis of structural downwarping. The amount of downwarping increases seaward along the axis to approximately 500 feet at the shelf margin near the canyon (Fisk and McFarlan, 1955), and the section of near-surface deposits is abnormally thick in this area. Substratum sands and gravels in the trench are more than 400 feet thick, and the topstratum at the shelf margin in the vicinity of the modern birdfoot delta reaches a known thickness of 700 feet. Both units thin toward the eastern and western margins of the Louisiana shelf

FIGURE 3.—CROSS SECTION OF NEAR-SURFACE SHELF DEPOSITS ALONG LINE APPROXIMATELY PARALLEL TO LOUISIANA SHORE

where the effects of downwarping are less pronounced (Fig. 3).

Characteristics of the shelf topography are directly related to the nature and thickness of underlying deposits. A series of east-trending irregular gulf-floor ridges is present seaward from Sabine Bank in the western part of the region where the topstratum is very thin. Each ridge surface commonly exhibits 5–10 feet of local relief, and its seaward margin is a linear zone of steeper slope which in some places connects a number of irregular ridge elements to establish the east–west trend. The zones of steeper slope are 10–30 feet high and are similar to the modern shore-face zone of Grand Isle, Timbalier Island, or the arc of Chandeleur Islands. The ridges disappear eastward beneath the thick topstratum deposits offshore from the deltaic plain. In this region the shelf surface is comparatively smooth but is marked by broad terraces with gently sloping platforms and steeper arcuate frontal zones bowed in a seaward direction. The best developed submarine terraces lie close to sea level offshore from Timbalier Island and Marsh Island. In this area, the 30-foot bottom contour lies almost 30 miles seaward of its normal near-shore position and outlines three lobate terraces with shoal platforms, each with an arcuate steep frontal zone. The terrace platforms include Tiger and Trinity shoals on the west, offshore from Marsh Island; Ship Shoal on the east, offshore from Timbalier Island; and unnamed shoals off Atchafalaya Bay. The gulf-floor terraces become progressively less well defined with distance offshore; in the deeper shelf waters in the vicinity of the Submarine Canyon, the platforms are obscured, and their positions are marked mainly by local arcuate zones of steeper slope.

### *Facies of Shelf Deposits*

Studies by Fisk and McFarlan (1955) have indicated the general character of the shelf deposits off Louisiana and the nature of the environments in which they accumulated. The substratum consists of fluviatile and strand-plain facies; the topstratum is a complex of facies laid down in deltaic and marginal-deltaic shelf environments. Fluviatile sands and gravels are localized in entrenched stream valleys and hold wood fragments. They grade both laterally and upward into marine strand-plain deposits containing typical beach mollusks, weathered and eroded shell fragments, and a few slabs of cemented beach rock.

The great bulk of deltaic sediments accumulates in the prodelta marine environments—i.e. the delta front and the deeper gulf floor surrounding the delta front. A relatively small proportion of the deltaic sediment is deposited in the near-sea-level complex of brackish-marine deltaic-plain environments, which include marshes, lakes and bays, beaches, and marginal islands. Sedimentary features and the presence of plant and animal remains are important in establishing the environment of deposition. The depth of water under which various facies accumulated can be determined by the dominance of diagnostic genera in the foraminiferal assemblages (Lowman, 1949).

Marsh deposits of the delta plain consist largely of massive silty clays containing roots and local peat beds. They also incorporate beds of oyster shells which accumulate in shallow-water bodies within the marshes. In contrast to marsh deposits, sediments laid down in lakes and bays of the deltaic plain are generally well bedded, and some are delicately laminated with alternating organic-rich silty clays and silty sands (Pl. 3, fig. 1). They also contain wood fragments, beds of oyster shells, and scattered invertebrate remains. The sparse foraminiferal assemblage in the deltaic-plain sediments is dominated by the arenaceous genus *Ammobaculites*. Sandy littoral facies of beaches and offshore bars are characterized by a mixed assemblage of Foraminifera and molluscan shells and are typically finely laminated (Pl. 3, fig. 2).

Shallow delta-front facies of the inner-neritic zone, deposited in less than 60 feet of water, are made up largely of massive silty clays. Portions of these deposits laid down in very shallow water contain sand lenses and silty sand laminae (Pl. 3, figs. 3, 4). The delta-front deposits include a sparse foraminiferal assemblage dominated by *Elphidium* and *Rotalia* and are characterized by wood fragments and disseminated carbonized plant remains. Inner-neritic-zone deposits of the shelf contain fewer wood fragments and more numerous lenses of silty sand. Shelf facies of the deeper mid-neritic zone, deposited in water between 60 and 250 feet deep, contain little or no plant remains and are characterized by delicate laminations (Pl. 4, fig. 1). The foraminiferal fauna in these beds is dominated by *Cibicides*, *Eponides*, *Nonion*, *Quinqueloculina*, and *Textularia*.

In the mid-neritic waters of the prodelta zone, plant remains are also scarce; the clays are more massive than those deposited in

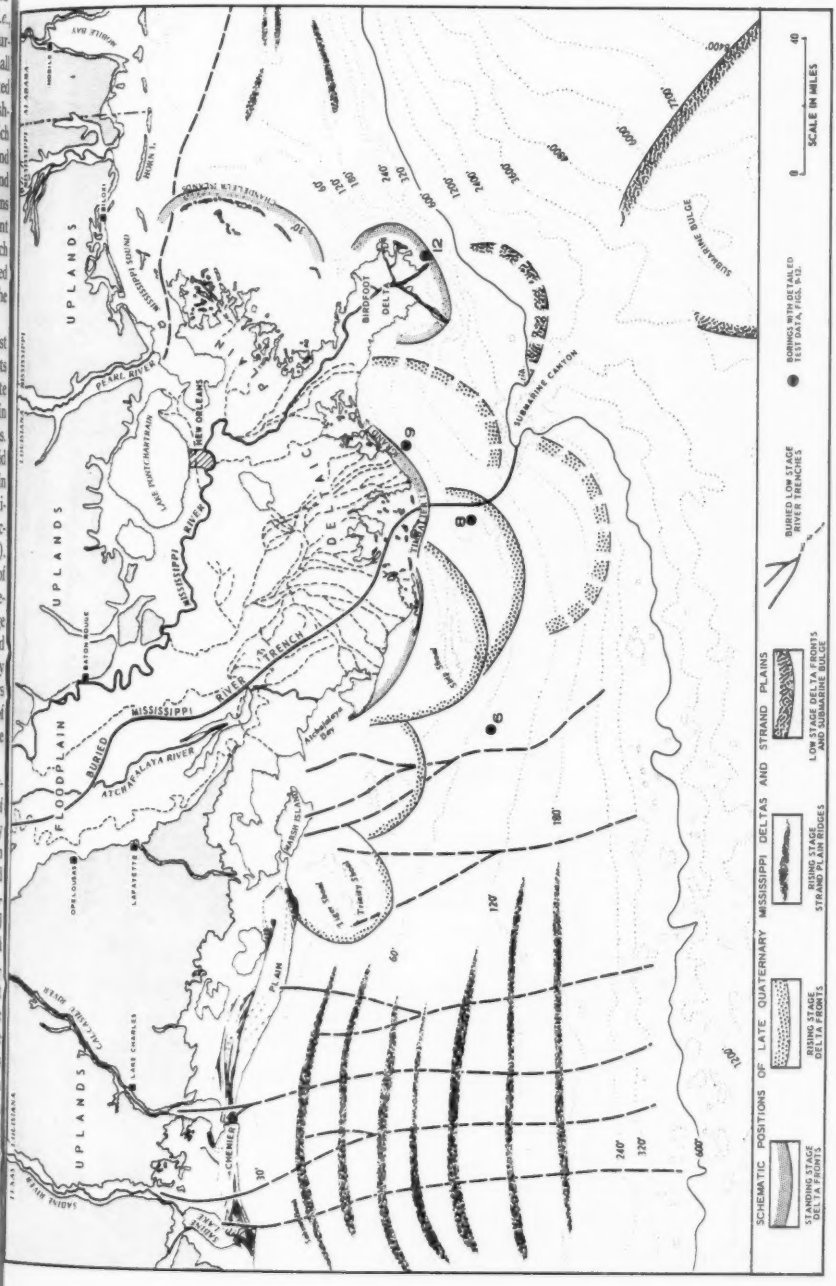


FIGURE 4.—POSITIONS OF LATE QUATERNARY BURIED TRENCHES, STRAND PLAINS, AND DELTAS OFF LOUISIANA COAST

shallower waters, and they are characterized by scattered small thin-shelled mollusks (Pl. 4, fig. 2). Both shelf and prodelta facies of the outer-neritic zone, deposited in water more than 250 feet deep, are massive clays with faint laminations (Pl. 4, fig. 3). A foraminiferal assemblage dominated by *Bolivina*, *Bulimina*, and *Uvigerina* characterizes these beds; scaphopods, echinoids, and thin-shelled pelecypods are also present.

Clay minerals in the various facies provide information as to the source of the deposits. The Mississippi River carries an assemblage of clay-sized minerals in which montmorillonite dominates, and muscovite (illite?), kaolinite, quartz, and feldspar are present. The Red River carries a similar clay-sized suite of minerals, in which kaolinite or muscovite (illite?) is dominant, and montmorillonite, quartz, feldspar, chlorite, and dolomite also occur. The Atchafalaya River, which carries a mixture of Mississippi and Red River waters, transports a mixed assemblage of clay minerals, including chlorite, to the gulf.

The weathered materials mantling the buried erosional surface are from a few inches to more than 50 feet thick. They consist typically of oxidized brown to yellow clays or reddish-brown sands and bear secondary calcium-carbonate nodules near the base of the zone. Original sedimentary structures, such as bedding, are largely destroyed (Pl. 4, fig. 4).

### *Age and Development of the Shelf Deposits*

The changing facies of shelf deposits penetrated in borings and the relationship of the facies to gulf-floor topography provide a basis for interpreting the development of the shelf region. These data, plus a knowledge of processes active in the development and destruction of deltas, make it possible to predict the nature and distribution of foundation materials in areas of no drilling.

The gradational sequence of topstratum and substratum shelf deposits and the eroded and weathered surface on which they rest provide a record of a cyclic change in sea level. The lowering of the sea which initiated the cycle and brought about stream erosion of the shelf is thought to have started approximately 80,000 years ago. Radiocarbon dates indicate that the subsequent rise in sea level and deposition of the substratum and topstratum deposits began at least 40,000 years ago (McFarlan, 1955). They also show that the final part of the cycle, that of standing sea level, began about 5000 years ago. The cycle is correlated with events of the last climatic cycle of the Quaternary period, and the shelf deposits are therefore considered to be of late Quaternary age (Fisk and McFarlan, 1955).

During the early stage of the late Quaternary cycle when the Pleistocene climates became colder, sea level was lowered approximately 450 feet by the withdrawal of water required to nourish the expanding Wisconsin-stage glaciers. Gulf-coast streams then eroded their valleys across the shelf as its exposed area was progressively increased (Fig. 4). The increase in stream gradients resulting from the lowering of stream base level permitted the rivers to transport sands and gravels to the shore line. At the time of maximum lowering of the sea, about 40,000 years ago, the delta of the Mississippi was located in the vicinity of the Submarine Canyon. Structural downwarping has depressed this area so that the low-stage delta location, marked by local flattening of the gulf-floor slope, lies seaward of the 600-foot contour. The original arcuate frontal zone of this delta is schematically shown on Figure 4 and is marked by a zone of steeper gulf-floor slope. A portion of the

PLATE 1.—SELF-CONTAINED MULTIPLE-WELL DRILLING STRUCTURE WITH HELICOPTER PLATFORM, GRAND ISLE AREA

Block 18 field, 8 miles offshore from Grand Isle, Louisiana. (Photograph courtesy Humble Oil & Refining Company)

PLATE 2.—LABORATORY TESTS FOR DETERMINATION OF THE SHEARING STRENGTH OF CLAYS

Photographs courtesy McClelland Engineers, Inc.

FIGURE 1.—Triaxial shear test, in which lateral pressure is applied to the sample to simulate *in situ* earth pressures

FIGURE 2.—Unconfined compression test

SELF-CONTAINED MULTIPLE-WELL DRILLING STRUCTURE WITH HELICOPTER PLATFORM, GRAND ISLE AREA

FIGURE 1

FIGURE 2

FIGURE 3

FIGURE 4

UNDISTURBED CORES OF DELTAIC FACIES FROM LATE QUATERNARY SHELF DEPOSITS

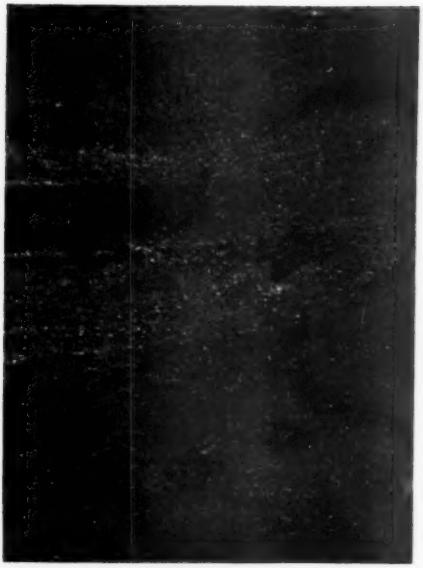

FIGURE 1

FIGURE 2

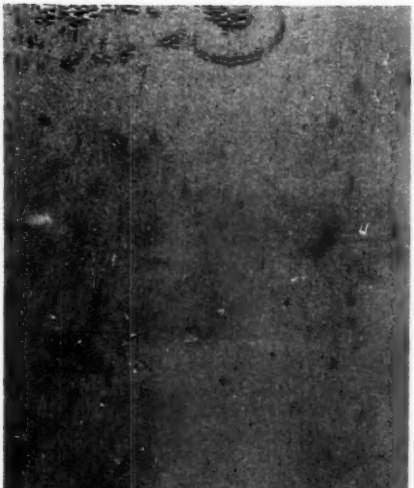

FIGURE 3

FIGURE 4

UNDISTURBED CORES OF SHELF AND PRODELTA FACIES, AND THE WEATHERED ZONE FROM LATE QUATERNARY SHELF DEPOSITS

Mississippi's load was swept down the Continental Slope by submarine currents during the time of lowering sea level. The Submarine Canyon was eroded by the sediment-laden currents (Bates, 1953), and the sediments settled around the mouth of the canyon to form the Submarine Bulge on the deep gulf floor (Fig. 4). These processes continued during the early stages of rising sea level.

Stream entrenchment during the early phase of the late Quaternary cycle was accompanied by a lowering of the ground-water table. As a result, late Pleistocene strata at the exposed shelf surface were desiccated, leached, and oxidized to form the weathered zone. These processes destroyed original sedimentary structures and brought about a concentration of calcium-carbonate nodules near the base of the weathered zone.

Warming of the Pleistocene climate during the middle of the cycle returned meltwaters to the ocean basins, raised sea level, and brought about a progressive decrease in the gradients and carrying capacities of streams. As a result, the gradational sequence of topstratum and substratum deposits gradually developed, filling the erosional valley systems and blanketing the interfluves. Some of the sands which reached the gulf floor throughout the epoch of rising sea level were swept laterally by longshore currents and were deposited as strand plains. The east-trending gulf-floor ridges at the eastern and western margins of the Louisiana shelf are directly related to the original strand-plain topography (Fig. 4).

Deltaic sedimentation of the Mississippi could not keep pace with the rise in sea level, and a series of retreatal deltas was constructed on the shelf. Terraces on the gulf floor above the 600-foot contour indicate the probable locations of some of these deltas; zones of steeper slope marking delta fronts are shown diagrammatically on Figure 4. After each delta was abandoned, it was subjected to wave erosion as it subsided, and a part of its surface section of deposits was removed. As the eroded surface became more deeply submerged, it became mantled by prodelta gulf-floor deposits of younger deltas. In the early stages of rising sea level, the Mississippi River was closely confined by its trench, and its deltas were built outward onto the gulf floor just beyond the trench mouth. As sea level continued to rise, the Mississippi Trench was progressively filled, and its ability to confine the river was gradually lost. Stream deltas were distributed over a progressively wider area along the shore, as may be seen by the location of delta fronts on Figure 4. The arcuate frontal zones of the three shoal areas offshore from Timbalier Island and Marsh Island indicate the position of deltas that were abandoned by the river just prior to the time of standing level. The westernmost of these, at Tiger and Trinity

PLATE 3.—UNDISTURBED CORES OF DELTAIC FACIES FROM LATE QUATERNARY SHELF DEPOSITS

FIGURE 1.—Laminated lake or bay deposits of organic-rich dark clays and light-gray silts; 227 feet below sea level, Grand Isle Area, Block 23 (*See* log, Fig. 10)

FIGURE 2.—Laminated beach sands; 121 feet below sea level, South Timbalier Area, Block 54 (*See* log, Fig. 12)

FIGURE 3.—Shallow inner-neritic delta-front clay with carbonized plant remains; 77 feet below sea level, South Timbalier Area, Block 54 (*See* log, Fig. 12)

FIGURE 4.—Shallow inner-neritic delta-front clays with lentils of silty sand; 230 feet below sea level, South Timbalier Area, Block 54 (*See* log, Fig. 12)

PLATE 4.—UNDISTURBED CORES OF SHELF AND PRODELTA FACIES, AND THE WEATHERED ZONE FROM LATE QUATERNARY SHELF DEPOSITS

FIGURE 1.—Mid-neritic shelf clays with delicate laminations; Modern gulf floor, 70 feet below sea level, Eugene Island Area, Block 188 (*See* log, Fig. 9)

FIGURE 2.—Mid-neritic prodelta massive clays with organic specks; 325 feet below sea level, South Pass Area, Block 20 (*See* log, Fig. 11)

FIGURE 3.—Outer-neritic prodelta massive clays with small mollusks and minor silt lenses; 385 feet below sea level, South Pass Area, Block 20 (*See* log, Fig. 11)

FIGURE 4.—Weathered-zone materials; 169 feet below sea level, Eugene Island Area, Block 188 (*See* log, Fig. 9)

shoals, is farther from the Mississippi Trench than any other delta of the river.

The middle phase of the cycle began to develop about 40,000 years ago, and by 10,000 years ago the sea had risen to within 100 feet of its present level (McFarlan, 1955). The well-defined near-shore abandoned and submerged delta surfaces were formed between 10,000 and 5000 years ago when the rise in sea level halted.

The late phase of the cycle, characterized by relative stability of climates and sea level, began when the sea reached its present level about 5000 years ago. The Mississippi delta was then located in the vicinity of Marsh Island. The gulf shore line west of the delta lay along the inner margin of the chenier plain; east of the delta it closely followed the upland margin, inland from New Orleans. The Mississippi River has subsequently changed its course several times and has constructed and abandoned several deltas to form the broad Mississippi deltaic plain (Fig. 1). The last change in the course of the river occurred near New Orleans and has resulted in the development of the modern birdfoot delta. This is the only delta within the deltaic plain that has been constructed in deep water near the shelf margin. It began to form approximately 450 years ago (Fisk *et al.*, 1954). While the deltaic plain has been developing, marginal deltaic sedimentation has created the chenier plain on the west. Oak-covered abandoned beach ridges (cheniers) mark stages in the development of this plain.

Although the topstratum consists chiefly of clays and silts, included sand bodies serve locally as foundation materials. Some of the sands bear a direct relationship to depositional processes in delta building. The sand load of the Mississippi that reaches the birdfoot delta consists of fine to very fine sands and is deposited largely on distributary-mouth bars. The mass of the sand bars compacts and displaces the underlying silty clays of the delta platform, and the bars settle as they accumulate. As a consequence of bar building and seaward lengthening of the passes, long and narrow "sand fingers" have developed (Fig. 3) beneath the distributaries to a thickness of approximately 250 feet (Fisk *et al.*, 1954). Earlier formed deltas within the Mississippi deltaic plain were constructed in shallower gulf waters than the modern birdfoot delta, and their growth was more rapid. Sands accumulated in thin widespread sheets at the periphery of an advancing delta, rather than in fingers (Fisk, 1955). The sheet sands contain scattered mollusks typical of those living on sandy near-shore bottoms. They grade upward into typical marsh deposits and downward into prodelta gulf-bottom silts and clays containing wood fragments.

Other sand bodies develop as a result of the destruction of deltas and the redistribution of the delta-plain sands. After each delta is abandoned by the Mississippi and substantial quantities of river-borne sediment no longer reach it, compaction of marsh sediments combines with regional subsidence to lower the marshland plain. Water bodies, such as tidal channels, lakes, and bays, enlarge and gradually destroy the seaward margin of the deltaic lands. Sands derived from the destruction of the marshland are swept seaward to accumulate as delta-margin islands marking the original delta front (Fisk, 1955). Typical of these deposits is Grand Isle, marginal to the abandoned Lafourche-Mississippi delta south of New Orleans (Fig. 4). Borings indicate that the accumulating sands compact the underlying silts and clays, and thicknesses are greatly in excess of the depth of water in which they are deposited.

The frayed seaward margin of the Lafourche-Mississippi delta is typical of an early stage of marshland deterioration. More extensive destruction of the deltaic plain is illustrated by long-continued subsidence of the La Loutre-Mississippi delta to form Chandeleur Sound, east of New Orleans. The arc of the Chandeleur Islands, 25–50 miles offshore, probably was formed in the same manner as Grand Isle. The location of the island sand bodies marks the approximate location of the old La Loutre-Mississippi delta front.

## Foundation Characteristics of the Shelf Deposits

In evaluating the engineering characteristics of the shelf deposits, the individual needs of mobile and fixed offshore platforms must be considered. The near-surface beds provide the support for mobile structures, and the characteristics of these beds determine foundation performance. Fixed platforms are not supported entirely by near-surface deposits because part of their loads are transferred to deeper sediments. Characteristics of the shelf sediments to relatively great depths are important and may affect piling penetrations and in this way relate to costs of fixed structures. The foundation engineer is interested in the

character and thickness of the topstratum and the character of the substratum and Pleistocene beds where these underlie the topstratum at a shallow depth.

The topstratum blankets the entire shelf and can be divided into four principal units (Fig. 5), distinguished on the basis of thickness (greater or less than 50 feet) and on the presence or absence of sand beds in the upper part of the section. Each unit thus occupies a broad area of the shelf.

The two topstratum units thicker than 50 feet are located offshore from the Mississippi deltaic plain; that containing near-surface sands lies inshore and grades seaward into the sand-free unit. The two units less than 50 feet thick occur in the eastern and western portions of the shelf where little offshore drilling has been conducted. Comparatively little is known about their characteristics except in near-shore areas. The thin units are important from the standpoint of foundations because, where they occur, the substratum sand or the weathered zone is present at a shallow depth.

The topstratum unit, greater than 50 feet thick and sand-bearing, forms a belt around the deltaic plain. It is more than 200 feet thick on the west, in the area of Ship Shoal and Trinity Shoal, and thickens to an average of 400 feet around the margin of the birdfoot delta. It thins rapidly to approximately 100 feet on the eastern side of the deltaic plain in the vicinity of the Chandeleur Islands. The sand bodies in this unit vary both in extent and thickness. Sand fingers of the modern birdfoot delta are narrow and thick, whereas in older deltaic deposits the sands form widespread sheets, generally less than 50 feet thick, and lenticular bar deposits.

The sand-free topstratum unit greater than 50 feet thick occupies the outer part of the shelf off the deltaic plain. Its greatest thickness is offshore from the modern birdfoot delta where 700 feet of massive silts and clays has been penetrated. The unit probably reaches its greatest thickness along the shelf margin in the vicinity of the Submarine Canyon. Inland from the head of the canyon, this topstratum unit mantles early rising-stage delta-front and prodelta deposits of the Mississippi. Sands, if present, are at depths of more than 100 feet beneath the gulf floor.

The thin sand-free topstratum unit is widely distributed offshore from the chenier plain where it covers approximately one-fourth the area of the Louisiana shelf. It gradually thickens from less than 10 feet near shore to a postulated thickness of more than 50 feet near the shelf margin. Throughout this area it rests upon the eroded Pleistocene surface or, locally, upon substratum sands. This unit is also present in a smaller area east of the Chandeleur Islands, where it is less than 10 feet thick offshore in waters approximately 200 feet deep.

The sand and clay unit less than 50 feet thick is made up of sands, silty sands, and silty clays. It occurs in the vicinity of Sabine Bank on the west and offshore from the Chandeleur Islands on the east.

In the thick sand-free unit, deep foundation-bearing piles are usually required. Such piles derive their support from skin friction unless the pile top develops end-bearing resistance in a substantial sand body. Such a condition is seldom encountered in this unit at less than 100-foot penetrations. If a deep sand is not encountered, safe pile penetrations depend upon the shear strengths of the clay sediments; these strengths vary widely within the unit, as revealed by the lines of equal cohesion shown on Figure 3. The bearing capacity of near-surface sediments is very low, so that foundation conditions are poor for mobile platforms supported either by near-surface footings or by short caissons.

In the thick unit with near-surface sands, deep piles are also required in most cases. Large-diameter caissons may receive substantial end-bearing support from shallow sands in the unit, but bearing piles with smaller diameters frequently punch through such sands. If so, the piles derive their support either from skin friction or from end bearing in a deeper sand. Locally, the near-surface clays of this unit offer more substantial bearing support than elsewhere because marine erosion has removed the shallow, softest part of the deposit.

The two topstratum units less than 50 feet thick provide the most favorable foundation conditions for both fixed-pile structures and for mobile platforms having pier foundations capable of moderate penetrations. This is particulary true in near-shore areas where the topstratum is underlain at a shallow depth either by substratum sands and gravels or by the stiffer materials of the late Pleistocene weathered zone. Surface-bearing capacities, of importance to mobile structures with foundation barges, are low except where the topstratum contains sand.

Low resistance to scour must be anticipated in both topstratum units that contain near-surface sands. This is also true in the areas of

UPLANDS
FLOODPLAIN
DELTAIC PLAIN
ABANDONED MISSISSIPPI RIVER COURSES AND INTERDISTRIBUTARY BASINS ON DELTAIC PLAIN
ABANDONED BEACH RIDGES
CHENIER PLAIN
MISSISSIPPI CANYON
LINE OF SECTION FIGURE 5
CONTINENTAL SHELF TOPSTRATUM DEPOSITS (MODIFIED AFTER FISK, 1960)
CLAYS AND SILTS WITH SANDS NEAR SURFACE (<30 FT.) THICK
CLAYS AND SILTS (<30 FT.) THICK
SANDS AND CLAYS (<30 FT.) THICK
OFFSHORE WELLS
TEST BORINGS ON FIGURE 3
BORINGS WITH DETAILED TEST DATA, FIGS. 4-10
SCALE IN MILES

very soft near-surface clay sediments in that part of the thick topstratum unit which forms the seaward margin of the birdfoot delta (Fig. 3).

## Engineering-Geology Relationships

### *Typical Strength Profiles of Clay Sediments*

A deposit of relatively uniform clay-sized particles laid down in water and with its volume fully adjusted at all depths to the pressure of the overlying material is "normally consolidated." Its strength is approximately a linear function of the overburden pressure, and its cohesion varies with depth (Fig. 6a). Even at zero depth, however, the clays have a small cohesion derived from colloidal attraction between particles. This minimum cohesion has a value of about 0.05 ton per square foot (Terzaghi, 1956).

Modifications from the normally consolidated strength pattern can be produced by a number of geologic processes. One of the most easily recognized pattern variations is the increase in strength which results from desiccation, as at the surface of Pleistocene marine clays which were exposed to weathering during sea-level lowering in the late Quaternary cycle. As water contents were reduced by drainage and by evaporation, the exposed Pleistocene clays consolidated by shrinking and gained in strength. The modified strength profile was then approximately as illustrated by Figure 6b. Subsequent resubmergence does not materially alter the profile because consolidation produced by desiccation can be only partly reversed by swelling. The Pleistocene strata that have been so stiffened or strengthened are readily recognizable; the process of desiccation was accompanied by oxidation of all organic matter, and the clays were altered from dark gray to yellow, red, or brown.

Significant modifications of the normally consolidated strength profile can also occur in clays that have remained submerged. Such effects can result either from marine planation of near-surface sediments or from very rapid deposition of new sediment. As the process of consolidation is not fully reversible, stiffer clays that are unburdened by erosion of overlying sediment do not suffer appreciable loss of strength. An important area where such an occurrence has been recognized lies south of Timbalier Island, where pre-modern deltas of the Mississippi River once extended seaward of the present coast line (Fig. 4). After each delta was abandoned, the gulf transgressed its frontal zone, and wave action removed sediment. As a result, the strength of existing sediment in the eroded areas is appreciably greater than that of a normally consolidated clay and is described as being overconsolidated. A typical strength profile for marine sediments in an area which has experienced significant erosion is shown by Figure 6c.

If substantial thicknesses of new sediments are deposited quite rapidly, as for example near the mouths of passes of the modern Mississippi River, clay strengths remain very low for an extended period of time (Terzaghi, 1956). Strengths of underlying clay sediments will also respond very slowly to the increased overburden pressures. A strength profile resulting under such conditions is illustrated by Figure 6d. The depth of deposits of negligible strength in the modern birdfoot delta of the Mississippi River exceeds 250 feet (McClelland, 1956).

### *Effect of Clay Minerals on Sediment Strength*

Engineering properties of clay sediments have long been correlated with the Atterberg liquid and plastic limits—*i.e.*, the upper and lower limits of the water-content range within which the sediment behaves as a plastic. The difference in these two limits is called the plasticity index, or *PI*. Skempton (1953) has demonstrated that *PI* varies directly with the percentage of clay-sized minerals present for any given type or assemblage of clay minerals. The ratio of *PI* to the percentage of clay minerals present is called the activity ratio. Typical values of this ratio for different clay minerals are given in Figure 7, which indicates that the normal range of activity ratios for clay is bracketed by 0.75 to 1.25. Late Quaternary shelf clays off Louisiana fall within the normal activity range, and data form a 100-foot section of these clays are plotted on Figure 7 for comparison. An average line through the plotted points has a slope corresponding to the activity ratio of 0.90 which is shown by Skempton to be typical of illite. The clay minerals throughout this section represent a typical mixed Mississippi River–Red River assemblage: in order of decreasing abundance, montmorillonite, muscovite (illite?), quartz, feldspar, and chlorite.

The rate of strength increase with depth is an engineering property of clay sediment closely related to the plasticity index, and therefore to the type and abundance of clay minerals;

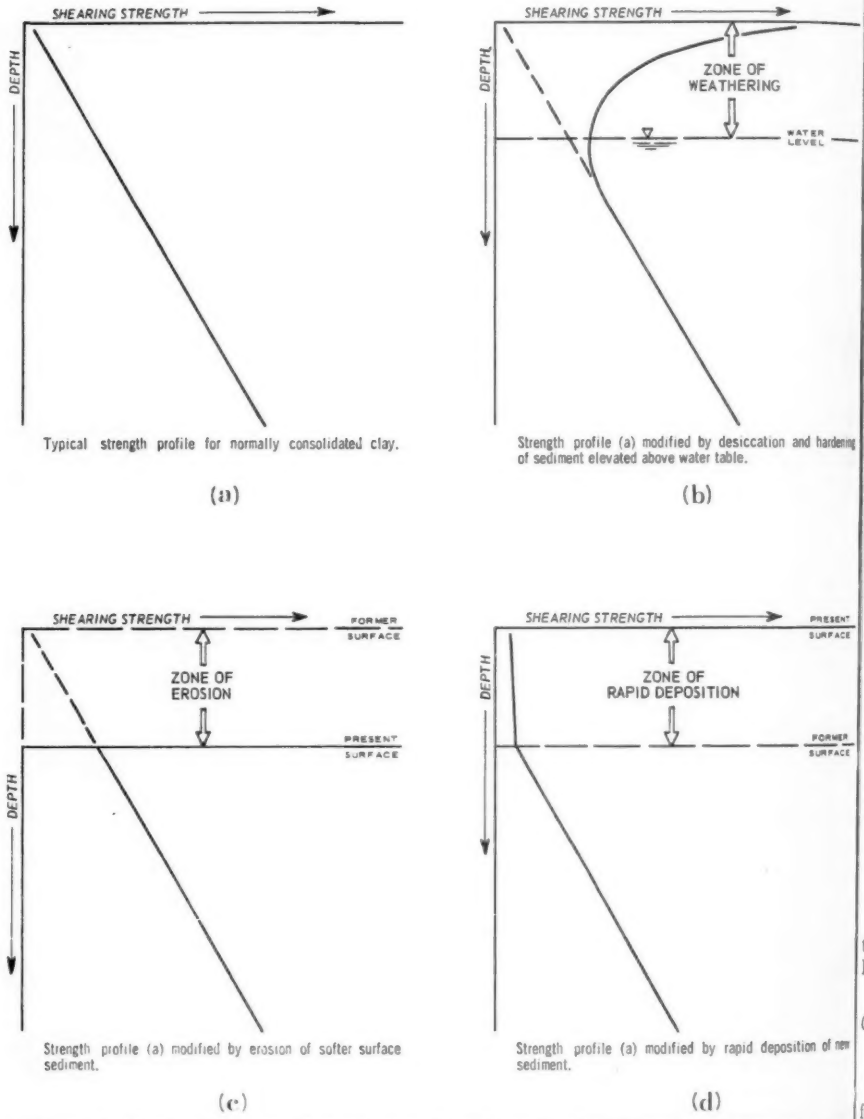


FIGURE 6.—TYPICAL STRENGTH PROFILES FOR CLAY DEPOSITS, ILLUSTRATING THE EFFECTS OF GEOLOGIC PROCESSES

it is expressed by the ratio $c/p$, where $c$ is cohesion, and $p$ the effective overburden pressure. Skempton (1948; 1953) and Bjerrum (1954) have shown that strength increases more rapidly with depth for clays with higher plasticity-index values, as indicated by the correlation of $c/p$ with $PI$ for normally consolidated clays (Fig. 8). Normally consolidated clays on the Louisiana shelf conform with the correlation. Data from a continuous section of

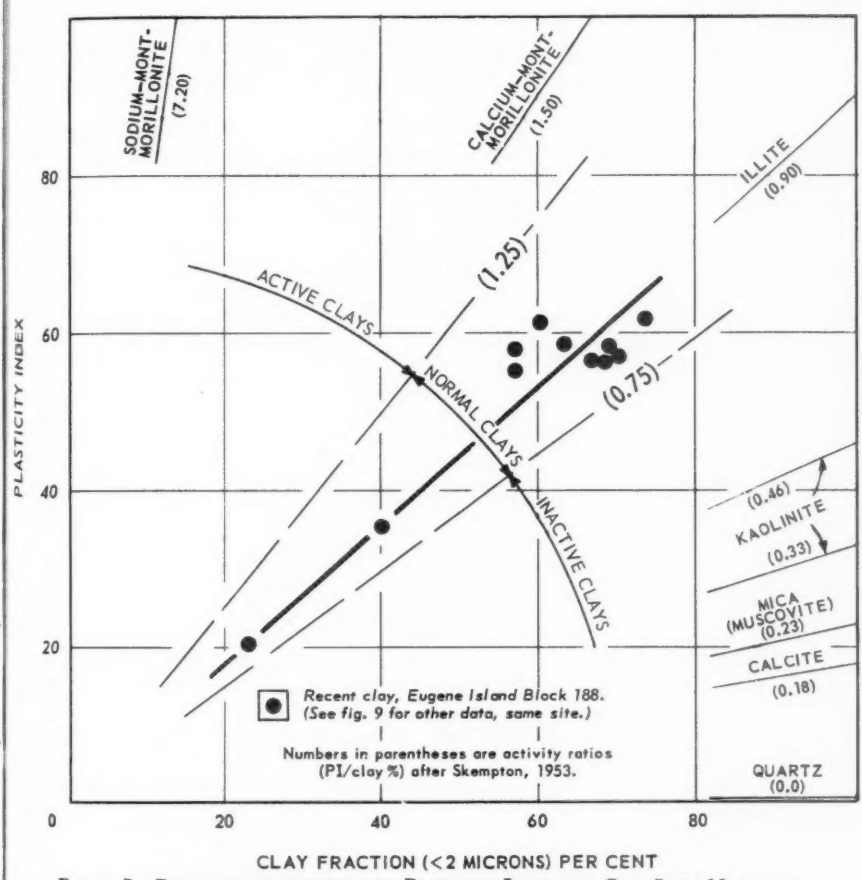


FIGURE 7.—RELATIONSHIP BETWEEN THE PLASTICITY INDEX AND CLAY-SIZED MINERALS
With data from Eugene Island Area, Block 188 boring

these clays are represented by a point on Figure 8.

*Correlation of Engineering and Geological Data at Specific Sites*

*General Statement.*—Undisturbed samples from four selected borings have been subjected to detailed engineering and geological tests. Results of these tests have been analyzed to develop more fully the engineering-geology relationships of shelf sediments. Particular attention was given to the clays which typify the following categories of strength variation with depth:

*Normally consolidated clays:* Deposits at equilibrium under existing overburden pressure and having linear increase in strength with depth.

*Underconsolidated clays, approaching the normal state of consolidation:* Deposits increasing in strength with depth, but more slowly than normally consolidated clays.

*Underconsolidated clays:* Recently and rapidly deposited sediments with very low rate of strength increase with depth.

*Overconsolidated clays:* Deposits consolidated under pressure greater than existing overburden pressure.

The undisturbed samples from each boring were analyzed for their clay mineralogy, their included fossils, and significant lithologic and

textural variations. These and other geological data were interpreted to establish the environments of deposition in which the sediments accumulated. The samples were also subjected

feet lower than at present. The location of the section with respect to rising-sea-level-stage Mississippi River delta fronts is shown on Figure 4. The deposits hold a mixed Mississippi

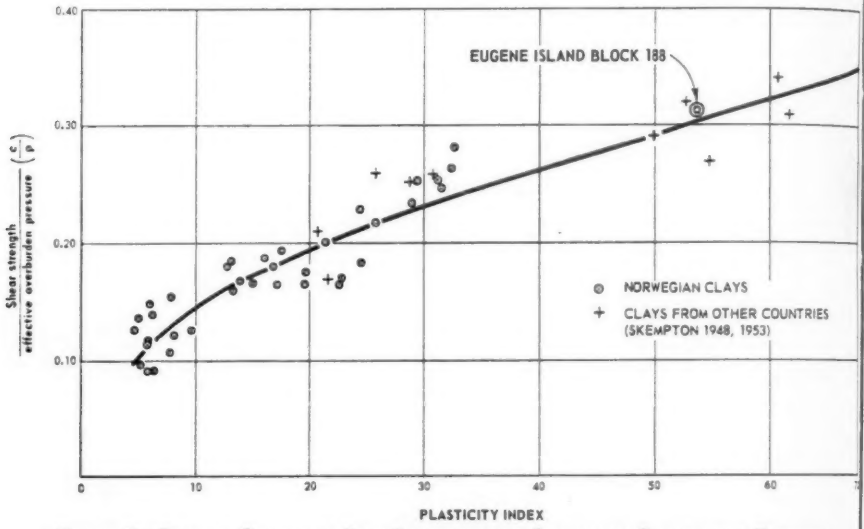


FIGURE 8.—RATE OF CHANGE IN CLAY STRENGTH WITH INCREASING OVERBURDEN PRESSURE
Data from Eugene Island Area, Block 188 boring compared with compilation by Bjerrum (1954)

to detailed laboratory tests to establish their engineering properties. These tests included determinations of strength, water content, plastic and liquid limits, and unit dry weight (density). Grain-size analyses were made to confirm visual classifications of the materials and to permit computation of activity ratios. The combined plots of the geologic and engineering characteristics of sediments penetrated in the borings are presented on Figures 9–12 These plots were prepared to facilitate comparison of the two types of information.

*Normally consolidated clay deposits.*—The upper 96 feet of the section of shelf deposits penetrated in a boring made at Eugene Island Block 188 (Fig. 9) typifies normally consolidated clays. This boring is 45 miles offshore in Atchafalaya Bay in 67 feet of water and was drilled to a depth of 249 feet below sea level. The normally consolidated section consists of massive gray clays and rests beneath a layer of modern gulf-floor clays less than 10 feet thick. It accumulated as prodelta gulf-floor deposits, beginning more than 10,000 years ago during the middle part of the late Quaternary cycle when the rising gulf waters were more than 100

River–Red River assemblage of clay minerals, and their uniformity indicates long-continued unvaried conditions of gulf-floor sedimentation.

The late Quaternary deposits rest upon the weathered late Pleistocene surface at a depth of 164 feet below sea level. The weathered zone is approximately 12 feet thick and appears to represent the basal part of a typical soil zone in which original sedimentary structures have been largely destroyed. The soils are oxidized to a red brown and contain nodules of secondary calcium carbonate (Pl. 4, fig. 4). The clay-mineral assemblage of the late Pleistocene deposits underlying the weathered zone differs from that of the late Quaternary beds. The tabulation (Fig. 9) indicates that muscovite (illite?), rather than montmorillonite, is the dominant mineral, and that kaolinite, quartz, and chlorite occur in smaller amounts.

The average-strength profile shown by the dotted line on the shear-strength plot on Figure 9 is typical of that of a normally consolidated clay deposit, as diagrammed in Figure 6a. The strength, as determined by unconfined compression tests, increases linearly with depth throughout the late Quaternary section. The

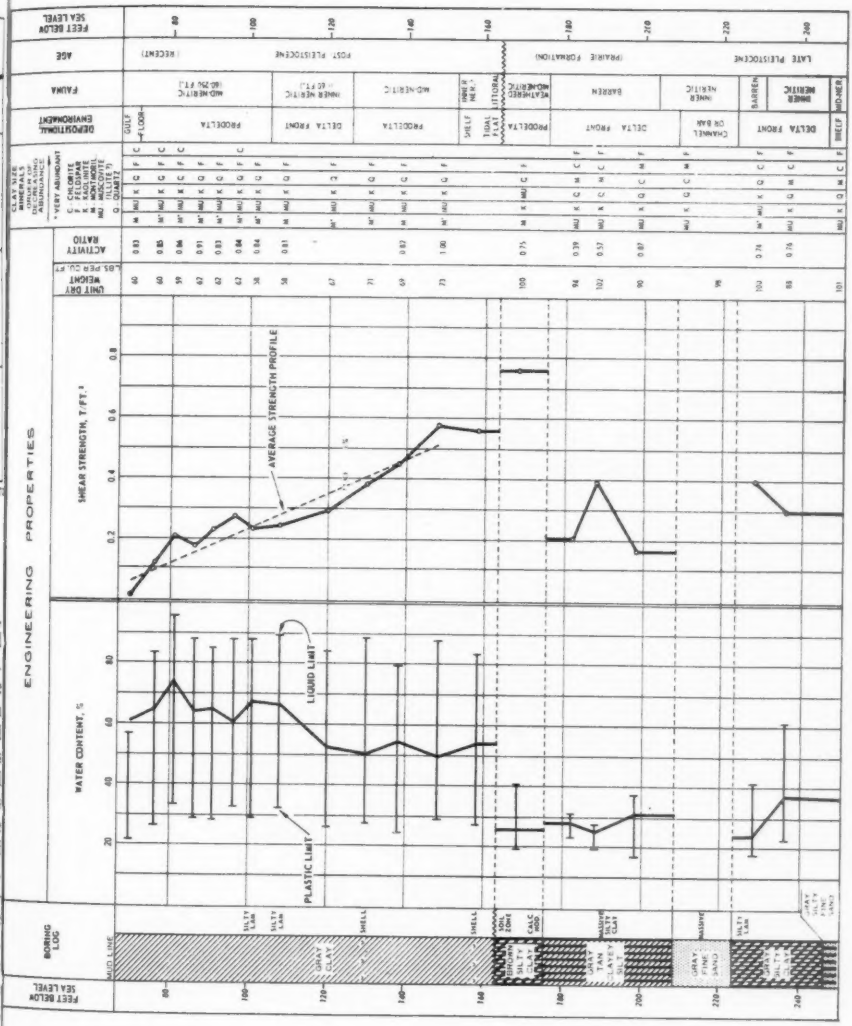
ENGINEERING PROPERTIES
SHEAR STRENGTH, T/FT.²
AVERAGE STRENGTH PROFILE
WATER CONTENT, %
LIQUID LIMIT
PLASTIC LIMIT
ACTIVITY RATIO
UNIT DRY WEIGHT
BORING LOG
MUD LINE
FEET BELOW SEA LEVEL
AGE
FAUNA
DEPOSITIONAL ENVIRONMENT
DELTA FRONT
PRODELTA
BARRIER
CHANNEL OR BAR
MARSH OR MUD FLAT
SHELF
BELFAST
MONTEREY
SALINAS
SAN LORENZO
SAN ANDREAS
SAN GREGORIO
SAN MATEO
SAN FRANCISCO
SAN JOAQUIN
SAN JOSE

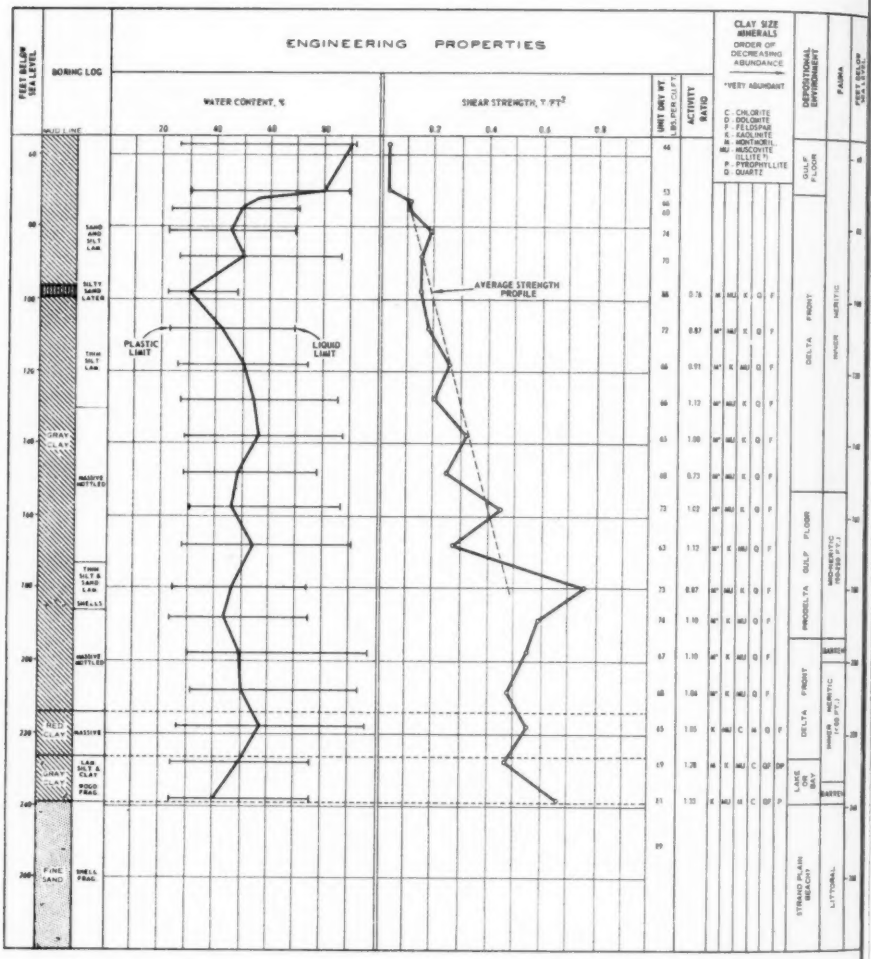


FIGURE 10.—ENGINEERING AND GEOLOGIC DATA FROM UNDISTURBED SAMPLES

Samples taken in Humble Oil & Refining Company foundation test boring No. 4, Grand Isle Area, Block 23. For location *see* Figure 1, boring 9.

average ratio between the shear-strength value ($c$) and effective overburden pressure ($p$), as computed from the unit dry weights, is 0.31; the average plasticity index is 53. These values agree closely with the correlation developed by Skempton (1953) and Bjerrum (1954) (Fig. 8). This correlation and the linear-strength increase confirm the fact that the topstratum is fully consolidated under existing overburden pressure, except for the thin layer of gulf-floor clays at the mud line.

A sharp increase in strength at a depth of 164 feet below sea level clearly marks the top of the weathered surface of the late Pleistocene formation. Other physical properties which accompany this strength change at the weathered surface include a notable increase in unit dry weight and a sharp decrease in water content. These characteristics all reflect the exposure of the shelf which occurred in the early stage of the late Quaternary cycle and the consequent desiccation of the late Pleistocene.

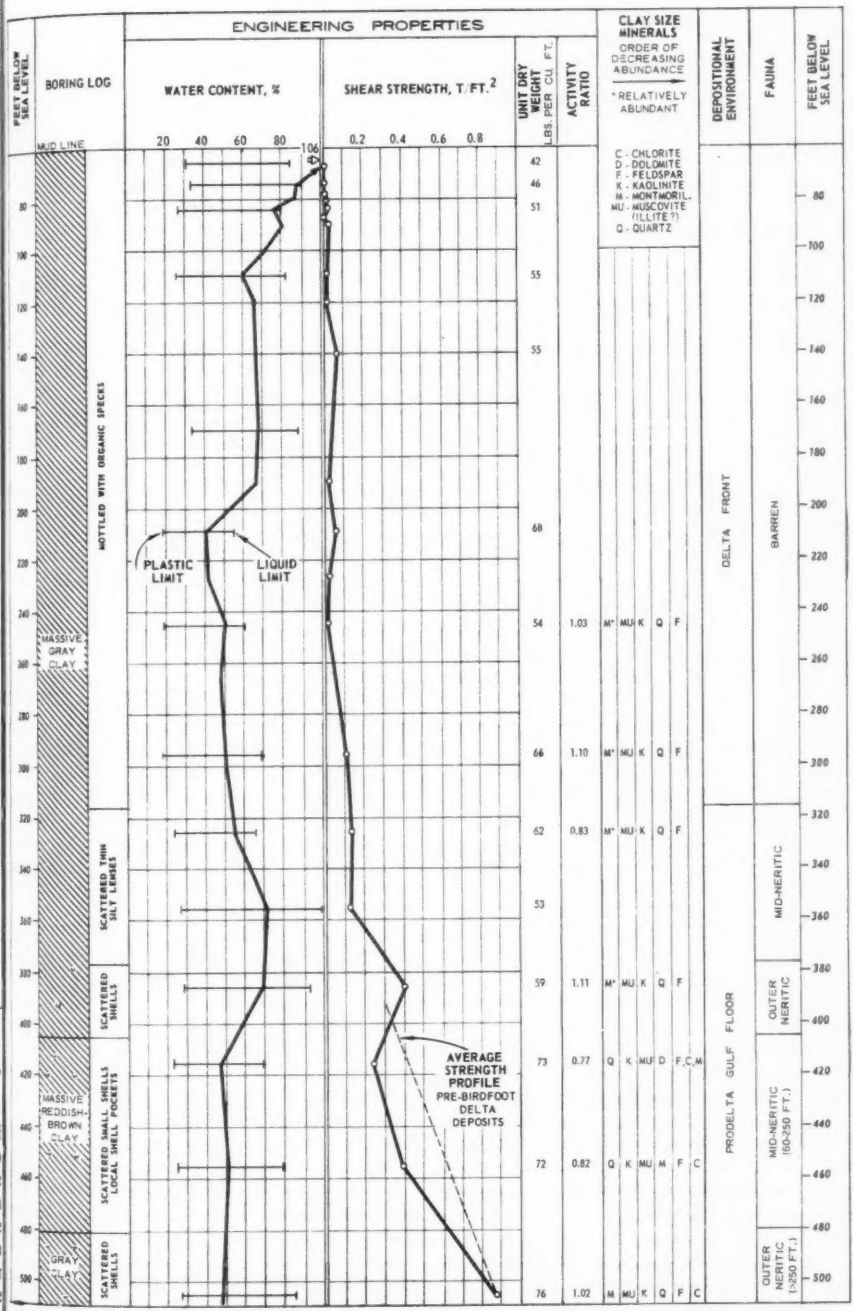


FIGURE 11.—ENGINEERING AND GEOLOGIC DATA FROM UNDISTURBED SAMPLES

Samples taken in Humble Oil & Refining Company foundation test boring No. 1, South Pass Area, Block 20. For location *see* Figure 1, boring 12.

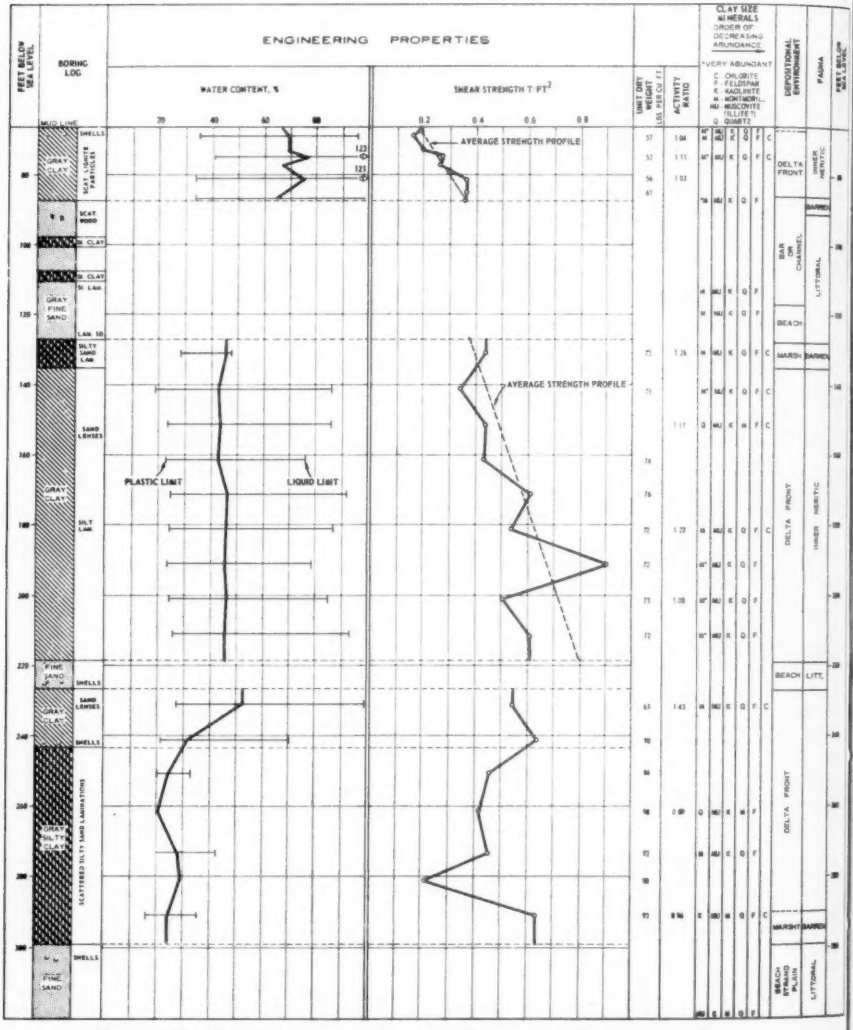


FIGURE 12.—ENGINEERING AND GEOLOGIC DATA FROM UNDISTURBED SAMPLES

Samples taken in Humble Oil & Refining Company foundation test boring No. 2, South Timbalier Area, Block 54. For location *see* Figure 1, boring 8.

beds. The strength values for the beds beneath the weathered zone should not be compared with those of the overlying topstratum clays because of the strong influence of silt and sand layers in the older deposits.

The activity ratio of the late Quaternary clays ranges from 0.83 to 1.00, establishing these deposits as "normal" clays on the basis of this property (Fig. 7). Somewhat lower values of activity, 0.39 to 0.87, were found for the late Pleistocene clays. Their average activity ratio is approximately 0.75 which is the division between normal and inactive clays.

*Underconsolidated clays approaching normal state of consolidation.*—A section of delta-front and underlying prodelta clays sampled in a boring at Grand Isle Block 23 was less well consolidated than the older prodelta clays

penetrated at Eugene Island Block 188. The boring is located in 55 feet of water, approximately 8 miles offshore from Grand Isle, Louisiana, and close to the frontal zone of the abandoned Lafourche-Mississippi delta. The facies of the abandoned delta underlie 15 feet of gulf-floor clays and extend to approximately 195 feet below sea level. They overlie earlier formed deltaic deposits which rest upon substratum sands at 240 feet below sea level. The log of this boring and related information are tabulated in Figure 10.

The upper 15-foot layer of modern gulf-floor clays carries a typical shallow-marine inner-neritic fauna. The shallow delta-front clays of the Lafourche-Mississippi delta extend to approximately 155 feet below sea level where they grade into the prodelta sediments which accumulated in the mid-neritic zone. Radiocarbon analyses indicate that the Lafourche-Mississippi delta began to develop approximately 1500 years ago and was abandoned about 800 years ago (McFarlan, 1955).

The assemblage of clay minerals in the Lafourche-Mississippi delta-front and prodelta gulf-floor clays is remarkably uniform and appears to be of Mississippi River origin. The clay minerals in the underlying, older deltaic deposits contain chlorite, indicating a Red River source. The color of the 10-foot bed of massive red clay at 215 feet below sea level confirms the Red River origin. These deposits rest upon finely laminated dark clays and gray silts (Pl. 3, fig. 1) which contain a high percentage of kaolinite and chlorite, indicating a mixed Mississippi River-Red River source.

The values of cohesive shear strength are plotted on Figure 10. The average-strength profile throughout Lafourche-Mississippi delta deposits is shown by a dashed line. As indicated by these data, strengths are quite negligible in the 15-foot layer of modern gulf-floor clays, and water content is correspondingly high. These physical characteristics are compatible with the youthful nature of the deposit. In the underlying Lafourche-Mississippi delta deposits, the shear strength increases steadily with depth but more slowly than in the normally consolidated topstratum clays at Eugene Island Block 188. The rate of strength increase with depth corresponds to a $c/p$ ratio of 0.15. This value is much lower than would be expected for clays with a plasticity index of approximately 55, based on the correlation shown in Figure 8. Probably the explanation for this relatively low rate of strength increase lies in the fact that the deposits are less than 1500 years old. It may be concluded, therefore, that the major part of the topstratum has not consolidated fully with respect to existing overburden pressures, and that it may be properly classified as an underconsolidated clay.

Both the type and abundance of clay minerals are relatively uniform as indicated by the tabulated values of activity and the plotted values of liquid and plastic limits in Figure 10. Water contents are very near the liquid limit in the soft, modern gulf-floor clay; they decrease gradually with depth and are much nearer the plastic limit at the bottom of the topstratum. Except for the two deepest samples of clay, activity ratios are normal (Fig. 7). The two deep samples, with activity ratios of 1.28 and 1.38, are probably more active because of organic colloids present in the dark clays. They were deposited in brackish-marine delta-plain environments rather than in offshore marine environments (Pl. 3, fig. 1).

*Underconsolidated clays.*—A thick section of massive gray clays which have consolidated very little under existing overburden pressures was penetrated by a boring located in South Pass Block 20, near the frontal margin of the modern Mississippi birdfoot delta. The platform of the birdfoot delta has been created during the past 450 years, and the frontal zone is building seaward at rates up to 350 feet per year (Fisk *et al.*, 1954). The South Pass boring was drilled in 59 feet of water and penetrated the base of the modern deltaic deposits at approximately 380 feet below sea level. Below this depth are older gulf-floor sediments, some of which may have accumulated during the middle phase of the late Quaternary cycle when sea level was rising. Information from this boring, which was drilled to a total depth of 510 feet below sea level, is shown on Figure 11.

Shallow-water delta-front deposits compose the upper 255 feet of the section and consist of massive clays with disseminated organic specks. These beds grade downward into mid-neritic prodelta clays, approximately 55 feet thick, which contain less organic material and include scattered silt lenses (Pl. 4, fig. 2). The mid-neritic facies grade into outer-neritic laminated clays containing scattered small molluscan shells (Pl. 4, fig. 3). Because the entire section of clays to 400 feet below sea level holds the same clay-mineral assemblage, it is difficult to establish the exact base of the birdfoot-delta deposits. Although the consistent mineral assemblage suggests a common source,

some of the outer-neritic and mid-neritic facies deeper than 360 feet below sea level could have accumulated earlier when the Mississippi River was constructing its older deltas of the deltaic plain.

The deposits deeper than 400 feet below sea level were laid down prior to the formation of the birdfoot delta. An 80-foot section of reddish-brown mid-neritic gulf-floor clays underlies the outer-neritic facies of questionable age. These reddish deposits bear a typical suite of Red River clay minerals, and at 480 feet below sea level they grade into outer-neritic clays which indicate a mixed Mississippi River-Red River source.

Engineering properties of the sediments at this site bear a striking relationship to the geological factors described above. The outstanding characteristic of the section is the near absence of strength in the sediment down to a depth of 360 feet below sea level. The unit dry weight of the sediment within this same depth range is low and shows only a slight tendency to increase with depth; water contents are correspondingly high and show only a moderate decrease with depth. These combined physical properties demonstrate that the sediment has experienced negligible consolidation; in its lower part, the section exhibits strength and density very little greater than the material at the gulf floor. This section of the topstratum is, therefore, properly classified as an underconsolidated clay deposit.

Below the underconsolidated section the strength of the pre-birdfoot-delta deposits increases appreciably with depth, as shown by the average-strength profile (Fig. 11). The strength profile of these older sediments is probably very little changed, if any, from that which characterized it prior to the deposition of modern delta-front overburden.

The clay-mineral assemblages at this location are all of normal activity as shown by the tabulation of activity ratios. The two lowest values are associated with the massive pre-birdfoot-delta reddish-brown clays which are high in quartz.

*Overconsolidated clays.*—Near-surface clays at South Timbalier Block 54 are stiffer than those usually found at comparable depths in the topstratum and indicate the effects of overconsolidation. A test boring in this block, approximately 15 miles south of Timbalier Island in 66 feet of water, was drilled to approximately 320 feet below sea level. The log of this boring and related test data are presented in Figure 12. The boring lies close to the front of a Mississippi River delta that was constructed near the end of the late Quaternary rising-sea-level stage. Deposits of this delta probably began to accumulate about 6000 years ago when sea level was 30 feet lower than at present. The local gulf-floor topography is irregular, and steep slopes mark the effects of wave erosion by rising gulf waters prior to submergence of the delta.

The deposits penetrated by the boring are representative of the thick sand-bearing topstratum unit (Fig. 5). They consist of shallow-water deltaic facies covered by modern gulf-floor muds less than 1 foot thick. The premodern deltaic deposits consist of two clay sections separated by a 40-foot sand bed. The upper section is 20 feet thick and consists of massive gray clays with local silt laminations, wood fragments, and abundant carbonized plant remains (Pl. 3, fig. 3). This section is the portion of shallow-water delta-front deposits remaining after marine erosion. The underlying 40-foot-thick gray sand bed is made up of offshore bar deposits with finely laminated beach deposits at its base (Pl. 3, fig. 2). The sands overlie the lower clay section which consists of deltaic and littoral deposits that extend to the substratum sands at a depth of 300 feet below sea level. The topstratum clays at depths greater than 225 feet below sea level contain more silt and sand than does the upper clay section (Pl. 3, fig. 4).

Evidence of erosion at this site is readily apparent in the engineering properties of the deposits underlying the thin veneer of modern gulf-floor sediments. The strength of 0.2 ton per square foot determined for a sample directly beneath the mud line at the top of the eroded deltaic deposits is representative of strengths found at a depth of about 30 feet in normally consolidated deposits of similar clays. Below this sample, the strength in the upper clay section increases with depth to the top of the 40-foot sand bed. Below this sand body, strength increases in the lower clay section at a uniform rate to a depth of 200 feet below sea level. The average-strength profiles for both clay sections, shown by dashed lines on Figure 12, intersect at 30 feet above the gulf floor. This strength relationship, which is supported by the relatively low water contents of the clays, indicates that the topstratum clays have been consolidated under deposits 30 feet thicker than the present overburden. Marine erosion has apparently removed the excess overburden. Strengths of clay sediments in the vicinity of the South Timbalier Block 54

lite may be contrasted with those in adjacent blocks by the lines of equal shear strength shown on Figure 3.

Strengths of clay deposits deeper than 220 feet below sea level are erratic, a fact attributable to the presence of numerous silty sand laminations in the clay sections.

Activity ratios of the clay sediments, except for the sample at a depth of 230 feet, are in the range of 0.89 to 1.26, indicating that all these deltaic clays are of normal activity. No explanation is readily apparent for the unusually high activity ratio of 1.43 for the sample at the 230-foot depth.

## Summary and Conclusions

The foundation conditions on the Continental Shelf off Louisiana have been strongly affected by depositional, erosional, and weathering processes active during the late Quaternary cycle of changing sea level. These geological factors, together with structural downwarping, have controlled the distribution, thickness, and rate of deposition of sediments brought to the shelf. Foundation conditions seaward of the Mississippi deltaic plain are poorer than elsewhere in the region; this portion of the shelf is underlain by thick topstratum clay deposits. The poorest foundation conditions are at the seaward margin of the Mississippi birdfoot-delta platform where very recently deposited underconsolidated silty clays are up to several hundred feet thick. Generally speaking, conditions are more favorable for foundations in the near-shore areas south of the chenier plain and east of the Chandeleur Islands, where the topstratum is underlain at shallow depth by either substratum sands or by the firm weathered late Pleistocene surface. In the area of thick clays, south of the deltaic plain, the most favorable conditions exist where marine erosion has removed a portion of the section of soft near-surface sediments and where sands are locally present.

Detailed study of engineering properties and geological relationships at several offshore locations has permitted confirmation and extension of important correlations between the shear strength of clay deposits and the type and abundance of clay minerals. Off western Louisiana where delta-front deposits accumulated over many thousand years, these clay sediments are normally consolidated and are at equilibrium under existing overburden pressures. The rate of strength increase with depth found for samples in that area and the average plasticity index conform to the previously established relationship of the two properties. Different relationships were determined, however, for younger deltaic deposits which started to accumulate about 1500 years ago; the rate of strength increase with depth in these clays is appreciable but not so high as in the older deposits. In the modern Mississippi birdfoot-delta clays, which have accumulated in the last few hundred years, strength increase with depth is negligible. These findings emphasize that time is an important factor in establishing full consolidation of clay sediments under their existing overburden pressures.

Certain general foundation conditions can be associated with particular areas of the Continental Shelf. Local variations and exceptional conditions inherent in most natural deposits prevent the use of such generalizations in the detailed design of foundations. It is useful, however, to recognize these identifying characteristics of the various shelf areas when examining the feasibility of new structural methods, planning future operations, preparing cost estimates, or anticipating the hazards of operations in the open gulf.

## References Cited


Bates, C. C., 1953, Rational theory of delta formation: Am. Assoc. Petroleum Geologists Bull., v. 37, p. 2119–2162

Bjerrum, Laurits, 1954, Geotechnical properties of Norwegian marine clays: Géotechnique, v. 4, p. 49–69

Fisk, H. N., 1955, Sand facies of Recent Mississippi Delta deposits: Rome, 4th World Petroleum Cong. Proc., sec. 1, p. 377–398

—— 1956, Nearsurface sediments of the Continental Shelf off Louisiana: 8th Texas Conf. on Soil Mechanics and Foundation Engineering Proc., 36 p.

Fisk, H. N., and McFarlan, E., Jr., 1955, Late Quaternary deltaic deposits of the Mississippi River, p. 279–302 *in* Poldervaart, A., *Editor*, Crust of the Earth: Geol. Soc. America Special Paper 62, 762 p.

Fisk, H. N., *et al.*, 1954, Sedimentary framework of the modern Mississippi Delta: Jour. Sed. Petrology, v. 24, p. 76–99

Howe, R. J., 1954, The design of offshore drilling structures: Am. Soc. Mech. Engineers, 9th Annual Petroleum Mechanical Engineering Conf., Paper No. 54-PET-19, 50 p.

Lowman, S. W., 1949, Sedimentary facies in Gulf Coast: Am. Assoc. Petroleum Geologists Bull., v. 33, p. 1939–1997

McClelland, Bramlette, 1956, Engineering properties of soils on the Continental Shelf of the Gulf of Mexico: 8th Texas Conf. on Soil Mechanics and Foundation Engineering Proc., 28 p.

McFarlan, E., Jr., 1955, Radiocarbon dating of the

Quaternary in southern Louisiana (Abstract): Geol. Soc. America Bull., v. 66, p. 1594

Osterhoudt, W. J., 1946, The seismograph discovery of an ancient Mississippi River channel (Abstract): Geophysics, v. 11, p. 417

Rechtin, E. C., Steele, J. E., and Scales, R. E., 1957, Engineering problems related to the design of offshore mobile platforms: Soc. Naval Architects and Marine Engineers Annual Meeting, Paper 10, 30 p.

Skempton, A. W., 1948, Vane tests in the alluvial plain of the River Forth: Géotechnique, v. 1, p. 111–124

Skempton, A. W., 1953, The colloidal "activity" of clays: 3rd Intern. Conf. on Soil Mechanics and Foundation Engineering Proc., v. 1, p. 57–61

Terzaghi, Karl, 1956, Varieties of submarine slope failures: 8th Texas Conf. on Soil Mechanics and Foundation Engineering Proc., 41 p.

HUMBLE OIL & REFINING COMPANY, HOUSTON, TEXAS; McCLELLAND ENGINEERS, INC., HOUSTON, TEXAS

MANUSCRIPT RECEIVED BY THE SECRETARY OF THE SOCIETY, MARCH 28, 1958

# Short Notes

BULLETIN OF THE GEOLOGICAL SOCIETY OF AMERICA
VOL. 70, PP. 1395-1398 OCTOBER 1959

## LAYERED INTRUSIONS OF WILLOW LAKE TYPE

BY ARIE POLDERVAART AND WILLIAM H. TAUBENECK

Wager (1953, p. 335-340) distinguished two main types of layering in igneous plutons: *cryptic* layering and *rhythmic* layering. Cryptic layering is produced by changes in composition of constituent minerals, with or without changes in modal compositions of the rocks. This type of layering may or may not be apparent in the field. It results from fractional crystallization of magma, with or without gravitational accumulation of particular minerals. Most large to medium-sized plutons show some cryptic layering.

Rhythmic layering is formed by repetitious layers in which alternative minerals predominate. The writers propose a subdivision of rhythmic layering into: (1) layering of Skaergaard type, and (2) layering of Willow Lake type. The type localities are, respectively, the Skaergaard pluton, Kangerdlugssuaq, East Greenland, and the Willow Lake intrusion in the Elkhorn Mountains, northeastern Oregon. Other types of rhythmic layering may exist, but to date there are no well-studied examples.

Skaergaard-type layering is displayed by many large gabbroic plutons. Characteristically crystals of the constituent minerals show a preferred orientation of their longer axes in the plane of banding. The layering is due to crystal sedimentation under the influence of gravity, accompanied and rendered repetitious by periodic disturbances in the magma. Single layers may be produced when the magma passes into a condition of lower variance, but repetitious layering by this means is not possible in a quiescent magma. Repetitious disturbing factors may be physical or chemical: slow, periodic convective overturn, a rhythmic convection system, or turbulent currents caused by slumping of crystal mush, stoping of blocks of country rocks from roof or walls of the pluton, or periodic sagging of the floor of the pluton; or periodic increments of undifferentiated magma or assimilation following periodic stoping of country rocks. Understanding of Skaergaard-type rhythmic layering has increased greatly as a result of the brilliant studies of Wager and Deer (1939) on the Skaergaard pluton, East Greenland, and of Hess (in press) on the Stillwater pluton, Montana.

Yoder (1954, p. 107) has suggested that periodic variations in water pressure during crystallization may result in rhythmic layering similar to that of the Skaergaard type. The writers do not believe this process accounts for rhythmic layering in most gabbroic plutons. Periodic variations in water pressure may be expected in magmas emplaced at shallow depths, but they become more problematical at depths of several miles. Yoder and Tilley (1956; 1957) have argued that basaltic magmas cannot contain much water, and Boyd's (1956) work also indicates that at moderate water pressures basaltic magmas crystallize to plagioclase-hornblende rather than to plagioclase-pyroxene-(olivine) assemblages. However, the mechanism of varying water pressures probably accounts for the rhythmic layering observed in some more silicic rocks, including pegmatites (*e.g.*, Eckelmann *et al.*, 1958). Rhythmic layering in silicic rocks, produced by differential movements of crystal mush and magma, also appears to be possible (*e.g.*, Alper and Poldervaart, 1957, p. 961–962). Detailed petrologic studies of such occurrences will enable distinction and definition of these additional types.

Willow Lake-type rhythmic layering is displayed by many small gabbroic plutons in western North America, to date found in a region extending from northeastern Oregon to east-central California. Characteristically the igneous bodies are small (down to dikelets less than an inch wide), have steep (50°–90°) walls, are found in the greenschist facies of regional metamorphism, and are associated with younger granitic batholiths. Typically also, crystals of the constituent minerals are arranged with their longer axes at high angles (60°–90°) to the layering. The crystals are

commonly elongated, curved, and branching. The layers are rarely more than a foot thick and are commonly much thinner, down to 1 mm. The writers have selected the Willow Lake intrusion as the type example of such layering. The pluton is funnel-shaped, about 1 mile long by half a mile wide, and lies athwart the southern contact of the Bald Mountain batholith (Taubeneck, 1957). It was selected for detailed study because of the excellent exposures. Layered sequences in the pluton commonly extend right to the contact with the country rocks. Some xenoliths are also surrounded by layered rocks, in which banding is parallel to the margins of the xenoliths, and crystals are oriented with their longer axes at high angles thereto. The central part of the pluton contains several autoliths of layered rocks. Associated dikes are also layered; the layers are parallel to the dike contacts, and crystals are oriented with their longer axes at high angles to the contacts. The investigation of the Willow Lake pluton (Taubeneck and Poldervaart, in preparation) is near completion.

The writers believe that Willow-Lake type of rhythmic layering is due to undercooling and crystallization in the oversaturated region, combined with periodic disturbances in the magma. The disturbances can be of the same type as in Skaergaard-type layering and serve only to bring fresh portions of the magma to the sites of crystalization. In the Willow Lake pluton disturbances in the magma were probably mainly turbulent currents associated with the initial emplacement of the magma, somewhat later stoping of large blocks of country rocks from the roof and walls of the pluton, and yet later enlargement of the pluton by lateral intrusion. The main sites of initial crystallization in the supersaturated region were the steep walls of the pluton. Currents caused continuation of magmetic undercooling against the crystallizing walls. As a result, the magma which was initially probably near a univariant condition (*cf.*, Yoder and Tilley, 1957, p. 159) moved away from this condition instead of toward it. Continued undercooling requires unusually efficient heat flow away from crystallization sites. It is suggested that this is likely only in steep-walled intrusions, emplaced at the peak of epizonal regional metamorphism, when water migrated through the country rocks at rates which may well have exceeded the rate of conduction of heat through the country rocks. Rather to their own surprise the writers have found that Willow-Lake-type rhythmically layered intrusions are by no means rare in western North America.

As noted by Hess (in press), nearly monomineralic layers in rhythmically layered sequences are the products of reaction between earlier crystals and interstitial melt, combined with diffusion between the interstitial melt and overlying magma, or the interstitial melt in the next contrasted layer. Small amounts of minerals late in the reaction series (*e.g.*, biotite in picrites) testify to the former presence of the interstitial melt and the importance of reaction-diffusion in the formation of these rocks. Willow Lake-type layered sequences may also include nearly monomineralic layers. Similar top- and bottom criteria may be observed in both Skaergaard- and Willow Lake-type layered sequences. Such criteria as sharply defined bottom boundaries with gradational top boundaries have been interpreted as evidence for gravitational sedimentation of crystals (Peoples, 1936, p. 358), but their presence in Willow Lake-type layered rocks indicates that these features do not invariably result from gravity controls. Van Zyl (in press) has attributed rhythmic layering in the Kapalagulu pluton, Tanganyika, to periodic undercooling. From his descriptions of the layered rocks, however, it appears that layering is of Skaergaard type, and not of Willow Lake type.

Characteristic features of crystallization in the supersaturation region are elongated, curved, and branching crystals oriented with their longer axes roughly at right angles to the cooling front. Although not associated with rhythmic layering, such typical crystal forms are also commonly observed adjacent to chilled contacts or in the interior portions of many small and large intrusions, including also the Skaergaard (perpendicular feldspar rock: Wager and Deer, 1939, p. 144–150) and Sudbury (feather norite; Bain, 1926a, p. 113–114; 1926b, p. 286–287) plutons, and the ultramafic intrusions on the island of Rhum (harrisite structure; Brown, 1956, p. 10). Orbicular rocks are also being studied in detail (D. L. Leveson, in preparation). Probably their origin requires a special type of crystallization in the supersaturated region, in which metastable crystallization on few crystal nuclei is combined with Liesegang-type variations in concentrations of various elements.

## *References Cited*

Alper, A. M., and Poldervaart, Arie, 1957, Zircons from the Animas stock and associated rocks, New Mexico: Econ. Geology, v. 52, p. 952–97.

Bain, G. W., 1926a, Killarneyan intrusives of Sudbury: Pan-Am. Geologist, v. 45, p. 109–12

Bain, G. W., 1925b, Chemistry of Killarneyan magma of Sudbury: Pan-Am. Geologist, v. 45, p. 277–294

Boyd, F. R., Jr., 1956, Amphiboles, p. 198–200 *in* Abelson, P. H., Annual Report of the Director, Geophysical Laboratory: Carnegie Inst. Washington Yearbook 55, p. 153–229

Brown, G. M., 1956, The layered ultrabasic rocks of Rhum, Inner Hebrides: Roy. Soc. London Philos. Trans., ser. B, v. 240, no. 668, p. 1–53

Echelmann, F. D., Long, L. E., and Olson, E. A., 1958, Origin and occurrence of extensively developed layered structures in leucogranite-granite pegmatite, Huron Claim-Johnston Lake area, Southeast Manitoba, Canada (Abstract): Geol. Soc. America Bull., v. 69, p. 1558

Hess, H. H., in press, Stillwater igneous complex, a quantitative mineralogical study: Geol. Soc. America Mem.

Peoples, J. W., 1936, Gravity stratification as a criterion in the interpretation of the structure of the Stillwater complex, Montana: 16th Internat. Geol. Congr. Repts., 1933 (U. S.), v. 1, p. 353–360

Taubeneck, W. H., 1957, Geology of the Elkhorn Mountains, northeastern Oregon; Bald Mountain batholith: Geol. Soc. America Bull., v. 68, p. 181–238

Van Zyl, Colin, in press, An outline of the geology of the Kapalagulu complex, Kungwe Bay, Tanganyika, Territory, and aspects of the evolution of layering in basic intrusives: Geol. South Africa Trans., v. 61

Wager, L. R., 1953, Layered intrusions: Meddeleser fre Dansk Geol. Forening, v. 12, p. 335–349

Wager, L. R., and Deer, W. A., 1939, Geological investigations in East Greenland. 3. The petrology of the Skaergaard intrusion, Kangerdlugssuaq, East Greenland: Meddelelser om Grönland, v. 105, no. 4, p. 1–352

Yoder, H. S., Jr., 1954, Synthetic basalt, p. 106–107 *in* Abelson, P. H., Annual Report of the Director, Geophysical Laboratory: Carnegie Inst. Washington Yearbook 53, p. 95–145

Yoder, H. S., Jr., and Tilley, C. E., 1956, Natural tholeiite basalt-water system, p. 169–171 *in* Abelson, P. H., Annual Report of the Director, Geophysical Laboratory: Carnegie Inst. Washington Yearbook 55, p. 153–229

—— 1957, Basalt magmas, p. 156–161 *in* Abelson, P. H., Annual Report of the Director, Geophysical Laboratory: Carnegie Inst. Washington Yearbook 56, p. 151–252

Department of Geology, Columbia University, New York 27, N. Y.; Department of Geology, Oregon State College, Corvallis, Ore.

Manuscript Received by the Secretary of the Society, April 7, 1959